Dacarbazine and Its Structural Analogues:

Systematic computational studies of the configurations, tautomers, tautomerization pathways and bimolecular nucleophilic substitution reaction mechanisms of Dacarbazine; a triazene containing anti-neoplastic agent, and its structural analogues.

By
Katherine Grace Doucet

A Thesis Submitted to
Saint Mary's University, Halifax, Nova Scotia
in Partial Fulfillment of the Requirements for
the Degree of Masters of Science in Applied Science.

October 2007, Halifax, Nova Scotia

Approved:	Dr. Stacey Wetmore, External Examiner Department of Chemistry and Biochemistry University of Lethbridge
Approved:	Dr. Cory C. Pye, Senior Supervisor Department of Chemistry
Approved:	Dr. Keith Vaughan, Supervisory Committee Department of Chemistry
Approved:	Dr. Susan Bjornson, Supervisory Committee Department of Biology
Approved:	Dr. Pawan Lingras, Program Co-ordinator
Approved:	Dr. Kevin Vessey, Dean of Graduate Studies
Date:	August 31, 2007

Your file Votre référence
ISBN: 978-0-494-35765-1
Our file Notre référence
ISBN: 978-0-494-35765-1

Certification

Dacarbazine and Its Structural Analogues: Systematic computational studies of the configurations, tautomers, tautomerization pathways and bimolecular nucleophilic substitution reaction mechanisms of Dacarbazine, a triazene containing anti-neoplastic agent, and its structural analogues.

by

Katherine Doucet

A Thesis Submitted to Saint Mary's University, Halifax, Nova Scotia,
in Partial Fulfillment of the Requirements for the
Degree of Master of Science in Applied Science

August 31, 2007

Examining Committee:

Approved: Dr. Stacey Wetmore, External Examiner
Department of Chemistry and Biochemistry
University of Lethbridge

Approved: Dr. Cory Pye, Senior Supervisor
Department of Chemistry

Approved: Dr. Keith Vaughan, Supervisory Committee
Department of Chemistry

Approved: Dr. Susan Bjornson, Supervisory Committee
Department of Biology

Approved: Dr. Pawan Lingras, Program Co-ordinator

Approved: Dr. Kevin Vessey, Dean of Graduate Studies

Abstract

Dacarbazine and Its Structural Analogues:
Systematic computational studies of the configurations, tautomers, tautomerization pathways and bimolecular nucleophilic substitution reaction mechanisms of Dacarbazine, a triazene containing anti-neoplastic agent, and its structural analogues.

by Katherine Grace Doucet

Abstract: A monomethyltriazene is believed to be the active metabolite of triazene containing anti-neoplastic agents and is thought to methylate the O6-oxygen of guanine to form methylguanine. Methylguanine is believed to be responsible for the observed cytotoxic properties of triazene containing anti-neoplastic agents. Dacarbazine, a triazene containing anti-neoplastic agent, has been shown to be the single most active agent for the treatment of malignant melanoma. Computational studies, including conformational and tautomer analysis, tautomerization pathways and a model mechanism of action, were conducted in the hopes that a better understanding of the chemical and physical properties of triazene containing anti-neoplastic compounds could be provided. This study found that the tautomerization of a monomethyltriazene is a relatively low energy process and the tautomer form will preferentially undergo an S_N2 type reaction. It is proposed that following demethylation DTIC would preferentially undergo tautomerization followed by an S_N2 type reaction to form methylguanine.

October 4, 2007

ACKNOWLEDGEMENTS

The author wishes to thank Dr. Cory Pye for supervising this project. The author also wishes to thank Drs. Susan Bjornson and Keith Vaughan for acting as members of her supervisory committee and Dr. Stacey Wetmore for acting as her external examiner. The author wishes to thank the Department of Astronomy and Physics, Saint Mary's University (SMU) for providing access to Cygnus* and the Atlantic Computational Excellence Network (ACEnet) for access to Placentia, Herzberg, Verdandi, Skuld and Urdur† that are part of ACEnet and located at Memorial University of Newfoundland. The author would like to acknowledge the financial support of SMU's Faculty of Graduate Studies and Research for this project.

On a personal note, the author would like to thank her friends as well as her immediate and extended family for their continued support throughout the duration of this project.

---

* Cygnus is a 10-processor Sun Server, purchased with the assistance of the Canadian Foundation for Innovation, Sun Microsystems, the Atlantic Canada Opportunity Agent and SMU.

† Placentia is a 96 core GigE/16-way cluster, 6 octal socket SunFire x4600 nodes populated with 2.6 GHz dual-core Opteron 285 processors and 4 GB RAM per core. Herzberg is a SGI Onyx 3400 with 8 MIPS R12000 400MHz CPUs and 4GB of shared memory. Verdandi is a SGI Altix 350 with 10 1.5Ghz Itanium2 CPUs and 10GB RAM. Skuld and Urdur are two SGI Altix 350 with 16 1.5Ghz Itanium2 CPUs and 16GB of RAM.

TABLE OF CONTENTS

LIST OF FIGURES & SCHEMES

Chapter 1: Introduction

Chapter 6: Tautomers and Tautomerization

LIST OF TABLES

CHAPTER ONE: INTRODUCTION

1. Canadian Cancer Rates

Recent publications by the Canadian Cancer Society, the National Cancer Institute of Canada (1) and Cancer Care Nova Scotia (2) have estimated that 153,100 new cases of cancer will have been diagnosed and 70,400 Canadians will have lost their lives to cancer in 2006. Canadian mortality rates of certain cancers, such as prostate cancer, are decreasing, while the incidence and mortality rates of lung cancer, malignant melanoma and non-Hodgkin lymphoma continue to increase. In Canada, cancer mortality rates are the highest in Atlantic Canada and Quebec (1,2). It has been predicted that 38% of Canadian women and 44% of Canadian men will develop cancer in their lifetime; the increase in cancer is due in part to the increase in the life expectancy of the Canadian population (1,2). Based on current mortality rates, 1 in 4 Canadians will die from cancer (1,2).

Cancer is a broad term used to describe a group of diseases. There are over 100 types of disease that are classified as cancer. Cancer occurs when cells grow at an abnormal rate and prevent healthy cells from functioning properly. Masses of cancerous cells are called malignant tumors. There are four major categories of cancer;

carcinomas*, leukemias†, lymphomas‡ and sarcomas§ (3,4). When cancer cells travel through the lymph or blood system to other parts of the body the cancer is said to have metastasized.

Due to medical advances, there are various treatment options available for the treatment of cancer. The primary goals of cancer treatment options are to remove or shrink the cancer, kill any cancer cells that may have spread and reduce the risk of recurrence. Depending on the type of cancer, more than one treatment option may be needed. Current treatment options include chemotherapy, radiation therapy, surgery, immunotherapy and bone marrow or stem cell transplants. The 2002 Cancer Care Nova Scotia report concluded that the most realistic means of cancer control were prevention, early detection and the use of chemotherapy (2).

---

* Carcinomas are malignant tumors that occur in epithelial tissues and can affect any organ or part of the body (3,4).

† Leukemias are cancers that affect white blood cells, when immature white blood cells multiply at the expense of mature white blood cells (3,4). As normal blood cells are depleted, anemia, infection, hemorrhage or death can occur (3,4).

‡ Lymphomas are malignant neoplasms originating from lymphocytes, white blood cells involved in immune protection (3,4).

§ Sarcomas are cancers that arise from the mesenchymal tissues and may affect bones, bladder, kidneys, liver, lungs, parotids and spleen (3,4).

2. Chemotherapy

Chemotherapy is the use of pharmaceuticals to treat cancer, specifically cytotoxic drugs used to kill cancer cells. Chemotherapy may be used alone or in combination with surgery and / or radiation therapy. Chemotherapeutics are designed to stop cancer cells from growing and proliferating, which shrinks the tumor. There are approximately 50 chemotherapy drugs currently used in Canada. Most of these drugs are anti-neoplastic agents that are designed to inhibit the growth of tumors (1,2).

2.1 Anti-neoplastic Agents

Anti-neoplastic agents are chemical agents that prevent, inhibit or halt the development and growth of a neoplasm, a tumor or abnormal growth of tissue (1,2). It should be noted that neoplasm and cancer are not synonymous terms. A neoplasm can be benign or malignant, whereas a cancer is always malignant. Most chemotherapeutics are anti-neoplastic agents. Chemotherapeutics are administered in the hopes of stopping and possibly reversing the growth of malignant tumors.

2.1.1 Triazene Containing Anti-neoplastic Agents

Anti-neoplastic agents that contain triazene (Figure 1.1) are proven to be effective in the treatment of malignant melanoma (skin cancer), gliomas (brain cancer) and non-Hodgkin's lymphoma (5,6). Dacarbazine (Figure 1.2) and Temozolomide

(Figure 1.3) are triazene-containing anti-neoplastic agents.

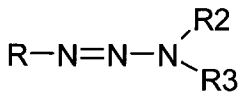

Figure 1.1: The chemical structure of triazene, a functional group comprised of three nitrogen atoms bonded together in sequence.

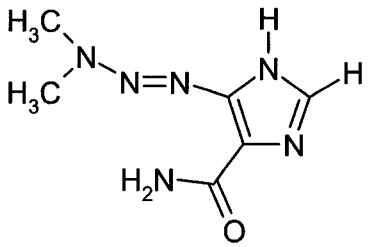

Figure 1.2: Chemical structure of 5-(3,3-dimethyl-1-triazenyl)imidazole-4-carboxamide (Dacarbazine, DTIC ®).

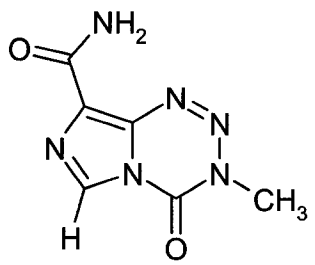

Figure 1.3: The chemical structure of Temozolomide (3,4-dihydro-3-methyl-4-oxoimidazo-[5,1,d]-1,2,3,5-tetrazine-8-carboxamide, Temodal ®)

2.1.2 Dacarbazine

Dacarbazine is a cell-cycle non-specific anti-neoplastic agent currently used as a palliative** measure for metastatic malignant melanoma (7). The exact mechanism of Dacarbazine is unknown but there are various hypotheses about its mechanism of

** Palliative measures are treatment that is designed to alleviate symptoms rather than cure a disease (3,4).

action. The most widely accepted theory is that Dacarbazine is a DNA alkylating agent activated by liver metabolism (5,6,7). Other hypotheses include the inhibition of DNA synthesis by acting as a purine analogue and interacting with the thiol groups (7). While Dacarbazine is a structural analogue of 5-amino-imidazole-4-carboxamide, an intermediate of purine synthesis, there is no concrete evidence to support or negate either hypothesis.

Dacarbazine is currently used as a palliative measure because of the severity of the adverse effects associated with the administration of the compound. The most common side effect is depression of the hematopoietic system[††]. In addition, leucopenia and thrombocytopenia are common side effects and may be severe or fatal. Nausea and vomiting commonly occurred in patients after the initial dose. Other adverse effects include facial flushing, electrocardiogram abnormalities, orthostatic hypotension, blurred vision, seizure, headache, confusion, malaise, lethargy and facial paresthesiae. Diarrhea, anaphylaxis, flu-like symptoms, hepatic and renal failure have also been reported (7).

Dacarbazine is the single most active agent for the treatment of malignant melanoma (8,9) but other dimethyltriazenes also demonstrate anti-tumor properties (10). Dimethyltriazenes are demethylated through an oxidative process carried out by

---

[††] Depression of the hematopoietic system results in reduced production of all blood cells: neutrophils, eosinophils, basophils, monocytes, and lymphocytes (white blood cells); erythrocytes (red blood cells); and thrombocytes (platelets) (7).

hepatic cytochrome P450 enzymes (11). The hepatic oxidative demethylation yields a methyltriazene (Scheme 1), which are known DNA and RNA alkylating agents (12-15). Methyltriazenes are believed to methylate the O6-oxygen of guanine through a bimolecular nucleophilic substitution (S_N2) reaction at the methyl carbon. This S_N2 reaction results in the formation of an aryl amine (RNH_2), molecular nitrogen (N_2) and methylated DNA ($NuCH_3$) (Scheme 2) (6,7).

Scheme 1: The metabolic formation of monomethyltriazene from Dacarbazine, through hepatic cytochrome P450 enzymatic oxidation.

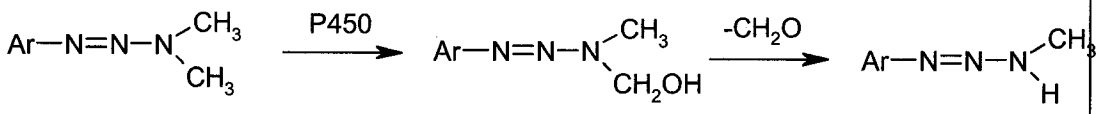

Scheme 2: Methylation of DNA by monomethyltriazene occurs through nucleophilic attack by the DNA base guanine on the methyl group of the triazene moiety.

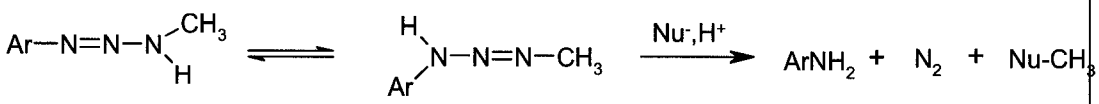

It is believed that the methylation of the O6-oxygen of guanine (Figure 1.4) is responsible for the cytotoxic properties of triazene containing anti-neoplastic compounds (9,12,16). However, Dacarbazine is poorly metabolized in the human body (17). Recent work has focused on designing compounds that do not require oxidative metabolism by hepatic cytochrome P450 enzymes to form a monomethyltriazene (11,18).

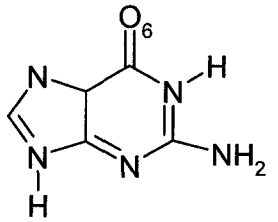

Figure 1.4: The chemical structure of the DNA base guanine.

3. Describing the Potential Energy Surface of Dacarbazine

This study aims to provide an accurate description of the potential energy surface (PES) of Dacarbazine and its structural analogues in an attempt to provide more information about the chemical and physical properties of triazene containing anti-neoplastic agents. Various configurations of Dacarbazine and its structural analogues, certain tautomers of interest, the tautomerization pathway, and the S_N2 reaction that is proposed to occur between a monomethyltriazene and the O6-oxygen of guanine, will be included in this computational study. With this information, it is hoped that more effective triazene containing anti-neoplastic agents may be designed.

3.1 Configurational Possibilities

Configurational analysis of 5-(1-triazenyl)imidazole (TI) (Figure 1.5), 5-(3-methyl-1-triazenyl)imidazole (MTI) (Figure 1.6), 5-(3,3-dimethyl-1-triazenyl)imidazole (DTI) (Figure 1.7), 5-(1-triazenyl)imidazole-4-carboxamide (TIC) (Figure 1.8), 5-(3-methyl-1-triazenyl)imidazole-4-carboxamide (MTIC) (Figure 1.9) and Dacarbazine (5-(3,3-dimethyl-1-triazenyl)imidazole-4-carboxamide, DTIC) (Figure 1.10) will be performed. Specific configurations of Temozolomide (TEMO) (Figure

1.11) and Mitozolomide (MTIO) (Figure 1.12), analogues of Dacarbazine, will be studied in an attempt to more accurately describe the PES of triazene containing anti-neoplastic agents. The configurational analysis will be restricted to the available configurations with respect to the nitrogen-nitrogen double bond of the triazene moiety. A geometrical analysis and relative energy comparison of the identified configurations will be conducted. A similar study of triazene, including its mono-, di- and trimethyl analogues has been previously conducted (19).

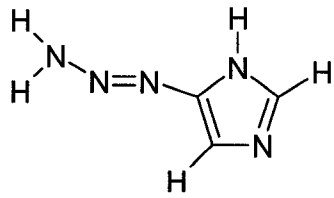

Figure 1.5: The chemical structure of 5-(1-triazenyl)imidazole (TI).

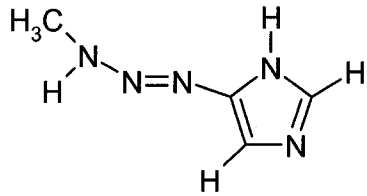

Figure 1.6: The chemical structure of 5-(3-methyl-1-triazenyl)imidazole (MTI).

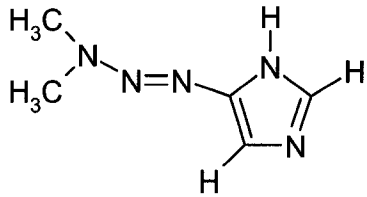

Figure 1.7: The chemical structure of 5-(3,3-dimethyl-1-triazenyl)imidazole (DTI).

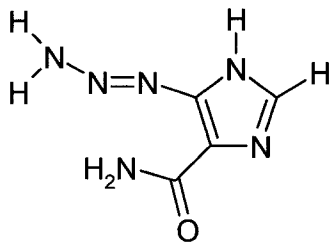

Figure 1.8: The chemical structure of 5-(1-triazenyl)imidazole-4-carboxamide (TIC).

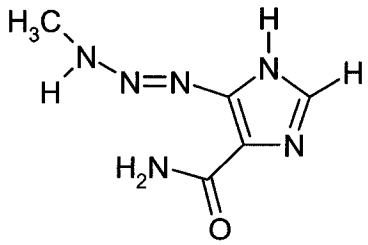

Figure 1.9: The chemical structure of 5-(3-methyl-1-triazenyl)imidazole-4-carboxamide (MTIC).

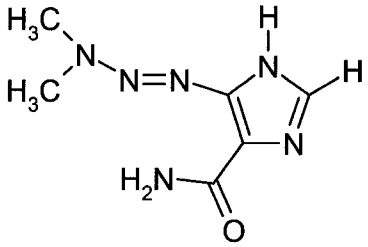

Figure 1.10: The chemical structure of 5-(3,3-dimethyl-1-triazenyl)imidazole-4-carboxamide (Dacarbazine or DTIC).

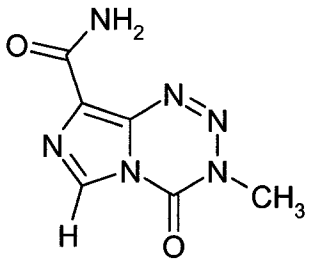

Figure 1.11: The chemical structure of 3,4-dihydro-3-methyl-4-oxoimidazo-[5,1,d]-1,2,3,5-tetrazine-8-carboxamide (Temozolomide, TEMO).

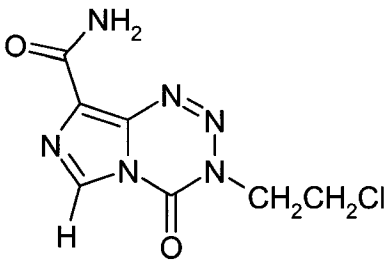

Figure 1.12: The chemical structure of 3,4-dihydro-3-(2-chloroethyl)-4-oxoimidazo-[5,1,d]-1,2,3,5-tetrazine-8-carboxamide (Mitozolomide, MITO).

3.2 Bimolecular Nucleophilic Substitution Reaction Pathways

In addition to describing the configurational possibilities of Dacarbazine and its structural analogues, a series of model S_N2 reactions involving a monomethyltriazene and O6-oxygen of guanine will be carried out. These reactions will be based on results from previous studies involving the S_N2 reactions between mono-, di- and trimethyltriazene and halide ions (20,21,22). These model S_N2 reactions will use halide ions as a simplified model for the O6-oxygen of guanine. It is acknowledged that the halide ions are not the most realistic model for the O6-oxygen of guanine (i.e.; not demonstrating the same chemical behaviour). Fluoride, chloride and bromide provide relatively good models for an exothermic, slightly endothermic and an endothermic reaction, respectively (20,21,22).

The proposed mechanism of action of triazene containing anti-neoplastic agents is a carbon centered S_N2 reaction. These have been widely studied (23,24). Various methods have been employed to study S_N2 reactions, including kinetic experiments (25-34), *ab initio* quantum mechanical and semi-classical dynamical methods and trajectory simulations (35-41), statistical mechanical studies (42-49), *ab initio* and density functional structural analyses (50-62) and electron-transfer investigations (63-69).

3.3 Tautomers and Tautomerization Pathways

This study also includes the tautomeric configurations of 5-(3-methyl-1-triazenyl)imidazole and 5-(3-methyl-1-triazenyl)imidazole-4carboxamide (Figure 1.13)

and both the gas-phase (Scheme 3) and water mediated (Scheme 4) tautomerization reaction pathway. The identified tautomers will also be considered in the series of S_N2 reaction pathways.

MTI_T **MTIC_T**

Figure 1.13: The chemical structure of 5-(3-methyl-1-triazenyl)imidazole tautomer (MTI_T) and 5-(3-methyl-1-triazenyl)imidazole-4carboxamide tautomer (MTIC_T).

Scheme 3: Tautomerization of 5-(3-methyl-1-triazenyl)imidazole

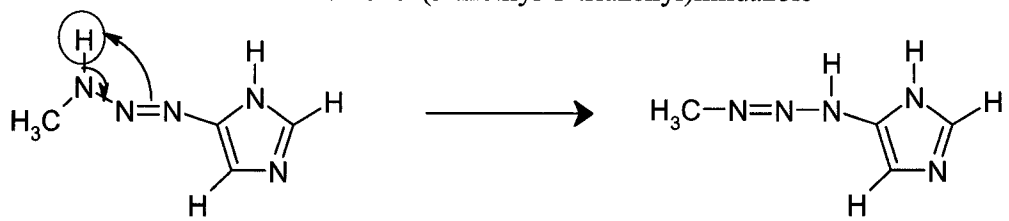

Scheme 4: Water mediated tautomerization of 5-(3-methyl-1-triazenyl)imidazole.

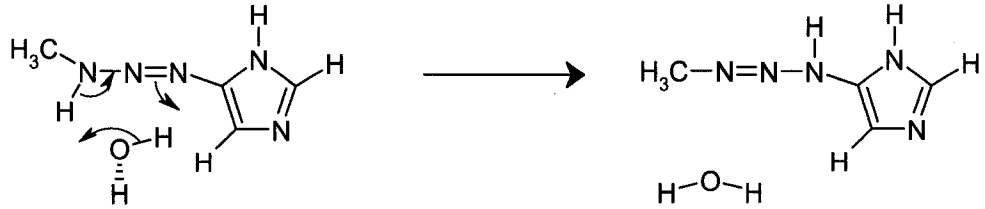

3.4 Analysis of Computational Methods Employed

The final objective of this study is to determine a computational method that is both accurate and efficient for describing triazene-containing anti-neoplastic agents and their chemical behaviour. Various computational methods will be employed throughout this study. These will be discussed in Chapter 2.

CHAPTER TWO: COMPUTATIONAL CHEMISTRY

1. Introduction

Computational chemistry (70-73) is a sub-discipline of theoretical chemistry. Theoretical chemistry, a sub-discipline of physical chemistry, is a conglomeration of chemistry, mathematics, physics and computer science. Theoretical chemists strive to develop mathematical equations and algorithms to develop computer programs in order to predict chemical properties. Computational chemistry applies these computer programs to specific chemical problems. The solutions provide an approximate qualitative and quantitative description of a chemical system.

As with any scientific discipline there are various methods that comprise computational chemistry, each with their own advantages and disadvantages. Three computational methods used in this study will be discussed including Hartree-Fock (70-79), Møller-Plesset perturbation (74-81), and density functional (74-76,82-86,87-98) theories. The role of basis sets (70-76) will also be examined.

2. *ab initio* Methods

Ab initio theory is derived from the first principles of quantum mechanics. The goal of *ab initio* theory is to solve the Schrödinger equation in order to calculate the

observables of a system of interest (i.e.; the properties of a chemical system). Approximations are needed because the Schrödinger equation cannot be solved exactly for systems larger than H_2. However, no empirical parameters are used in *ab initio* molecular orbital theory. The fundamental aspects of *ab initio* molecular orbital theory will be discussed by examining the assumptions that are applied to the Schrödinger equation to derive the time independent Schrödinger equation.

2.1 Solving the Time Independent Schrödinger Equation

The time-dependent Schrödinger equation describes the mathematical relationship upon which *ab initio* molecular orbital theory is based,

$$\hat{H}\Psi = i\hbar\frac{\partial}{\partial t}\Psi . \tag{1}$$

In this equation, the Hamiltonian operator ($\hat{H}$) is the sum of the kinetic energy operator of the nuclei ($\hat{T}_n$), the potential energy operator between nuclei ($\hat{V}_{nn}$), the kinetic energy operator of the electrons ($\hat{T}_e$), the potential energy operator between electrons ($\hat{V}_{ee}$) and the potential energy operator between nuclei and electrons ($\hat{V}_{ne}$) such that

$$\hat{H} = \hat{T}_n + \hat{V}_{nn} + \hat{T}_e + \hat{V}_{ee} + \hat{V}_{ne} . \tag{2}$$

If we assume that $\hat{H}$ does not explicitly depend on time, we can write the wavefunction as the product of a time dependent part (Ψ_t) and a space (nuclear and electronic positions) dependent part (Ψ_x). The equation is therefore separable and the time-dependent part is easily solved. The separation constant of the time-independent equation

$$\hat{H}\Psi = E\Psi \tag{3}$$

is the energy (E). Under the Born-Oppenheimer approximation we can assume that nuclear and electronic contributions can be separated because the nucleus is much more massive than the electrons. We essentially assume that the nuclei are fixed. The total energy of the system is

$$E_{total} = E_{electron} + E_{nuclei}\,. \tag{4}$$

Under the Born-Oppenheimer approximation the nuclear kinetic energy is zero. Therefore, the nuclear energy contribution is only due to nuclear potential energy

$$E_{nuclei} = \sum_{A<B} \frac{Z_A Z_B}{r_{AB}} \tag{5}$$

and results in a simpler electronic Hamiltonian ($\hat{H}_{elec}$) that can be expressed as

$$\hat{H}_{elec} = \sum_{i=1}^{N} \tfrac{1}{2}\nabla_i^2 + \sum \frac{1}{r_{ij}} + \sum_{i=1}^{N}\sum_{A=1}^{n} \frac{Z_A}{r_{iA}}\,. \tag{6}$$

Under the Born-Oppenheimer approximation, the Schrödinger equation is simplified to the electronic time-independent Schrödinger equation. In order to solve the electronic time-independent Schrödinger equation we need more information about the wavefunction.

If the independent orbital approximation* is applied then the total wavefunction of a poly-electron wavefunction can be written as the product of one electron wavefunctions

* The independent orbital approximation states that for a poly-electronic system the wavefuntion can be written as a product of one electron wavefunctions, known as a Hartree product.

(ϕ_i) called orbitals. Probability theory dictates that the position of one electron is independent of the position of another electron in the system. The total wavefunction of a system can then be written as

$$\Psi(1,2,...,N) = \phi_1(1)\phi_2(2)\phi_3(3)...\phi_N(N) = \prod_{i=1}^{N}\phi_i(i) \qquad (7)$$

which known as a Hartree product. Hartree products are allowed due to the Aufbau principle[†]. The independent orbital approximation introduces a problem because the position of electrons and their energy contribution *are* dependent on the other electrons in the system. The impact of this assumption will be discussed later when the role of electron correlation is examined.

Another assumption used is the Pauli exclusion principle[‡], which allows a molecular orbital to have two electrons of opposite spin (α and β). It is the Pauli exclusion principle that allows for the wavefunction of a poly-electronic system to be written as a Hartree product of spin orbitals (χ_i) such that

$$\Psi(1,2,...,2N) = \chi_1(1)\chi_2(2)...\chi_{2N}(2N) \text{ where } \chi_1(1) = \phi_1\alpha(1),\ \chi_2(2) = \phi_1\beta(2) \qquad (8)$$

and each spatial orbital is associated with an α-spin function and a β-spin function. However, a Hartree product of spin orbitals is not anti-symmetric. A wavefunction is

---

[†] Under the Aufbau principle electrons are placed in orbitals of the lowest possible energy while obeying the Pauli exclusion principle and Hund's rules.

[‡] Under the Pauli exclusion principle no two electrons may have the all the same four quantum numbers.

anti-symmetric when the interchange of any two electrons (i.e.; i, j) changes the sign of the wavefunction

$$\hat{P}_{ij}\Psi(1,2...i,j...N) = \Psi(1,2...j,i...N) = -\Psi(1,2...i,j...N)\,. \tag{9}$$

The Pauli exclusion principle satisfies the anti-symmetry requirement of electronic wavefunctions by expressing the total wavefunction as a linear combination of Hartree products. A wavefunction written as a linear combination of Hartree products can be made to satisfy the anti-symmetry requirement by being expressed as a Slater determinant[§].

To solve for the energy of the electronic time independent Schrödinger equation a Slater determinant of a known set of ortho-normal spin orbitals must be assumed to represent the total wavefunction of a poly-electronic system. This is accomplished by assuming that the electronic time-independent Schrödinger equation Hamiltonian operator ($\hat{H}_{elec}$) is separable. This allows the Hamiltonian to be separated into two Hamiltonians, the one-electron Hamiltonian ($\hat{H}_1$)

$$\hat{H}_1 = \sum_i -\frac{1}{2}\nabla_i^2 - \sum_i \sum_A \frac{Z_A}{r_{1A}}, \tag{10}$$

which contains only the terms that rely on one electron and the two-electron Hamiltonian ($\hat{H}_2$)

[§] The use of a Slater determinant to express a wavefunction written as a linear combination of Hartree products upon expansion generates all permutations of all 2N electrons among the 2N spin orbitals as well as satisfying the anti-symmetry requirement and the Pauli exclusion principle.

$$\hat{H}_2 = \sum_{i<j} \frac{1}{r_{ij}}, \tag{11}$$

which is comprised of terms that depend on two electrons.

Under the conditions and assumptions mentioned to this point, evaluation of the energy of a normalized poly-electronic system results in three distinct parts, the core Hamiltonian

$$H_{ii}^{core} = \int \chi_i(1) \left(-\frac{1}{2}\nabla^2 - \sum_A \frac{Z_A}{r_{iA}} \right) \chi_i(1) d\tau_1, \tag{12}$$

the Coulomb integral

$$J_{ij} = \int\int \chi_i^2(1) \frac{1}{r_{12}} \chi_j^2(2) d\tau_1 d\tau_2, \tag{13}$$

and the exchange integral

$$K_{ij} = \int\int \chi_i(1)\chi_j(2) \frac{1}{r_{12}} \chi_j(1)\chi_i(2) d\tau_1 d\tau_2 . \tag{14}$$

The core Hamiltonian can be interpreted as one electron moving in the field of the bare nucleus and is represented by a one-electron integral. The Coulomb integral is a classical mechanics effect and represents the repulsion between two charge distributions. The exchange integral is a quantum mechanics effect and arises from the anti-symmetry principle. The total energy is the sum of the electronic energy;

$$E_{elec} = 2\sum_{i=1}^{N} H_{ii} + \sum_{i=1}^{N}\sum_{j=1}^{N} (2J_{ij} - K_{ij}), \tag{15}$$

and the energy of the nuclear repulsion;

$$E_{nuclear} = \sum_{A<B} \frac{Z_A Z_B}{R_{AB}}. \quad (16)$$

The molecular orbitals must be known in order to calculate the electronic energy of the system. Hartree-Fock theory introduces a way to describe molecular orbitals to calculate the electronic energy of a system.

2.2 Hartree-Fock Theory

The derivation of Hartree-Fock theory from *ab initio* molecular orbital theory includes the Hartree-Fock equations and the Roothaan-Hall equations. It should be noted that Hartree-Fock theory builds upon *ab initio* molecular orbital theory and provides a solution for the spin orbitals, which allows the wavefunction to be solved.

2.2.1 Hartree-Fock Equations

The Hartree-Fock equations are a set of integral-differential equations. Application of the Lagrange method of undetermined multipliers to the constrained variation problem of finding the best orbitals gives stationary values of the electronic energy subject to the ortho-normality condition;

$$S_{ij} = \langle \psi_i | \psi_j \rangle = \delta_{ij}, \quad (17)$$

where the Kronecker δ (δ_{ij}) equals 1 if $i = j$ and 0 if $i \neq j$. Here we have introduced Dirac notation** for the overlap integral (S_{ij}). The ortho-normality condition gives rise to the Hartree-Fock equations which are expressed as

$$\hat{F}\chi_i = \varepsilon_i \chi_i, \; i = 1,2,3...,N. \tag{18}$$

The Hartree-Fock equations are comprised of an eigenvalue (ε_i) known as the orbital energy of the ith molecular orbital, eigenfunctions that correspond to the spin orbitals that need to be solved and the Hartree-Fock operator ($\hat{F}$), which is defined as the sum of the core Hamiltonian ($\hat{H}^{core}$), the Coulomb operator ($\hat{J}_j$) and the exchange operator ($\hat{K}_j$) and is expressed as

$$\hat{F} = H^{core} + \sum_{j=1}^{N}\left(2\hat{J}_j - \hat{K}_j\right), \tag{19}$$

The Coulomb operator ($\hat{J}_j(1)$) of the Hartree-Fock equations is the potential experienced by one electron at a specific distance (r_{12}) due to electron two in a spin orbital (χ_i) and is expressed as

$$\hat{J}_j(1) = \int \chi_j(2)\frac{1}{r_{12}}\chi_j(2)d\tau_2. \tag{20}$$

Unlike the Coulomb operator, the Exchange operator ($\hat{K}_{ij}$), which is expressed as

$$K_j\chi_i(1) = \left[\int \chi_j(2)\frac{1}{r_{12}}\chi_i(2)d\tau_2\right]\chi_j(1) \tag{21}$$

is not a simple function.

** Dirac or Bra-ket notation is a shorthand method introduced by P. A. M. Dirac.

The Hartree-Fock equations must be solved through an iterative process because the Hartree-Fock operator depends on the spin orbital used. The requirement of an iterative process makes Hartree-Fock theory a self-consistent field (SCF) method; once the orbitals no longer change noticeably they are said to be self consistent with the field or potential that is generated. While the Hartree-Fock equations are solved through an iterative process the direct solution to the equations is not practical for use in molecular calculations.

2.2.2 Roothaan-Hall Equations

The major obstacle preventing the Hartree-Fock equations from being solved for molecules is that mathematical form of the molecular orbitals is unknown. In order to solve this problem molecular orbitals of the Hartree-Fock equations are expanded as a linear combination of atomic orbitals (LCAO). The LCAO approach and the application of the ortho-normality condition to the orbitals in the Hartree-Fock equations gives rise to the Roothaan-Hall equations, which are expressed as

$$\sum_{\nu=1}^{M}\left(F_{\mu\nu}-\varepsilon_i S_{\mu\nu}\right)c_{\nu i}=0, \qquad \mu=1,2...M\,. \tag{22}$$

The Roothaan-Hall equations are comprised of a Fock matrix operator ($F_{\mu\nu}$);

$$F_{\mu\nu}=H_{\mu\nu}^{core}+\sum_{\lambda=1}^{K}\sum_{\sigma=1}^{K}P_{\lambda\sigma}\left[\left(\mu\nu|\lambda\sigma\right)-\frac{1}{2}\left(\mu\lambda|\nu\sigma\right)\right], \tag{23}$$

the number of atomic orbitals (M), the expectation value of the ith molecular orbital (ε_i), the overlap integral ($S_{\mu\nu}$) and the coefficient matrix ($C_{\nu i}$). The expression that makes up

the Fock matrix operator is comprised of the core Hamiltonian matrix ($H_{\mu\nu}^{core}$);

$$H_{\mu\nu}^{core} = \int \varphi_{\mu}(1)\left[-\frac{1}{2}\nabla^2 - \sum_{A=1}^{M}\frac{Z_A}{r_{iA}}\right]\varphi_{\nu(1)}d\tau_1, \tag{24}$$

the density matrix ($P_{\lambda\sigma}$);

$$P_{\lambda\sigma} = 2\sum_{i=1}^{occ} c_{\lambda i}c_{\sigma i} \tag{25}$$

and the two-electron repulsion integrals ($(\mu\nu|\lambda\sigma)$);

$$(\mu\nu|\lambda\sigma) = \iint \varphi_{\mu}(1)\varphi_{\nu}(1)\frac{1}{r_{12}}\varphi_{\lambda}(2)\varphi_{\sigma}(2)d\tau_1 d\tau_2. \tag{26}$$

While the Hartree-Fock equations and the Roothaan-Hall equations are linked through the LCAO approach and the ortho-normality condition, there are significant differences between the two sets of equations. One of the most important differences is that the Hartree-Fock equations can only be solved numerically, which is not practical for molecules. Additionally, the Hartree-Fock equations are integral-differential equations whereas the Roothaan-Hall equations are algebraic. This means that numerical values are used to find the coefficient values of the Roothaan-Hall equations as opposed to integration and differentiation as is seen in the Hartree-Fock equations, which makes the Roothaan-Hall equations easier to solve. An interesting point is that the two sets of equations are both solved iteratively.

The Roothaan-Hall equations are solved by first generating an initial guess for $F_{\mu\nu}$. For example, one can neglect the two-electron repulsion integrals and use $H_{\mu\nu}$ to approximate the initial guess for $F_{\mu\nu}$. Then the eigenvectors for the Hamiltonian matrix

are used to make a guess at the Fock matrix, which is then used to solve for the initial coefficient matrix that in turn generates the density matrix, and then the total energy (E_{total}) of the system, which can then be used to generate a new Fock matrix. This process continues until the coefficients converge. The criteria for convergence are generally the total energy and the density matrix. It should be noted that there are other ways to solve the Roothaan-Hall equations.

The relationship between the Hartree-Fock equations and the Roothaan-Hall equations is very important. However, it is the Roothaan-Hall Equations that are used in molecular calculations, as the Hartree-Fock equations are not practical for this purpose. It is important to keep in mind that while the Roothaan-Hall equations are used for molecular calculations there are some very fundamental assumptions that were made during the derivation of the Hartree-Fock equations that impact on that accuracy and usefulness of the Roothaan-Hall equation set.

3. Basis Functions and Basis Sets

While the LCAO is applied to derive the Roothaan-Hall equations to allow for molecular calculations, a problem arises because the mathematical form of atomic orbitals is not known. To provide a solution for this problem, the atomic orbitals are represented by basis functions. These can either be Slater Type Orbitals (STO) or Gaussian Type Orbitals (GTO). STOs are expressed as

$$S_{nlm}^{\xi}(r,\vartheta,\varphi) = Nr^{n-1}e^{-\xi r}Y_l^m(\vartheta,\varphi) \qquad (27)$$

where N is the normalization factor and Y_l^m is the spherical harmonics. GTOs are expressed as

$$G_{i.j.k}^{\alpha,r}(r) = N_{i,j,k}^{\alpha}(x-R_1)^i(y-R_2)^j(z-R_e)^k e^{-\alpha(r-R)^2} \quad (28)$$

where $N_{i,j,k}^{\alpha}$, R and α are the normalization factor, the center of the Gaussian function and the exponent of the Gaussian function, respectively.

It is interesting to note that STOs are very similar to the solution for hydrogen atoms and represent atomic orbitals most effectively. However, integral evaluation of STOs is very difficult due to their mathematical form and as a result calculations involving STOs are generally reserved for small molecules. On the other hand GTOs are much easier to evaluate due to the Gaussian Product Theorem. This theorem states that the product of two GTOs on two different centers equals a GTO on a third center (i.e.; $\varphi_A\varphi_B=\varphi_C$). However, GTOs do not accurately represent an atomic orbital but a linear combination of GTOs may be used to form a STO to outweigh the limitations of both types of basis functions.

The most demanding part of the solving the Roothaan-Hall equations are the sheer number of two-electron repulsion integrals which depend on the size of the basis set used. There are a number of basis sets that can be utilized in a molecular calculation. These basis sets include minimal basis sets, double zeta basis sets, doubly-split basis sets and the inclusion of diffuse or polarizable functions to suit the system of interest. The larger the

basis set is (i.e.; more basis functions that are included) the more variational parameters that are available, which provides a better description of the molecular orbitals. However, under Hartree-Fock theory the best that a very large basis set with infinite flexibility can do is known as the Hartree-Fock Limit. The consequence of the Hartree-Fock Limit will be discussed in the next section.

4. Electron Correlation

Hartree-Fock Theory assumes that electrons move in an average potential that is due to the nuclei and other electrons of the system. As a result, in Hartree-Fock theory the instantaneous position of an electron is not dependent on the position of the other electrons in the system. This theory is inherently wrong because the motion of the electrons is correlated (i.e.; the location of one electron depends on the location of the other electrons in the system).

The correlation energy is the difference between the Hartree-Fock energy of a system and the real energy of a system and the effect of not including the correlation energy in Hartree-Fock theory prevents calculations from predicting the real energy of the system of interest. Some methods, which will be discussed later, improve upon Hartree-Fock theory by including correlation energy to provide a more accurate prediction of the energy of a system.

Including electron correlation in molecular calculations is important for a number

of reasons. While Hartree-Fock calculations give reasonable geometries, the inclusion of electron correlation will lead to more quantitative results. Electron correlation is also important for modeling intermolecular interactions, improves properties, provides correct trends for transition metals and improves both absolute and relative energies. In the next section, methods that go beyond Hartree-Fock theory will be discussed.

5. Post-Hartree-Fock Methods

Hartree-Fock theory is an *ab initio* method that uses only the first principles of quantum mechanics. However, Hartree-Fock theory makes various assumptions about the Schrödinger equation and subsequently its sets of solutions. Specifically, the Born-Oppenheimer approximation is assumed, which does not hold for a true wavefunction as the wavefunction should be a function of the coordinates of each nuclei. Additionally, the momentum operator is assumed to be completely classical (i.e; relativistic effects are ignored). The basis set is made up of a finite set of functions, where as the true wavefunction is a linear combination of functions from a complete (infinite) basis set. Finally, the energy eigenfunctions are assumed to be the products of one-electron wavefunctions, which results in the effects of electron correlation being included only as an average.

For various systems (i.e.; excited states, transition states) inclusion of electron correlations is very important for the accurate description of the PES. Methods that are based on Hartree-Fock theory and include a way to approximate a more accurate electron

correlation are broadly termed post-Hartree-Fock methods. Generally, post-Hartree-Fock methods provide a more accurate result than Hartree-Fock; however, the accuracy is at additional computational expense. There are various post-Hartree-Fock methods, for example, configuration interaction, coupled cluster, and Møller-Plesset perturbation theory.

5.1 Møller-Plesset Perturbation Theory

Perturbation theory uses a factor that prevents the exact solution of the Hamiltonian Operator in the Schrödinger Equation. In Møller-Plesset Perturbation Theory (MP*n*) the Hamiltonian is represented as the sum of the perturbation ($\hat{H}'$) and the Hartree-Fock Hamiltonian (H^{HF}), such that

$$\hat{H} = \hat{H}^{HF} + \hat{H}'. \tag{29}$$

H^{HF} is treated as the zeroth-order Hamiltonian. Furthermore, under perturbation theory, the wavefunction (Ψ_i) and eigenfunction (E_i) are each treated as power series such that

$$\Psi_i = \Psi_i^{HF} + \lambda\Psi_i^{(1)} + \lambda^2\Psi_i^{(2)} + \lambda^3\Psi_i^{(3)} \ldots \tag{30}$$

and

$$E_i = E_i^{HF} + \lambda E_i^{(1)} + \lambda^2 E_i^{(2)} + \lambda^3 E_i^{(3)} \ldots\ldots \tag{31}$$

These power series are then substituted back into the Schrödinger equation. The resulting products are then expanded and the coefficients (λ^n) of equal powers are equated so that

$$\lambda^0 : \hat{H}^{HF}\Psi_i^{HF} = E_i^{HF}\Psi_i^{HF}$$
$$\lambda^1 : \hat{H}^{HF}\Psi_i^{(1)} + \hat{H}\Psi_i^{HF} = E_i^{HF}\Psi_i^{(1)} + E_i^{(1)}\Psi_i^{HF} \quad (32)$$
$$\lambda^2 : \hat{H}^{HF}\Psi_i^{(2)} + \hat{H}\Psi_i^{(1)} = E_i^{HF}\Psi_i^{(2)} + E_i^{(1)}\Psi_i^{(1)} + E_i^{(2)}\Psi_i^{HF}.$$

This results in a series of equations that are progressively higher orders of perturbation. Once the coefficients of the same powers have been equated and the power series for the wavefunction and eigenfunction are inserted in to the Schrödinger equation the energy expressions are generated such that

$$\begin{aligned} E_i^{HF} &= \left\langle \Psi_i^{HF} \middle| \hat{H}^{HF} \middle| \Psi_i^{HF} \right\rangle \\ E_i^{(1)} &= \left\langle \Psi_i^{HF} \middle| \hat{H}' \middle| \Psi_i^{HF} \right\rangle \\ E_i^{(2)} &= \left\langle \Psi_i^{HF} \middle| \hat{H}' \middle| \Psi_i^{(1)} \right\rangle \\ E_i^{(3)} &= \left\langle \Psi_i^{HF} \middle| \hat{H}' \middle| \Psi_i^{(2)} \right\rangle. \end{aligned} \quad (33)$$

However, in order to solve these expressions the wavefunctions must first be solved and then the energy expression for the desired perturbation, $E_i^{(n)}$, where n is the order of the perturbation (i.e.; 1, 2, 3 … n), can be solved.

It should be noted that the perturbation can be truncated at any point. Furthermore, depending upon where the perturbation expansion is truncated, different levels of perturbation theory will be generated. For instance, the MP2 level of theory indicates that the perturbation was truncated at the second-order energy correction ($E_i^{(2)}$). Likewise, MP3 and MP4 indicate that the perturbation was truncated at the third-order energy correction ($E_i^{(3)}$) and fourth-order energy correction ($E_i^{(4)}$); respectively. It should be noted that the MP1 perturbation is possible; however, the first-order energy

correction ($E_i^{(1)}$) simply gives back the Hartree-Fock energy. As such, MP2 is the first level of perturbation theory that improves upon the Hartree-Fock energy.

In addition to being the first level of Møller-Plesset perturbation theory that improves upon the Hartree-Fock energy, MP2 is a widely used method. Furthermore, MP3 offers little improvement on MP2 but is much more costly computationally. For improvement upon MP2 results MP4 is generally used. However, MP4 is more costly computationally and is as accurate as a configuration interaction single double (CISD) calculation. Finally MP4 is generally the limit for Møller-Plesset Perturbation Theory as MP5 offers little improvement on MP4 calculations and is an extremely costly method when compared to MP4.

5.2 Advantages and Disadvantages of Møller-Plesset Perturbation Theory

As with any theoretical method Møller-Plesset perturbation theory has various advantages and disadvantages. Specifically, MP2 has some favorable theoretical properties including easily-evaluated gradients. However, MP*n* methods are nonvariational[††] and occasionally MP*n* methods exhibits divergent behaviour.

[††] The energy calculated with a variational method is an upper bound to the exact energy.

6. Density Functional Theory

6.1 Hohenberg-Kohn Theorems

Density Functional Theory is based on two theorems by Hohenberg and Kohn. The first theorem states that for a ground-state molecule the energy and all other properties, including the external potential due to the nucleus ($v(\boldsymbol{r})$) and the total number of electrons (N), are determined by the ground-state electron probability density ($\rho(\boldsymbol{r})$). The total number of electrons and the external potential determine the Hamiltonian operator, which is expressed as

$$\hat{H} = -\sum_{i}^{N}\frac{1}{2}\nabla_i^2 - \sum_{A}^{n}\sum_{i}^{N}\frac{Z_A}{r_{iA}} - \sum_{i<j}^{N}\sum_{j}^{N}\frac{1}{r_{ij}} + \sum_{B<A}^{n}\sum_{A}^{n}\frac{Z_A Z_B}{R_{AB}}. \quad (34)$$

When the Hamiltonian, which is determined by the total number of electrons and the electron probability density, is used in the Schrödinger Equation it is implied that the electron probability density also determines the energy of the system. It should be noted that due to the dependence of the Hamiltonian operator on the electron probability density, the energy of the system can be represented as a functional[‡‡] of the electron probability density of the system where

$$E = E[\rho]. \quad (35)$$

The second theorem states that, for a trial density ($\rho'(\boldsymbol{r})$) satisfying $\rho'(\boldsymbol{r}) \geq 0$ and $\int \rho'(\boldsymbol{r})d\boldsymbol{r} = N$, then the true energy of the system ($E[\rho]$) is less than or equal to the energy of the trial system ($E[\rho']$). In essence this theorem states that DFT is a

[‡‡] A functional can be thought of as a function of a function.

variational method. The Hohenberg-Kohn Theorems provide the fundamental ideas that DFT is based on. However, the form of the energy functional is unknown.

6.2 The Kohn-Sham Method

The primary problem facing DFT is that the exact form of the energy functional is unknown. In order to solve this problem the Kohn-Sham Method is applied. The Kohn-Sham Method introduces orbitals, known as the Kohn-Sham orbitals, which are analogous to those used in Hartree-Fock Theory. However, the Kohn-Sham orbitals are not single electron orbitals. However, the sum of the square of the Kohn-Sham orbitals must give the electron density, which is expressed as

$$\rho(r) = \sum_{i=1}^{N} \left| \Psi_i^{KS} \right|^2 \tag{36}$$

The introduction of the Kohn-Sham orbitals (Ψ_i^{KS}) allows the energy functional to be expressed as a mathematical expression. The Kohn-Sham Method establishes a relationship between the electron density and the orbitals but does not give a physical significance to the orbitals.

6.3 The Energy Functional

Under the Hohenberg-Kohn Theorem it was established that the energy is a functional of the electron density. The Kohn-Sham orbitals were introduced under the Kohn-Sham Method. The mathematical form of the energy functional will be briefly

considered.

The energy functional under the Born-Oppenheimer Approximation can be expressed as the sum of the kinetic energy of the electrons ($T[\rho]$), the potential energy between the electrons ($V_{ee}[\rho]$) and the potential energy between the nuclei and the electrons ($V_{ne}[\rho]$) and is expressed as

$$E[\rho] = T[\rho] + V_{ee}[\rho] + V_{ne}[\rho]. \tag{37}$$

There also exists an alternative but equivalent form of the energy function. The alternative form is the sum of the potential energy between the nuclei and electrons ($V_{ne}[\rho]$) and the Hohenberg-Kohn Functional ($F_{HK}[\rho]$), which is expressed as

$$E[\rho] = V_{ne}[\rho] + F_{HK}[\rho]. \tag{38}$$

The Hohenberg-Kohn Functional

$$F_{HK}[\rho] = T_s[\rho] + J[\rho] + E_{xc}[\rho], \tag{39}$$

is the summation of the kinetic energy functional

$$T_s[\rho] = \sum_i^N \left\langle \Psi_i^{KS} \left| -\frac{1}{2}\nabla_i^2 \right| \Psi_i^{KS} \right\rangle, \tag{40}$$

the classical Coulombic interaction between the electrons

$$J[\rho] = \frac{1}{2}\iint \frac{\rho(r)\rho(r')}{|r-r'|} dr dr', \tag{41}$$

and the exchange correlation functional

$$E_{xc}[\rho] = T[\rho] - T_s[p] + V_{ee}[\rho] - J[\rho]. \tag{42}$$

The exchange correlation functional suggested by Kohn and Sham is the summation of

the difference between the true kinetic energy and the kinetic energy functional and the difference between the non-classical portion of the potential energy and the Coulombic interaction. The exchange correlation functional is a non-classical term and describes the repulsion between electrons. The various approximate models of the exchange correlation functional are what differentiate the various forms of DFT.

6.4 The Kohn-Sham Equations

The Kohn-Sham equations are introduced due to the application of the Kohn-Sham method to the Hohenberg-Kohn theories and the introduction of the Kohn-Sham orbitals. The first important step in developing the Kohn-Sham equations is the introduction of the Kohn-Sham orbitals, which have previously been described. A reference Hamiltonian operator

$$H_{ref} = -\sum_{i}^{N} \frac{1}{2} \nabla_i^2 + \sum_{i}^{N} v_i(r) = \sum_{i} h_{ref,i} \tag{43}$$

describes a reference system of N-electrons that were non-interacting. The electron density of the reference system has the same electron density as the interacting system.

The introduction of the one-electron Hamiltonian ($h_{ref,i}$) and the alternate form of energy functional provides the basis for the Kohn-Sham equations. As previously mentioned, the Hohenberg-Kohn Second Theorem states that the DFT is a variational method. The electron density is such that the energy of the system at a minimum and the electron density integrates to the total number of electrons in the system (i.e.;

$\int \rho(r)dr = N$). The mathematical interpretation of the Hohenberg-Kohn Second is an Euler equation that is expressed as

$$\delta(E - \mu\rho(r)) = 0 \tag{44}$$

where E is the energy, μ is the Lagrange multiplier and $\rho(r)$ is the electron density. Using the Hohenberg-Kohn Functional ($F_{HK}[\rho]$), the kinetic energy functional ($T_s[\rho]$) and the classic Coulombic interaction between electrons ($J[\rho]$) there is a Lagrange multiplier;

$$\mu = v_{eff}(r) + \frac{T_s}{\delta\rho}. \text{ where } v_{eff}(r) = v(r) + \frac{\delta J}{\delta\rho} + \frac{\delta E_{xc}}{\delta\rho} = v(r) + \int \frac{\rho(r)}{|r - r'|} dr' + v_{xc}(r), \tag{45}$$

that satisfies the Euler equation formed from the Hohenberg-Kohn Second Theorem.

The Lagrange multiplier introduces an effective potential ($v_{eff}(r)$) that in turn introduces the exchange correlation potential (v_{xc}). The latter is a functional derivative of the exchange-correlation functional (i.e.; $v_{xc} = \frac{\delta E_{xc}}{\delta\rho(r)}$) whose mathematical form is unknown thus preventing DFT from being an exact method. The introduction of the effective potential by the Lagrange method of multipliers generates a mathematical form for the potential of the system that can be used in the one-electron reference Hamiltonian ($h_{ref,i}$). This form of the one-electron reference Hamiltonian in combination with the Kohn-Sham orbitals yields a set of equations that are analogous to the Schrödinger time-independent equation and are known as the Kohn-Sham equations. The Kohn-Sham equations are expressed as

$$\hat{h}_i^{KS}\Psi_i^{KS} = \varepsilon_i^{KS}\Psi_i^{KS} \quad i = 1,2\ldots N \tag{46}$$

where $\hat{h}_i^{KS} = -\frac{1}{2}\nabla_i^2 + v_{eff}(r)$, ε_i^{KS} is the energy of the ith Kohn-Sham orbital, and the Kohn-Sham orbitals (Ψ_i^{KS}) satisfy $\rho(r) = \sum_i^N \left|\Psi_i^{KS}\right|^2$.

Due to the manner in which the Kohn-Sham equations were originally derived, they share certain similarities with the Hartree-Fock equations. Like the Hartree-Fock equations, the Kohn-Sham equations are one electron equations. The Kohn-Sham equations must also be solved iteratively. They both have a one-electron kinetic energy operator ($-\frac{1}{2}\nabla_i^2$), as well as terms that account for the potential energy between the electrons and the nuclei and the potential energy between the electrons. What differentiates these two sets of equations is that the Kohn-Sham equations contain the exchange-correlation potential (v_{xc})

7. Types of Density Functionals

It was mentioned previously that the form of the exchange-correlation functional distinguishes the various DFT methods. Due to the popularity of DFT methods, there are a variety of exchange-correlation functions that are available. Some of the more common and popular forms will be discussed in the current section. These include functionals which employ only the Local Spin Density Approximation (LSDA), those that employ the Generalized Gradient Approximation (GGA), and Hybrid Functionals.

7.1 The Local Spin Density Approximation

The Local Spin Density Approximation (LSDA) was first described by Vosko, Wilk and Nusair thus the method is sometimes abbreviated VWN. The basic approximation made in LSDA is that the electron density is uniform throughout the system and is expressed as

$$E_{xc}^{LSDA} = \int \rho(r)\varepsilon_{xc} dr, \tag{47}$$

where $\rho(r)$ is the electron density, ε_{xc} is the exchange-correlation and their product is integrated over r. The form of the LSDA functional is similar to the exchange-correlation energy functional for a uniform electron gas. In order to achieve this uniform system under LSDA, the electron density of a molecular system is divided into infinitesimal parts. Furthermore, under the LSDA it is proposed that the electron-correlation energy functional for a non-uniform system can be summed from the infinitesimal portions that comprise the system.

Under the LSDA method it is assumed that the results are more accurate than those given by Hartree-Fock because the electron correlation and the electron exchange are both incorporated into the mathematical form of the function. However, this is not the case. The accuracy of LSDA is on par with Hartree-Fock. The problem with LSDA is that it is only valid for a system whose density varies slowly, which is not the case for molecules. As a result, the accuracy of density functionals based on LSDA are generally poor and the qualitative results for trends are sometimes incorrect.

Due to the poor results and inaccurate trends given by LSDA density functionals there are few that are commonly used. However, the most commonly used LSDA density functional is comprised of Slater's exchange and Vosko-Wilk-Nusair's (VWN's) correlation. This density functional is abbreviated SVWN.

7.2 The Generalized Gradient Approximation

The main problem with LSDA is that the method does not account for the non-homogeneity of the electron density in a molecular system. One way to improve upon the LSDA is to apply the Generalized Gradient Approximation (GGA). The form for an exchange-correlation energy functional under GGA is expressed as

$$E_{xc}^{GGA}[\rho] = \int f(\rho(r), \nabla\rho(r))dr\,. \tag{48}$$

The GGA accounts for the non-homogenous nature of a molecular system by including spin density gradients ($\nabla\rho(r)$) in addition to the spin density ($\rho(r)$). Energy functionals that include spin density gradients along with the spin density are called gradient-corrected functionals.

The advantage of gradient-corrected functionals is that they include how the electron density changes within a system. In some instances functionals are fit to experimental data by introducing parameters into the exchange-correlation energy functional. In other functional forms the exchange interaction ($E_x[\rho]$) and the

correlation interaction ($E_c[\rho]$) are represented as two unique contributions to the exchange-correlation energy functional (i.e.; $E_{xc}[\rho]=E_x[\rho]+E_c[\rho]$). This method of splitting up the two contributions allows for a more accurate representation of each energy contribution, which is important as the exchange interaction is very different from the correlation interaction.

Due to the improvement of GGA density functionals over LSDA there are several density functionals that are based on GGA. Several GGA density functionals that were developed in the 1986 – 1992 period have since become standard DFT tools. These GGA density functionals include the Becke (B), Becke88 (B88), Becke Parr (BP) exchange functionals, and the Lee, Yang and Parr (LYP) and the Perdew and Wang (PW91) correlation functionals, which when combined form the BLYP or BPW91 density functionals. More recent GGA density functionals include the exchange functionals of Perdew, Burke, and Ernzerhof (PBE), Filatov and Thiel (FT97), or Hamprecht, Cohen, Tozer, and Handy (HCTH/93, HCTH/402), along with the correlation functional of Colle and Salvetti. Finally, in a series of studies, which analyzed the errors associated with GGA density functionals, it was found that the largest errors were caused by the exchange energies, which are compensated for by the correlation errors. The rationale for the extreme exchange energy error is due to the localized GGA exchange of the electrons.

7.3 Hybrids

As previously discussed, the Generalized Gradient Approximation faces a major problem in describing the exchange properly. A solution to this problem was introduced in 1993 by Becke and includes the Hartree-Fock exchange (E_x^{HF}) in the functional form of the exhange-correlation energy function and is expressed as

$$E_{xc} = a_o E_x^{HF} + a_x E_x + a_c E_c . \qquad (49)$$

Furthermore, Becke initially introduced a hybrid functional that included three parameters, later hybrid functionals include more parameters (i.e.; Becke's 1997 functional includes 10 parameters), with predetermined coefficients (a_0, a_x, a_c) to mix in the Hartree-Fock exchange. The coefficients are predetermined by experimental values including atomization energies, ionization potentials and proton affinities. It should be noted that the Hartree-Fock exchange is evaluated using the Kohn-Sham orbitals in this hybrid functional. The introduction of hybrid functionals has established an increased success with Density Functional Theory.

Due to the ability of hybrid density functionals to accurately describe a molecular system there are various hybrid functionals available (i.e.; BH&HLYP, B3LYP, B3P86, B3PW91, PBE1-PBE and X3LYP). However, the most popular hybrid density functional is B3LYP, which is formed from the combination of the VWN and Lee-Yang-Parr (LYP) correlation functional, the Hartree-Fock correlation functional and a mixed exchange functional comprised of three terms; the exact exchange, the Slater local exchange and the non-local gradient correction of Becke88.

7.4 The Advantages & Disadvantages of DFT

The advantages of Density Functional Theory are simple and attractive. The primary advantage of DFT is that even at its simplest level of theory, electron correlation is included. As previously noted in the Hartree-Fock discussion, electron correlation must be included to obtain accurate molecular properties (i.e., geometries, dipole moment, atomization energy etc.). Furthermore, it was previously noted that electron correlation is not included in Hartree-Fock Theory due to the assumptions made in deriving the theory. In addition to including electron correlation, DFT is also a computationally efficient method when compared with *ab initio* methods that require more memory and disk than DFT.

A major disadvantage of approximate DFT is that it is not a variational method even though the Hohenberg-Kohn Second Theorem states that DFT is a variational method. In addition, due to the manner in which the various electron density functionals were developed, there is no way to systematically improve results.

In addition to considering the advantages and disadvantages of Density Functional Theory, accuracy should also be considered. Briefly, the accuracy of DFT depends on the form of the electron density functional, the basis set being used and the property being examined. For the most part when a reasonable functional is used (i.e.; B3LYP, B3PW91) the results obtained are comparable with MP2. However, the behaviour of the system plays a major role in the performance of DFT (i.e.; B3LYP poorly describes S_N2 reaction pathways).

CHAPTER THREE: CONFIGURATIONS OF TI, MTI & DTI

1. Introduction

The reactive site of Dacarbazine (Figure 3.1) is the triazene moiety (99). Previous studies have examined the configurational possibilities of triazene and its mono-, di- and trimethyl derivatives (19). The 1,3-proton transfer of triazene and its monomethyl derivative, in addition to the methyl transfer of 1,3-dimethyltriazene and 3,3-dimethyltriazene were also examined in previous studies (19). Previous *ab initio* study of triazene and its methyl derivates helped to lay the foundation for future computational investigations of triazene containing anti-neoplastic agents.

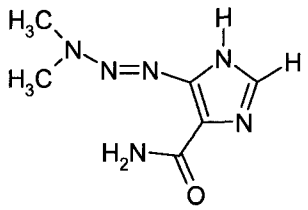

Figure 3.1: Chemical structure of Dacarbazine.

To further the understanding of the chemical and physical behaviour of triazene containing anti-neoplastic agents, the results of a configurational study of three simple structural analogues of Dacarbazine; 5-(1-triazenyl)imidazole (TI), 5-(3-methyl-1-triazenyl)imidazole (MTI) and 5-(3,3-dimethyl-1-triazenyl)imidazole (DTI) (Figure 3.2), are presented here. These models correspond to increasing methylation of the triazene

sp3 nitrogen.

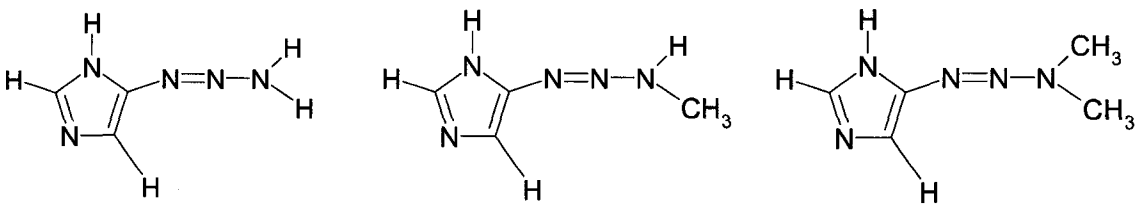

TI **MTI** **DTI**

Figure 3.2: The chemical structures of TI, MTI and DTI.

2. Computational Methods

All calculations for this computational study of 5-(1-triazenyl)imidazole were performed with Gaussian 98 (100). Geometries of the (E) and (Z) stereoisomers of 5-(1-triazenyl)imidazole were optimized in the same manner as a previous study of triazene and its methyl derivatives (19). Briefly, the approach involved the sequential optimizations at nine different levels of theory; HF/STO-3G, HF/3-21G, HF/6-31G(d), HF/6-31+G(d), MP2/6-31G(d), MP2/6-31+G(d), B3LYP/6-31G(d), B3LYP/6-31+G(d) and B3LYP/6-31G(d,p). This approach was undertaken in order to evaluate the ability of these levels of theory in predicting molecular properties (i.e., bond lengths, bond angles and dihedral angles). Harmonic vibrational frequencies and zero-point vibrational energy (ZPVE) corrections were calculated at the same levels of theory to properly characterize each structure. Zero-point vibrational energies were corrected by including an appropriate scaling factor (101).

3. Results and Discussion

This discussion is limited to the outstanding features, geometric and energetic, of each configuration identified. Important geometrical features, namely bond lengths, bond angles and dihedral angles of interest can be found in the supplemental data section (Tables S3). The absolute energies of all structures at all levels of theories employed during this study can be found in Appendix I.

For clarity, a systematic numbering system will be used throughout this discussion for all configurations of TI, MTI and DTI (Figure 3.3). The number assigned to each atom refers only to its connectivity and place in the molecule. Additionally, the individual configurations of TI, MTI and DTI will be distinguished according to the imidazole (Im) conformation with respect to the nitrogen-nitrogen double bond of the triazene moiety, s-trans (t) or s-cis (c). The configurations of MTI will also be distinguished with respect to the methyl (Me) conformation relative to the nitrogen-nitrogen double bond of the triazene moiety, s-trans (t) or s-cis (c).

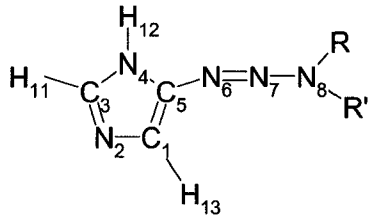

Figure 3.3: The systematic numbering of TI (R=H, R′=H), MTI (R=H, R′=CH_3) and DTI (R=CH_3, R′=CH_3).

3.1 5-(1-triazenyl)imidazole

5-(1-triazenyl)imidazole is a simple structural analogue of Dacarbazine. Two isomers of TI were identified, E and Z (Figure 3.4). The E isomer (Section 3.1.1) will be discussed first followed by an analysis of the Z isomer (Section 3.1.2).

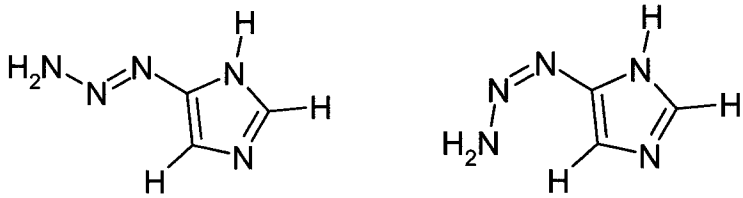

Figure 3.4: The (E)-5-(1-triazenyl)imidazole and (Z)-5-(1-triazenyl)imidazole isomers.

3.1.1 (E)-5-(1-triazenyl)imidazole: Two distinct configurations of (E)-TI were identified: (E)-TI Im s-trans and (E)-TI Im s-cis (Figure 3.5). (E)-TI Im (t) was found to be more energetically favorable than (E)-TI Im (c) (Table 1). The N_6-N_7 and N_7-N_8 bond length of (E)-TI (t) and (E)-TI (c) can be found in Table S3-1 of the supplemental data section. By examining the ‹($C_1N_2N_3N_4$) and ‹($C_3N_4C_5C_1$) dihedral angles, the imidazole rings of (E)-TI (t) and (E)-TI (c) were determined to be planar (to within 0.1 deg) at all levels of theory (Table S3-2). Furthermore, the triazene moieties of (E)-TI (t) and (E)-TI (c) were found to lie in the same plane as the imidazole ring (Table S3-3). However, for both (E)-TI (t) and (E)-TI (c), the terminal N_8 hydrogen atoms were out of plane with the rest of the molecule (Table S3-4).

3.1.2 (Z)-5-(1-triazenyl)imidazole: Two distinct configurations of (Z)-TI were characterized: (Z)-TI Im s-trans and (Z)-TI Im s-cis (Figure 3.6). (Z)-TI (c) was more

energetically favorable than (Z)-TI (t) but less energetically favorable than (E)-TI (t) and (E)-TI (c) (Table 1).

The N_6-N_7 and N_7-N_8 bond lengths of (Z)-TI configurations can be found in Table S3-5 of the supplemental data section. As was seen with the E configurations of TI, (Z)-TI (t) and (Z)-TI (c) demonstrate nearly planar imidazole rings. The deviation from planarity is larger than (E) configurations, especially for the s-trans conformer (Table S3-6). However, unlike (E)-TI (t) and (E)-TI (c), the triazene moieties of (Z)-TI (t) and (Z)-TI (c) are not in the same plane as the imidazole ring (Table S3-7). The steric repulsion between the amine group and the imidazole hydrogens ortho to the triazene substituent partially breaks the conjugation between the triazene double bond and the imidazole ring.

Table 1: Zero-point corrected relative energy comparison of the TI configurations with respect to (E)-TI Im s-trans.

Level of Theory	Relative Energy (kJ mol^{-1})		
	(E)-TI s-cis	(Z)-TI s-trans	(Z)-TI s-cis
HF/STO-3G	8.7	51.4	36.8
HF/3-21G	7.9	72.6	42.8
HF/6-31G(d)	7.6	57.3	42.3
HF/6-31+G(d)	7.4	57.3	42.4
MP2/6-31G(d)	8.1	43.0	25.7
MP2/6-31+G(d)	8.0	43.7	26.1
B3LYP/6-31G(d)	6.8	48.6	32.5
B3LYP/6-31+G(d)	6.7	48.9	32.7
B3LYP/6-31G(d,p)	6.8	48.6	32.5

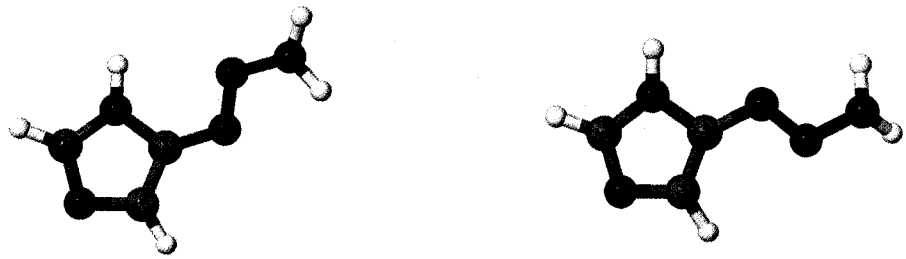

(E)-TI Im s-trans **(E)-TI Im s-cis**

Figure 3.5: The identified configurations of (E)-5-(1-triazenyl)imidazole.

(Z)-TI Im s-trans **(Z)-TI Im s-cis**

Figure 3.6: The two identified (Z) configurations of 5-(1-triazenyl)imidazole.

3.2 5-(3-methyl-1-triazenyl)imidazole

5-(3-methyl-1-triazenyl)imidazole (MTI) had (E) and (Z) isomers with respect to the nitrogen-nitrogen double bond of the triazene moiety.

3.2.1 (E)-5-(3-methyl-1-triazenyl)imidazole: Four (E) configurations of MTI were identified (Figure 3.7). (E)-MTI (t,c) was found to be the most energetically favorable configuration of (E)-MTI (Table 2). (E)-MTI (t,t), (E)-MTI (c,c) and (E)-MTI (c,t) were found to be less stable than (E)-MTI (t,c) (Table 2). The N_6-N_7 and N_7-N_8 bond lengths are reported in the supplemental data section (Table S3-8). The imidazole ring of

the (E)-MTI configurations was found to be planar in all cases (Table S3-9).

Upon further comparison it was found that the E configurations of MTI may be differentiated by the ‹($N_4C_5N_6N_7$) dihedral angle. Namely, (E)-MTI (t,c) and (E)-MTI (t,t) share a similar ‹($N_4C_5N_6N_7$) dihedral angle and (E)-MTI (c,c) and (E)-MTI (c,t) share a similar ‹($N_4C_5N_6N_7$) dihedral angle (Table S3-10). Furthermore, (E)-MTI (t,c) differs from (E)-MTI (t,t) and (E)-MTI (c,c) differs from (E)-MTI (c,t) by the ‹($CN_8N_7N_6$) dihedral angle formed (Table S3-11).

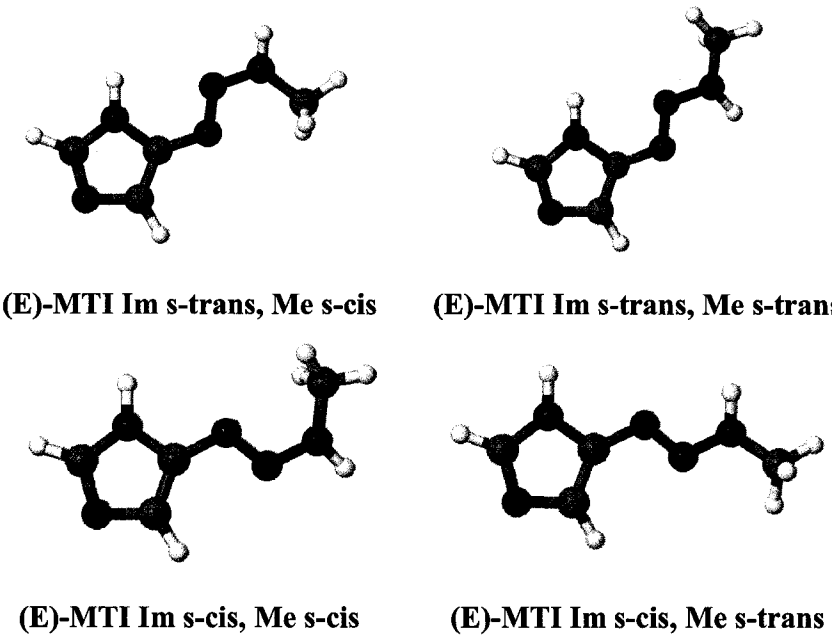

(E)-MTI Im s-trans, Me s-cis **(E)-MTI Im s-trans, Me s-trans**

(E)-MTI Im s-cis, Me s-cis **(E)-MTI Im s-cis, Me s-trans**

Figure 3.7: The four identified (E)-5-(3-methyl-1-triazenyl)imidazole configurations.

3.2.2 (Z)-5-(3-methyl-1-triazenyl)imidazole: Four (Z) configurations of MTI were identified: (Z)-MTI Im s-cis, Me s-trans; (Z)-MTI Im s-trans, Me s-cis; (Z)-MTI Im s-cis, Me s-cis and (Z)-MTI Im s-trans, Me s-trans (Figure 3.8). All (Z) configurations of MTI were less stable than (E) configurations (Table 2).

Table 2: Zero-point corrected relative energy comparison of the MTI configurations with respect to (E)-MTI Im s-trans, Me s-cis.

Level of Theory	Relative Energy (kJ mol^{-1})						
	(E)-MTI			(Z)-MTI			
	(t,t)	(c,c)	(c,t)	(c,t)	(t,c)	(c,c)	(t,t)
HF/STO-3G	3.3	1.1	-2.4	31.8	42.0	44.7	38.0
HF/3-21G	4.2	3.4	6.9	39.1	47.0	55.3	46.4
HF/6-31G(d)	0.2	5.6	5.5	38.6	63.8	67.7	52.7
HF/6-31+G(d)	0.2	6.1	6.7	43.1	69.0	72.5	57.3
MP2/6-31G(d)	3.5	7.1	10.4	27.0	52.1	56.1	43.6
MP2/6-31+G(d)	4.2	7.2	11.4	32.3	57.9	60.9	48.8
B3LYP/6-31G(d)	0.4	5.8	6.0	28.9	57.7	62.4	45.4
B3LYP/6-31+G(d)	1.5	5.9	7.3	34.9	65.2	67.4	52.4
B3LYP/6-31G(d,p)	0.8	5.8	6.4	29.0	58.3	62.5	46.0

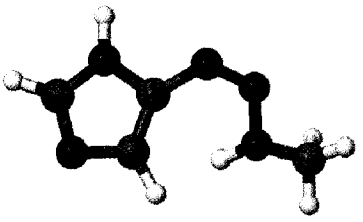

(Z)-MTI Im s-cis, Me s-trans

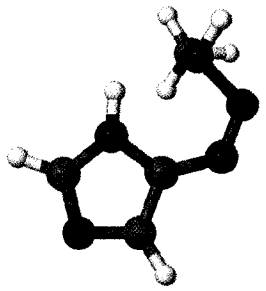

(Z)-MTI Im s-trans, Me s-cis

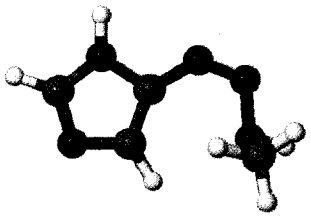

(Z)-MTI Im s-cis, Me s-cis

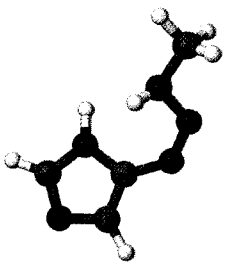

(Z)-MTI Im s-trans, Me s-trans

Figure 3.8: The (Z)-5-(3-methyl-1-triazenyl)imidazole configurations.

The N_6-N_7 and N_7-N_8 bond lengths of the (Z) configurations can be found in the supplemental data section (Table S3-12). The imidazole ring of each configuration was relatively planar at all levels of theory (Table S3-13). The most distinguishing features of the (Z) configurations of MTI are the ‹($N_4C_5N_6N_7$) dihedral angle and the ‹($CN_8N_7N_6$) dihedral angle. (Z)-MTI (c,t) and (Z)-MTI (c,c) share similar ‹($N_4C_5N_6N_7$) dihedral angles of 159.5 – 166.0 and 167.1 – 179.6°; respectively, whereas the ‹($N_4C_5N_6N_7$) dihedral angle of (Z)-MTI (t,c) and (Z)-MTI (t,t) was 8.0 – 16.4 and 23.2 – 34.7°, respectively (Table S3-14). The ‹($CN_8N_7N_6$) angle of (Z)-MTI (c,t), (Z)-MTI (t,c), (Z)-MTI (c,c) and (Z)-MTI (t,t) was 164.1 – 165.9, 79.6 – 96.6, 50.6 – 88.0 and 165.2 – 170.5°, respectively (Table S3-15).

3.3 5-(3,3-dimethyl-1-triazenyl)imidazole

DTI, the dimethyl derivative of TI, had two (E) configurations and two (Z) configurations (Figure 3.9).

3.3.1 (E)-5-(3,3-dimethyl-1-triazenyl)imidazole: (E)-DTI Im s-trans was found to be the most stable configurations of (E)-DTI (Table 3). The N_6-N_7 and N_7-N_8 bond lengths are reported in the supplemental data section (Table S3-16). By examining the ‹($C_1N_2C_3N_4$) and ‹($C_3N_4C_5C_1$) dihedral angles, the imidazole ring of the (E) configurations was found to be planar (Table S3-17). Examination of the ‹($N_4C_5N_6N_7$) dihedral angle revealed that the triazene moiety of each (E) configuration was in the same plane as the imidazole ring (Table S3-18).

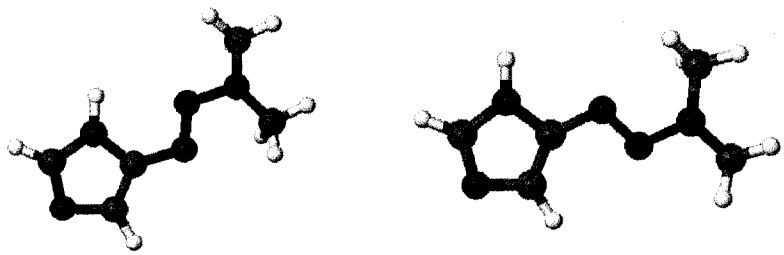

(E)-DTI Im s-trans **(E)-DTI Im s-cis**

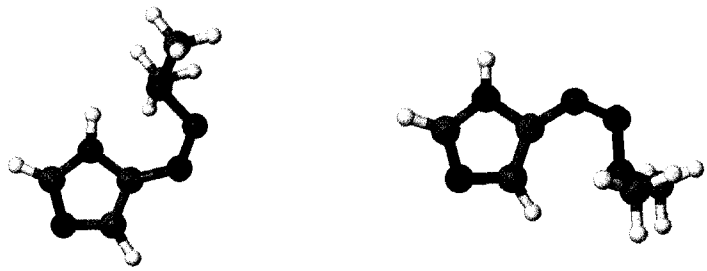

(Z)-DTI Im s-trans **(Z)-DTI Im s-cis**

Figure 3.9: The four identified DTI configurations.

Table 3: Zero-point corrected relative energy comparison of the DTI configurations with respect to (E)-DTI Im s-trans.

Level of Theory	Relative Energy (kJ mol^{-1})		
	(E)-DTI Im s-cis	(Z)-DTI Im s-trans	(Z)-DTI Im s-cis
HF/STO-3G	0.9	42.7	45.3
HF/3-21G	2.8	41.9	49.7
HF/6-31G(d)	5.3	62.5	66.3
HF/6-31+G(d)	6.0	66.6	70.1
MP2/6-31G(d)	6.9	51.3	56.7
MP2/6-31+G(d)	7.3	54.7	59.1
B3LYP/6-31G(d)	5.4	59.9	65.6
B3LYP/6-31+G(d)	5.7	65.3	68.8
B3LYP/6-31G(d,p)	5.5	59.7	65.7

3.3.2 (Z)-5-(3,3-dimethyl-1-triazenyl)imidazole: The (Z)-DTI configurations were significantly less stable than the (E) configurations (Table 3). The N_6-N_7 and N_7-N_8 bond lengths are reported in the supplemental data section (Table S3-16). Much like the (E)-DTI configurations, the imidazole ring of the (Z)-DTI configurations was planar (Table S3-17) and the triazene moiety was in the same plane as the imidazole ring (Table S3-18).

4. Conclusion

The study of TI identified four distinct configurations, (E)-TI (t), (E)-TI (c), (Z)-TI (t) and (Z)-TI (c). (E) configurations were more stable than (Z) configurations. (E)-TI (t) was the most energetically favorable configuration of TI, whereas (Z)-TI (t) was the least favorable configuration. Eight configurations of MTI were identified: four (E) and four (Z) configurations. (E)-MTI (t,c) was the most stable configuration. (Z)-MTI (c,c) was the least stable configuration of MTI. Four configurations of DTI were identified. (E)-DTI (t) and (Z)-DTI (c) were the most stable and the least stable configurations, respectively.

All configurations of TI, MTI and DTI demonstrated similar N_6-N_7 and N_7-N_8 bond lengths. In all cases, the imidazole ring was planar. The triazene moiety was in the same plane as the imidazole ring of the (E) configurations of TI, MTI and DTI. However, in (Z) configurations, especially for the TI and some MTI, the triazene moiety was found to be out of the plane with respect to the imidazole ring. It appears that methylation of

the (Z) configurations at N_8 forces the triazene moiety to lie in the same plane as the imidazole ring.

During this *ab initio* study of TI, MTI and DTI nine distinct levels of theory were utilized. This approach was intended to provide insight into which method is most appropriate for the determination of various properties of Dacarbazine. Methods that employ 6-31G(d), 6-31G(d,p) or 6-31+G(d) basis functions did a reasonable job of describing geometrical features such as bond lengths, bond angles and dihedral angles. The HF/STO-3G and HF/3-21G methods are less accurate at estimating the geometrical features and do not follow the same trends as the other methods. This result was expected with these methods. Furthermore, MP2 and B3LYP are in agreement with each other, which is expected. When consideration is given to computational time, B3LYP/6-31G(d) appears to be an adequate level of theory for the determination of geometrical properties of compounds such as TI, MTI and DTI. However, it may be appropriate to include polarization and or diffuse functions when dealing with charged or hydrogen bonded compounds.

CHAPTER FOUR: CONFIGURATIONS OF TIC, MTIC & DTIC

1. Introduction

In the previous chapter, configurational possibilities of 5-(1-triazenyl)imidazole (TI), 5-(3-methyl-1-triazenyl)imidazole (MTI), and 5-(3,3-dimethyl-1-triazenyl)imidazole (DTI) were investigated. As an extension of this study, and in an attempt to establish the effect of a carboxamide group at the 4-position of the imidazole ring, the results of a configurational study of 5-(1-triazenyl)imidazole-4-carboxamide (TIC), 5-(3-methyl-1-triazenyl)imidazole-4-carboxamide (MTIC) and 5-(3,3-dimethyl-1-triazenyl)imidazole-4-carboxamide (DTIC) (Figure 4.1) were examined.

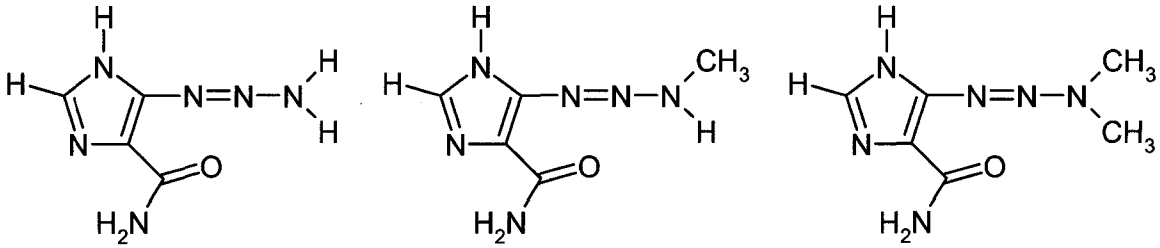

Figure 4.1: The chemical structures of TIC, MTIC and DTIC.

2. Computational Methods

All calculations were performed using the methods specified in Chapter 3; however, Gaussion 98 and Gaussian 03 (102) were used.

3. Results and Discussion

As an extension of previous studies concerning Dacarbazine structural analogues, configurational possibilities identified on the potential energy surfaces of TIC, MTIC and DTIC are discussed here. This discussion is limited to the outstanding geometric features and relative energy comparisons of each configuration identified.* A systematic numbering system employed during the discussion of TI, MTI and DTI (Chapter 3) will be used for the discussion of TIC, MTIC and DTIC (Figure 4.2).

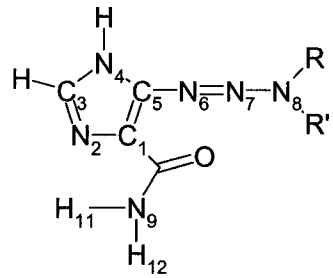

Figure 4.2: The systematic numbering system utilized during the discussion of TIC (R=H, R′=H), MTIC (R=H, R′=CH_3) and DTIC (R=CH_3, R′=CH_3).

The individual configurations of TIC, MTIC and DTIC will be distinguished by the imidazole (Im) C_1-C_5 conformation with respect to the N_6-N_7 bond of the triazene moiety and the carbonyl (C=O) conformation with respect to the C_1-C_5 bond of the imidazole ring. The conformations will be either s-trans (t) or s-cis (c). The MTIC

* All bond lengths and dihedral angles of interest are presented in the supplemental data section (Tables S4). The absolute energies of all structures at all levels of theories utilized during this study can be found in Appendix I.

configurations will be further distinguished by the methyl (Me) conformation relative to the N_6-N_7 double of the triazene moiety using the same labels.

3.1 5-(1-triazenyl)imidazole-4-carboxamide

Eight distinct configurations of 5-(1-triazenyl)imidazole-4-carboxamide (TIC) were identified: four (E)-TIC configurations and four (Z)-TIC configurations.

3.1.1 (E)-TIC: Of the four configurations of (E)-TIC (Figure 4.3) that were identified, (E)-TIC Im s-trans, C=O s-cis was the most stable (Table 1). The N_6-N_7 and N_7-N_8 bond lengths of the (E)-TIC configurations are reported in the supplemental data section (Table S4-1).

With the exception of MP2 levels of theory, the carboxamide group of the (E)-TIC configurations was relatively planar with respect to the imidazole ring. The ‹(OCC_1C_5) dihedral angle of (E)-TIC (t,c), (E)-TIC (t,t), (E)-TIC (c,c) and (E)-TIC (c,t) were 1.2 – 2.6, 176.7 – 179.6, 1.8 – 6.7 and 175.6 – 180.0°; respectively (Table S4-2). At MP2 levels of theory, the ‹(OCC_1C_5) dihedral angle of (E)-TIC (t,c), (E)-TIC (t,t), (E)-TIC (c,c) and (E)-TIC (c,t) were 7.1 – 12.7, 167.3 – 172.0, 11.1 -14.7 and 151.1 -160.2°, respectively (Table S4-2). The imidazole ring of (E)-TIC (t,c), (E)-TIC (t,t) and (E)-TIC (c,t) was relatively planar at all levels of theory. The ‹($C_1C_5N_6N_7$) dihedral angle of (E)-TIC (t,c), (E)-TIC (t,t) and (E)-TIC (c,t) was 171.6 – 176.0, 176.9 – 178.5 and (for most levels) 2.0 – 6.1°, respectively (Table S4-2). At HF/6-31+G(d) and MP2/6-31+G(d), the ‹($C_1C_5N_6N_7$) dihedral angle of (E)-TIC (c,t) was 38.0 and 17.0° (Table

S4-2), respectively. This is not in agreement with the other levels of theory. The imidazole ring of (E)-TIC (c,c) was out of plane at all levels of theory with a ‹($C_1C_5N_6N_7$) dihedral angle of 27.1 – 43.7° (Table S4-2).

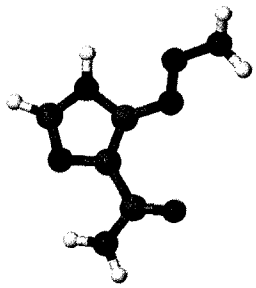

(E)-TIC Im s-trans, C=O s-cis

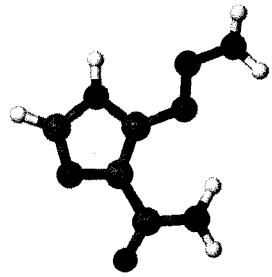

(E)-TIC Im s-trans, C=O s-trans

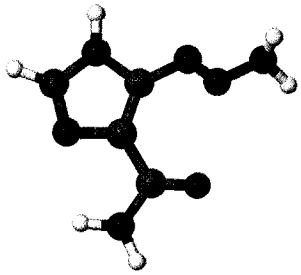

(E)-TIC Im s-cis, C=O s-cis

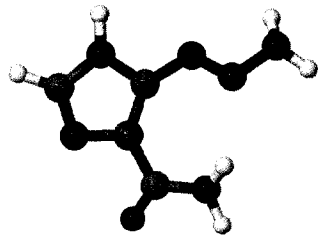

(E)-TIC Im s-cis, C=O s-trans

Figure 4.3: The four (E)-TIC configurations.

It appears that conjugation of the π-system through the triazene moiety and the imidazole ring may increase the stability of the (E)-TIC configurations. Additional stabilizing factors may come from weak hydrogen-bond type interactions between H_{11} and either N_2, N_6 or N_7. (E)-TIC Im (t,c) and (E)-TIC (c,c) form a $N_2\cdots H_{11}$ hydrogen-nitrogen interaction, whereas (E)-TIC (t,t) and (E)-TIC (c,t) form a $N_6\cdots H_{11}$ and a $N_7\cdots H_{11}$ hydrogen-nitrogen interaction, respectively (Table S4-3).

Table 1: Zero-point corrected relative energy comparison of (E)-TIC configurations with respect to (E)-TIC Im s-trans, C=O s-cis.

Level of Theory	Relative Energy (kJ mol^{-1})		
	(t,t)	(c,c)	(c,t)
HF/STO-3G	8.5	8.1	20.7
HF/3-21G	18.7	7.0	36.7
HF/6-31G(d)	17.8	6.4	38.7
HF/6-31+G(d)	17.2	9.9	38.8
MP2/6-31G(d)	12.1	15.0	28.0
MP2/6-31+G(d)	13.0	11.8	28.4
B3LYP/6-31G(d)	11.5	12.8	25.7
B3LYP/6-31+G(d)	12.0	9.4	27.4
B3LYP/6-31G(d,p)	11.2	12.1	25.6

3.1.2 (Z)-TIC: The four (Z)-TIC configurations (Figure 4.4) were all significantly less stable than the (E)-TIC configurations. (Z)-TIC Im s-cis, C=O s-cis was the most stable (Z)-TIC configuration (Table 2).

The N_6-N_7 and N_7-N_8 bond lengths of (Z)-TIC configurations are reported in the supplemental data section (Table S4-4). Furthermore, by examining the ‹(OCC_1C_5) dihedral angle of the (Z)-TIC configurations, the carboxamide group is in the same plane as the imidazole ring (± 10°), with the exception of (Z)-TIC (c,t) (Table S4-5). The carboxamide group of (Z)-TIC (c,t) was significantly out of plane with respect to the imidazole ring with a ‹(OCC_1C_5) dihedral angle of 62.7 – 163.5° (Table S4-5). The out of plane distortion of the carboxamide group is possibly due to steric interaction between the carboxamide group and the triazene moiety. Examination of the ‹($C_1C_5N_6N_7$) dihedral

angle revealed that the imidazole ring of all four (Z)-TIC configurations were significantly out of plane with respect to the triazene moiety (Table S4-5). It is reasonable to conclude that steric interactions between the imidazole ring and the amine of the triazene are responsible for this observation. The ‹($C_1C_5N_6N_7$) dihedral angle of (Z)-TIC (t,t), (Z)-TIC (t,c), (Z)-TIC (c,c) and (Z)-TIC (c,t) were 146.7 – 164.4, 146.7 – 151.3, 37.7 – 57.9 and 54.1 -120.5°, respectively (Table S4-5). The distortion of the ‹(OCC_1C_5) and ‹($C_1C_5N_6N_7$) dihedral angles would indicate that the π-system of the (Z)-TIC configurations is not conjugated through the triazene moiety and for (Z)-TIC (c,t) the carboxamide group.

Table 2: Zero-point corrected relative energy comparison of (Z)-TIC configurations with respect to (E)-TIC Im s-trans, C=O s-cis.

Level of Theory	Relative Energy (kJ mol^{-1})			
	(t,t)	(t,c)	(c,c)	(c,t)
HF/STO-3G	48.7	41.6	14.8	57.9
HF/3-21G	65.8	55.5	7.0	75.1
HF/6-31G(d)	68.3	75.8	26.4	69.3
HF/6-31+G(d)	71.2	78.5	30.9	84.0
MP2/6-31G(d)	47.3	41.5	9.9	50.3
MP2/6-31+G(d)	52.7	45.1	15.6	62.4
B3LYP/6-31G(d)	52.1	47.8	7.0	59.3
B3LYP/6-31+G(d)	58.3	53.4	15.2	72.7
B3LYP/6-31G(d,p)	52.6	48.2	6.1	59.1

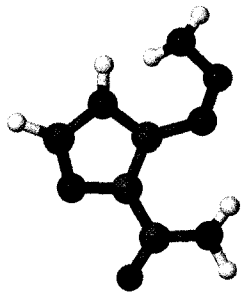

(Z)-TIC Im s-trans, C=O s-trans

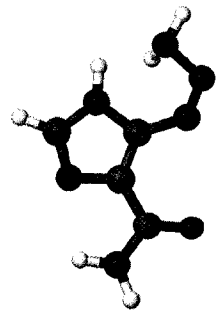

(Z)-TIC Im s-trans, C=O s-cis

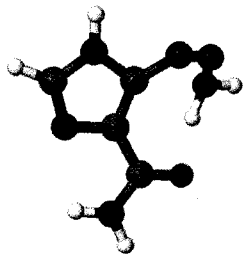

(Z)-TIC Im s-cis, C=O s-cis

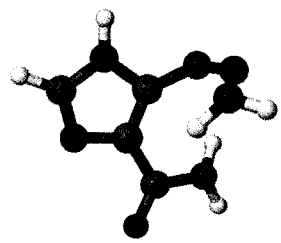

(Z)-TIC Im s-cis, C=O s-trans

Figure 4.4: The four configurations of (Z)-TIC.

The (Z)-TIC configurations demonstrate similar hydrogen-nitrogen interactions (Table S4-6) as were found in the (E)-TIC configurations. Of particular interest is the N_8-H···O hydrogen-bond of (Z)-TIC (c,c) (Table 8). The formation of this hydrogen-bond may be responsible for the increased stability of (Z)-TIC (c,c) in comparison to the other (Z)-TIC configurations (~ 30 – 50 kJ mol^{-1}) (Table 2).

3.2 5-(3-methyl-1-triazenyl)imidazole-4-carboxamide

5-(3-methyl-1-triazenyl)imidazole-4-carboxamide (MTIC), the monomethyl form of TIC, was found to have eight (E) configurations and eight (Z) configurations.

3.2.1 (E)-MTIC: (E)-MTIC Im s-trans, Me s-cis, C=O s-cis was the most stable configuration of MTIC (Figure 4.5) (Table 3). The methyl s-trans conformation is nearly always less stable than the methyl s-cis conformation.

Table 3: Zero-point relative energy comparison of (E)-MTIC configurations with respect to (E)-MTIC Im s-trans, Me s-cis, C=O s-cis

Level of Theory	Relative Energy (kJ mol^{-1})						
	(t,t,c)	(t,c,t)	(t,t,t)	(c,c,c)	(c,t,c)	(c,c,t)	(c,t,t)
HF/STO-3G	-2.9	8.5	5.3	4.5	7.6	23.2	26.5
HF/3-21G	5.8	19.3	23.4	9.9	8.0	42.2	38.0
HF/6-31G(d)	1.8	18.0	19.0	7.2	6.9	40.2	39.8
HF/6-31+G(d)	2.8	17.3	19.3	6.7	5.8	41.2	40.0
MP2/6-31G(d)	5.7	12.4	17.2	15.9	12.0	33.0	29.6
MP2/6-31+G(d)	7.3	13.1	19.5	14.3	9.0	34.8	30.3
B3LYP/6-31G(d)	2.2	12.6	13.4	11.4	11.5	28.5	27.5
B3LYP/6-31+G(d)	4.3	13.0	16.0	12.3	11.3	32.0	30.2
B3LYP/6-31G(d,p)	2.6	12.4	13.7	11.9	11.8	28.9	27.4

The N_6-N_7 and N_7-N_8 bond lengths of the (E)-MTIC configurations are reported in the supplemental data section (Tables S4-7 and S4-8). With the exception of the MP2 levels of theory, the four most stable (E)-MTIC configurations were (E)-MTIC (t,c,c), (E)-MTIC (t,t,c), (E)-MTIC (t,c,t) and (E)-MTIC (t,t,t). These configurations had relatively planar ‹(OCC_1C_5) (Table S4-9) and ‹($C_1C_5N_6N_7$) (Table S4-10) dihedral angles.

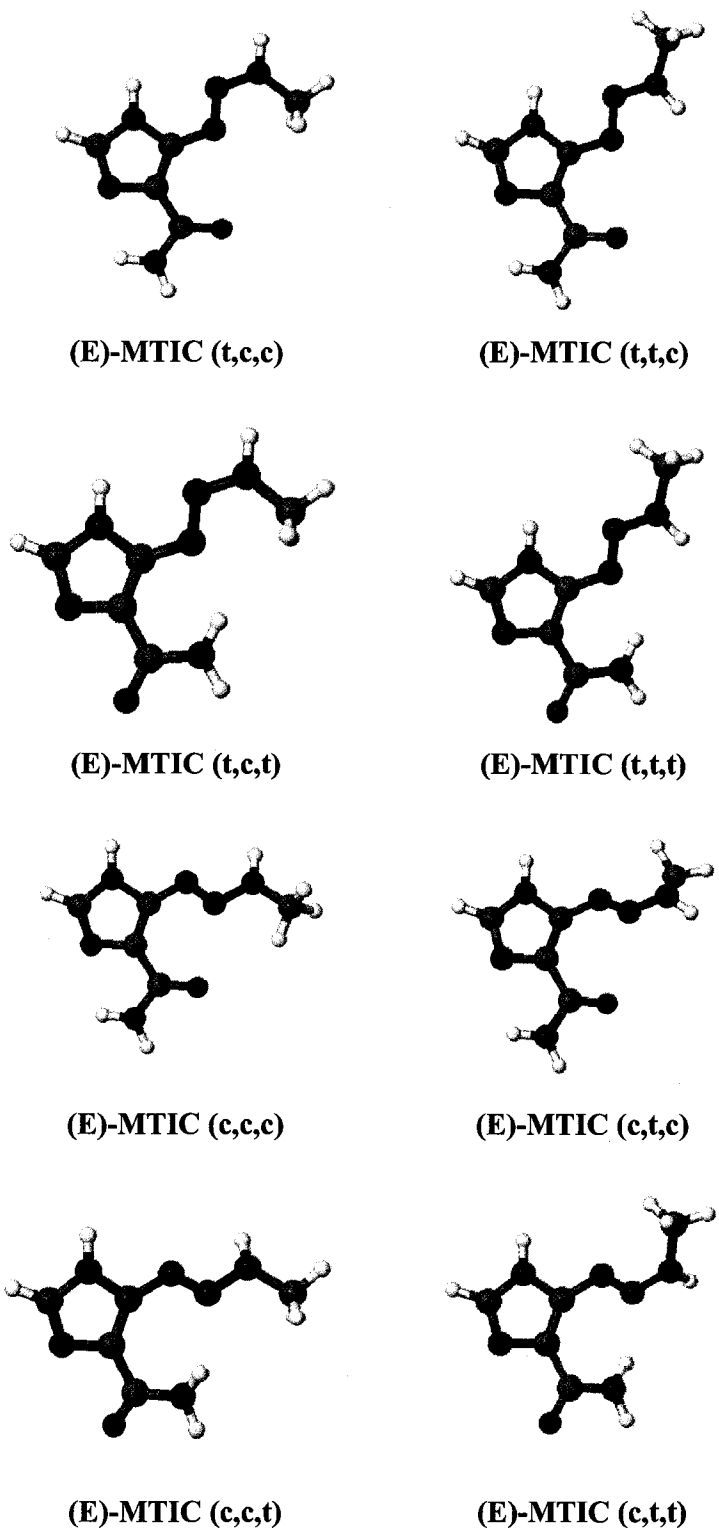

Figure 4.5: The identified configurations of (E)-MTIC.

The four less stable (E)-MTIC configurations were (E)-MTIC (c,c,c), (E)-MTIC (c,t,c), (E)-MTIC (c,c,t) and (E)-MTIC (c,t,t). These configurations had a triazene group that was out of plane with respect to the imidazole ring (Table S4-10). At the B3LYP levels of theory, (E)-MTIC (c,c,c), (E)-MTIC (c,t,c), (E)-MTIC (c,c,t) and (E)-MTIC (c,t,t) had a triazene moiety that was in the same plane as the imidazole ring with a ‹($C_1C_5N_6N_7$) dihedral angle of 0.4 – 1.7 and 0.6 – 2.1°, respectively (Table S4-10). (E)-MTIC (c,c,c) and (E)-MTIC (c,t,c) had a relatively planar carboxamide group with respect to the imidazole ring at HF and B3LYP levels of theory (Tables S4-9). However, at MP2 levels of theory, the ‹(OCC_1C_5) dihedral angle of (E)-MTIC (c,c,c) and (E)-MTIC (c,t,c) was 9.3 – 12.3 and 9.6 – 12.3°, respectively (Table S4-9). At B3LYP levels of theory, (E)-MTIC (c,c,t) and (E)-MTIC (c,t,t) had a relatively planar carboxamide group with respect to the imidazole ring. However, at HF and MP2 levels of theory, the ‹(OCC_1C_5) dihedral angle of (E)-MTIC (c,c,t) and (E)-MTIC (c,t,t) was 152.5 – 156.8° and 146.8 – 158.6°, respectively (Table S4-9).

As with the configurations of TIC, a hydrogen bonding interaction is present in each (E)-MTIC configuration (Table S4-11). Of specific interest are (E)-MTIC (c,c,c) and (E)-MTIC (c,t,c), which both demonstrate a $H_{11}\cdots N_2$ interaction. Both (E)-MTIC (c,c,c) and (E)-MTIC (c,t,c) are characterized by a ‹($C_1C_5N_6N_7$) dihedral angle (Table S4-10). This indicates that the imidazole ring is significantly out of plane with respect to the triazene moiety. However, (E)-MTIC (c,c,c) and (E)-MTIC (c,t,c) are comparable in energy to (E)-MTIC (t,c,t) and (E)-MTIC (t,t,t) (Table 3), which demonstrates a planar triazene moiety and carboxamide group with respect to the imidazole ring.

3.2.2 (Z)-MTIC: The (Z)-MTIC configurations (Figure 4.6) were significantly less stable than the (E)-MTIC configurations, with the exception of (Z)-MTIC Im s-cis, Me s-trans, C=O s-cis (Table 4).

The N_6-N_7 and N_7-N_8 bond lengths of the (Z)-MTIC configurations are reported in the supplemental data section (Tables S4-12 and S4-13). The carboxamide group of (Z)-MTIC (t,t,c), (Z)-MTIC (t,c,c), (Z)-MTIC (t,t,t), (Z)-MTIC (t,c,t), (Z)-MTIC (c,t,c), (Z)-MTIC (c,c,c) and (Z)-MTIC (c,c,t) was slightly out of plane with respect to the imidazole as indicated (Table S4-14). The carboxamide group of (Z)-MTIC (c,t,t) was significantly out of plane with respect to the imidazole ring. The ‹(OCC_1C_5) dihedral angle was 146.4 – 167.6° (Table S4-14).

The ‹($C_1C_5N_6N_7$) dihedral angle of (Z)-MTIC (t,t,c), (Z)-MTIC (t,c,c) and (Z)-MTIC (t,c,t) indicates that the triazene moiety was slightly out of plane with respect to the imidazole ring (Table S4-15). The triazene moiety of (Z)-MTIC (t,t,t), (Z)-MTIC (c,t,c), (Z)-MTIC (c,t,t), (Z)-MTIC (c,c,c) and (Z)-MTIC (c,c,t) was out of plane with respect to with the imidazole (Table S4-15). A lack of planar carboxamide and triazene groups with respect to the imidazole ring would indicate a lack of conjugation of the π-system.

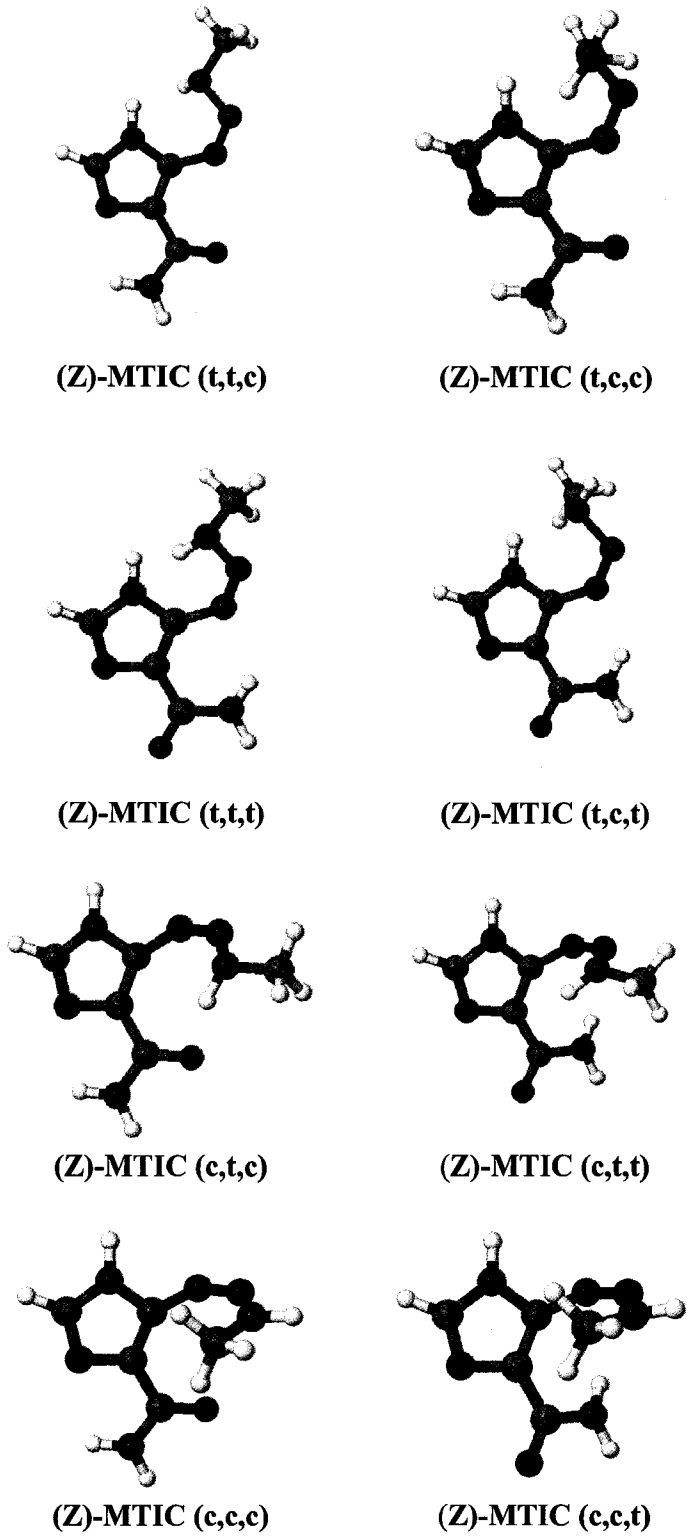

Figure 4.6: The identified configurations of (Z)-MTIC.

Table 4: Zero-point relative energy comparison of (Z)-MTIC configurations with respect to (E)-MTIC Im s-trans, Me s-cis, C=O s-cis.

Level of Theory	Relative Energy (kJ mol^{-1})							
	(t,t,c)	(t,c,c)	(t,t,t)	(t,c,t)	(c,t,c)	(c,t,t)	(c,c,c)	(c,c,t)
HF/STO-3G	47.1	47.3	48.4	51.7	12.8	55.3	-	-
HF/3-21G	61.0	62.6	70.7	72.4	10.4	77.8	-	-
HF/6-31G(d)	76.1	79.5	71.0	87.3	29.1	69.6	75.8	103.6
HF/6-31+G(d)	83.6	83.6	72.6	91.8	33.6	72.6	78.3	105.8
MP2/6-31G(d)	61.6	61.6	54.8	64.9	14.4	53.8	55.1	77.7
MP2/6-31+G(d)	62.3	62.3	60.0	71.1	19.9	55.0	53.8	74.9
B3LYP/6-31G(d)	71.7	71.7	58.1	73.9	9.9	60.3	60.2	88.3
B3LYP/6-31+G(d)	79.5	79.5	65.5	82.0	19.5	65.9	63.9	92.4
B3LYP/6-31G(d,p)	72.3	72.3	58.8	74.6	9.2	60.7	60.1	88.8

As with the (E)-MTIC configurations, some of the (Z)-MTIC configurations demonstrate a hydrogen bonding interaction (Table S4-16). Of particular interest is (Z)-MTIC (c,t,c), which is significantly more stable than the other (Z)-MTIC configurations and comparable in stability to the (E)-MTIC configurations. As previously noted, the carboxamide group and triazene moiety are out of plane with respect to the carboxamide group in (Z)-MTIC (c,t,c). This would decrease the stability of the configuration due to a lack of conjugation of the π-system through the triazene moiety, imidazole ring and carboxamide group. However, (Z)-MTIC (c,t,c) demonstrates a N_8-H···O hydrogen-bond interaction (Table S4-16) that may be responsible for its increased stability.

3.3 5-(3,3-dimethyl-1-triazenyl)imidazole-4-carboxamide

5-(3,3-dimethyl-1-triazenyl)imidazole-4-carboxamide (DTIC) had four (E) configurations and four (Z) configurations.

3.3.1 (E)-DTIC: (E)-DTIC Im s-trans, C=O s-cis was the most stable (Table 5) of the four (E)-DTIC configurations that were identified (Figure 4.7). The N_6-N_7 and N_7-N_8 bond lengths of the (E)-DTIC configurations are reported in the supplemental data section (Table S4-17).

Table 5: Zero-point relative energy comparison of DTIC configurations with respect to (E)-DTIC Im s-trans, C=O s-cis

Level of Theory	Relative Energy (kJ mol^{-1})						
	(E)-DTIC				(Z)-DTIC		
	(t,t)	(c,c)	(c,t)	(t,c)	(t,t)	(c,c)	(c,t)
HF/STO-3G	8.5	7.5	21.1	48.3	52.2	55.6	68.1
HF/3-21G	18.8	5.2	38.4	58.0	67.5	71.6	
HF/6-31G(d)	18.1	6.1	40.3	79.5	86.4	86.3	106.7
HF/6-31+G(d)	17.3	4.6	40.4	83.1	89.8	88.2	108.1
MP2/6-31G(d)	12.4	11.2	29.2	62.2	64.8	51.7	86.5
MP2/6-31+G(d)	12.8	7.7	29.8	68.6	68.5	49.3	
B3LYP/6-31G(d)	14.0	21.0	28.9	82.0	77.2	60.1	92.0
B3LYP/6-31+G(d)	13.4	9.7	31.1	81.5	83.2	62.9	95.0
B3LYP/6-31G(d,p)	12.6	10.4	28.7	74.6	77.0	59.7	92.2

(E)-DTIC (t,c) and (E)-DTIC (t,t) are characterized by a triazene moiety that lies in the same plane as the imidazole ring. The ‹($C_1C_5N_6N_7$) dihedral angle of (E)-DTIC

(t,c) and (E)-DTIC (t,t) were 177.6 - 179.3 and 175.2 – 178.9°, respectively (Table S4-18). The triazene moiety of (E)-DTIC (c,c) and (E)-DTIC (c,t) was out of plane with respect to the imidazole ring. (E)-DTIC (c,c) and (E)-DTIC (c,t) had a ‹($C_1C_5N_6N_7$) dihedral angle of 31.5 – 47.7 and 19.5 – 29.6°, respectively (Table S4-18). At B3LYP levels of theory, the ‹($C_1C_5N_6N_7$) dihedral angle of (E)-DTIC (c,t) was 1.9 – 3.8° (Table S4-18).

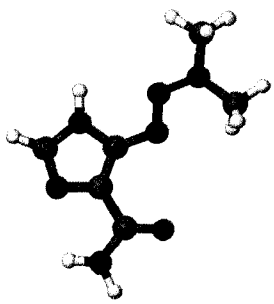

(E)-DTIC Im s-trans, C=O s-cis

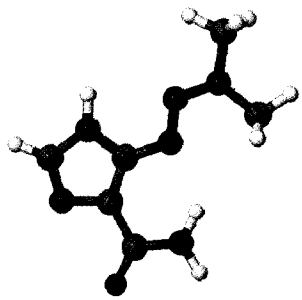

(E)-DTIC Im s-trans, C=O s-trans

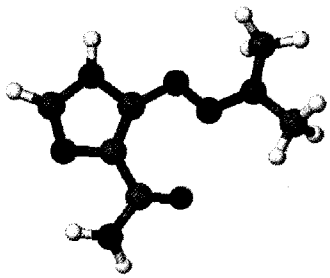

(E)-DTIC Im s-cis, C=O s-cis

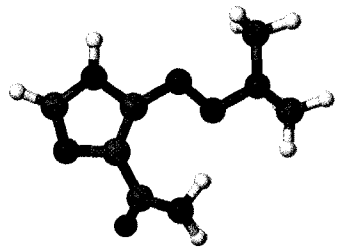

(E)-DTIC Im s-cis, C=O s-trans

Figure 4.7: The four identified (E)-DTIC configurations.

(E)-DTIC (t,c), (E)-DTIC (t,t) and (E)-DTIC (c,c) had a ‹(OCC_1C_5) dihedral angle of 0.2 – 1.4, 175.7 –179.4 and 4.0 – 5.8°; respectively, at B3LYP and HF levels of theory. At MP2 levels of theory, the ‹(OCC_1C_5) dihedral angle of (E)-DTIC (t,c), (E)-DTIC (t,t), and (E)-DTIC (c,c) was 5.1 – 9.6, 166.5 – 169.9 and 9.4 – 11.7°, respectively (Table S4-18). The ‹(OCC_1C_5) dihedral angle of (E)-DTIC (c,t) was 171.9 – 176.0° at B3LYP

levels of theory and 147.6 – 155.3° at MP2 and HF levels of theory (Table S4-18). This trend would indicate that at B3LYP levels of theory, the carboxamide group lies in the plane of the imidazole ring and at HF and MP2 levels of theory, the carboxamide group lies out of the plane.

3.3.2 (Z)-DTIC: The (Z)-DTIC configurations (Figure 4.8) were significantly less stable than the (E)-DTIC configurations (Table 5). The N_6-N_7 and N_7-N_8 bond lengths of the (Z)-DTIC configurations are reported in the supplemental data section (Table S4-19).

The carboxamide group of (Z)-DTIC (t,t) and (Z)-DTIC (c,c) was in the same plane as the imidazole ring with a ‹(OCC_1C_5) dihedral angle of 175.7 – 179.4 and 0.6 – 7.5°, respectively (Table S4-20). The carboxamide group of (Z)-DTIC (t,c) was out of plane with respect to the imidazole ring with a ‹(OCC_1C_5) dihedral angle of 0.0 – 17.2° (Table S4-20). The triazene moiety of (Z)-DTIC (t,c) and (Z)-DTIC (t,t) was relatively planar with respect to the imidazole ring with a ‹($C_1C_5N_6N_7$) dihedral angle of 164.1 – 180.0 and 172.8 – 177.2°, respectively (Table S4-20). The triazene moiety of (Z)-DTIC (c,c) was out of plane with a ‹($C_1C_5N_6N_7$) dihedral angle of 48.2 – 64.9° (Table S4-20). Both the carboxamide group and the triazene moiety of (Z)-DTIC (c,t) were out of the plane with respect to the imidazole ring with ‹(OCC_1C_5) and ‹($C_1C_5N_6N_7$) dihedral angles of 92.5 – 164.8 and 15.3 – 65.0°, respectively (Table S4-20).

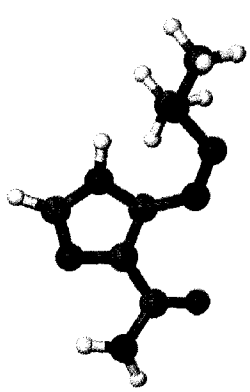

(Z)-DTIC Im s-trans, C=O s-cis

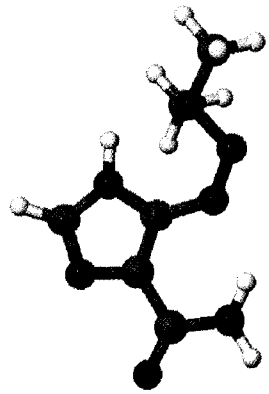

(Z)-DTIC Im s-trans, C=O s-trans

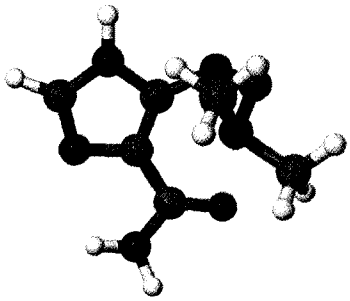

(Z)-DTIC Im s-cis, C=O s-cis

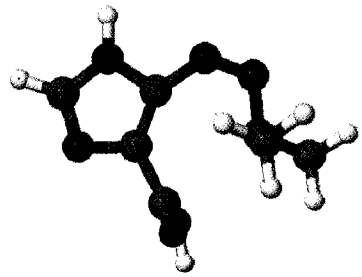

(Z)-DTIC Im s-cis, C=O s-trans

Figure 4.8: The four identified (Z)-MTIC configurations.

4. Conclusion

During the course of this study, eight configurations of TIC, 16 configurations of MTIC and eight configurations of DTIC were identified. In all cases, the configuration that was most stable was an (E) configuration where the N_6-N_7 bond of the triazene moiety was s-trans to the C_1-C_5 bond of the imidazole ring and the carbonyl of the carboxamide group was s-cis to the C_1-C_5 double bond of the imidazole ring. Furthermore, the most stable configurations demonstrate planar or relatively planar triazene moiety, imidazole rings and carboxamide groups with respect to each other.

It is believed that the primary stabilizing influence is the conjugation of the π-system through the triazene moiety, the imidazole ring and the carboxamide group. It appears that hydrogen-bond interactions may provide a stabilizing influence in some cases. The role of hydrogen bond stabilization is most evident in (Z)-TIC (c,c) and (Z)-MTIC (c,t,c), which both demonstrate a N_8-H···O interaction and increased stabilization despite the fact that neither configuration has a conjugated π-system. Steric interactions, between the imidazole ring and the amine of the triazene and the triazene moiety and the carboxamide group appear to be the greatest destabilizing influence in the (Z) configurations.

Overall there appears to be good agreement between the various levels of theory employed with respect to the geometrical features of the configurations studied. There is some discrepancy in relative energy comparisons at the various levels of theory. Furthermore, B3LYP levels of theory are in agreement with the MP2 levels of theory, particularly B3LYP/6-31+G(d) with MP2/6-31+G(d). Diffuse functions appear to have an effect on relative energy comparisons and dihedral angle measurements of certain configurations of TIC, MTIC and DTIC, particularly at the HF and MP2 levels of theory. These factors and consideration of computational expenses, B3LYP/6-31+G(d) may prove to be a useful level of theory for the study of DTIC and its structural analogues.

CHAPTER FIVE: TEMOZOLOMIDE & MITOZOLOMIDE

1. Introduction

Temozolomide (Figure 5.1), an imidazotetrazine derivative of the alkylating agent Dacarbazine, is believed to undergo a conversion to a monomethyl triazene imidazole carboxamide (MTIC). Like Dacarbazine, Temozolomide (TEMO) is believed to interfere with DNA replication. TEMO is spontaneously hydrolyzed to MTIC at physiological pH. Because of this, TEMO is administered orally and is rapidly absorbed. However, Dacarbazine is poorly metabolized by the human body and is believed to require oxidative metabolism by hepatic cytochrome P450 enzymes to form a monomethyltriazene (12,20).

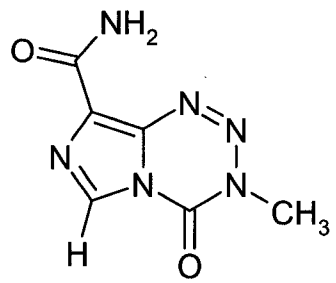

Figure 5.1: The chemical structure of Temozomide (3,4-dihydro-3-methyl-4-oxoimidazo-[5,1,d]-1,2,3,5-tetrazine-8-carboxamide, Temodal ®).

TEMO has demonstrated activity against recurrent brain cancer (gliomas). In combination with radiation therapy, TEMO chemotherapy significantly has improved the overall survival rate of patients diagnosed with glioblastoma multiforme (stage IV brain

cancer). As such, Health Canada recently approved TEMO in combination with radiotherapy for the treatment of glioblastoma multiforme or anaplastic astrocytoma after recurrence with standard therapy. Due to the serious and numerous side effects associated with TEMO, this treatment option is reserved for the treatment of recurrent aggressive brain cancers, such as glioblastoma multiforme or anaplastic astrocytoma (103,104,105,106).

Initially, Mitozolomide (MITO) (Figure 5.2), a chloroethyl analogue of TEMO, was thought to have significant anti-tumor properties. Animal testing of MITO did show a significant effect on various tumors. However, MITO has not proven effective against human cancer and the compound possesses serious toxic effects in the human system (107).

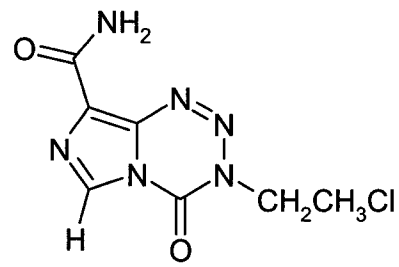

Figure 5.2: The chemical structure of Mitozolomide (3,4-dihydro-3-(2-chloroethyl)-4-oxoimidazo-[5,1,d]-1,2,3,5-tetrazine-8-carboxamide).

This study of TEMO and MITO will focus on the various configurations of each with respect to the orientation of the carboxamide group. This study is an extension of previous studies concerned with Dacarbazine and its structural analogues (Chapters 3 and 4).

2. Computational Methods

All calculations were performed using the methods specified in Chapter 4.

3. Results and Discussion

As an extension of previous Dacarbazine structural analogues studies the configurations of TEMO and MITO are discussed here. Individual configurations of TEMO and MITO are distinguished by the carbonyl (C=O) conformation with respect to the C_8-C_9 bond of the imidazole ring. The conformations will be either s-trans (t) or s-cis (c). MITO configurations are further distinguished by the orientation of the chloroethyl group. The Cl-C bond are either antiperiplanar (a) or gauche to the C-N_3 bond with respect to the ‹($ClCCN_3$) dihedral angle of the configuration. The gauche orientations are either syn- (sg) or anti- (ag) with respect to the triazene moiety of the configuration. This discussion will be limited to the outstanding geometric features and relative energy comparisons of each configuration identified. All bond lengths and dihedral angles of interest are reported in the supplemental data section (Tables S5). The absolute energies of all structures at all levels of theories utilized during this study can be found in Appendix I. The systematic numbering system used in previous discussions (Chapter 3 and Chapter 4) will be employed for the discussion of TEMO and MITO (Figure 5.3).

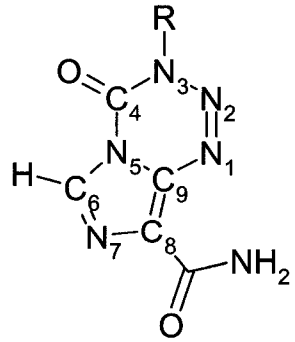

Figure 5.3: The systematic numbering system utilized during the discussion of TEMO ($R=CH_3$) and MITO ($R=CH_2CH_2Cl$).

3.1 Temozolomide: Two configurations of TEMO (Figure 5.4) were identified. TEMO C=O s-cis was more stable than TEMO C=O s-trans (Table 1). The N_1-N_2 and N_2-N_3 bond lengths of the triazene moiety of TEMO (t) and TEMO (c) are reported in the supplemental data section (Table S5-1). The triazene moiety of TEMO (t) and TEMO (c) was in plane with respect to the imidazole ring. The ‹($C_8C_9N_1N_2$) dihedral angle of TEMO (t) and TEMO (c) was 178.2 – 180.0 and 179.7 – 180.0°, respectively (Table S5-2). The ‹(OCC_8C_9) dihedral angle of TEMO (t) and TEMO (c) was 167.3 – 180.0 and 179.7 – 180.0°, respectively (Table S5-2). This suggests that the carboxamide group is in the same plane as the imidazole ring. Both TEMO configurations had a weak hydrogen-bond interaction (Table S5-3).

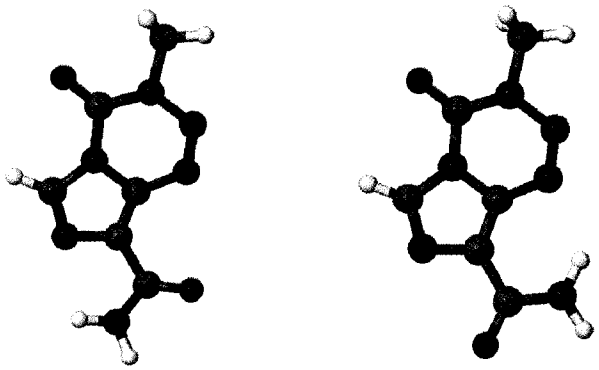

TEMO C=O s-cis **TEMO C=O s-trans**

Figure 5.4: The identified configurations of Temozolomide.

Table 1: Zero-point relative energy comparison of TEMO C=O s-trans with respect to TEMO C=O s-cis.

Level of Theory	Relative Energy (kJ mol^{-1})
HF/STO-3G	4.0
HF/3-21G	13.3
HF/6-31G(d)	10.6
HF/6-31+G(d)	10.1
MP2/6-31G(d)	5.7
MP2/6-31+G(d)	6.0
B3LYP/6-31G(d)	6.5
B3LYP/6-31+G(d)	6.2
B3LYP/6-31G(d,p)	6.5

3.2 Mitozolomide: Six configurations of Mitozolomide were identified (Figure 5.5)*. MITO C=O s-cis, EtCl antiperiplanar was the most stable MITO

* Attempts to generate other conformations by rotations about the N_3-C bond resulted in coalescence to structures already obtained.

configuration (Table 2). The N_1-N_2 and N_2-N_3 bonds of the triazene moiety of the MITO configurations are reported in the supplemental data section (Table S5-4). The triazene moiety and carboxamide group were in the same plane as the imidazole ring. The ‹(OCC_8C_9) dihedral angle of the MITO s-trans and MITO s-cis configurations were 174.6 – 180.0 and 0.1 – 2.7°, respectively (Tables S5-5 and S5-6). The ‹($C_8C_9N_1N_2$) dihedral angle was 179.9 – 180.0 and 179.6 – 179.9°, respectively (Tables S5-5 and S5-6). All MITO configurations had a weak intra-molecular hydrogen bond interaction (Table S5-7).

Table 2: Zero-point relative energy comparison of the MITO configurations with respect to MITO C=O s-cis, EtCl antiperiplanar.

Level of Theory	Relative Energy (kJ mol^{-1})				
	(c,ag)	(c,sg)	(t,a)	(t,ag)	(t,sg)
HF/STO-3G	-2.2	1.2	4.6	2.6	4.6
HF/3-21G	-0.1	0.9	14.6	15.1	13.7
HF/6-31G(d)	2.3	2.8	11.5	14.3	12.6
HF/6-31+G(d)	2.6	2.9	11.0	14.0	12.2
MP2/6-31G(d)	-0.6	0.1	6.5	6.9	6.2
MP2/6-31+G(d)	-	-	-	-	-
B3LYP/6-31G(d)	1.7	1.7	7.2	9.1	7.8
B3LYP/6-31+G(d)	1.9	2.1	6.9	9.0	7.8
B3LYP/6-31G(d,p)	1.4	1.5	7.2	8.8	7.6

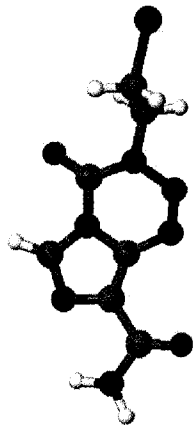

MITO C=O s-cis, EtCl antiperiplanar

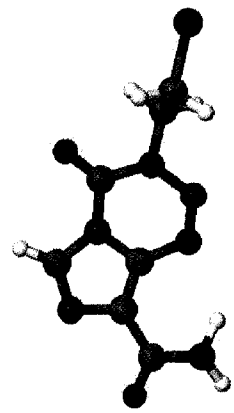

MITO C=O s-trans, EtCl antiperiplanar

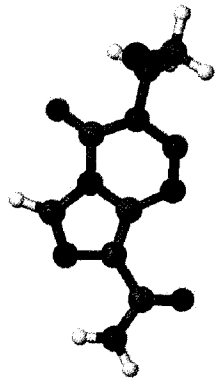

MITO C=O s-cis, EtCl anti-gauche

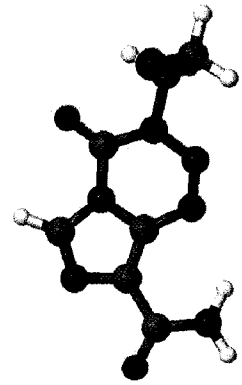

MITO C=O s-trans, EtCl anti-gauche

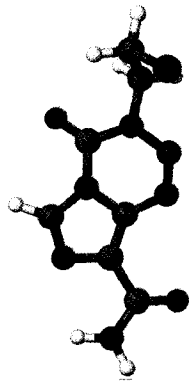

MITO C=O s-cis, EtCl syn-gauche

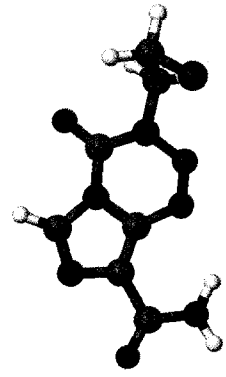

MITO C=O s-trans, EtCl syn-gauche

Figure 5.5: The identified configurations of Mitozolomide.

4. Conclusion

All configurations of TEMO and MITO demonstrated similar characteristics. Furthermore, the carboxamide group, imidazole ring and triazene moiety of both configurations of TEMO and MITO are in the same plane. Therefore, it is reasonable to conclude that there is conjugation of the π-system. The relative energy differences between configurations of TEMO and MTIO were comparable at 5.7 – 10.6 and 6.2 – 14.3 kJ mol^{-1}, respectively. The chloroethyl group is not believed to have a significant influence on the relative stability of the MITO configurations and the anti- and gauche- configurations are expected to readily interchange in the gas-phase.

CHAPTER SIX:
TAUTOMERS & TAUTOMERIZATION

1. Introduction

Tautomers are structural isomers that can interconvert by the migration of a hydrogen atom and the exchange of a single bond with an adjacent double bond (108). Various factors can influence the ability of tautomers to interconvert (108), including temperature, solvent, and pH. Tautomerism is among the most important chemistry reactions in living systems (108-111). MTIC, the active metabolite of Dacarbazine could interconvert to its tautomer form (MTIC_T) (Figure 6.1) under the right conditions.

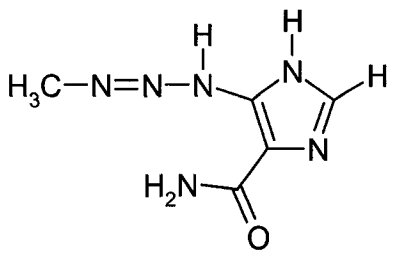

Figure 6.1: Chemical structure of the 5-(3-methyl-1-triazenyl)imidazole-4-carboxamide tautomer.

The relationships between various tautomers have been of interest for several years and studied through various methods. For instance, formamide and its tautomer have been studied by Classical Monte Carlo (112-114), molecular dynamics simulations (115-117) and quantum chemical calculations (118) in both gas phase and aqueous conditions. Monohydrated formamide–water complexes have been studied at *ab initio* and DFT levels of theory (119-124).

Water stabilizes different tautomers if hydrogen bonding is possible (125,126). In addition, water mediated hydrogen atom transfer has been shown to lower the energy barrier of various tautomerization processes (125-127). For instance, previous theoretical studies concerning tautomers of guanine noted that the energy barrier of the gas-phase tautomerization process was 125 – 167 kJ mol^{-1} and the water mediated energy barrier was 42 kJ mol^{-1} (125,126). The barrier for water mediated tautomerization is significantly lowered due to the ability of a water molecule to act as both a proton acceptor and proton donor (111,128-130).

Scheme 1: The tautomerization of MTIC to MTIC_T.

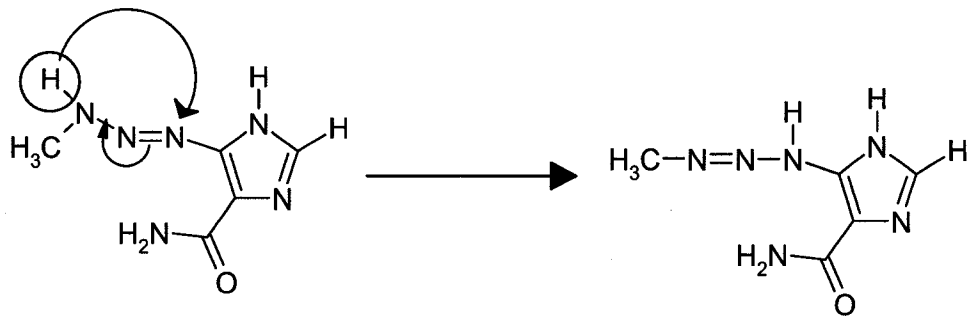

It is plausible that MTIC will undergo tautomerization in various situations (Scheme 1). MTIC_T could be responsible for the observed anti-neoplastic properties of DTIC. In order to gain more information about the relationship between MTIC and its tautomer form, a configurational search of MTIC_T was carried out. A configurational search of the 5-(3-methyl-1-triazenyl)imidazole tautomers (MTI_T) was also conducted in order to assess the influence of the carboxamide group on the stability of these compounds. Furthermore, the tautomerizations of MTI to MTI_T and MTIC to MTIC_T in both the gas-phase and as a water mediated process were investigated.

2. Computational Methods

All calculations were performed using the methods specified in Chapter 4.

3. Results and Discussion

The various configurations of MTI_T (Section 3.1.1) and MTIC_T (Section 3.1.2) along with specific gas-phase and water mediated tautomerization pathways of MTI to MTI_T (Section 3.2) and MTIC to MTIC_T (Section 3.3) are presented here. The tautomer configurations will be distinguished by the orientation of the C_1-C_5 bond of the imidazole ring (Im) with respect to the N_6-N_7 bond of the triazene moiety and the orientation of the hydrogen on N_6 will be defined with respect to the N_7-N_8 bond of the triazene moiety. The MTIC_T configurations will be further distinguished by the orientation of the carbonyl (C=O) conformation with respect to the C_1-C_5 bond of the imidazole ring. The gas-phase transition structures (TS) and the water mediated transition structures (TS H_2O) will be distinguished by the orientation of the imidazole ring (Im) with respect to the N_6-N_7 bond of the triazene moiety. The MTIC to MTIC_T transition structures will also be distinguished by the carbonyl (C=O) conformation of the carboxamide group with respect to the C_1-C_5 bond of the imidazole ring. The conformations will be either s-trans (t) or s-cis (c). Relative energy comparisons and specific geometrical features of interest will be discussed.

The geometrical features of interest are reported in the supplemental data section (Tables S6). The absolute energies of all structures at all levels of theories utilized during this study are reported in Appendix I. A systematic numbering system similar to the one used in previous discussions concerning MTI and MTIC will be employed during this discussion of MTI_T and MTIC_T (Figure 6.2).

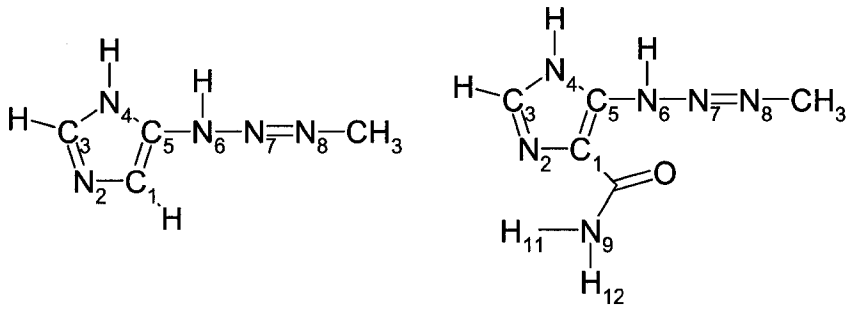

MTI_T **MTIC_T**

Figure 6.2: The systematic numbering system of MTI_T and MTIC_T.

3.1 MTI and MTIC Tautomers

3.1.1 MTI_T: Four 5-(3-methyl-1-triazenyl)imidazole tautomer configurations were identified and characterized (Figure 6.3)*. (E)-MTI_T Im s-trans, H s-cis and (E)-MTI_T Im s-trans, H s-trans were comparable in energy and the most stable MTI_T configurations (Table 1). The N_6-N_7 and N_7-N_8 bond lengths of the triazene moiety of the MTI_T configurations are reported in the supplemental data section (Table S6-1). The ‹($C_1C_5N_6N_7$) dihedral angle indicates that the triazene moiety of (Z)-MTI_T (c,t) is significantly out of plane with respect to the imidazole ring (Table S6-2). At the

* In attempts to identify other tautomer configurations, PES scans were conducted by rotation about the N_6-N_7 bond; however no further tautomers were identified.

HF/6-31G(d) and B3LYP levels of theory, the triazene moiety and the imidazole ring of (Z)-MTI_T (t,c), (E)-MTI_T (t,c) and (E)-MTI_T (t,t) was planar. The triazene moiety of (Z)-MTI_T (t,c), (E)-MTI_T (t,t) and (E)-MTI_T (t,c) was out of plane with respect to the imidazole ring at HF/6-31+G(d) and MP2 levels of theory (Table S6-2).

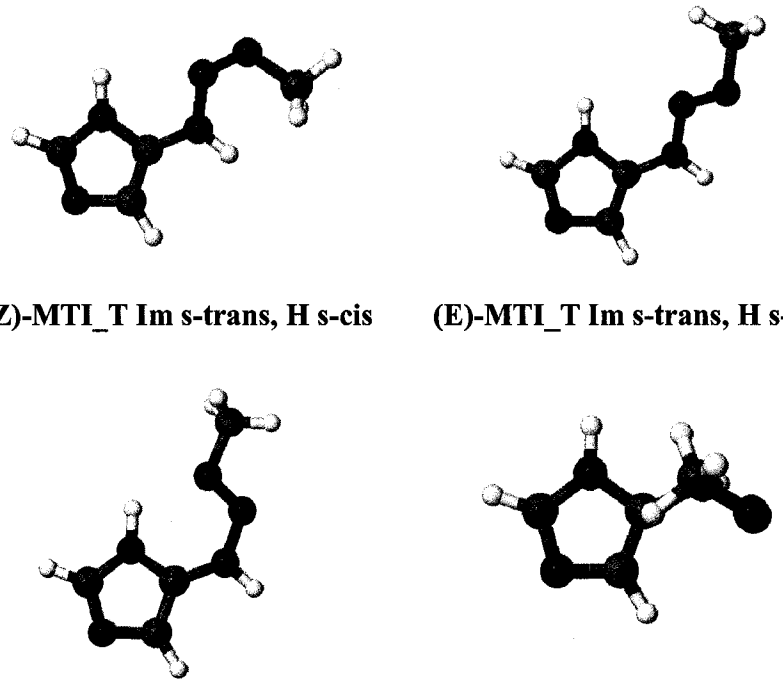

(Z)-MTI_T Im s-trans, H s-cis **(E)-MTI_T Im s-trans, H s-cis**

(E)-MTI_T Im s-trans, H s-trans **(Z)-MTI_T Im s-cis, H s-trans**

Figure 6.3: Identified configurations of the 5-(3-methyl-1-triazenyl)imidazole tautomers.

3.1.2 MTIC_T: Six MTIC_T configurations were identified (Figure 6.4)†. (E)-MTIC_T Im s-trans, C=O s-cis, H s-trans was the most stable configuration of MTIC_T (Table 2). The N_6-N_7 and N_7-N_8 bond lengths of the MTIC_T configurations are reported in Tables S6-3 and S6-4 of the supplemental data section. Examination of

† In attempts to identify other tautomer configurations, PES scans were conducted by rotation about the N_6-N_7 bond; however no further tautomers were identified.

the ‹($C_1C_5N_6N_7$) dihedral angle indicates that the triazene moiety was in the same plane as the imidazole ring for all MTIC_T configurations (Table S6-5). However, at the MP2 levels of theory, the ‹($C_1C_5N_6N_7$) dihedral angle indicates that the triazene moiety is slightly out of plane with respect to the imidazole ring (Table S6-5). The ‹(OCC_1C_5) dihedral angle of (Z)-MTIC_T (t,c,c), (Z)-MTIC_T (t,t,c) and (E)-MTIC_T (t,c,t) was 0.0 – 0.9, 0.0 – 0.3 and 0.0 – 0.3°; respectively, indicating that the carboxamide group is in the same plane as the imidazole ring (Table S6-6). The ‹(OCC_1C_5) dihedral angle of (E)-MTIC_T (t,c,c), (E)-MTIC_T (t,t,c) and (E)-MTIC_T (t,t,t) was 145.0 – 167.0, 145.5 – 153.8 and 148.6 – 152.5°; respectively, indicating that the carboxamide group is slightly out of plane with respect to the imidazole ring (Table S6-6).

Table 1: Relative energy comparison of MTI_T configurations with respect to (E)-MTI_T (t,c).

Level of Theory	Relative Energy (kJ mol^{-1})		
	(Z)-MTI_T (t,c)	(E)-MTI_T (t,t)	(Z)-MTI_T (c,t)
HF/STO-3G	30.0	4.7	44.7
HF/3-21G	32.8	1.7	54.1
HF/6-31G(d)	37.1	5.2	60.7
HF/6-31+G(d)	44.1	5.9	66.8
MP2/6-31G(d)	24.2	-7.4	42.1
MP2/6-31+G(d)	31.8	-2.7	46.1
B3LYP/6-31G(d)	26.7	-3.3	57.0
B3LYP/6-31+G(d)	31.4	-1.7	60.2
B3LYP/6-31G(d,p)	26.2	-3.7	57.4

Table 2: Zero-point relative energy comparison of MTIC_T configurations with respect to (E)-MTIC_T (t,c,t).

Level of Theory	Relative Energy (kJ mol^{-1})				
	(Z) (t,c,c)	(Z) (t,c,c)	(E) (t,c,c)	(E) (t,t,c)	(E) (t,t,t)
HF/STO-3G	21.8	-2.5	42.1	15.1	19.2
HF/3-21G	25.6	4.6	105.1	74.0	75.0
HF/6-31G(d)	28.1	-1.8	88.3	51.5	58.2
HF/6-31+G(d)	30.9	-2.5	91.7	51.0	58.7
MP2/6-31G(d)	29.9	13.6	81.7	59.8	52.0
MP2/6-31+G(d)	31.0	10.5	82.7	55.9	50.2
B3LYP/6-31G(d)	28.0	8.7	85.6	60.3	55.8
B3LYP/6-31+G(d)	30.1	6.3	88.9	58.6	56.3
B3LYP/6-31G(d,p)	27.9	9.2	86.3	61.5	56.6

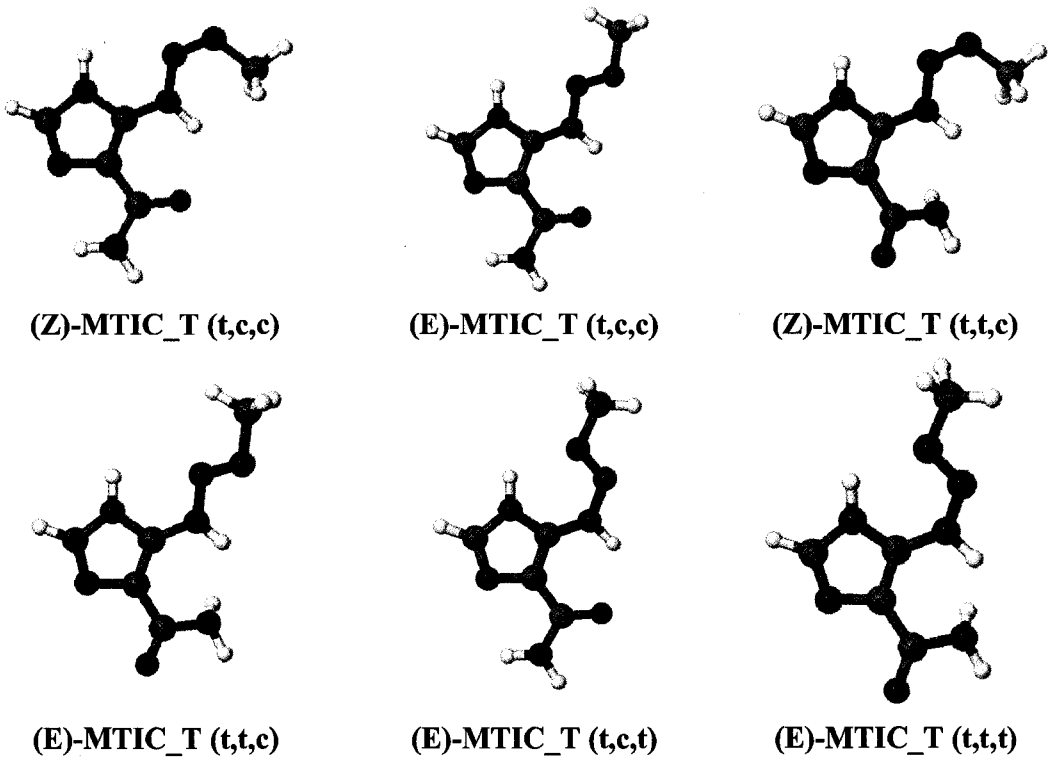

Figure 6.4: The identified configurations of the MTIC tautomer.

3.2 MTI to MTI_T Tautomerization Pathways

The tautomerization of MTI to MTI_T was studied by examining the (E)-MTI (t,t) to (E)-MTI_T (t,c) and (E)-MTI (c,t) to (Z)-MTI_T (c,t) pathways.

3.2.1 Gas-phase Tautomerization: Overall, the (E)-MTI (t,t) to (E)-MTI_T (t,c) and (E)-MTI (c,t) to (Z)-MTI_T (c,t) gas-phase tautomerizations were endothermic reactions (Table 3). Tautomerization of (E)-MTI (t,t) to (E)-MTI_T (t,c) occurs through TS Im s-trans (Figure 6.5) and the central energy barrier associated with TS (t) was 153.1 – 230.9 kJ mol^{-1} (Table 3). Tautomerization of (E)-MTI (c,t) to (Z)-MTI_T (c,t) occurs through TS Im s-cis (Figure 6.5), which is characterized by a central energy barrier of 150.5 – 228.5 kJ mol^{-1} (Table 3). Both TSs are characterized by a four-membered ring involved in the transfer of the hydrogen from N_8 to N_6. Along each reaction pathway there is obvious breaking and making of the N_8-H bond and the N_6-H bond, respectively (Tables S6-8 and S6-10). The N_6-N_7 and N_7-N_8 bond distances of TS (t) and TS (c) are reported in the supplemental data section (Tables S6-7 and S6-9).

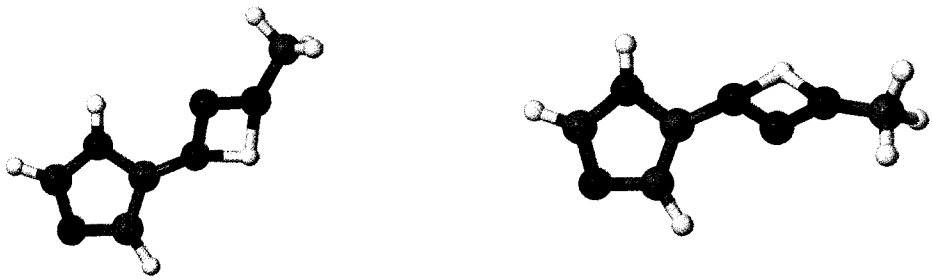

TS Im s-trans **TS Im s-cis**

Figure 6.5: The gas-phase tautomerization of MTI to MTI_T transition structures.

Table 3: Relative energy comparison of the gas-phase tautomerization (E)-MTI (t,t) to (E)-MTI_T (t,c) with respect to (E)-MTI (t,t) and (E)-MTI (c,t) to (Z)-MTI_T (c,t) with respect to (E)-MTI (c,t).

Level of Theory	Relative Energy (kJ mol^{-1})			
	(E)-MTI (t,t) to (E)-MTI_T (t,c)		(E)-MTI (c,t) to (Z)-MTI_T (c,t)	
	TS (t)	(E)-MTI_T (t,c)	TS (c)	(Z)-MTI_T (c,t)
HF/STO-3G	225.6	3.9	224.2	47.7
HF/3-21G	205.7	2.9	204.0	54.3
HF/6-31G(d)	230.9	11.4	225.1	66.5
HF/6-31+G(d)	235.4	9.1	228.5	69.5
MP2/6-31G(d)	153.1	17.9	148.1	53.2
MP2/6-31+G(d)	157.8	15.8	151.9	54.8
B3LYP/6-31G(d)	159.8	16.1	156.6	67.5
B3LYP/6-31+G(d)	166.3	16.5	162.5	70.8
B3LYP/6-31G(d,p)	153.4	15.4	150.5	67.3

3.2.2 Water Mediated Tautomerization: Separated reactants (SR), consisting of a MTI configuration and a water molecule, are the first structures on the tautomerization pathway, followed by the formation of a reactant complex (RC). The transition structure (TS H_2O) that follows is characterized by a pseudo-six-membered ring, consisting of the triazene moiety, the N_8-hydrogen and the water molecule. TS H_2O was involved in the transfer of the N_8-hydrogen to N_6. A product complex (PC) consisting of a MTI_T configuration and the water molecule follows. The tautomerization pathway is completed by the separated products (SP).

3.2.2 A (E)-MTI (t,t) to (E)-MTI_T (t,c): Formation of RC Im s-trans, Me s-trans (a (E)-MTI (t,t) and water complex) and PC Im s-trans, H s-cis (a (E)-MTI_T (t,c) and water complex) occurs during the water mediated tautomerization of (E)-MTI (t,t) to (E)-MTI_T (t,c) (Figure 6.6). RC (t,t) and PC (t,c) were more stable than the SR ((E)-MTI (t,t) and a water molecule at infinite distance) (Table 4). At higher levels of theory, the central energy barrier associated with the water mediated tautomerization transition structure (TS H_2O Im s-trans) (Figure 6.7) was 56.5 – 145.8 kJ mol^{-1} (Table 4). A break in the N_6-N_7 double bond (Table S6-11) and formation of a N_7-N_8 double bond (Table S6-12) is demonstrated along the reaction pathway. A break of the H-N_8 bond (Table S6-13) and formation of the H-N_6 bond (Table S6-14) is also observed.

Table 4: Relative energy comparison of the water mediated tautomerization of (E)-MTI (t,t) to (E)-MTI_T (t,c), with respect to the separated reactants.

Level of Theory	Relative Energy (kJ mol^{-1})			
	RC (t,t)	TS H_2O (t)	PC (t,c)	SP
HF/STO-3G	-23.5	37.1	-22.6	3.9
HF/3-21G	-53.5	15.0	-51.1	2.9
HF/6-31G(d)	-21.0	124.3	-10.4	11.4
HF/6-31+G(d)	-17.1	128.6	-6.2	9.1
MP2/6-31G(d)	-38.5	36.7	-24.3	17.9
MP2/6-31+G(d)	-32.3	46.9	-16.2	15.8
B3LYP/6-31G(d)	-39.5	24.7	-25.8	16.1
B3LYP/6-31+G(d)	-26.6	42.9	-11.8	16.5
B3LYP/6-31G(d,p)	-39.6	17.0	-26.4	15.4

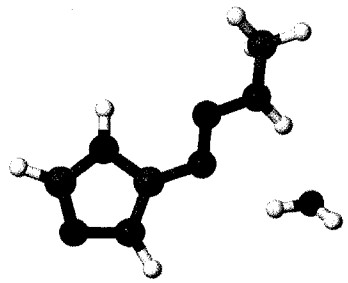

RC Im s-trans, Me s-trans

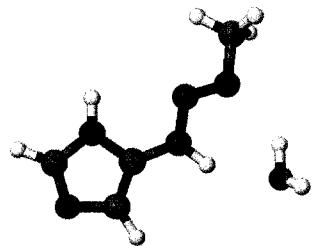

PC Im s-trans, H s-cis

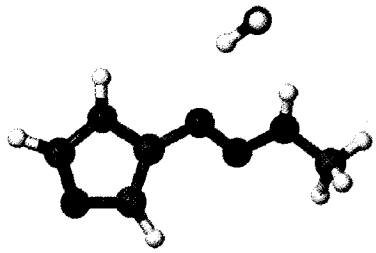

RC Im s-cis, Me s-trans

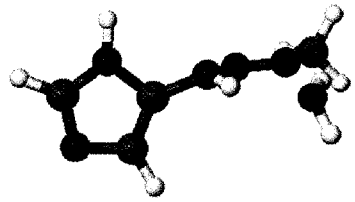

PC Im s-cis, H s-trans

Figure 6.6: The reactant complexes and product complexes of the water mediated tautomerizations of (E)-MTI (t,t) to (E)-MTI_T (t,c) and (E)-MTI (c,t) to (Z)-MTI_T (c,t).

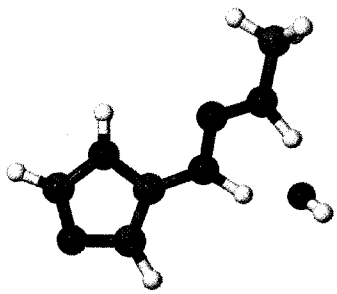

TS H_2O Im s-trans

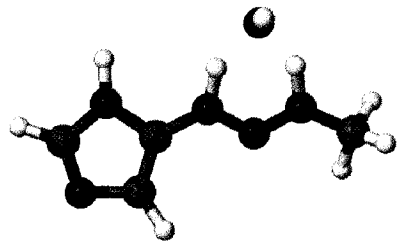

TS H_2O Im s-cis

Figure 6.7: The TS of the water mediated tautomerizations of (E)-MTI (t,t) to (E)-MTI_T (t,c) and (E)-MTI (c,t) to (Z)-MTI_T (c,t)

3.2.2 B (E)-MTI (c,t) to (Z)-MTI_T (c,t): RC Im s-cis, Me s-trans (a (E)-MTI (c,t) water complex) and PC Im s-cis, H s-trans (a (Z)-MTI_T (c,t) water complex) are formed during the water mediated tautomerization of (E)-MTI (c,t) (Figure 6.6). RC (c,t) and PC (c,t) were more stable than SR (Table 5). At higher levels of theory the central energy barrier associated with the water mediated tautomerization of (E)-MTI (c,t) to (Z)-MTI_T (c,t) (TS H_2O Im s-cis) (Figure 6.7) was 56.8 - 137.8 kJ mol^{-1} (Table 5). Along the reaction pathway, there is breaking and making of N_6-N_7 and N_7-N_8 double bonds (Tables S6-15 and S6-16). Breaking and making of the H-N_8 and H-N_6 bonds (Tables S6-17 and S6-18) is also observed.

Table 5: Relative energy comparison of the water mediated tautomerization of (E)-MTI (c,t) to (Z)-MTI_T (c,t), with respect to the separated reactants.

Level of Theory	Relative Energy (kJ mol^{-1})			
	RC (c,t)	TS H_2O (c)	PC (c,t)	(Z)-MTI_T (c,t)
HF/STO-3G	-19.7	40.7	-23.7	47.7
HF/3-21G	-49.4	17.8	-53.8	54.3
HF/6-31G(d)	-17.3	120.5	-14.5	66.5
HF/6-31+G(d)	-13.2	122.3	-12.7	69.5
MP2/6-31G(d)	-34.4	38.9	-25.5	53.2
MP2/6-31+G(d)	-28.1	46.5	-21.8	54.8
B3LYP/6-31G(d)	-36.5	27.3	-31.3	67.5
B3LYP/6-31+G(d)	-23.2	43.9	-17.6	70.8
B3LYP/6-31G(d,p)	-36.9	20.0	-32.0	67.3

3.3 MTIC to MTIC_T Tautomerization Pathways

Four MTIC tautomerization pathways were studied in the gas-phase and as water mediated processes. The tautomerization of (E)-MTIC (t,t,c) to (E)-MTIC_T (t,c,c), (E)-MTIC (t,t,t) to (E)-MTIC_T (t,t,c), (E)-MTIC (c,c,c) to (E)-MTIC_T (t,c,c) and (E)-MTIC (c,c,t) to (E)-MTIC_T (t,t,c) will be discussed.

3.3.1 Gas-Phase: Gas-phase tautomerization of MTIC to MTIC_T was an exothermic process (Table 6). The tautomerization of (E)-MTIC (t,t,c) to (E)-MTIC_T (t,c,c), (E)-MTIC (t,t,t) to (E)-MTIC_T (t,t,c), (E)-MTIC (c,c,c) to (E)-MTIC_T (t,c,c) and (E)-MTIC (c,c,t) to (E)-MTIC_T (t,t,c) proceeded through TS Im s-trans, C=O s-cis; TS Im s-trans, C=O s-trans; TS Im s-cis, C=O s-cis and TS Im s-cis, C=O s-trans (Figure 6.8), respectively. Each TS was characterized by a four-membered ring that was involved in the transfer of N_8-hydrogen to N_6. The TSs demonstrate breaking and making of the H-N_8 and H-N_6 bonds (Tables S6-19, S6-21, S6-23 and S6-25). Breaking and the making of the N_6-N_7 and N_7-N_8 double bonds (Table S6-20, S6-22, S6-24 and S6-26) is also observed. The central energy barriers associated with each TS were significantly high (Table 6).

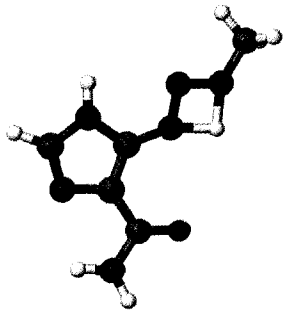

TS Im s-trans, C=O s-cis

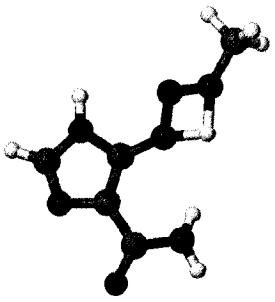

TS Im s-trans, C=O s-trans

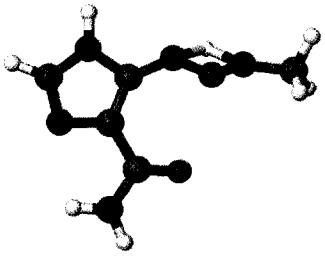

TS Im s-cis, C=O s-cis

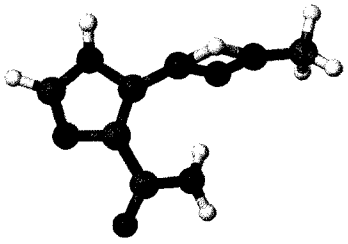

TS Im s-cis, C=O s-trans

Figure 6.8: The TSs involved during the gas-phase tautomerization of MTIC to MTIC_T.

Table 6: Relative energy comparison of the gas-phase tautomerization of MTIC to MTIC_T.

Level of Theory	Relative Energy (kJ mol^{-1})‡							
	TS (t,c)	(t,c,c)	TS (t,t)	(t,t,c)	TS (c,c)	(t,c,c)	TS (c,t)	(t,t,c)
HF/STO-3G	215.4	-13.9	222.7	-4.5	212.8	-21.3	215.9	-22.4
HF/3-21G	185.8	-44.6	212.3	7.2	188.4	-48.6	202.2	-11.5
HF/6-31G(d)	212.4	-29.8	231.3	6.3	213.2	-35.2	218.3	-14.9
HF/6-31+G(d)	215.5	-29.6	234.8	7.4	217.1	-33.6	221.5	-14.5
MP2/6-31G(d)	144.0	-18.7	157.7	15.9	140.8	-29.0	146.5	0.2
MP2/6-31+G(d)	147.0	-17.8	159.0	15.4	144.6	-24.8	148.5	0.1
B3LYP/6-31G(d)	146.3	-21.3	167.3	19.1	150.1	-30.5	157.5	4.1
B3LYP/6-31+G(d)	151.9	-20.7	171.7	19.9	156.1	-28.8	162.6	3.8
B3LYP/6-31G(d,p)	140.4	-21.8	161.5	19.4	144.1	-31.1	151.5	4.2

‡ The relative energy is calculated with respect to the original MTIC configuration.

3.3.2 Water Mediated: All four water mediated tautomerization pathways of MTIC to MTIC_T were characterized by five stationary points: the separated reactants (SR), a reactant complex (RC) comprised of a MTIC configuration and a water molecule (Figure 6.9), a transition structure (TS H_2O) characterized by a pseudo-six membered ring involved in a hydrogen transfer from N_6 to N_8 (Figure 6.10), a product complex (PC) comprised of a MTIC_T configuration and a water molecule (Figure 6.11) and the separated products (SP). The separated reactants and products are considered to be at an infinite distance.

3.3.2 A (E)-MTIC (t,t,c) to (E)-MTIC_T (t,c,c): Formation of RC Im s-trans, Me s-trans, C=O s-cis occurs during the water mediated tautomerization of (E)-MTIC (t,t,c) to (E)-MTIC_T (t,c,c). RC (t,t,c) was more stable than the SR ((E)-MTIC (t,t,c) and a water molecule) (Table 7). TS H_2O Im s-trans, C=O s-cis was associated with the (E)-MTIC (t,t,c) tautomerization pathway and was characterized by a central energy barrier of 55.1 – 146.8 kJ mol^{-1} (Table 7). PC Im s-trans, C=O s-cis, H s-cis formed along the tautomerization pathway and the SP ((E)-MTIC_T (t,c,c) and a water molecule) were found to be more stable than the SR, respectively (Table 7). The tautomerization pathway shows breaking and making of N_6-N_7 (Table S6-27) and N_7-N_8 double bonds (Table S6-28). Also evident is the breaking and making of H-N_8 (Table S6-29) and H-N_6 bonds (Table S6-30).

Table 7: Relative energy comparison of the water mediated tautomerization of (E)-MTIC (t,t,c) with respect to the SR, (E)-MTIC (t,t,c) and a water molecule.

Level of Theory	Relative Energy (kJ mol^{-1})			
	RC (t,t,c)	TS H_2O (t,c)	PC (t,c,c)	SP
HF/STO-3G	-36.6	17.3	-65.9	-13.9
HF/3-21G	-88.7	-21.7	-115.9	-44.6
HF/6-31G(d)	-44.5	96.0	-55.0	-29.8
HF/6-31+G(d)	-41.5	105.4	-50.1	-29.6
MP2/6-31G(d)	-60.6	12.5	-60.3	-18.7
MP2/6-31+G(d)	-57.2	24.7	-53.3	-17.8
B3LYP/6-31G(d)	-60.7	3.6	-63.9	-21.3
B3LYP/6-31+G(d)	-49.7	24.8	-48.9	-20.7
B3LYP/6-31G(d,p)	-60.0	-4.9	-64.8	-21.8

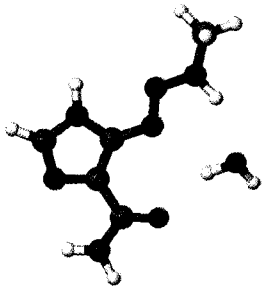

RC Im s-trans, Me s-trans, C=O s-cis

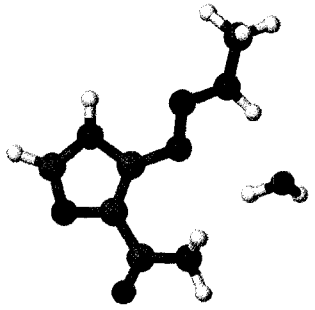

RC Im s-trans, Me s-trans, C=O s-trans

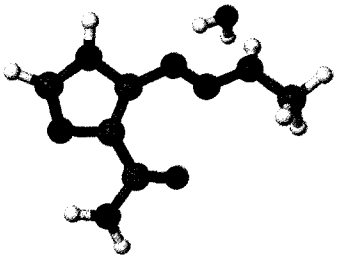

RC Im s-cis, Me s-cis, C=O s-cis

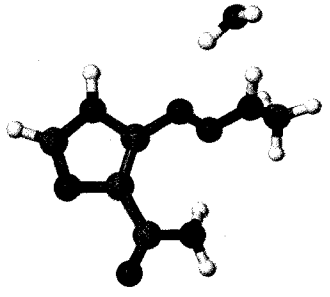

RC Im s-cis, Me s-cis, C=O s-trans

Figure 6.9: The MTIC and water molecule reactant complexes formed along the MTIC

to MTIC_T water mediated tautomerization pathways.

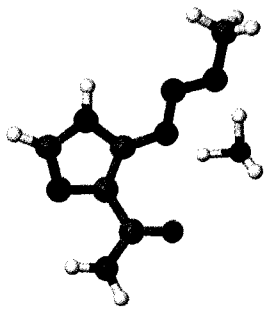

TS H_2O Im s-trans, C=O s-cis

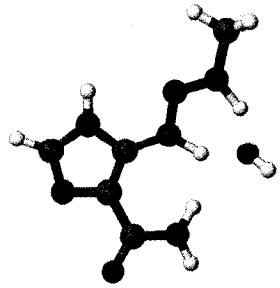

TS H_2O Im s-trans, C=O s-trans

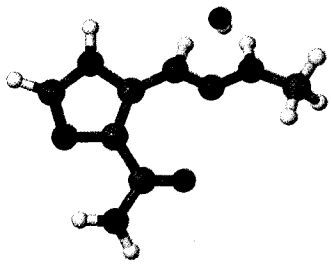

TS H_2O Im s-cis, C=O s-cis

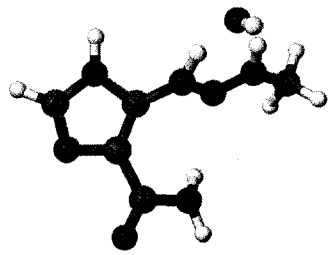

TS H_2O Im s-cis, C=O s-trans

Figure 6.10: The transition structures of the water mediated MTIC tautomerization.

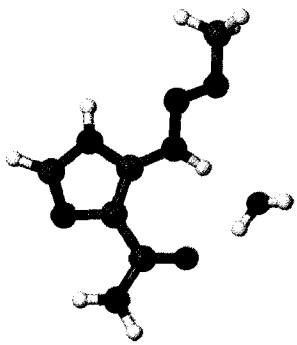

PC Im s-trans, C=O s-cis, H s-cis

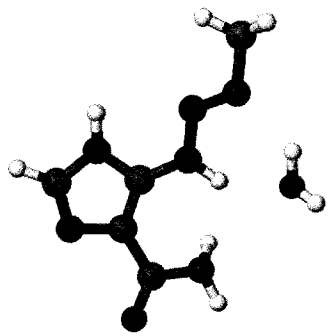

PC Im s-trans, C=O s-trans, H s-cis

Figure 6.11: The MTIC_T water complexes formed along the MTIC to MTIC_T water mediated tautomerization pathway.

3.3.2 B (E)-MTIC (t,t,t) to (E)-MTIC_T (t,t,c): RC Im s-trans, Me s-trans, C=O s-trans (Figure 6.9) is formed during the water mediated tautomerization

of (E)-MTIC (t,t,t) to (E)-MTIC_T (t,t,c). RC (t,t,t) was more stable than the SR ((E)-MTIC (t,t,t) and a water molecule) (Table 8). TS H_2O Im s-trans, C=O s-trans was associated with the tautomerization of (E)-MTIC (t,t,t) (Figure 6.10). TS H_2O (t,t) was associated with a central energy barrier of 57.7 – 150.0 kJ mol^{-1} (Table 8). PC Im s-trans, C=O s-trans, H s-cis is formed along the tautomerization pathway (Figure 6.11). PC (t,t,c) was more stable than the SR (Table 8). The SP ((E)-MTIC_T (t,t,c) and a water molecule) were less stable than the SR (Table 8). Again the tautomerization pathway shows breaking and making of the N_6-N_7 (Table S6-31) and N_7-N_8 double bonds (Table S6-32). Breaking and making of the H-N_8 (Table S6-33) and H-N_6 bonds (Table S6-34) is also evident.

Table 8: Relative energy comparison of the water mediated tautomerization of (E)-MTIC (t,t,t) to (E)-MTIC_T (t,t,c) with respect to (E)-MTIC (t,t,t) and a water molecule.

Level of Theory	Relative Energy (kJ mol^{-1})			
	RC (t,t,t)	TS H_2O (t,t)	PC (t,t,c)	SP
HF/STO-3G	-25.8	28.2	-35.3	-4.5
HF/3-21G	-49.2	18.2	-48.6	7.2
HF/6-31G(d)	-21.3	126.4	-13.1	6.3
HF/6-31+G(d)	-16.8	133.2	-7.1	7.4
MP2/6-31G(d)	-38.5	37.2	-23.8	15.9
MP2/6-31+G(d)	-34.8	46.4	-17.2	15.4
B3LYP/6-31G(d)	-35.4	30.3	-20.8	19.1
B3LYP/6-31+G(d)	-23.0	50.3	-5.8	19.9
B3LYP/6-31G(d,p)	-35.0	22.7	-20.9	19.4

3.3.2 C (E)-MTIC (c,c,c) to (E)-MTIC_T (t,c,c): RC Im s-cis, Me s-cis, C=O s-cis (Figure 6.9) is formed along the water mediated tautomerization pathway of (E)-MTIC (c,c,c). RC (c,c,c) was more stable than the SR ((E)-MTIC (c,c,c) and a water molecule) (Table 9). TS H_2O Im s-cis, C=O s-cis was associated with the tautomerization of (E)-MTIC (c,c,c) (Figure 6.10). The central energy barrier associated with TS H_2O (c,c) was 50.0 – 133.3 kJ mol^{-1} (Table 9). PC Im s-trans, C=O s-cis, H s-cis is formed along the tautomerization pathway (Figure 6.11). PC (t,c,c) and the SP ((E)-MTIC_T (t,c,c) and a water molecule) were more stable than the SR (Table 9). Along the tautomerization pathway breaking of the N_6-N_7 double bond (Table S6-35) and the H-N_8 bond (Table S6-37) along with making of the N_7-N_8 double bond (Table S6-36) and H-N_6 bond (Table S6-38) is demonstrated.

Table 9: Relative energy comparison of the water mediated tautomerization of (E)-MTIC (c,c,c) to (E)-MTIC_T (t,c,c) with respect to (E)-MTIC (c,c,c).

Level of Theory	Relative Energy (kJ mol^{-1})			
	RC (c,c,c)	TS H_2O (c,c)	PC (t,c,c)	SP
HF/STO-3G	-23.2	—	-73.3	-21.3
HF/3-21G	-54.6	4.7	-119.9	-48.6
HF/6-31G(d)	-22.6	110.7	-60.4	-35.2
HF/6-31+G(d)	-18.4	114.2	-54.0	-33.6
MP2/6-31G(d)	-39.3	2.3	-70.5	-29.0
MP2/6-31+G(d)	-46.2	17.7	-60.3	-24.8
B3LYP/6-31G(d)	-39.9	20.4	-73.1	-30.5
B3LYP/6-31+G(d)	-27.4	37.2	-57.0	-28.8
B3LYP/6-31G(d,p)	-36.6	13.4	-74.0	-31.1

3.3.2 D (E)-MTIC (c,c,t) to (E)-MTIC_T (t,t,c): RC Im s-cis, Me s-cis, C=O s-trans is formed during the water mediated tautomerization of (E)-MTIC (c,c,t) (Figure 6.9). RC (c,c,t) was more stable than the SR ((E)-MTIC (c,c,t) and a water molecule) (Table 10). TS H_2O Im s-cis, C=O s-trans was associated with the tautomerization of (E)-MTIC (c,c,t) (Figure 6.10) and characterized by a central energy barrier of 55.9 – 136.7 kJ mol^{-1} (Table 10). PC Im s-trans, C=O s-trans, H s-cis is formed along the tautomerization pathway (Figure 6.11). It was more stable than the SR (Table 10). The SP ((E)-MTIC_T (t,t,c) and a water molecule) were less stable than the SR (Table 10). Along the tautomerization pathway, breaking and making of the N_6-N_7 (Table S6-39) and N_7-N_8 double bonds (Table S6-40) is demonstrated. The breaking and making of the H-N_8 (Table S6-41) and H-N_6 and bonds (Table S6-42) is observed.

Table 10: Relative energy comparison of the water mediated tautomerization of (E)-MTIC (c,c,t) with respect to (E)-MTIC (c,c,t) and a water molecule.

Level of Theory	Relative Energy (kJ mol^{-1})			
	RC (c,c,t)	TS H_2O (c,t)	PC (t,t,c)	SP
HF/STO-3G	-27.0	—	-53.2	-22.4
HF/3-21G	-48.3	17.7	-67.4	-11.5
HF/6-31G(d)	-20.1	116.6	-34.4	-14.9
HF/6-31+G(d)	-16.6	120.0	-28.9	-14.5
MP2/6-31G(d)	-35.3	34.5	-39.6	0.2
MP2/6-31+G(d)	-484.2	40.5	-32.6	0.1
B3LYP/6-31G(d)	-35.0	28.7	-35.8	4.1
B3LYP/6-31+G(d)	-22.2	45.5	-21.8	3.8
B3LYP/6-31G(d,p)	-34.7	21.2	-36.0	4.2

4. Conclusions

Various configurations of the MTI and MTIC tautomers were characterized. Configurations with an imidazole ring in a s-trans configuration with respect to the triazene moiety were most stable. (E)-MTI_T (t,c) and (E)-MTIC_T (t,c,t) were the most stable MTI_T and MTIC_T configurations, respectively. The stability of these configurations is believed to be due to minimal steric effects.

MTI_T and MTIC_T configurations that are characterized by a triazene moiety and imidazole ring with an s-cis configuration, such as (Z)-MTI_T (c,t), were the least stable configurations. This trend is believed to be caused by steric effects between the terminal amine of the triazene and the imidazole ring. The MTIC_T configurations with a s-trans carboxamide group with respect to the imidazole ring, such as (E).MTIC_T (t,c,c), were further destabilized by the steric effects between the carboxamide group and the terminal amine of the triazene.

Gas-phase and water mediated tautomerization pathways were investigated for the tautomerization of MTI and MTIC. In the gas-phase studies, the transition structure in both situations was characterized by a four-membered ring involved in the transfer of the hydrogen from N_8 to N_6. Breaking and making of the N_6-N_7 and N_7-N_8 double bonds was observed. The central energy barriers associated with the gas-phase tautomerization of MTI and MTIC were significant in all cases (140.4 – 230.9 kJ mol^{-1}).

The transition structure of the water mediated tautomerization pathways (TS H_2O) was characterized by a pseudo-six-membered ring. TS H_2O involved transfer of the N_8-hydrogen atom to N_6 via the water molecule in both MTI and MTIC tautomerizations. Along the water-mediated tautomerization pathways, the breaking and making of the H-N_8 and H-N_6 bonds and breaking and making of the N_6-N_7 and N_7-N_8 double bonds was observed. The central energy barriers associated with the water mediated tautomerization are significant (41.6 – 150.0 kJ mol^{-1}); however, they are significantly less than the gas-phase barriers. Furthermore, the water complexes formed along the tautomerization pathway significantly stabilizes the reactants and the products.

Configurations of MTI and MTIC were stabilized by conjugation of the π-system; however, the tautomers of MTI and MTIC are not capable of extended π-system conjugation and steric effects significantly decrease the stability of the tautomer. The tautomerization of MTI and MTIC as a water mediated process was the most favorable situation for tautomerization to occur. The water molecule acted as a catalyst for the tautomerization. Furthermore, the water molecule stabilized the reactant and product through the formation of complexes, which increased the favorability of the tautomerization.

CHAPTER SEVEN: MTI & MTI_T S_N2 REACTION PATHWAYS

1. Introduction

The S_N2 reaction that is believed to occur between monomethyltriazene and the O6-oxygen of guanine as the mechanism of action for DTIC and other triazene containing anti-neoplastic agents has been previously studied. These studies have modeled the S_N2 reaction between 1- and 3-methyltriazene and halide ions; fluoride, chloride, bromide and iodide (20). Follow-up work has examined the S_N2 reactions of dimethyl- (21) and trimethyltriazenes (22). As an extension of these studies, the S_N2 reaction between 5-(3-methyl-1-triazenyl)imidazole or its tautomer (Figure 7.1) and a series of halide ions, including fluoride, chloride and bromide, was investigated.

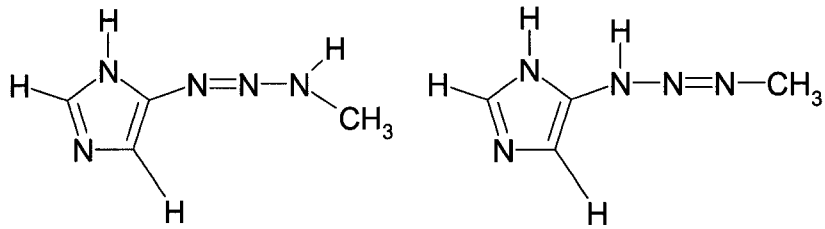

MTI **MTI_T**

Figure 7.1: The chemical structures of MTI and MTI_T.

The S_N2 reaction that occurs between MTI and a halide ion results in a halomethane and a 5-imidazolyltriazenide ion (Scheme 1). The S_N2 reaction that occurs between MTI_T and a halide ion results in a halomethane, molecular nitrogen and a

5-imidazolylamide ion (Scheme 2), which is the best representation of the proposed mechanism of action of triazene containing anti-neoplastic agents. This series of studies concerning monomethyltriazene will facilitate a better understanding of the mechanism of action of DTIC and other triazene containing anti-neoplastic agents.

Scheme 1: The S_N2 reaction between 5-(3-methyl-1-triazeneyl)imidazole and a halide ion results in a halomethane and 5-imidazolyltriazenide ion.

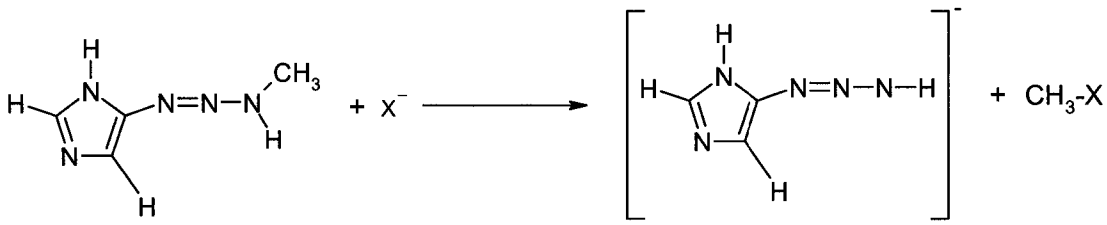

Scheme 2: The S_N2 reaction between a 5-(3-methyl-1-triazeneyl)imidazole tautomer and a halide ion results in a halomethane, molecular nitrogen and a 5-imidazolylamide ion.

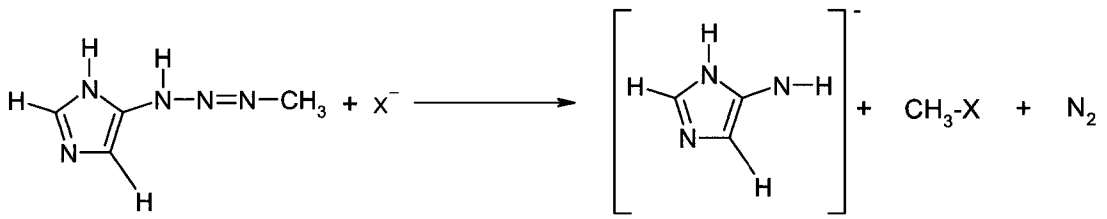

2. Computational Methods

All calculations were performed as specified in Chapter 4.

3. Results and Discussion

This study is an extension of a previous study concerning the S_N2 reaction between isomers of monomethyltriazene and a halide ion (20). For this study eight 5-(3-methyl-1-triazenyl)imidazole configurations (MTI) and four MTI tautomers (MTI_T) were used. The MTI configurations and tautomers were previously characterized in Chapters 3 and 6. The S_N2 reaction pathways involve a MTI or MTI_T configuration and a fluoride, chloride or bromide ion. The S_N2 reactions will be considered in terms of relative energy comparisons and specific geometrical features along the reaction pathways will be discussed. The S_N2 reactions between the configurations of MTI and the various halide ions (Section 3.1) will be discussed first followed by the S_N2 reactions between configurations of MTI_T and the halide ions (Section 3.2).

3.1 MTI

There are two isomers of MTI, E and Z with respect to the nitrogen-nitrogen double bond of the triazene moiety. There are four E configurations and four Z configurations of MTI. The relative energy comparisons and geometrical features of these configurations are reported in Chapter 3.

Structures along the MTI + X^- reaction pathways follow the same pattern: the separated reactants (SR), followed by a reactant complex (RC), a transition structure (TS) with a flattened methyl group corresponding to inversion of this center, a product

complex (PC), and the separated products (SP). For the purposes of this discussion the results of the various reactions will be discussed in terms of the halide involved. Similar RC, TS and PC were found for each (E)-MTI (Figure 7.2) and (Z)-MTI (Figure 7.3) configuration regardless of the halide involved. Furthermore, the SR, a halide ion and a MTI configurations, and the SP, a halomethane and a 5-imidazolyltriazenide ion configuration, are assumed to be at an infinite distance.

3.1.1 Fluoride ion: The fluoride and MTI S_N2 reactions were thermodynamically favorable (Tables 1 – 8). F-C, C-N_8, N_8-N_7 and N_7-N_6 bond lengths pertaining to the MTI and fluoride S_N2 reactions can be found in the supplemental data section (Tables S7-1 – S7-8). Along the reaction pathways, there is clearly making of the C-F bond, breaking of the C-N_8 bond, shortening of the N_8-N_7 bond and lengthening of the N_7-N_6 bond (Tables S7-1 – S7-8). Formation of the reactant complex does not significantly affect the C-N_8 bond length. However, the N_8-N_7 and N_7-N_6 bond lengths of the RCs are noticeably shortened and lengthened with respect to the MTI configuration of interest at an infinite distance from the fluoride ion.

The influence of diffuse functions on the F^- reaction pathway is of interest. The RC formed between (E)-MTI (t,c) and F^- at the HF/6-31G(d) level of theory is 276.1 kJ mol^{-1} more stable than the SR, whereas at the HF/6-31+G(d) level of theory the same RC is 161.2 kJ mol^{-1} more stable than the SR. This trend was also observed at the MP2 and B3LYP levels of theory for all MTI and F^- RCs. At all levels of theory, the inclusion of diffuse functions depressed the overall transition barrier by approximately 33 - 52 kJ

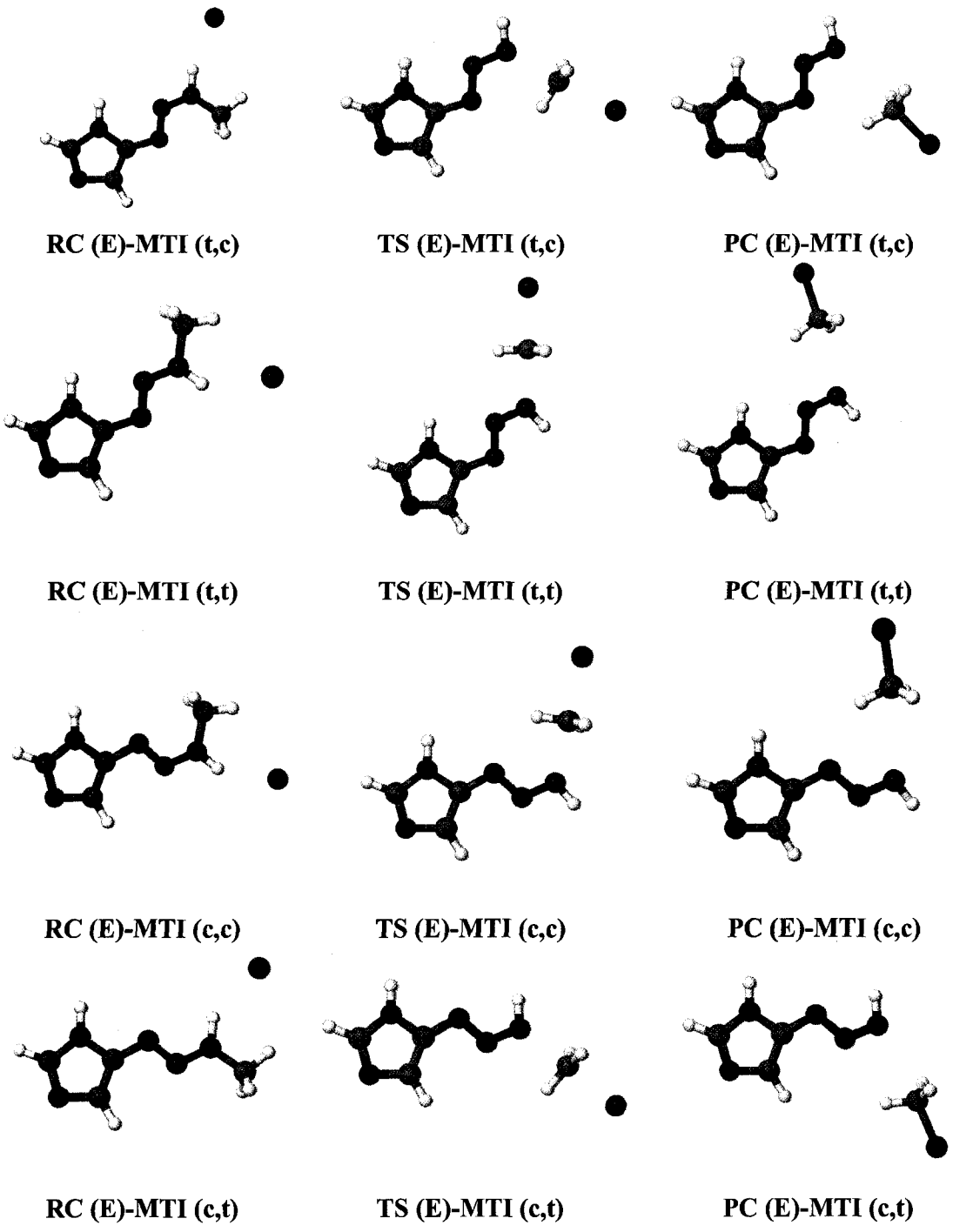

Figure 7.2: The reactant complexes (RC), transition structures (TS) and product complexes (PC) along the (E)-MTI + X^- S_N2 reaction pathway; where X = F, Cl or Br.

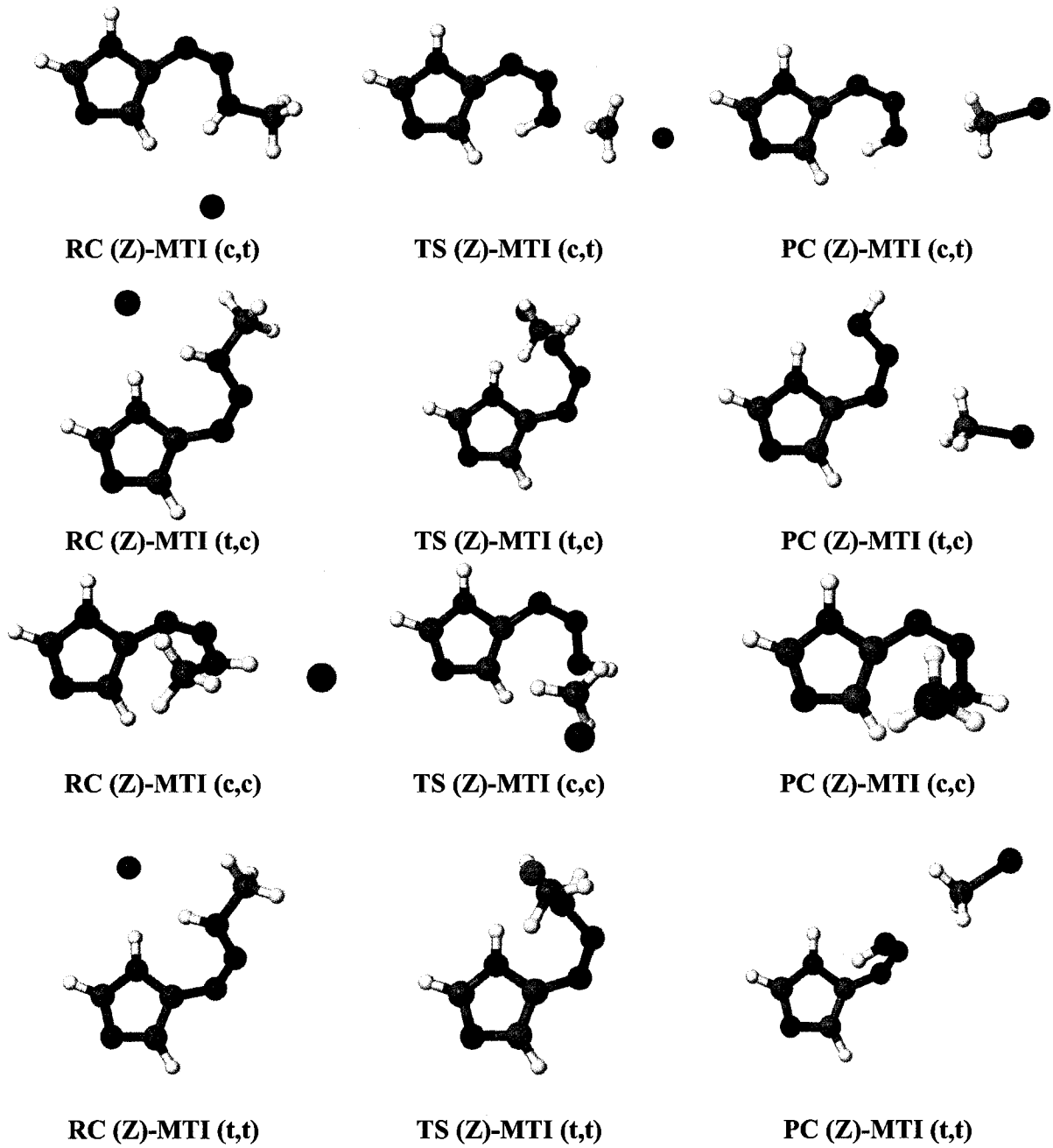

Figure 7.3: The reactant complexes (RC), transition structures (TS) and product complexes (PC) along the (Z)-MTI + X^- S_N2 reaction pathway.

mol^{-1} for all MTI configurations, with the exception of (Z)-MTI (t,c). At the MP2/6-31+G(d) level of theory, inclusion of diffuse functions depressed the overall transition barrier for (Z)-MTI (t,c) + F^- by 110.4 kJ mol^{-1}. At all levels of theory, diffuse functions decreased the stability of the PC and SP along the MTI and F^- S_N2 reaction pathways.

3.1.2 Chloride ion: The reaction between a chloride ion and a configuration of MTI were found to be thermodynamically unfavorable, with the exception of the (Z)-MTI (t,c) + Cl^- reaction pathway (Tables 1 – 8). The (Z)-MTI (t,c) + Cl^- pathway was slightly thermodynamically favorable at MP2 and B3LYP levels of theory (Table 6). The RC, TS and PC of the MTI and chloride ion pathways are analogous to the fluoride pathways. The specific geometrical features of the MTI + Cl^- pathways are reported in Tables S7-9 – S7-15 of the supplemental data section. As was found with the fluoride pathways, the chloride pathways were characterized by a breaking of the C-N_8 bond, making of the Cl-C bond, shortening of the N_8-N_7 bond and lengthening of the N_7-N_6 bond.

Of particular interest is the (Z)-MTI (t,c) and a chloride ion RC, which is 118.0 – 169.9 kJ mol^{-1} more stable than the SR (Table 6). RC (Z)-MTI (t,c) was significantly more stable than the other MTI and chloride ion RC. However, the central barriers were comparable for all MTI configurations, with the exception of the (Z)-MTI (c,c) and a chloride ion pathway. The (Z)-MTI (c,c) and a chloride ion transition barrier was 146.8 – 188.2 kJ mol^{-1} (Table 7). The remaining MTI and chloride ion transition barriers were

160.7 – 246.6 kJ mol^{-1}.

3.1.3 Bromide ion: The MTI and bromide ion reactions were thermodynamically unfavorable (Tables 1 – 8). Structures along the MTI and bromide ion reaction pathway are similar to the chloride pathway. Relevant geometrical features are reported in Tables S7-16 – S7-22 of the supplemental data section. At the HF and B3LYP levels of theory, the 6-31+G(d) basis set decreased the stability of the RC by 10 – 20 kJ mol^{-1} when compared with the 6-31G(d) series. The central barriers were 161.5 – 254.8 kJ mol^{-1} with the exception of the (Z)-MTI (c,c) and bromide ion pathway. The (Z)-MTI (c,c) central barrier was 142.2 – 188.3 kJ mol^{-1} (Table 7), which is significantly less than the other MTI and bromide transition barriers.

Table 1: The relative energy comparison of the (E)-MTI (t,c) and halide ion S_N2 reaction pathways with respect to the separated reactants.

Level of Theory	Relative Energy (kJ mol^{-1})			
	RC	TS	PC	SP
Fluoride				
HF/6-31G(d)	-276.1	-18.1	-202.0	-164.3
HF/6-31+G(d)	-161.2	57.4	-83.2	-50.3
MP2/6-31G(d)	-337.9	-65.9	-222.5	-176.5
MP2/6-31+G(d)	-195.3	34.3	-65.5	-25.0
B3LYP/6-31G(d)	-356.0	-115.9	-265.9	-226.4
B3LYP/6-31+G(d)	-196.4	10.0	-81.1	-49.0
B3LYP/6-31G(d,p)	-364.7	-118.7	-267.6	-227.5
Chloride				
HF/6-31G(d)	-89.6	149.9	95.0	138.6
HF/6-31+G(d)	-79.7	154.7	95.1	132.3
MP2/6-31G(d)	-117.5	110.1	48.4	100.5
MP2/6-31+G(d)	-112.3	109.1	42.0	85.3
B3LYP/6-31G(d)	-118.7	77.4	44.7	94.3
B3LYP/6-31+G(d)	-99.6	92.0	54.3	90.8
B3LYP/6-31G(d,p)	-120.9	76.1	43.8	94.1
Bromide				
HF/6-31G(d)	-92.9	146.0	101.5	147.4
HF/6-31+G(d)	-81.5	157.4	102.4	160.1
MP2/6-31G(d)	-118.0	110.1	69.7	125.9
MP2/6-31+G(d)	-205.6	17.3	-37.1	28.3
B3LYP/6-31G(d)	-121.4	69.6	44.0	95.2
B3LYP/6-31+G(d)	-100.2	90.6	53.3	109.2
B3LYP/6-31G(d,p)	-123.7	67.7	40.5	93.9

Table 2: The relative energy comparison of the (E)-MTI (t,t) and halide ion S_N2 reaction pathways with respect to the separated reactants.

Level of Theory	Relative Energy (kJ mol^{-1})			
	RC	TS	PC	SP
Fluoride				
HF/6-31G(d)	-260.5	-34.4	-212.7	-182.8
HF/6-31+G(d)	-146.0	45.2	-90.1	-62.5
MP2/6-31G(d)	-319.2	-85.8	-239.0	-201.2
MP2/6-31+G(d)	-175.4	18.0	-78.0	-42.0
B3LYP/6-31G(d)	-340.7	-133.0	-278.9	-247.4
B3LYP/6-31+G(d)	-177.5	-4.2	-91.0	-63.2
B3LYP/6-31G(d,p)	-349.6	-136.0	-280.3	-248.4
Chloride				
HF/6-31G(d)	-67.3	141.0	87.0	120.1
HF/6-31+G(d)	-57.7	148.3	90.3	120.2
MP2/6-31G(d)	-92.7	95.7	34.4	75.7
MP2/6-31+G(d)	-87.3	96.8	31.1	68.3
B3LYP/6-31G(d)	-95.9	67.1	35.0	73.3
B3LYP/6-31+G(d)	-77.5	83.2	46.4	76.6
B3LYP/6-31G(d,p)	-98.2	66.0	34.3	73.2
Bromide				
HF/6-31G(d)	-73.0	137.6	94.4	128.9
HF/6-31+G(d)	-61.8	151.9	104.6	148.0
MP2/6-31G(d)	-96.8	97.5	56.8	101.1
MP2/6-31+G(d)	-184.8	6.2	-40.2	11.2
B3LYP/6-31G(d)	-101.2	60.3	35.4	74.2
B3LYP/6-31+G(d)	-80.6	82.6	52.7	94.9
B3LYP/6-31G(d,p)	-103.4	58.1	33.5	72.9

Table 3: The relative energy comparison of the (E)-MTI (c,c) and halide ion S_N2 reaction pathways with respect to the separated reactants.

Level of Theory	Relative Energy (kJ mol^{-1})			
	RC	TS	PC	SP
Fluoride				
HF/6-31G(d)	-271.8	-24.4	-205.1	-167.0
HF/6-31+G(d)	-157.1	50.7	-87.5	-55.0
MP2/6-31G(d)	-328.6	-67.7	-220.1	-172.8
MP2/6-31+G(d)	-186.5	32.3	-64.7	-24.2
B3LYP/6-31G(d)	-348.5	-118.4	-263.7	-222.8
B3LYP/6-31+G(d)	-188.5	6.8	-80.3	-48.3
B3LYP/6-31G(d,p)	-357.0	-120.9	-265.2	-223.6
Chloride				
HF/6-31G(d)	-83.3	144.4	91.7	135.9
HF/6-31+G(d)	-73.6	148.5	91.0	127.7
MP2/6-31G(d)	-108.2	109.6	50.3	104.1
MP2/6-31+G(d)	-103.3	107.5	42.8	86.1
B3LYP/6-31G(d)	-110.9	75.5	46.0	97.9
B3LYP/6-31+G(d)	-91.9	89.4	54.8	91.5
B3LYP/6-31G(d,p)	-112.9	74.3	45.3	98.0
Bromide				
HF/6-31G(d)	-87.6	140.4	98.1	144.7
HF/6-31+G(d)	-76.2	151.0	104.0	155.5
MP2/6-31G(d)	-110.1	109.8	71.3	129.5
MP2/6-31+G(d)	-198.1	15.2	-29.7	29.1
B3LYP/6-31G(d)	-114.5	67.6	44.9	98.8
B3LYP/6-31+G(d)	-93.3	87.8	59.3	109.9
B3LYP/6-31G(d,p)	-116.7	65.8	43.0	97.7

Table 4: The relative energy comparison of the (E)-MTI (c,t) and halide ion S_N2 reaction pathways with respect to the separated reactants.

Level of Theory	Relative Energy (kJ mol^{-1})			
	RC	TS	PC	SP
Fluoride				
HF/6-31G(d)	-264.8	-31.0	-211.8	-181.0
HF/6-31+G(d)	-152.1	47.1	-90.8	-62.1
MP2/6-31G(d)	-317.2	-77.7	-232.8	-194.0
MP2/6-31+G(d)	-176.0	24.8	-74.1	-36.9
B3LYP/6-31G(d)	-339.5	-126.3	-273.3	-240.9
B3LYP/6-31+G(d)	-179.1	0.9	-87.2	-58.6
B3LYP/6-31G(d,p)	-348.2	-129.0	-274.6	-241.7
Chloride				
HF/6-31G(d)	-72.6	142.7	87.1	121.9
HF/6-31+G(d)	-63.7	149.0	89.0	120.5
MP2/6-31G(d)	-94.8	103.3	40.0	82.9
MP2/6-31+G(d)	-90.9	103.1	34.2	73.4
B3LYP/6-31G(d)	-98.5	73.0	40.2	79.8
B3LYP/6-31+G(d)	-80.9	87.8	50.0	81.2
B3LYP/6-31G(d,p)	-100.6	72.1	39.8	79.9
Bromide				
HF/6-31G(d)	-77.8	139.3	94.4	130.6
HF/6-31+G(d)	-67.2	152.5	100.4	148.3
MP2/6-31G(d)	-98.5	99.7	62.4	108.4
MP2/6-31+G(d)	-187.0	6.0	-41.7	16.4
B3LYP/6-31G(d)	-103.4	63.7	40.5	80.7
B3LYP/6-31+G(d)	-83.7	83.3	55.6	99.6
B3LYP/6-31G(d,p)	-105.4	61.3	38.9	79.6

Table 5: The relative energy comparison of the (Z)-MTI (c,t) and halide ion S_N2 reaction pathways with respect to the separated reactants.

Level of Theory	Relative Energy (kJ mol^{-1})			
	RC	TS	PC	SP
Fluoride				
HF/6-31G(d)	-267.9	-26.2	-201.4	-168.5
HF/6-31+G(d)	-150.0	52.0	-81.7	-50.9
MP2/6-31G(d)	-324.3	-303.9	-220.1	-179.1
MP2/6-31+G(d)	-174.8	30.6	-61.9	-22.0
B3LYP/6-31G(d)	-347.5	-120.3	-260.9	-226.4
B3LYP/6-31+G(d)	-172.7	7.0	-76.4	-45.5
B3LYP/6-31G(d,p)	-356.6	-123.0	-262.3	-227.3
Chloride				
HF/6-31G(d)	-66.0	148.3	96.8	134.4
HF/6-31+G(d)	-56.2	154.3	97.4	131.8
MP2/6-31G(d)	-91.9	109.2	51.8	97.9
MP2/6-31+G(d)	-88.5	109.0	45.9	88.2
B3LYP/6-31G(d)	-92.3	79.5	51.5	94.3
B3LYP/6-31+G(d)	-74.9	94.0	60.0	94.3
B3LYP/6-31G(d,p)	-94.9	78.5	50.9	94.3
Bromide				
HF/6-31G(d)	-74.7	144.8	103.9	143.1
HF/6-31+G(d)	-61.6	157.3	110.9	159.6
MP2/6-31G(d)	-98.4	105.6	73.9	123.3
MP2/6-31+G(d)	-186.4	5.0	-25.8	31.2
B3LYP/6-31G(d)	-102.4	72.9	51.5	95.1
B3LYP/6-31+G(d)	-80.2	87.4	65.9	112.6
B3LYP/6-31G(d,p)	-104.2	71.0	49.7	94.1

Table 6: The relative energy comparison of the (Z)-MTI (t,c) and halide ion S_N2 reaction pathways with respect to the separated reactants.

Level of Theory	Relative Energy (kJ mol^{-1})			
	RC	TS	PC	SP
Fluoride				
HF/6-31G(d)	-330.9	-44.9	-263.6	-267.4
HF/6-31+G(d)	-221.8	28.6	-147.0	-147.0
MP2/6-31G(d)	-404.0	-101.2	-290.7	-288.0
MP2/6-31+G(d)	-200.4	-8.0	-135.2	-126.9
B3LYP/6-31G(d)	-430.6	-149.0	-332.1	-328.3
B3LYP/6-31+G(d)	-256.5	-26.8	-149.4	-144.1
B3LYP/6-31G(d,p)	-438.3	-152.6	-335.5	-329.5
Chloride				
HF/6-31G(d)	-130.1	116.3	34.6	35.5
HF/6-31+G(d)	-118.0	121.6	32.2	35.7
MP2/6-31G(d)	-164.0	62.5	-18.9	-11.1
MP2/6-31+G(d)	-160.6	60.2	-27.7	-16.7
B3LYP/6-31G(d)	-166.8	35.2	-19.7	-7.6
B3LYP/6-31+G(d)	-146.3	48.6	-12.8	-4.3
B3LYP/6-31G(d,p)	-169.9	33.0	-22.2	-7.9
Bromide				
HF/6-31G(d)	-135.2	111.5	41.7	44.3
HF/6-31+G(d)	-122.3	120.6	41.3	63.5
MP2/6-31G(d)	-164.1	60.8	3.1	14.4
MP2/6-31+G(d)	-253.5	-36.7	-104.4	-73.7
B3LYP/6-31G(d)	-172.5	26.3	-19.6	-6.7
B3LYP/6-31+G(d)	-149.5	43.1	-12.2	14.1
B3LYP/6-31G(d,p)	-175.8	23.4	-23.3	-8.1

Table 7: The relative energy comparison of the (Z)-MTI (c,c) and halide ion S_N2 reaction pathways with respect to the separated reactants.

Level of Theory	Relative Energy (kJ mol^{-1})			
	RC	TS	PC	SP
Fluoride				
HF/6-31G(d)	-243.8	-32.9	-248.5	-218.1
HF/6-31+G(d)	-130.6	37.8	-133.8	-107.3
MP2/6-31G(d)	-313.5	-84.3	-266.3	-224.9
MP2/6-31+G(d)	-252.1	7.2	-138.2	-76.1
B3LYP/6-31G(d)	-337.0	-135.0	-337.0	-274.0
B3LYP/6-31+G(d)	-258.6	-13.0	-179.1	-99.2
B3LYP/6-31G(d,p)	-345.8	-137.9	-345.8	-275.1
Chloride				
HF/6-31G(d)	-65.8	122.4	49.3	84.7
HF/6-31+G(d)	-56.8	126.7	45.0	75.4
MP2/6-31G(d)	-98.2	78.5	4.7	52.0
MP2/6-31+G(d)	-95.6	74.4	-10.7	34.2
B3LYP/6-31G(d)	-104.1	48.5	7.8	46.7
B3LYP/6-31+G(d)	-85.8	61.0	11.5	40.6
B3LYP/6-31G(d,p)	-106.0	47.4	7.2	46.5
Bromide				
HF/6-31G(d)	-70.9	117.4	56.4	93.5
HF/6-31+G(d)	-59.1	124.9	52.3	103.2
MP2/6-31G(d)	-101.3	76.5	26.3	77.4
MP2/6-31+G(d)	-191.2	-23.6	-91.9	-22.8
B3LYP/6-31G(d)	-108.8	39.4	7.5	47.6
B3LYP/6-31+G(d)	-87.2	55.0	10.1	59.0
B3LYP/6-31G(d,p)	-110.8	37.5	4.5	46.3

Table 8: The relative energy comparison of the (Z)-MTI (t,t) and halide ion S_N2 reaction pathways with respect to the separated reactants.

Level of Theory	Relative Energy (kJ mol^{-1})			
	RC	TS	PC	SP
Fluoride				
HF/6-31G(d)	-333.5	-34.5	-207.8	-174.8
HF/6-31+G(d)	-211.8	43.0	-88.8	-57.8
MP2/6-31G(d)	-395.5	-88.3	-231.0	-190.7
MP2/6-31+G(d)	-240.1	19.1	-75.1	-35.6
B3LYP/6-31G(d)	-418.3	-128.6	-271.3	-237.9
B3LYP/6-31+G(d)	-243.6	-1.9	-86.3	-56.3
B3LYP/6-31G(d,p)	-426.0	-131.7	-273.0	-239.2
Chloride				
HF/6-31G(d)	-119.0	134.3	90.4	128.1
HF/6-31+G(d)	-106.3	140.1	90.4	124.9
MP2/6-31G(d)	-155.4	-	41.2	86.2
MP2/6-31+G(d)	-151.6	-	-	74.7
B3LYP/6-31G(d)	-154.5	63.0	41.6	82.8
B3LYP/6-31+G(d)	-133.3	76.5	50.4	83.5
B3LYP/6-31G(d,p)	-157.4	61.5	40.6	82.4
Bromide				
HF/6-31G(d)	-124.1	130.7	97.6	136.8
HF/6-31+G(d)	-110.5	143.2	104.1	152.7
MP2/6-31G(d)	-155.5	-	63.4	111.6
MP2/6-31+G(d)	-	-	-	114.1
B3LYP/6-31G(d)	-160.2	55.7	41.7	83.6
B3LYP/6-31+G(d)	-136.7	75.2	56.0	101.9
B3LYP/6-31G(d,p)	-163.5	53.4	39.5	82.2

3.2 MTI_T

There are two isomers of MTI_T, E and Z with respect to the N_8-N_7 double bond of the triazene moiety. There are two E configurations and two Z configurations of MTI_T. The relative energy comparisons and geometrical features of these configurations are reported in Chapter 6.

The structures along the MTI_T + X^- reaction pathways follow a similar pattern as the MTI and a halide ion reaction pathways: SR followed by a RC, TS with a flattened methyl group corresponding to inversion of this center, a PC and SP. For the purposes of this discussion the results of the various reactions will be discussed in terms of the halide involved. Similar RC, TS and PC were found for each MTI_T configuration regardless of the halide involved (Figure 7.4). The SR (a halide ion and a MTI_T configuration) and the SP (a halomethane, molecular nitrogen and a 5-imidazolylamide ion) are assumed to be at an infinite distance.

3.2.1 Fluoride ion: The MTI_T and fluoride ion S_N2 reactions were thermodynamically favorable at all levels of theory (Tables 9 – 12). Along the reaction pathway there is breaking of the C-N_8 bond, making of the F-C bond, shortening of the N_8-N_7 bond and breaking of the N_7-N_6 bond. The relevant geometrical features can be found in Tables S7-23 – S7-26 (supplemental data section). RC stability was similarly influenced by diffuse functions as was observed in the MTI and fluoride ion pathways. RC and PC of the (Z)-MTI_T and fluoride ion S_N2 reactions are approximately 20 – 40 kJ

mol^{-1} more stable than the corresponding (E)-MTI_T reactions. Furthermore, the central barriers for the MTI_T and a fluoride ion are significantly less than the corresponding SR. The favorability of the TS in comparison to the SR seems to indicate that even though the central barriers are significant (169.8 – 295.9 kJ mol^{-1}; Tables 9 – 12), this series of reaction would be more likely to occur than the MTI and a fluoride ion S_N2 reactions.

3.2.2 Chloride ion: The reactions between a chloride ion and MTI_T were thermodynamically favorable (Tables 9 – 12). The relevant geometrical features of these reactions are reported in Tables S7-27 – S7-30 (supplemental data section). The same pattern as the fluoride and MTI_T S_N2 reactions was observed. Formation of the RC is more favorable than the SR. There is an influence on the stability of the RC at levels of theory where diffuse functions are included in the basis set. The TS* is characterized by carbon-chloride bond making, carbon-nitrogen bond breaking, N_8-N_7 bond shortening and N_7-N_6 bond breaking. The central barrier associated with the TS is significant (93.8 – 194.6 kJ mol^{-1}; Tables 9 – 12). However, the barrier is less than the corresponding MTI_T and fluoride ion S_N2 reactions and the MTI and chloride ion S_N2 reactions. RC and PC of the (Z)-MTI_T and chloride S_N2 reactions are approximately 30 kJ mol^{-1} more stable than the corresponding (E)-MTI_T reactions.

---

*Distinct RCs were found for each MTI_T configurations and Cl^- combination. The S_N2 reaction pathways for MTI_T and Cl^- appear to coalesce before the TS at the higher levels of theory. A similar finding was observed in an analogous study of dimethyltriazene (21).

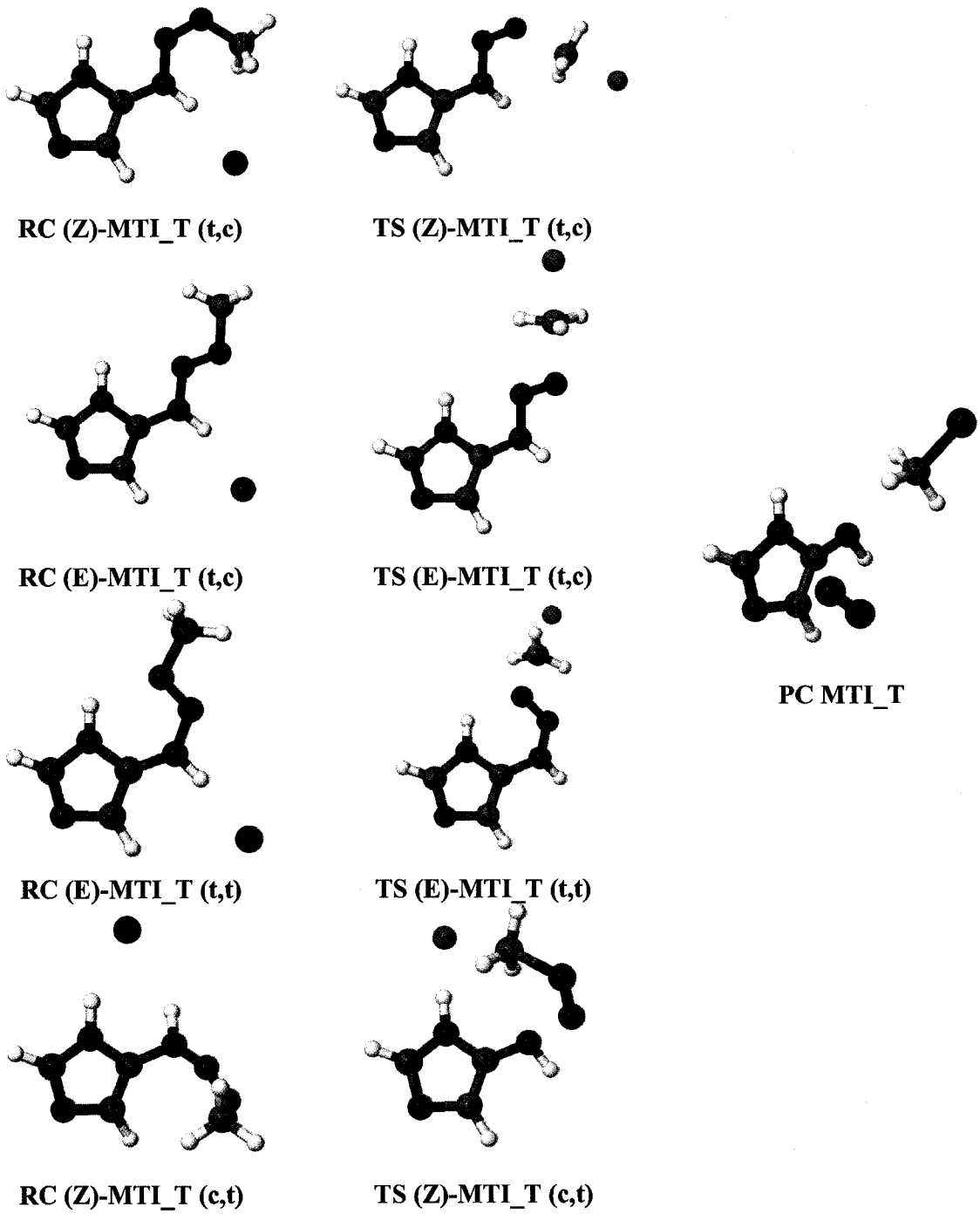

Figure 7.4: The reactant complexes (RC), transition structures (TS) and product complexes (PC) along the MTI_ T + X^- S_N2 reaction pathway.

Table 9: The relative energy comparison of the (Z)-MTI_T (t,c) and halide ion S_N2 reaction pathways with respect to the separated reactants.

Level of Theory	Relative Energy (kJ mol^{-1})			
	RC	TS	PC	SP
Fluoride				
HF/6-31G(d)	-315.2	-19.4	-472.4	-430.5
HF/6-31+G(d)	-196.0	37.2	-362.1	-326.5
MP2/6-31G(d)	-378.0	-105.2	-459.8	-395.3
MP2/6-31+G(d)	-226.2	-29.6	-311.9	-253.6
B3LYP/6-31G(d)	-392.4	-139.2	-446.1	-392.6
B3LYP/6-31+G(d)	-218.4	-30.3	-265.8	-229.1
B3LYP/6-31G(d,p)	-400.7	-143.1	-448.3	-394.2
Chloride				
HF/6-31G(d)	-98.7	85.4	-173.9	-127.6
HF/6-31+G(d)	-87.2	88.0	-182.4	-143.8
MP2/6-31G(d)	-131.7	2.7	-187.2	-118.3
MP2/6-31+G(d)	-125.6	-1.7	-203.7	-143.3
B3LYP/6-31G(d)	-126.3	-10.1	-135.4	-71.9
B3LYP/6-31+G(d)	-106.1	7.0	-132.3	-89.3
B3LYP/6-31G(d,p)	-128.6	-12.0	-137.0	-72.6
Bromide				
HF/6-31G(d)	-106.0	76.1	-167.4	-118.8
HF/6-31+G(d)	-90.3	83.0	-171.7	-116.0
MP2/6-31G(d)	-137.6	-6.0	-166.6	-92.9
MP2/6-31+G(d)	-222.9	-101.3	-280.7	-200.3
B3LYP/6-31G(d)	-134.0	-25.5	-137.8	-71.0
B3LYP/6-31+G(d)	-108.6	-1.4	-131.0	-71.0
B3LYP/6-31G(d,p)	-136.7	-27.7	-140.6	-72.9

Table 10: The relative energy comparison of the (E)-MTI_T (t,c) and halide ion S_N2 reaction pathways with respect to the separated reactants.

Level of Theory	Relative Energy (kJ mol^{-1})			
	RC	TS	PC	SP
Fluoride				
HF/6-31G(d)	-275.1	-5.7	-436.5	-393.4
HF/6-31+G(d)	-157.6	76.9	-317.9	-282.3
MP2/6-31G(d)	-338.4	-61.1	-435.6	-371.1
MP2/6-31+G(d)	-189.4	-	-280.1	-221.8
B3LYP/6-31G(d)	-357.5	-103.5	-418.2	-365.8
B3LYP/6-31+G(d)	-189.8	5.7	-234.4	-197.7
B3LYP/6-31G(d,p)	-366.0	-213.5	-421.1	-368.0
Chloride				
HF/6-31G(d)	-62.0	122.4	-136.9	-90.5
HF/6-31+G(d)	-48.4	132.2	-138.3	-99.6
MP2/6-31G(d)	-107.5	26.9	-163.0	-94.1
MP2/6-31+G(d)	-93.7	30.1	-171.9	-111.5
B3LYP/6-31G(d)	-93.7	16.7	-108.7	-45.2
B3LYP/6-31+G(d)	-73.9	38.5	-100.9	-57.9
B3LYP/6-31G(d,p)	-96.3	14.2	-110.8	-46.4
Bromide				
HF/6-31G(d)	-67.7	113.1	-130.3	-81.8
HF/6-31+G(d)	-52.5	127.1	-127.6	-71.9
MP2/6-31G(d)	-97.8	18.2	-142.4	-68.7
MP2/6-31+G(d)	-182.7	-69.5	-248.9	-168.5
B3LYP/6-31G(d)	-98.6	1.2	-111.1	-44.3
B3LYP/6-31+G(d)	-76.5	30.0	-99.5	-39.6
B3LYP/6-31G(d,p)	-101.3	-1.5	-114.3	-46.6

Table 11: The relative energy comparison of the (E)-MTI_T (t,t) and halide ion S_N2 reaction pathways with respect to the separated reactants.

Level of Theory	Relative Energy (kJ mol^{-1})			
	RC	TS	PC	SP
Fluoride				
HF/6-31G(d)	-280.8	-8.0	-441.7	-398.6
HF/6-31+G(d)	-162.1	75.4	-323.9	-288.2
MP2/6-31G(d)	-350.2	-73.7	-428.3	-363.7
MP2/6-31+G(d)	-202.6	4.9	-277.4	-219.1
B3LYP/6-31G(d)	-367.0	-109.1	-414.9	-362.5
B3LYP/6-31+G(d)	-199.0	2.9	-232.6	-196.0
B3LYP/6-31G(d,p)	-376.0	-113.2	-417.4	-364.3
Chloride				
HF/6-31G(d)	-77.3	117.2	-142.1	-95.7
HF/6-31+G(d)	-63.8	126.3	-144.2	-105.5
MP2/6-31G(d)	-111.2	34.2	-155.7	-86.8
MP2/6-31+G(d)	-107.4	32.8	-169.2	-108.8
B3LYP/6-31G(d)	-111.1	20.0	-105.3	-41.8
B3LYP/6-31+G(d)	-90.8	40.2	-99.1	-56.2
B3LYP/6-31G(d,p)	-113.7	17.9	-107.1	-42.7
Bromide				
HF/6-31G(d)	-81.8	107.9	-135.6	-87.0
HF/6-31+G(d)	-66.8	121.2	-133.5	-77.8
MP2/6-31G(d)	-113.2	25.5	-135.1	-61.4
MP2/6-31+G(d)	-201.2	-66.8	-246.2	-165.8
B3LYP/6-31G(d)	-114.7	4.6	-107.7	-40.9
B3LYP/6-31+G(d)	-92.3	31.8	-97.8	-37.8
B3LYP/6-31G(d,p)	-117.7	2.2	-110.6	-42.9

Table 12: The relative energy comparison of the (Z)-MTI_T (c,c) and halide ion S_N2 reaction pathways with respect to the separated reactants.

Level of Theory	Relative Energy (kJ mol^{-1})			
	RC	TS	PC	SP
Fluoride				
HF/6-31G(d)	-266.5	-95.6	-497.2	-454.2
HF/6-31+G(d)	-220.0	-8.4	-384.8	-349.1
MP2/6-31G(d)	-342.6	-103.2	-477.8	-413.2
MP2/6-31+G(d)	-231.5	-	-326.3	-267.9
B3LYP/6-31G(d)	-393.1	-264.5	-475.2	-422.8
B3LYP/6-31+G(d)	-224.3	-99.9	-294.6	-257.9
B3LYP/6-31G(d,p)	-444.0	-271.0	-478.5	-425.4
Chloride				
HF/6-31G(d)	-107.6	61.7	-197.6	-151.3
HF/6-31+G(d)	-95.4	65.4	-205.0	-166.4
MP2/6-31G(d)	-136.0	-15.3	-205.2	-136.3
MP2/6-31+G(d)	-124.9	-16.0	-218.0	-157.6
B3LYP/6-31G(d)	-138.7	-40.3	-165.6	-102.1
B3LYP/6-31+G(d)	-115.6	-21.7	-161.1	-118.1
B3LYP/6-31G(d,p)	-141.4	-43.2	-168.2	-103.8
Bromide				
HF/6-31G(d)	-113.5	52.4	-191.1	-142.5
HF/6-31+G(d)	-97.4	60.3	-194.4	-138.6
MP2/6-31G(d)	-139.9	-23.9	-184.6	-110.9
MP2/6-31+G(d)	-222.2	-115.6	-295.1	-214.7
B3LYP/6-31G(d)	-145.0	-55.8	-168.1	-101.3
B3LYP/6-31+G(d)	-117.2	-30.2	-159.7	-99.8
B3LYP/6-31G(d,p)	-147.6	-58.9	-171.7	-104.1

3.2.3 Bromide ion: The reactions between bromide and MTI_T were thermodynamically favorable (Table 9 – 12). The relevant geometrical features of these reactions are reported in Tables S7-31 – S7-34 (supplemental data section). The same pattern of bond breaking and making as was exhibited in the corresponding fluoride and chloride reaction pathways was found in the bromide and MTI_T S_N2 reactions. RC and PC of the (Z)-MTI_T and bromide S_N2 reactions are approximately 30 – 40 kJ mol^{-1} more stable than the corresponding (E)-MTI_T reactions. The central barriers associated with the $TS^{\dagger}$ are significant (87.0 – 189.7 kJ mol^{-1}; Tables 9 – 12). However, they are comparable to the MTI_T and chloride central barriers and less than the MTI_T and fluoride central barriers.

4. Conclusions

Two distinct S_N2 reaction pathways involving MTI or MTI_T and various halide ions were investigated as model reaction pathways for DTIC and other triazene containing anti-neoplastic agents. The structures along the MTI and halide ion pathways were analogous to a previous study involving 3-methyltriazene and various halide ions, whereas MTI_T and halide ion pathways were analogous to 1-methyltriazene and various halide ion S_N2 pathway structures (20). The MTI_T and halide ion reaction pathways were more energetically favorable than the MTI and halide ion reaction pathways. The

---

†Distinct RCs were found for each MTI_T configuration and Br^- combination. The S_N2 reaction pathways of MTI_T and Br^- appear to coalesce before the TS at all levels of theory.

MTI and fluoride ion reaction were thermodynamically favorable; however, the MTI and chloride or bromide ion reaction pathways were thermodynamically unfavorable. All of the MTI_T and halide ion reaction pathways were thermodynamically favorable.

Along the S_N2 reaction pathways for MTI or MTI_T and various halide ions the central barriers were significant. However, the central barriers of the MTI studies were more significant than in the MTI_T studies. The height of the central barriers and the favorability of the reaction pathways would indicate that the MTI_T and halide ions are more likely to occur. This would imply that MTI_T is a better candidate to undergo an S_N2 type reaction and may possibly be a better methylating agent when compared with MTI. These findings are in agreement with the results of a previous study of 1- and 3-methyltriazenes and halide ions (20). It was proposed that 1-methyltriazene would preferentially undergo S_N2 type reactions, whereas 3-methyltriazenes would likely undergo a hydrogen transfer to form a 1-methyltriazene to increase the favorability of the resulting S_N2 reaction. It is believed that MTIC and similar compounds would interconvert to a configuration that is capable of undergoing tautomerization (Chapter 6) to form MTIC_T which would then undergo the S_N2 reaction.

CHAPTER EIGHT:
MTIC & MTIC_T S_N2 REACTION PATHWAYS

1. Introduction

Recent work has focused on providing a better understanding of DTIC so as to facilitate the design of triazene compounds that will more readily methylate DNA (11,18,20). Of particular interest are a group of studies that investigated model mechanisms of action by investigating the S_N2 reactions that occur between mono, di- and trimethyltriazene and halide ions (20,21,22) and between MTI, the tautomer of MTI and halide ions (Chapter 7).

As an extension of these previous studies, this study will investigate the S_N2 reaction pathways of 5-(3-methyl-1-triazenyl)imidazole-4-carboxamide and its tautomer (Figure 8.1). The two reaction will be investigated: the S_N2 reaction that occurs between MTIC and halide ions which results in a halomethane and a 5-(4-carboxamido)imidazolyltriazenide ion (Scheme 1); and the S_N2 reaction that occurs between MTIC_T and a halide ion that results in a halomethane, molecular nitrogen and a 5-(4-carboxamido)imidazolylamide ion (Scheme 2). The S_N2 reaction pathway between MTIC_T and halide ions best represents the proposed mechanism of action that triazene containing anti-neoplastic agents utilize.

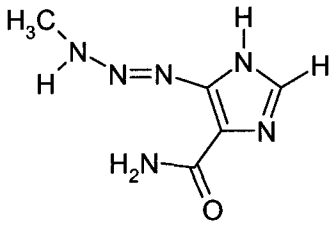

MTIC

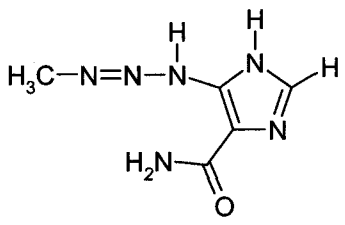

MTIC_T

Figure 8.1: Chemical structure of 5-(3-methyl-1-triazenyl)imidazole-4-carboxamide (MTIC) and its tautomer (MTIC_T).

Scheme 1: The S_N2 reaction between 5-(3-methyl-1-triazeneyl)imidazole-4-carboxamide and a halide ion results in a halomethane and a 5-(4-carboxamido)imidazolyltriazenide ion.

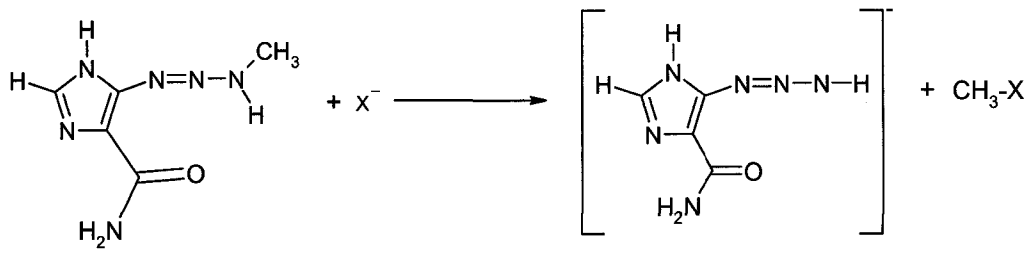

Scheme 2: The S_N2 reaction between the tautomer of 5-(3-methyl-1-triazeneyl)imidazole-4-carboxamide and a halide ion results in a halomethane, molecular nitrogen and a 5-(4-carboxamido)imidazolylamide ion.

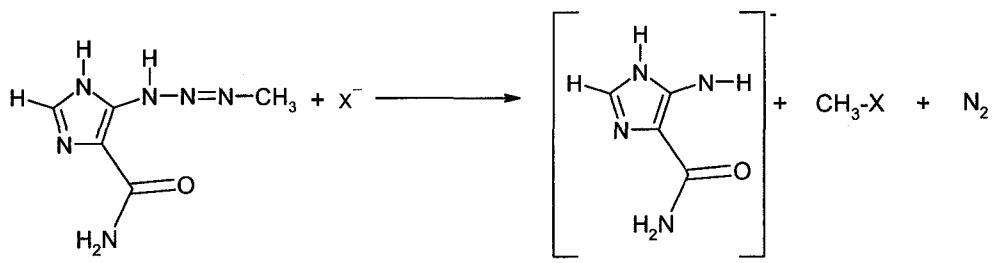

2. Computational Methods

All calculations were performed using the methods specified in Chapter 4. MP2 calculations were not performed because they were too time consuming.

3. Results & Discussion

This study is an extension of a previous study concerning the S_N2 reaction between isomers of 5-(3-methyl-1-triazenyl)imidazole and a halide ion (Chapter 7). For this study, 16 MTIC configurations and six MTIC tautomers were utilized. The MTIC configurations and tautomers were previously characterized (Chapters 4 and 6, respectively). The S_N2 reaction pathways involve a MTIC or MTIC_T configuration and a halide ion (fluoride, chloride or bromide). The S_N2 reactions will be considered in terms of relative energy comparisons. Specific geometrical features along the reaction pathways are presented in the supplemental data section (Tables S8).

3.1 MTIC

There are two isomers of MTIC, E and Z with respect to the nitrogen-nitrogen double bond of the triazene moiety. There are eight (E) configurations and eight (Z) configurations of MTIC. The relative energy comparisons and geometrical features of these configurations are reported in Chapter 4.

Structures along the MTIC + X^- reaction pathways follow the same pattern as was

noted for the MTI S_N2 reaction pathways. Specifically, the structures along the reaction pathways are the separated reactants (SR), followed by a reactant complex (RC), a transition structure (TS) with a flattened methyl group corresponding to inversion of this center, a product complex (PC) and the separated products (SP). For the purposes of this discussion the results of the various reactions will be discussed in terms of the halide involved. Similar RC, TS and PC were found for each (E)-MTIC (Figure 8.2) and (Z)-MTIC (Figure 8.3) configuration regardless of the halide involved. The SR and SP are assumed to be at an infinite distance.

3.1.1 Fluoride: The S_N2 reaction pathways between MTIC and F^- were thermodynamically favorable (Tables 1 – 16). However, in all cases the central barriers are significant. The (E)-MTIC and F^- central barriers were 168.7 – 278.6 kJ mol^{-1} and the (Z)-MTIC and F^- central barriers were 224.7 – 297.9 kJ mol^{-1} (Tables 1 – 16). As was previously observed with the MTI and F^- S_N2 reaction pathways (Chapter 7), the inclusion of diffuse functions significantly decreases the relative stabilization of the RC and PC with respect to the SR by 65.6 – 186.9 kJ mol^{-1} and 112.6 – 193.1 kJ mol^{-1}, respectively (Tables 1 – 18). Furthermore, in comparison with those levels of theory that utilized the 6-31G(d) or 6-31G(d,p) basis sets, the central barriers that were calculated with the 6-31+G(d) basis set are depressed by 37.3 – 60.2 kJ mol^{-1} (Tables 1 – 18).

Along the MTIC and F^- reaction pathways there is clearly making of the C-F bond, breaking of the C-N_8 bond, shortening of the N_8-N_7 bond and lengthening of the N_7-N_6 bond. The formation of the reactant complex does not significantly affect the C-N_8

bond length. However, RC formation does affect the N-N bonds of the triazene moiety. Specifically, when initial MTIC configuration at an infinite distance from F^- is compared to the corresponding RC there is noticeable shortening and lengthening of the N_8-N_7 and N_7-N_6 bond lengths. All important geometrical features pertaining to the MTIC and F^- S_N2 reaction pathways are reported in Tables S8-1 – S8-16 (supplemental data section). The bond lengths of interest (F-C, C-N_8, N_8-N_7 and N_7-N_6 bond lengths) are not significantly affected by the inclusion of diffuse functions (Tables S8-1 – S8-16).

3.1.2 Chloride: The S_N2 reaction pathways between Cl^- and a (E)-MTIC configuration were thermodynamically unfavorable (Tables 1 – 16). The (Z)-MTIC and Cl^- S_N2 reaction pathways were found to be thermodynamically favorable with the exception of the (Z)-MTIC (c,t,c) and (Z)-MTIC (c,t,t) reaction pathways (Tables 1 – 16). The central barriers were significant for all pathways; 125.8 – 254.6 kJ mol$^-$1. Unlike the F^- pathways, the central barriers of the Cl^- pathways were not significantly depressed by the inclusion of diffuse functions (0.6 – 8.6 kJ mol^{-1}; Tables 1 – 16). Nor did the inclusion of diffuse functions have as large an effect on the stabilization of the RC and PC (7.2 – 27.0 kJ mol^{-1} and 2.1 – 16.7 kJ mol^{-1}, respectively; Tables 1 – 16). The RC, TS and PC along the MTIC and Cl^- pathways are analogous to the F^- pathways. The MTIC and Cl^- pathways are characterized by a breaking of the C-N_8 bond, making of the Cl-C bond, shortening of the N_8-N_7 bond and lengthening on the N_7-N_6 bond. The specific geometrical features of the MTIC + Cl^- pathways are reported in Tables S8-17 – S8-32 (supplemental data section).

3.1.3 Bromide: The Br^- and (E)-MTIC reaction pathways were thermodynamically unfavorable. The (Z)-MTIC and Br^- pathways were thermodynamically favorable with the exception of the (Z)-MTIC (c,t,c) and (Z)-MTIC (c,t,t) reaction pathways (Table 1 – 16). The central barriers for all pathways were significant (134.9 – 257.6 kJ mol^{-1}; Tables 1 – 16). Diffuse functions did not significantly depress the central barriers (0.1 – 6.1 kJ mol^{-1}) or significantly affect the stabilization of the RC (9.5 – 28.9 kJ mol^{-1}) or PC (0.3 – 23.2 kJ mol^{-1}) (Tables 1 – 16). The structures along the MTIC and Br^- pathways were analogous to the previous pathways. Breaking of the C-N_8 bond, making of the Br-C bond, shortening of the N_8-N_7 bond and lengthening on the N_7-N_6 bond was found. The specific geometrical features of the MTIC + Br^- pathways are reported in Tables S8-33 – S8-48 (supplemental data section).

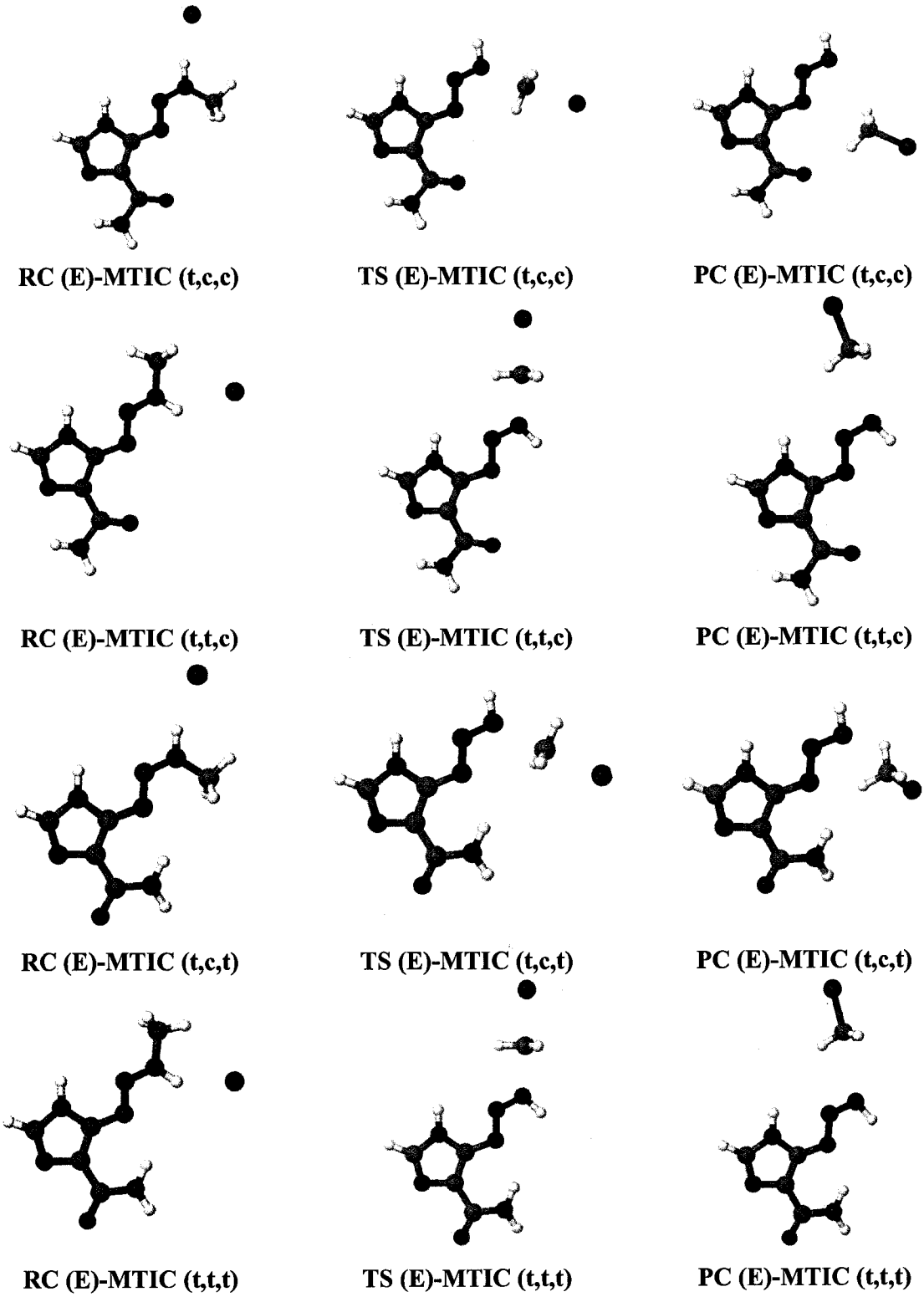

Figure 8.2a: (E)-MTIC and X^-; X = F, Cl, Br, S_N2 reaction pathway structures.

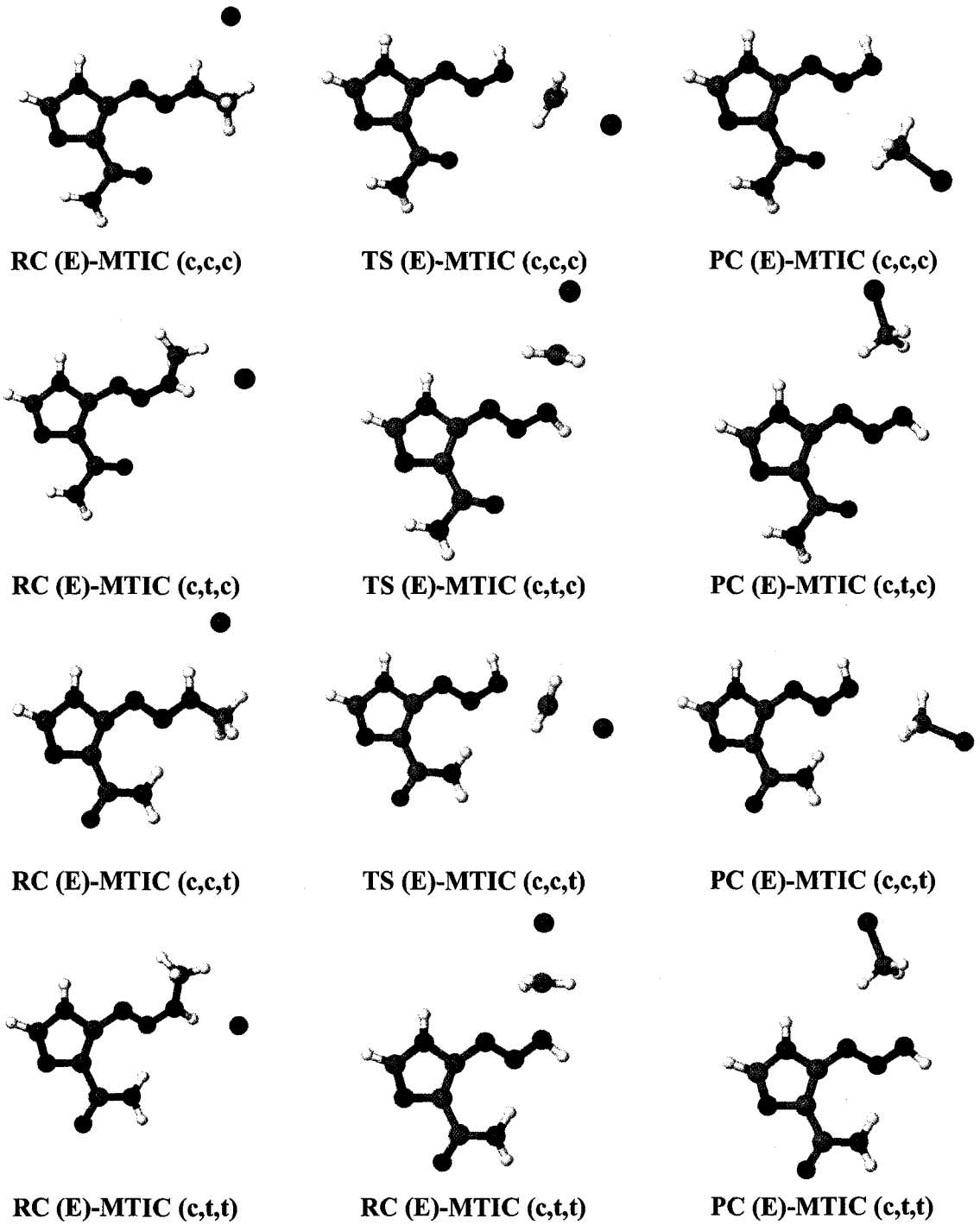

Figure 8.2b: (E)-MTIC and X^-; X = F, Cl, Br, S_N2 reaction pathway structures, continued.

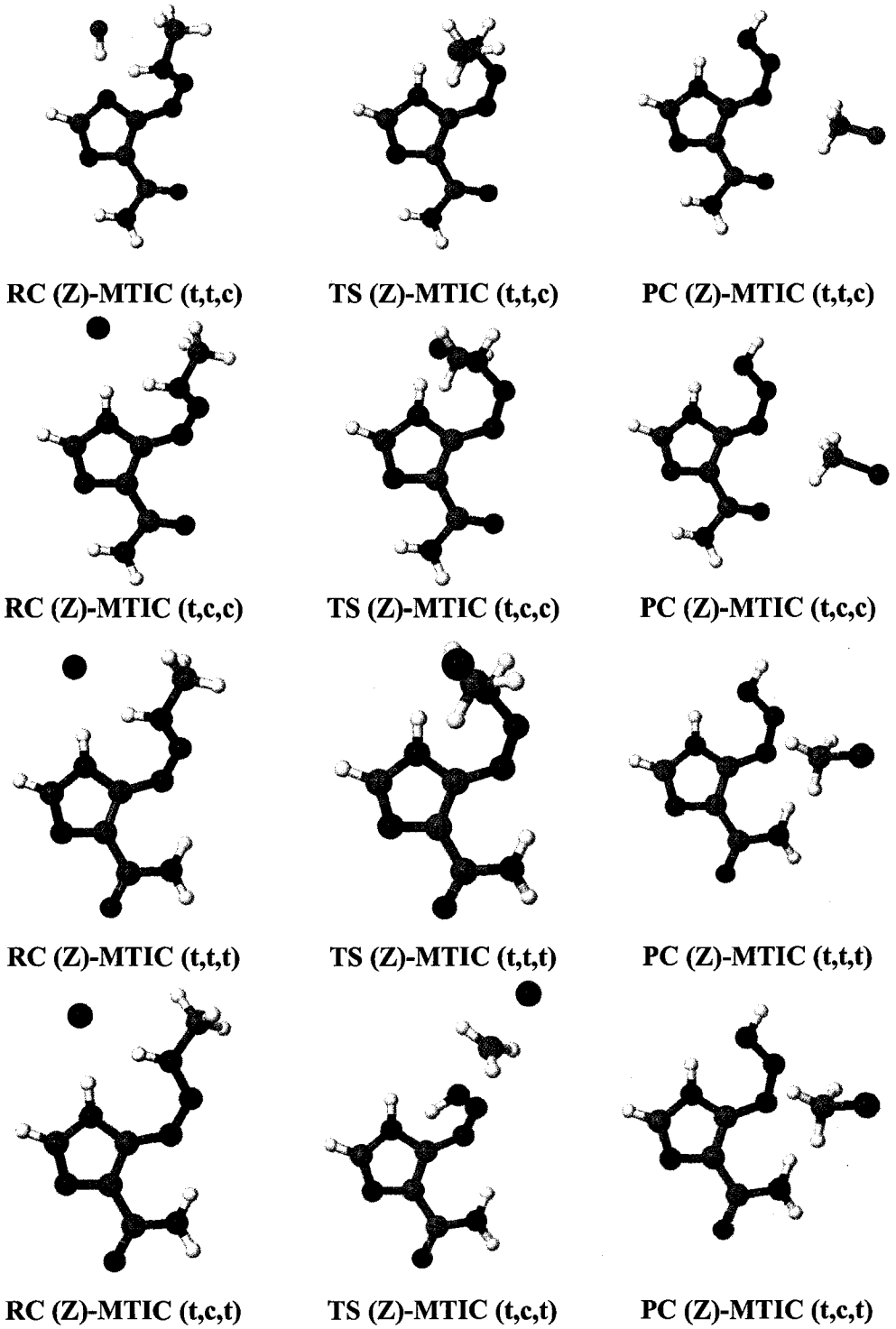

Figure 8.3a: (Z)-MTIC and X^-; X = F, Cl, Br, S_N2 reaction pathway structures.

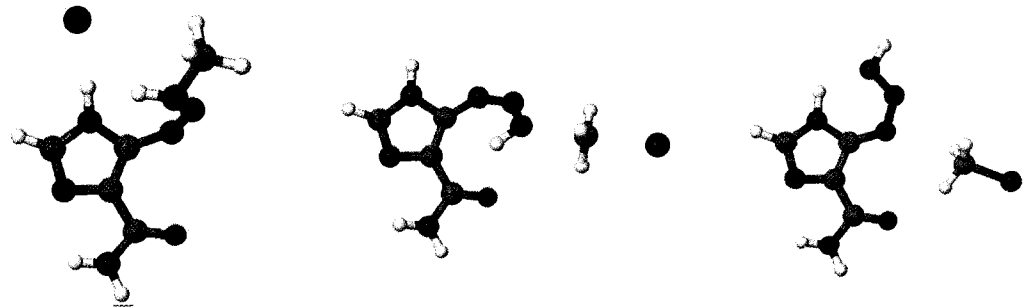

RC (Z)-MTIC (c,t,c) TS (Z)-MTIC (c,t,c) PC (Z)-MTIC (c,t,c)

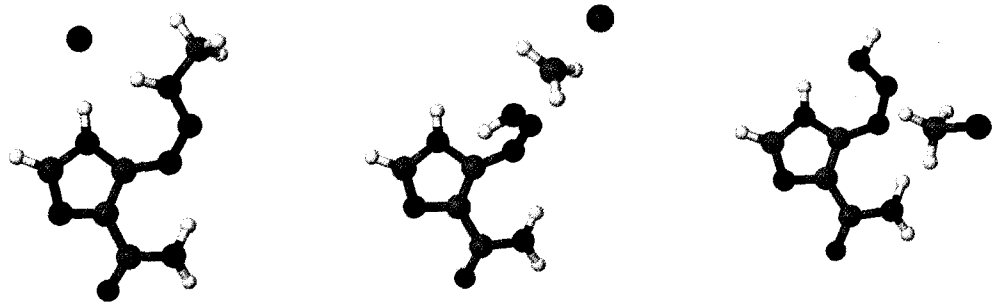

RC (Z)-MTIC (c,t,t) TS (Z)-MTIC (c,t,t) PC (Z)-MTIC (c,t,t)

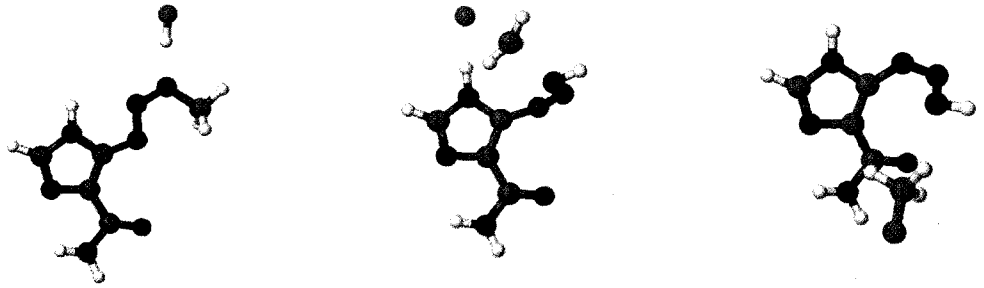

RC (Z)-MTIC (c,c,c) TS (Z)-MTIC (c,c,c) PC (Z)-MTIC (c,c,c)

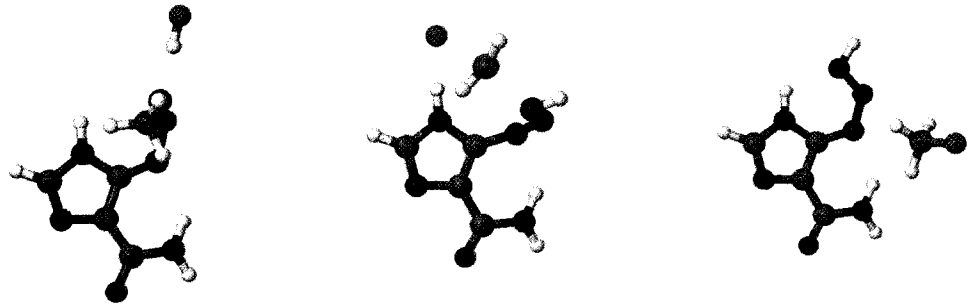

RC (Z)-MTIC (c,c,t) TS (Z)-MTIC (c,c,t) PC (Z)-MTIC (c,c,t)

Figure 8.3b: (Z)-MTIC and X^-; X = F, Cl, Br, S_N2 reaction pathway structures; continued.

Table 1: The relative energy comparison of the stationary points on the (E)-MTIC (t,c,c) and halide ion S_N2 reaction pathways with respect to the separated reactants.

Level of Theory	Relative Energy (kJ mol^{-1})			
	RC	TS	PC	SP
Fluoride				
HF/6-31G(d)	-300.5	-21.9	-236.5	-196.0
HF/6-31+G(d)	-183.1	52.9	-113.7	-76.4
B3LYP/6-31G(d)	-376.0	-118.5	-295.0	-254.2
B3LYP/6-31+G(d)	-211.6	7.6	-105.6	-70.8
B3LYP/6-31G(d,p)	-384.4	-121.1	-295.9	-254.7
Chloride				
HF/6-31G(d)	-97.1	139.4	58.2	106.9
HF/6-31+G(d)	-87.7	146.1	62.5	106.2
B3LYP/6-31G(d)	-126.8	70.8	14.6	66.5
B3LYP/6-31+G(d)	-107.5	87.1	28.9	69.0
B3LYP/6-31G(d,p)	-128.9	70.0	14.4	66.9
Bromide				
HF/6-31G(d)	-99.3	135.4	64.2	115.6
HF/6-31+G(d)	-89.2	147.5	69.5	134.0
B3LYP/6-31G(d)	-128.2	62.9	14.0	67.3
B3LYP/6-31+G(d)	-107.5	84.7	27.7	87.3
B3LYP/6-31G(d,p)	-130.8	61.4	12.4	66.7

Table 2: The relative energy comparison of the stationary points on the (E)-MTIC (t,t,c) and halide ion S_N2 reaction pathways with respect to the separated reactants.

Level of Theory	Relative Energy (kJ mol^{-1})			
	RC	TS	PC	SP
Fluoride				
HF/6-31G(d)	-282.0	-53.2	-247.0	-220.7
HF/6-31+G(d)	-164.7	26.2	-121.2	-96.5
B3LYP/6-31G(d)	-358.1	-148.5	-308.0	-280.1
B3LYP/6-31+G(d)	-189.2	-20.5	-117.3	-92.4
B3LYP/6-31G(d,p)	-366.6	-151.5	-308.7	-280.5
Chloride				
HF/6-31G(d)	-61.5	119.0	53.4	82.2
HF/6-31+G(d)	-54.3	128.0	59.7	86.2
B3LYP/6-31G(d)	-93.7	49.0	7.4	40.6
B3LYP/6-31+G(d)	-74.6	66.1	20.8	47.4
B3LYP/6-31G(d,p)	-96.1	48.3	7.4	41.1
Bromide				
HF/6-31G(d)	-66.4	115.6	61.2	90.9
HF/6-31+G(d)	-56.9	131.3	73.6	114.0
B3LYP/6-31G(d)	-99.1	42.2	8.0	41.5
B3LYP/6-31+G(d)	-77.8	57.1	26.7	65.7
B3LYP/6-31G(d,p)	-101.2	36.8	6.8	40.9

Table 3: The relative energy comparison of the stationary points on the (E)-MTIC (t,c,t) and halide ion S_N2 reaction pathways with respect to the separated reactants.

Level of Theory	Relative Energy (kJ mol^{-1})			
	RC	TS	PC	SP
Fluoride				
HF/6-31G(d)	-335.5	-66.3	-270.2	-243.6
HF/6-31+G(d)	-216.8	10.0	-147.9	-123.5
B3LYP/6-31G(d)	-405.6	-157.2	-322.7	-294.2
B3LYP/6-31+G(d)	-239.2	-31.7	-135.7	-112.1
B3LYP/6-31G(d,p)	-414.2	-159.8	-323.7	-294.9
Chloride				
HF/6-31G(d)	-120.5	100.5	29.8	59.3
HF/6-31+G(d)	-109.9	107.2	32.7	59.2
B3LYP/6-31G(d)	-149.1	36.2	-8.0	26.5
B3LYP/6-31+G(d)	-129.4	51.2	2.2	27.7
B3LYP/6-31G(d,p)	-151.4	35.5	-8.2	26.7
Bromide				
HF/6-31G(d)	-123.0	96.9	37.2	68.0
HF/6-31+G(d)	-111.1	108.7	39.3	87.0
B3LYP/6-31G(d)	-150.8	28.5	-7.8	27.4
B3LYP/6-31+G(d)	-129.4	48.4	5.3	46.1
B3LYP/6-31G(d,p)	-153.6	27.1	-9.2	26.5

Table 4: The relative energy comparison of the stationary points on the (E)-MTIC (t,t,t) and halide ion S_N2 reaction pathways with respect to the separated reactants.

Level of Theory	Relative Energy (kJ mol^{-1})			
	RC	TS	PC	SP
Fluoride				
HF/6-31G(d)	-327.2	-81.3	-283.1	-259.5
HF/6-31+G(d)	-210.6	-1.9	-156.4	-133.2
B3LYP/6-31G(d)	-395.6	-171.6	-338.4	-312.2
B3LYP/6-31+G(d)	-230.6	-44.3	-147.4	-123.8
B3LYP/6-31G(d,p)	-405.5	-174.7	-339.4	-312.9
Chloride				
HF/6-31G(d)	-103.3	89.3	17.6	43.3
HF/6-31+G(d)	-92.9	98.9	24.8	49.5
B3LYP/6-31G(d)	-131.6	24.4	-22.6	8.5
B3LYP/6-31+G(d)	-113.5	41.6	-9.0	16.0
B3LYP/6-31G(d,p)	-134.1	23.5	-22.8	8.8
Bromide				
HF/6-31G(d)	-107.6	86.0	25.5	52.1
HF/6-31+G(d)	-95.5	102.3	38.6	77.3
B3LYP/6-31G(d)	-135.3	17.5	-22.1	9.4
B3LYP/6-31+G(d)	-114.5	41.2	-3.4	34.3
B3LYP/6-31G(d,p)	-138.0	15.9	-23.8	8.5

Table 5: The relative energy comparison of the stationary points on the (E)-MTIC (c,c,c) and halide ion S_N2 reaction pathways with respect to the separated reactants.

Level of Theory	Relative Energy (kJ mol^{-1})			
	RC	TS	PC	SP
Fluoride				
HF/6-31G(d)	-280.0	-30.6	-229.4	-194.1
HF/6-31+G(d)	-163.0	48.4	-102.8	-68.9
B3LYP/6-31G(d)	-352.6	-126.1	-292.1	-255.6
B3LYP/6-31+G(d)	-187.7	1.5	-99.8	-67.3
B3LYP/6-31G(d,p)	-360.8	-128.4	-292.9	-255.7
Chloride				
HF/6-31G(d)	-71.6	138.4	66.1	108.8
HF/6-31+G(d)	-61.7	147.6	74.2	113.8
B3LYP/6-31G(d)	-100.6	69.6	18.1	65.1
B3LYP/6-31+G(d)	-81.9	86.7	34.8	72.5
B3LYP/6-31G(d,p)	-102.5	69.2	18.1	65.9
Bromide				
HF/6-31G(d)	-76.3	134.8	72.5	117.5
HF/6-31+G(d)	-65.4	150.7	85.1	141.6
B3LYP/6-31G(d)	-104.7	62.5	17.8	66.0
B3LYP/6-31+G(d)	-84.6	85.8	37.3	90.9
B3LYP/6-31G(d,p)	-106.8	61.3	16.5	65.6

Table 6: The relative energy comparison of the stationary points on the (E)-MTIC (c,t,c) and halide ion S_N2 reaction pathways with respect to the separated reactants.

Level of Theory	Relative Energy (kJ mol^{-1})			
	RC	TS	PC	SP
Fluoride				
HF/6-31G(d)	-274.0	-29.9	-222.8	-187.7
HF/6-31+G(d)	-154.9	46.6	-99.2	-69.0
B3LYP/6-31G(d)	-352.4	-126.1	-280.9	-243.4
B3LYP/6-31+G(d)	-185.8	0.9	-92.6	-62.9
B3LYP/6-31G(d,p)	-360.6	-128.4	-281.7	-243.7
Chloride				
HF/6-31G(d)	-74.7	135.1	74.8	115.1
HF/6-31+G(d)	-64.7	143.0	79.7	113.7
B3LYP/6-31G(d)	-103.9	65.3	30.1	77.3
B3LYP/6-31+G(d)	-84.5	82.4	43.1	76.9
B3LYP/6-31G(d,p)	-105.9	64.6	30.0	77.9
Bromide				
HF/6-31G(d)	-79.3	131.1	81.4	123.9
HF/6-31+G(d)	-67.5	145.2	83.8	141.5
B3LYP/6-31G(d)	-108.0	57.6	1.5	78.1
B3LYP/6-31+G(d)	-86.2	80.3	23.3	95.3
B3LYP/6-31G(d,p)	-110.2	56.1	0.1	77.7

Table 7: The relative energy comparison of the stationary points on the (E)-MTIC (c,c,t) and halide ion S_N2 reaction pathways with respect to the separated reactants.

Level of Theory	Relative Energy (kJ mol^{-1})			
	RC	TS	PC	SP
Fluoride				
HF/6-31G(d)	-319.5	-71.6	-275.1	-251.6
HF/6-31+G(d)	-202.3	7.0	-149.4	-127.0
B3LYP/6-31G(d)	-390.0	-164.4	-332.2	-307.0
B3LYP/6-31+G(d)	-224.4	-37.5	-142.7	-120.2
B3LYP/6-31G(d,p)	-399.2	-167.6	-333.7	-308.3
Chloride				
HF/6-31G(d)	-100.6	99.1	25.9	51.3
HF/6-31+G(d)	-90.7	107.7	31.9	55.7
B3LYP/6-31G(d)	-130.1	31.9	-15.9	13.7
B3LYP/6-31+G(d)	-111.7	48.4	-4.0	19.6
B3LYP/6-31G(d,p)	-133.1	30.6	-16.5	13.3
Bromide				
HF/6-31G(d)	-105.0	95.7	33.8	60.0
HF/6-31+G(d)	-94.1	111.0	46.9	83.5
B3LYP/6-31G(d)	-134.0	24.7	-15.4	14.6
B3LYP/6-31+G(d)	-113.9	48.2	2.4	37.9
B3LYP/6-31G(d,p)	-137.2	22.7	-17.4	13.1

Table 8: The relative energy comparison of the stationary points on the (E)-MTIC (c,t,t) and halide ion S_N2 reaction pathways with respect to the separated reactants.

Level of Theory	Relative Energy (kJ mol^{-1})			
	RC	TS	PC	SP
Fluoride				
HF/6-31G(d)	-327.5	-64.7	-266.3	-235.3
HF/6-31+G(d)	-209.0	11.7	-153.7	-115.6
B3LYP/6-31G(d)	-400.2	-157.0	-322.2	-287.9
B3LYP/6-31+G(d)	-234.2	-31.4	-134.3	-107.4
B3LYP/6-31G(d,p)	-409.3	-159.9	-323.9	-289.1
Chloride				
HF/6-31G(d)	-113.7	100.9	32.3	67.6
HF/6-31+G(d)	-103.1	107.8	36.6	67.1
B3LYP/6-31G(d)	-143.5	34.8	-9.5	32.8
B3LYP/6-31+G(d)	-123.9	50.3	2.4	32.4
B3LYP/6-31G(d,p)	-145.9	33.4	-10.3	32.5
Bromide				
HF/6-31G(d)	-116.4	97.0	39.3	76.4
HF/6-31+G(d)	-104.3	110.0	50.4	94.9
B3LYP/6-31G(d)	-145.2	27.2	-9.8	33.6
B3LYP/6-31+G(d)	-124.0	48.5	7.5	50.8
B3LYP/6-31G(d,p)	-148.3	25.0	-11.9	32.3

Table 9: The relative energy comparison of the stationary points on the (Z)-MTIC (t,t,c) and halide ion S_N2 reaction pathways with respect to the separated reactants.

Level of Theory	Relative Energy (kJ mol^{-1})			
	RC	TS	PC	SP
Fluoride				
HF/6-31G(d)	-377.6	-58.4	-305.5	-304.7
HF/6-31+G(d)	-261.2	12.6	-187.6	-183.1
B3LYP/6-31G(d)	-455.4	-165.7	-372.6	-364.9
B3LYP/6-31+G(d)	-276.6	-42.1	-186.3	-177.1
B3LYP/6-31G(d,p)	-463.5	-169.2	-361.2	-366.2
Chloride				
HF/6-31G(d)	-149.5	99.1	-9.8	-1.9
HF/6-31+G(d)	-141.3	103.7	-10.6	-0.4
B3LYP/6-31G(d)	-182.6	17.5	-61.9	-44.2
B3LYP/6-31+G(d)	-161.6	32.3	-51.1	-37.3
B3LYP/6-31G(d,p)	-185.6	15.4	-64.5	-44.6
Bromide				
HF/6-31G(d)	-155.7	94.3	-3.4	6.9
HF/6-31+G(d)	-147.1	102.5	-3.4	27.3
B3LYP/6-31G(d)	-189.0	8.4	-62.1	-43.4
B3LYP/6-31+G(d)	-165.9	26.7	-52.2	-18.9
B3LYP/6-31G(d,p)	-192.3	5.7	-65.9	-44.8

Table 10: The relative energy comparison of the stationary points on the (Z)-MTIC (t,c,c) and halide ion S_N2 reaction pathways with respect to the separated reactants.

Level of Theory	Relative Energy (kJ mol^{-1})			
	RC	TS	PC	SP
Fluoride				
HF/6-31G(d)	-334.3	-61.5	-308.9	-308.1
HF/6-31+G(d)	-212.1	12.6	-187.6	-183.1
B3LYP/6-31G(d)	-455.5	-164.9	-372.8	-364.9
B3LYP/6-31+G(d)	-276.6	-42.1	-186.3	-177.1
B3LYP/6-31G(d,p)	-463.5	-168.7	-361.2	-366.2
Chloride				
HF/6-31G(d)	-153.0	96.3	-13.2	-5.3
HF/6-31+G(d)	-141.3	103.7	-10.6	-0.4
B3LYP/6-31G(d)	-182.1	18.0	-61.9	-44.2
B3LYP/6-31+G(d)	-161.8	32.5	-51.1	-37.3
B3LYP/6-31G(d,p)	-185.3	15.7	-64.5	-44.6
Bromide				
HF/6-31G(d)	-159.3	91.5	-6.8	3.5
HF/6-31+G(d)	-147.1	102.5	-3.4	27.3
B3LYP/6-31G(d)	-188.5	9.1	-62.1	-43.4
B3LYP/6-31+G(d)	-165.9	26.9	-52.2	-18.9
B3LYP/6-31G(d,p)	-192.3	6.1	-65.9	-44.8

Table 11: The relative energy comparison of the stationary points on the (Z)-MTIC (t,t,t) and halide ion S_N2 reaction pathways with respect to the separated reactants.

Level of Theory	Relative Energy (kJ mol^{-1})			
	RC	TS	PC	SP
Fluoride				
HF/6-31G(d)	-356.5	-67.0	-315.4	-303.8
HF/6-31+G(d)	-241.7	7.9	-191.3	-177.1
B3LYP/6-31G(d)	-457.8	-169.8	-373.7	-363.7
B3LYP/6-31+G(d)	-280.9	-46.3	-187.1	-175.8
B3LYP/6-31G(d,p)	-466.0	-173.7	-376.5	-365.4
Chloride				
HF/6-31G(d)	-145.3	87.8	-16.0	-0.9
HF/6-31+G(d)	-130.1	97.4	-11.3	5.6
B3LYP/6-31G(d)	-184.2	12.6	-59.0	-43.0
B3LYP/6-31+G(d)	-162.8	27.3	-49.9	-35.9
B3LYP/6-31G(d,p)	-188.2	10.5	-61.5	-43.8
Bromide				
HF/6-31G(d)	-150.7	83.1	-8.4	7.9
HF/6-31+G(d)	-135.1	96.3	-6.7	33.4
B3LYP/6-31G(d)	-189.7	3.7	-58.8	-42.2
B3LYP/6-31+G(d)	-166.7	22.0	-52.7	-17.6
B3LYP/6-31G(d,p)	-194.0	0.8	-61.9	-44.1

Table 12: The relative energy comparison of the stationary points on the (Z)-MTIC (t,c,t) and halide ion S_N2 reaction pathways with respect to the separated reactants.

Level of Theory	Relative Energy (kJ mol^{-1})			
	RC	TS	PC	SP
Fluoride				
HF/6-31G(d)	-365.9	-90.0	-331.7	-320.1
HF/6-31+G(d)	-244.4	-12.8	-210.5	-196.2
B3LYP/6-31G(d)	-473.6	-180.6	-389.5	-379.5
B3LYP/6-31+G(d)	-297.5	-55.0	-203.7	-192.3
B3LYP/6-31G(d,p)	-393.8	-183.9	-392.3	-381.2
Chloride				
HF/6-31G(d)	-47.3	80.7	-32.3	-17.2
HF/6-31+G(d)	-37.9	87.9	-30.5	-13.6
B3LYP/6-31G(d)	-199.9	15.4	-74.8	-58.8
B3LYP/6-31+G(d)	-179.3	30.6	-66.5	-52.5
B3LYP/6-31G(d,p)	-204.0	13.9	-77.3	-59.6
Bromide				
HF/6-31G(d)	-167.0	77.3	-24.7	-8.4
HF/6-31+G(d)	-154.3	90.9	-25.9	14.2
B3LYP/6-31G(d)	-205.6	8.4	-74.5	-57.9
B3LYP/6-31+G(d)	-183.3	29.2	-69.3	-34.2
B3LYP/6-31G(d,p)	-209.9	6.2	-77.7	-59.9

Table 13: The relative energy comparison of the stationary points on the (Z)-MTIC (c,t,c) and halide ion S_N2 reaction pathways with respect to the separated reactants.

Level of Theory	Relative Energy (kJ mol^{-1})			
	RC	TS	PC	SP
Fluoride				
HF/6-31G(d)	-260.8	-19.0	-206.3	-171.9
HF/6-31+G(d)	-195.2	58.5	-81.9	-49.1
B3LYP/6-31G(d)	-393.7	-102.8	-256.8	-221.5
B3LYP/6-31+G(d)	-216.6	20.9	-71.1	-39.2
B3LYP/6-31G(d,p)	-330.6	-104.6	-256.7	-220.8
Chloride				
HF/6-31G(d)	-102.4	152.2	37.3	131.0
HF/6-31+G(d)	-91.3	159.1	39.4	133.6
B3LYP/6-31G(d)	-120.9	94.2	-0.1	99.1
B3LYP/6-31+G(d)	-101.7	106.6	8.8	100.6
B3LYP/6-31G(d,p)	-122.6	94.3	-1.4	100.8
Bromide				
HF/6-31G(d)	-108.6	148.5	43.7	139.7
HF/6-31+G(d)	-97.0	160.6	46.7	161.4
B3LYP/6-31G(d)	-127.3	87.1	-0.4	100.0
B3LYP/6-31+G(d)	-105.9	103.8	7.8	118.9
B3LYP/6-31G(d,p)	-129.2	86.6	-2.9	100.5

Table 14: The relative energy comparison of the stationary points on the (Z)-MTIC (c,t,t) and halide ion S_N2 reaction pathways with respect to the separated reactants.

Level of Theory	Relative Energy (kJ mol^{-1})			
	RC	TS	PC	SP
Fluoride				
HF/6-31G(d)	-348.4	-72.2	-268.3	-241.6
HF/6-31+G(d)	-225.2	6.4	-142.7	-116.8
B3LYP/6-31G(d)	-460.0	-167.0	-330.6	-303.0
B3LYP/6-31+G(d)	-281.3	-38.9	-139.7	-114.7
B3LYP/6-31G(d,p)	-467.9	-170.0	-332.0	-304.1
Chloride				
HF/6-31G(d)	-29.6	98.5	-14.5	61.3
HF/6-31+G(d)	-18.5	107.1	-11.3	65.9
B3LYP/6-31G(d)	-186.3	29.0	-61.1	17.7
B3LYP/6-31+G(d)	-163.2	46.8	-50.3	25.1
B3LYP/6-31G(d,p)	-190.2	27.8	-63.4	17.6
Bromide				
HF/6-31G(d)	-149.3	95.0	-7.0	70.1
HF/6-31+G(d)	-135.1	110.1	-6.7	93.7
B3LYP/6-31G(d)	-192.0	22.0	-60.9	18.5
B3LYP/6-31+G(d)	-167.1	45.3	-53.2	43.5
B3LYP/6-31G(d,p)	-196.0	20.0	-63.8	17.3

Table 15: The relative energy comparison of the stationary points on the (Z)-MTIC (c,c,c) and halide ion S_N2 reaction pathways with respect to the separated reactants.

Level of Theory	Relative Energy (kJ mol^{-1})			
	RC	TS	PC	SP
Fluoride				
HF/6-31G(d)	-376.3	-58.3	-250.5	-221.1
HF/6-31+G(d)	-261.4	17.9	-182.3	-103.6
B3LYP/6-31G(d)	-436.2	-172.6	-296.7	-265.7
B3LYP/6-31+G(d)	-275.6	-26.6	-112.2	-86.1
B3LYP/6-31G(d,p)	-444.5	-175.0	-297.3	-265.8
Chloride				
HF/6-31G(d)	-172.9	100.0	47.8	81.8
HF/6-31+G(d)	-166.0	109.0	-5.3	79.0
B3LYP/6-31G(d)	-186.9	29.5	16.1	55.0
B3LYP/6-31+G(d)	-171.5	48.0	24.4	53.7
B3LYP/6-31G(d,p)	-189.0	27.9	16.3	55.8
Bromide				
HF/6-31G(d)	-175.1	95.3	55.1	90.5
HF/6-31+G(d)	-167.5	107.8	1.9	106.8
B3LYP/6-31G(d)	-188.4	20.6	-50.6	55.8
B3LYP/6-31+G(d)	-171.4	42.5	-36.6	72.1
B3LYP/6-31G(d,p)	-190.9	18.3	-53.8	55.5

Table 16: The relative energy comparison of the stationary points on the (Z)-MTIC (c,c,t) and halide ion S_N2 reaction pathways with respect to the separated reactants.

Level of Theory	Relative Energy (kJ mol^{-1})			
	RC	TS	PC	SP
Fluoride				
HF/6-31G(d)	-322.6	-94.3	-348.0	-308.6
HF/6-31+G(d)	-288.9	-25.3	-224.5	-182.7
B3LYP/6-31G(d)	-464.3	-214.0	-403.9	-365.8
B3LYP/6-31+G(d)	-304.0	-73.2	-213.9	-174.2
B3LYP/6-31G(d,p)	-473.2	-217.5	-406.6	-366.8
Chloride				
HF/6-31G(d)	-63.6	55.2	-48.5	-33.4
HF/6-31+G(d)	-51.6	64.3	-44.4	-27.5
B3LYP/6-31G(d)	-214.3	-17.5	-89.1	-73.2
B3LYP/6-31+G(d)	-189.7	0.5	-76.8	-62.8
B3LYP/6-31G(d,p)	-218.3	-19.6	-91.5	-73.9
Bromide				
HF/6-31G(d)	-183.3	50.5	-41.0	-24.7
HF/6-31+G(d)	-168.3	63.2	-39.9	0.3
B3LYP/6-31G(d)	-220.0	-26.4	-88.9	-72.3
B3LYP/6-31+G(d)	-193.6	-4.8	-79.6	-44.5
B3LYP/6-31G(d,p)	-224.1	-29.2	-91.9	-74.1

3.2 MTIC_T

There are two isomers of MTIC_T, (E) and (Z) with respect to the N_8-N_7 double bond of the triazene moiety (Chapter 6). There are four (E) configurations and two (Z) configurations of MTIC_T. The relative energy comparisons and geometrical features of these configurations are reported in Chapter 6.

A similar pattern of structures is followed along the MTIC_T + X^- reaction pathways as was found for the MTIC + X^- reaction pathways. Specifically, the SR form a RC, which then proceeds to a TS with a flattened methyl group corresponding to inversion of the center. A PC is then formed followed by the SP. The SR and the SP are assumed to be at an infinite distance. Similar RC, TS and PC were found for each MTIC_T configuration regardless of the halide involved (Figure 8.4). For the purposes of this discussion the results of the various reactions will be discussed in terms of the halide involved.

3.2.1 Fluoride: The MTIC_T and F^- S_N2 reaction pathways were thermodynamically favorable at all levels of theory (Tables 17 – 22). While the central barriers are significant (102.9 – 308.1 kJ mol^{-1}) the formation of the RC, PC and SP is 130.0 – 453.3 kJ mol^{-1}, 269.0 – 548.5 kJ mol^{-1} and 238.8 – 514.4 kJ mol^{-1} more favorable than the SR, respectively (Tables 17 – 22). As was previously observed with the MTIC and F^- reaction pathways, the inclusion of diffuse functions in the MTIC_T and F^- reaction pathways depressed the central barriers and affected the relative stability of the RC, PC and SP with respect to the SR (Tables 17 - 22). Along the reaction pathways

there is breaking of the C-N_8 bond, making of the F-C bond, shortening of the N_8-N_7 bond and breaking of the N_7-N_6 bond. Relevant geometrical features are reported in Tables S8-49 – S8-54 (supplemental data section).

3.2.2 Chloride: The MTIC_T and Cl^- reaction pathways were thermodynamically favorable (Tables 17 – 22). Central barriers for (Z)-MTIC_T (t,c,c), (E)-MTIC_T (t,c,c) and (E)-MTIC_T (t,c,t) were 19.2 – 56.6 kJ mol^{-1} (Tables 17 - 22). Central barriers for (Z)-MTIC_T (t,t,c), (E)-MTIC_T (t,t,c) and (E)-MTIC_T (t,t,t) were 69.8 – 173.5 kJ mol^{-1} (Tables 17 - 22). The S_N2 reaction pathways of MTIC_T and Cl^- appear to coalesce at all levels of theory. This trend was previously observed in the MTI_T and X^- S_N2 reaction pathways (Chapter 7) and an analogous study of dimethyltriazene (21). The inclusion of diffuse functions did not have a significant affect on the central barriers or the relative stability of the RC, PC or SP with respect to the SR (Tables 17 - 22). Breaking of the C-N_8 bond, making of the Cl-C bond, shortening of the N_8-N_7 bond and breaking of the N_7-N_6 bond was found along the reaction pathways. Relevant geometrical features are reported in Tables S8-55 – S8-60 (supplemental data section).

3.2.3 Bromide: The MTIC_T and Br^- S_N2 reaction pathways were thermodynamically favorable (Tables 17 – 22). The central barriers were 43.5 – 169.4 kJ mol^{-1}, with the exception of (Z)-MTIC_T (t,c,c). The central barrier of (Z)-MTIC_T (t,c,c) and Br^- was 4.2 – 12.0 kJ mol^{-1} (Table 17). As was previously observed for the MTIC_T and Cl^- pathways, the S_N2 reaction pathways of MTIC_T and Br^- appear to

coalesce at all levels of theory. The inclusion of diffuse functions did not significantly depress the central barriers or affect the relative stability of the RC, PC or SP with respect to the SR (Tables 17 – 22). Along the MTIC_T and Br^- S_N2 reaction pathways, breaking of the C-N_8 bond, making of the Br-C bond, shortening of the N_8-N_7 bond and breaking of the N_7-N_6 bond was found. Relevant geometrical features area reported in Tables S8-61 – S8-66 (supplemental data section).

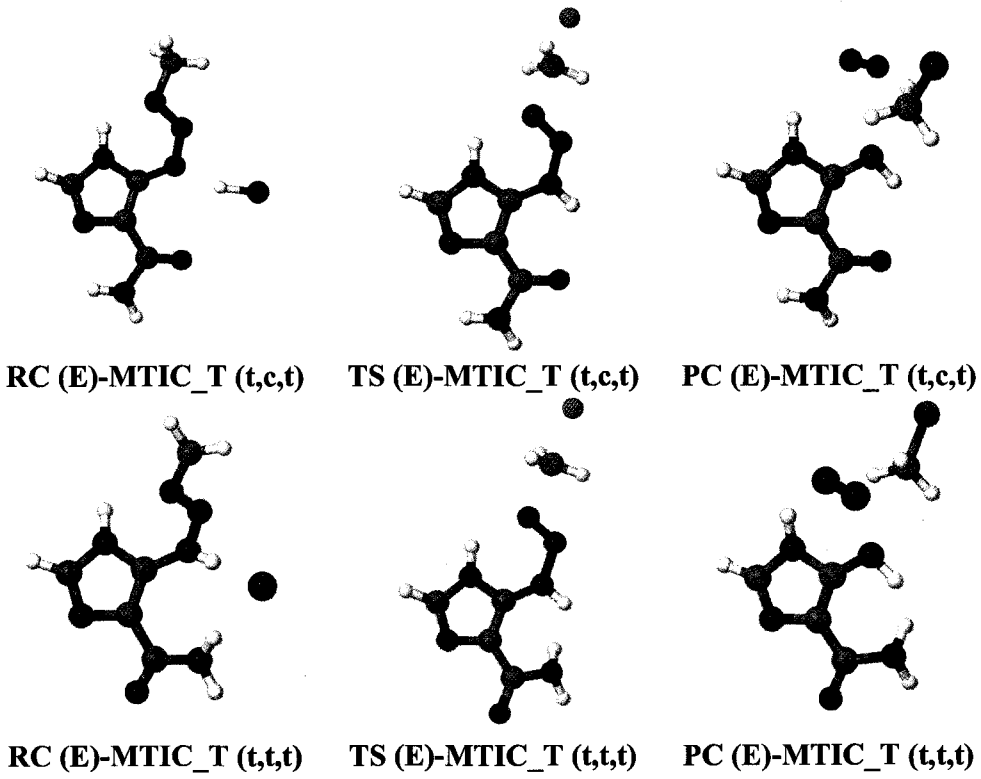

RC (E)-MTIC_T (t,c,t) **TS (E)-MTIC_T (t,c,t)** **PC (E)-MTIC_T (t,c,t)**

RC (E)-MTIC_T (t,t,t) **TS (E)-MTIC_T (t,t,t)** **PC (E)-MTIC_T (t,t,t)**

Figure 8.4a: MTIC_T and X^-; X = F, Cl, Br, S_N2 reaction pathway structures.

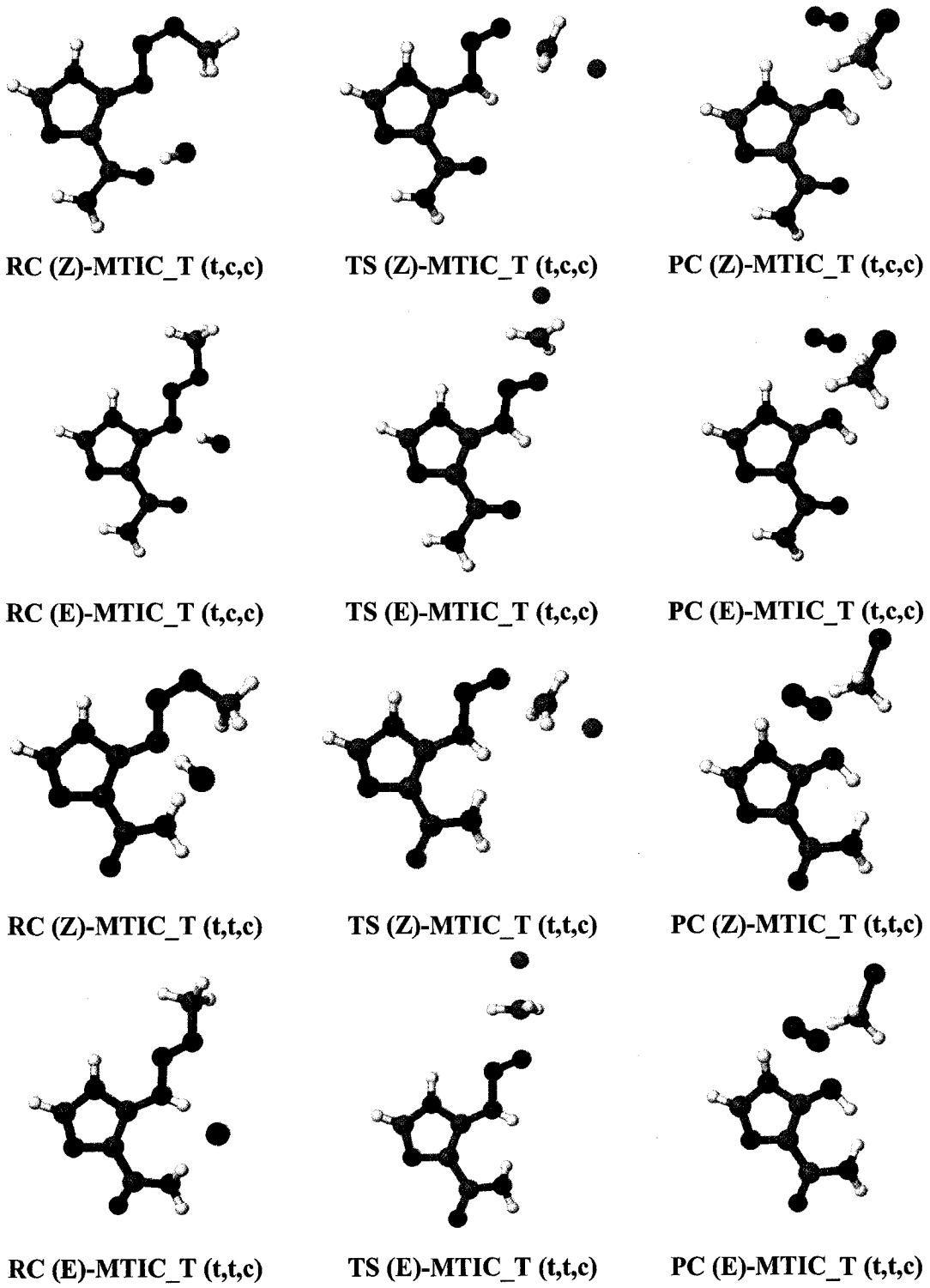

Figure 8.4b: MTIC_T and X^-; X = F, Cl, Br, S_N2 reaction pathway structures; continued.

Table 17: The relative energy comparison of the stationary points on the (Z)-MTIC_T (t,c,c) and halide ion S_N2 reaction pathways with respect to the separated reactants.

Level of Theory	Relative Energy (kJ mol^{-1})			
	RC	TS	PC	SP
Fluoride				
HF/6-31G(d)	-291.6	-7.8	-514.4	-478.3
HF/6-31+G(d)	-173.3	-8.4	-396.8	-365.6
B3LYP/6-31G(d)	-359.5	-244.8	-479.1	-438.8
B3LYP/6-31+G(d)	-182.8	-79.9	-299.1	-269.0
B3LYP/6-31G(d,p)	-367.7	-249.9	-480.1	-439.3
Chloride				
HF/6-31G(d)	29.5	65.3	-214.7	-175.4
HF/6-31+G(d)	35.3	63.9	-216.5	-182.9
B3LYP/6-31G(d)	-33.6	-13.9	-164.2	-118.1
B3LYP/6-31+G(d)	-16.8	3.0	-161.5	-129.2
B3LYP/6-31G(d,p)	-39.4	-15.2	-165.6	-117.7
Bromide				
HF/6-31G(d)	44.3	56.3	-207.5	-166.7
HF/6-31+G(d)	64.3	60.5	-212.2	-155.1
B3LYP/6-31G(d)	-32.9	-28.7	-164.6	-117.3
B3LYP/6-31+G(d)	-9.9	-5.5	-165.7	-110.8
B3LYP/6-31G(d,p)	-41.4	-30.3	-166.2	-117.9

Table 18: The relative energy comparison of the stationary points on the (E)-MTIC_T (t,c,c) and halide ion S_N2 reaction pathways with respect to the separated reactants.

Level of Theory	Relative Energy (kJ mol^{-1})			
	RC	TS	PC	SP
Fluoride				
HF/6-31G(d)	-253.7	-8.3	-484.6	-448.5
HF/6-31+G(d)	-134.9	71.7	-363.4	-332.2
B3LYP/6-31G(d)	-329.5	-120.4	-459.8	-419.5
B3LYP/6-31+G(d)	-154.5	4.1	-275.3	-245.1
B3LYP/6-31G(d,p)	-337.5	-125.5	-461.4	-420.6
Chloride				
HF/6-31G(d)	61.0	95.1	-184.8	-145.6
HF/6-31+G(d)	70.9	97.3	-183.1	-149.5
B3LYP/6-31G(d)	-38.2	5.4	-144.9	-98.9
B3LYP/6-31+G(d)	-21.8	26.8	-137.6	-105.3
B3LYP/6-31G(d,p)	-40.9	3.5	-146.9	-99.0
Bromide				
HF/6-31G(d)	-86.7	86.1	-177.6	-136.8
HF/6-31+G(d)	-71.9	93.9	-178.8	-121.8
B3LYP/6-31G(d)	-115.0	-9.4	-145.3	-98.0
B3LYP/6-31+G(d)	-89.3	18.3	-141.9	-87.0
B3LYP/6-31G(d,p)	-117.0	-11.6	-147.5	-99.3

Table 19: The relative energy comparison of the stationary points on the (Z)-MTIC_T (t,t,c) and halide ion S_N2 reaction pathways with respect to the separated reactants.

Level of Theory	Relative Energy (kJ mol^{-1})			
	RC	TS	PC	SP
Fluoride				
HF/6-31G(d)	-357.0	-48.9	-548.5	-514.4
HF/6-31+G(d)	-235.4	-22.4	-429.9	-400.6
B3LYP/6-31G(d)	-444.8	-183.3	-511.0	-474.0
B3LYP/6-31+G(d)	-258.7	-63.3	-332.1	-302.9
B3LYP/6-31G(d,p)	-453.4	-188.0	-513.2	-475.5
Chloride				
HF/6-31G(d)	-35.7	41.3	-248.1	-211.5
HF/6-31+G(d)	-27.4	42.5	-249.2	-217.9
B3LYP/6-31G(d)	-157.4	-43.9	-196.7	-153.3
B3LYP/6-31+G(d)	-137.9	-26.2	-192.4	-163.1
B3LYP/6-31G(d,p)	-160.1	-45.9	-197.9	-153.9
Bromide				
HF/6-31G(d)	-136.0	32.3	-240.7	-202.7
HF/6-31+G(d)	-121.2	39.3	-238.5	-190.1
B3LYP/6-31G(d)	-166.5	-59.4	-196.9	-152.4
B3LYP/6-31+G(d)	-143.0	-34.9	-191.8	-144.8
B3LYP/6-31G(d,p)	-169.0	-61.6	-199.4	-154.2

Table 20: The relative energy comparison of the stationary points on the (E)-MTIC_T (t,t,c) and halide ion S_N2 reaction pathways with respect to the separated reactants.

Level of Theory	Relative Energy (kJ mol^{-1})			
	RC	TS	PC	SP
Fluoride				
HF/6-31G(d)	-328.4	-34.2	-511.8	-477.6
HF/6-31+G(d)	-205.2	46.1	-389.3	-359.9
B3LYP/6-31G(d)	-417.5	-144.9	-485.7	-448.7
B3LYP/6-31+G(d)	-235.9	-17.0	-301.8	-272.6
B3LYP/6-31G(d,p)	-426.7	-150.8	-488.4	-450.7
Chloride				
HF/6-31G(d)	-94.2	78.0	-211.4	-174.7
HF/6-31+G(d)	-82.9	83.1	-208.5	-177.2
B3LYP/6-31G(d)	-129.6	-18.7	-171.4	-128.0
B3LYP/6-31+G(d)	-109.6	4.1	-162.1	-132.8
B3LYP/6-31G(d,p)	-132.7	-21.1	-173.0	-129.1
Bromide				
HF/6-31G(d)	-100.3	69.1	-203.9	-166.0
HF/6-31+G(d)	-87.5	79.9	-197.9	-149.5
B3LYP/6-31G(d)	-134.9	-34.2	-171.7	-127.2
B3LYP/6-31+G(d)	-112.0	-4.6	-161.5	-114.5
B3LYP/6-31G(d,p)	-138.0	-36.7	-174.5	-129.3

Table 21: The relative energy comparison of the stationary points on the (E)-MTIC_T (t,c,t) and halide ion S_N2 reaction pathways with respect to the separated reactants.

Level of Theory	Relative Energy (kJ mol^{-1})			
	RC	TS	PC	SP
Fluoride				
HF/6-31G(d)	-251.3	-12.3	-486.4	-450.3
HF/6-31+G(d)	-130.0	69.2	-365.9	-334.7
B3LYP/6-31G(d)	-329.6	-107.7	-451.1	-410.8
B3LYP/6-31+G(d)	-154.4	3.2	-269.0	-238.8
B3LYP/6-31G(d,p)	-338.8	-110.7	-452.2	-411.4
Chloride				
HF/6-31G(d)	62.8	93.3	-186.6	-147.4
HF/6-31+G(d)	75.7	94.8	-185.6	-152.0
B3LYP/6-31G(d)	-42.5	14.1	-136.2	-90.1
B3LYP/6-31+G(d)	-24.8	33.1	-131.3	-99.0
B3LYP/6-31G(d,p)	-45.6	12.7	-137.7	-89.8
Bromide				
HF/6-31G(d)	-17.3	84.3	-179.4	-138.6
HF/6-31+G(d)	-64.0	91.4	-181.3	-124.2
B3LYP/6-31G(d)	-44.2	-0.7	-136.6	-89.3
B3LYP/6-31+G(d)	-60.7	24.6	-135.6	-80.7
B3LYP/6-31G(d,p)	-47.9	-2.3	-138.3	-90.0

Table 22: The relative energy comparison of the stationary points on the (E)-MTIC_T (t,t,t) and halide ion S_N2 reaction pathways with respect to the separated reactants.

Level of Theory	Relative Energy (kJ mol^{-1})			
	RC	TS	PC	SP
Fluoride				
HF/6-31G(d)	-324.9	-35.3	-518.5	-484.3
HF/6-31+G(d)	-201.9	46.4	-396.9	-367.6
B3LYP/6-31G(d)	-420.2	-146.6	-481.1	-444.2
B3LYP/6-31+G(d)	-237.9	-19.8	-299.6	-270.4
B3LYP/6-31G(d,p)	-429.9	-152.0	-483.5	-445.8
Chloride				
HF/6-31G(d)	-102.2	71.3	-218.1	-181.4
HF/6-31+G(d)	-92.8	75.5	-216.1	-184.9
B3LYP/6-31G(d)	-137.4	-14.1	-166.8	-123.5
B3LYP/6-31+G(d)	-116.8	6.4	-159.8	-130.6
B3LYP/6-31G(d,p)	-140.9	-16.2	-168.1	-124.2
Bromide				
HF/6-31G(d)	-107.7	62.4	-210.6	-172.7
HF/6-31+G(d)	-98.0	72.3	-205.5	-157.1
B3LYP/6-31G(d)	-141.5	-29.6	-167.1	-122.6
B3LYP/6-31+G(d)	-117.1	-2.3	-159.3	-112.2
B3LYP/6-31G(d,p)	-145.2	-31.8	-169.6	-124.4

4. Conclusions

The S_N2 reaction pathways involving MTIC or MTIC_T and various halide ions were investigated as model reaction pathways for DTIC and other triazene containing anti-neoplastic agents. The structures along the MTIC and halide ion pathways were analogous to the MTI and various halide ions pathway structures, whereas the MTIC_T and halide ion pathways were found to be analogous to the MTI_T and various halide ion S_N2 pathway structures (Chapter 7).

The MTIC and F^- S_N2 reaction pathways were thermodynamically favorable while the MTIC and Cl^- or Br^- S_N2 reaction pathways were thermodynamically unfavorable. Along the S_N2 reaction pathways for MTIC and various halide ions the central barriers were significant in all cases. The MTIC_T and X^- reaction pathways were energetically favorable processes. The central barriers for the MTIC_T and X^- series were smaller than the MTIC and X^- central barriers. This would suggest that MTIC_T will more readily undergo an S_N2 type reaction in the gas-phase than MTIC. Along the MTIC_T and Cl^- reaction pathways, the MTIC_T configurations with C=O s-cis were found to proceed through a TS that is associated with much lower central barriers (19.2 – 56.6 kJ mol^{-1}) than those configurations with C=O s-trans (69.8 – 173.5 kJ mol^{-1}). In the (Z)-MTIC_T (t,c,c) and Br^- reaction pathway, the central barrier associated with the TS was 4.2 – 12.0 kJ mol^{-1}, which is significantly less than any of the other configurations. This may indicate that MTIC_T configurations with C=O s-cis will more readily undergo an S_N2 type reaction than those configurations with C=O s-trans.

These results suggest that MTIC_T is a better candidate than MTIC to undergo an S_N2 type reaction. When compared with MTIC, the ability of MTIC_T to undergo an S_N2 type reaction may suggest that MTIC_T is a better methylating agent. Furthermore, the orientation of the carboxamide group may play a role in the favorability of the reaction pathway. These findings are in agreement with a previous study of MTI or MTI_T and various halide ions (Chapter 7). It is believed that MTIC and similar compounds will interconvert to a configuration that is capable of undergoing tautomerization (Chapter 6) to form MTIC_T, which would then undergo the S_N2 reaction.

CHAPTER NINE: CONCLUSIONS & FUTURE WORK

1. Introduction

This study of Dacarbazine and its structural analogues was focused on describing the potential energy surface (PES) of these important compounds. Configurational studies of DTIC and its structural analogues were carried out (Chapters 3 and 4). In addition, configurational analysis of Temozolomide and Mitozolomide, imidazotetrazine derivatives of DTIC, were also conducted (Chapter 5). The tautomers and tautomerization pathways of MTI and MTIC were included in the description of the PES (Chapter 6). The PES was further described by investigating a series of S_N2 reaction pathways as model studies for the proposed method of action of DTIC and other triazene containing anti-neoplastic agents (Chapters 7 and 8). This study also intended to assess the ability of different computational methods and their ability to accurately describe the PES of DTIC and other triazene containing anti-neoplastic agents.

Global conclusions regarding DTIC and other triazene containing anti-neoplastic agents are also presented (Section 3). This study of DTIC, a triazene containing anti-neoplastic agents may be incomplete and suggestions for future projects are examined (Section 4).

2. DTIC and triazene containing anti-neoplastic studies

In order to better understand the chemical and physical properties of Dacarbazine and other triazene containing anti-neoplastic agents, various structural analogues of DTIC were identified and configurational, tautomerization and S_N2 reaction pathways were investigated.

2.1 Configurations

A configurational analysis of TI, MTI, DTI TIC, MTI and DTIC (Section 2.1.1) was performed first, followed by an analysis of the configurations of TEMO, MITO (Section 2.1.2). A configurational analysis of the tautomers of MTI and MTIC was also performed (Section 2.1.3).

2.1.1 TI, MTI, DTIC, TIC, MTIC & DTIC: Four TI, eight MTI and four DTI configurations were identified. All configurations of TI, MTI and DTI demonstrated a planar imidazole ring and the N_6-N_7 and N_7-N_8 bonds of the triazene moiety exhibited double and single bond characteristics. The (E) configurations were energetically preferred in all cases. All (E) configurations demonstrated a triazene moiety that was in the same plane as the imidazole ring. The less stable (Z) configurations tended to exhibit a triazene moiety that was out of plane with respect to the imidazole ring. The stability of the (E) configurations is believed to be due in part to the conjugation of the π-system through the triazene moiety and the imidazole ring.

Eight TIC, 16 MTIC and eight DTIC configurations were identified. Again, the (E) configurations were found to be the most stable in all cases. The most stable (E) configurations were those characterized by a triazene moiety that was s-trans to the imidazole ring and a carboxamide group that was s-cis with respect to the imidazole ring. The most stable configurations were those that demonstrated planar or relatively planar triazene moieties, imidazole rings and carboxamide groups with respect to each other.

The primary stabilizing influence on these structural analogues of Dacarbazine and other triazene containing anti-neoplastic agents is believed to be due to the conjugation of the π-system through the compound. In some cases, it appears that weak hydrogen-bond interactions may provide a stabilizing influence. Steric interactions between the imidazole ring and the amine of the triazene and between the triazene moiety and the carboxamide group appear to be the greatest destabilizing influence.

2.1.2 TEMO & MITO: Two TEMO and six MITO configurations were identified. TEMO and MITO were relatively planar molecules. The most stable configuration occurred when the carboxamide group was s-cis with respect to the imidazole ring. The relative stability of MITO was not significantly influenced by the orientation of the chloroethyl group. Furthermore, it is believed that the anti- and gauche-configurations of MITO will readily interchange in the gas-phase.

2.1.3 MTI_T & MTIC_T: Four MTI tautomer and six MTIC tautomer configurations were characterized. (E) configurations were the most stable. Decreased

stability of the (Z) configurations is believed to be due to steric effects between the terminal amine of the triazene and the imidazole ring. The MTIC_T configurations with a s-trans carboxamide group with respect to the imidazole ring were further destabilized by steric effects between the carboxamide group and the terminal amine of the triazene. The tautomers of MTI and MTIC are not capable of extended π-system conjugation and the presence of steric effects significantly decreases the stability of the tautomer configuration.

2.2 Tautomerization

The gas-phase and water mediated tautomerization pathways were investigated for the tautomerization of MTI and MTIC.

2.2.1 Gas-phase: In gas-phase tautomerization studies of both MTI and MTIC, transition structures were characterized by a four-membered ring involved in the transfer of the hydrogen from N_8 to N_6. Breaking and making of the N_6-N_7 double bond and the N_7-N_8 double bond was observed. The energy barriers associated with the gas-phase tautomerization of MTI and MTIC were significant in all cases.

2.2.2 Water mediated: In water mediated tautomerization pathways of MTI and MTIC, the transition structures were characterized by a pseudo-six-membered ring which involved the transfer of the N_8-hydrogen atom to N_6 via the water molecule. Energy barriers associated with the water mediated tautomerization were significant.

However, they were significantly less than the gas-phase barriers. The tautomerization of MTI and MTIC as a water mediated process was the most favorable situation for tautomerization to occur.

2.3 S_N2 reaction pathways

2.3.1 MTI & MTI_T: Two distinct S_N2 reaction pathways involving MTI or MTI_T and various halide ions were investigated as model reaction pathways for DTIC and other triazene containing anti-neoplastic agents. The MTI_T and halide ion reaction pathways were more energetically favorable than the MTI and halide ion reaction pathways. The MTI and fluoride ion reaction pathways were thermodynamically favorable; however, the MTI and chloride or bromide ion reaction pathways were thermodynamically unfavorable. All of the MTI_T and halide ion reaction pathways were thermodynamically favorable.

Along the S_N2 reaction pathways for MTI or MTI_T and various halide ions the central barriers were significant in all cases. However, the central barriers of the MTI studies were more significant than the MTI_T studies. The height of the central barriers and the favorability of the reaction pathways would indicate that S_N2 reactions between MTI_T and halide ions are more likely to occur. It is believed that MTI and similar compounds would interconvert to a configuration that is capable of undergoing tautomerization to form MTI_T which would then undergo the S_N2 reaction.

2.3.2 MTIC & MTIC_T: The S_N2 reaction pathways involving MTIC or MTIC_T and various halide ions were investigated as model reaction pathways for DTIC and other triazene containing anti-neoplastic agents. The MTIC and X^- S_N2 reaction pathways were thermodynamically unfavorable with the exception of the fluoride reaction pathways. The central barriers were significant in all cases. The MTIC_T and X^- reaction pathways were energetically favorable processes and the central barriers for most of the halide series were significant. The MTIC_T central barriers were significantly less than the MTIC and X^- central barriers. These findings would suggest that MTIC_T is a better candidate than MTIC to undergo an S_N2 type reaction. Furthermore, the orientation of the carboxamide group may play a role in the favorability of the reaction pathway. It is believed that MTIC and similar compounds will interconvert to a configuration that is capable of undergoing tautomerization to form MTIC_T, which would then undergo the S_N2 reaction.

3. Global Conclusions

The most stable configurations were the (E) configurations where conjugation of the π-system is possible and steric effects are avoided. Tautomer forms were found to be less stable; however, water mediated tautomerization was likely to occur.

In the S_N2 studies, the chloride ion was a reasonable nucleophile. Generally, the tautomer forms were more likely to undergo an S_N2 type reaction in the gas-phase than MTI or MTIC. These results, coupled with the ability of MTI and MTIC to undergo

water-mediated tautomerization, a process that is likely to occur in the human body, indicates that tautomerization would occur before a S_N2 type reaction. As such, it is believed that following the loss of a methyl group by heptatic cytochrome P450, the active metabolite of DTIC will undergo tautomerization in order to facilitate a more energetically favorable S_N2 type reaction with the O6-oxygen of guanine.

During the course of this computational study, nine distinct levels of theory were utilized. Generally, geometrical features at the MP2 and B3LYP levels of theory were in agreement. During the S_N2 studies, the central barriers of the B3LYP levels of theory were slightly depressed with respect to the MP2 levels of theory, which was expected. Furthermore, the computational time of the MP2 calculations was significantly greater than any of the B3LYP levels of theory. Due to the nature of the proposed method of action of this class of compounds, basis sets that include diffuse functions should be used for proper descriptions. At this point, it is difficult to determine which level of theory is best for the description of DTIC and other triazene containing anti-neoplastic agents. In order to make a true assessment of the appropriateness of the levels of theory, further investigation is required. These investigations should include, but not be limited to, intrinsic reaction coordinate pathway calculations, single point calculations, using larger nucleophile models and employing other computational methods such as molecular dynamics.

4. Future Work

Up to this point, configurational studies of DTIC and its structural analogues, including two tautomers, as well as a modeling of reaction pathways of the proposed method of action have been successfully carried out in the gas-phase at various levels of theory. However, more studies are required in order to gain further insight into this group of biologically important compounds. Some of this work could include using other levels of theory, solvation studies, and using more guanine-like nucleophiles in S_N2 studies.

By describing the PES with a larger level of theory (i.e.; using a larger basis set), a more accurate description of the PES may be gained. For instance, S_N2 reaction pathways that were considered in Chapters 7 and 8 involved a negative charge. In order to better describe these processes, basis sets like 6-31+G(d) that include diffuse functions should be used (131,132). However, the 6-31+G(d) basis set may not be enough for the accurate description of DTIC and other related compounds. The levels of theories should be expanded to include basis sets such as 6-31++G(d) in order to assess the need for more diffuse functions. In addition to using larger basis sets, it may be pertinent to employ other computational methods such as molecular dynamics. This type of theoretical study may provide a better understanding of chemical and physical properties of DTIC by providing a better understanding of kinetic properties of these compounds.

Although, this study of DTIC and it structural analogues was carried out in the gas-phase, the method of action of DTIC is a biological process where solvent (i.e.; water,

cytosol) is likely to be involved. As such, it would be worthwhile to study solvation effects on the reaction pathways. Solvation effects may alter configurational possibilities and the energy profile of the S_N2 reaction pathways.

Finally, a more realistic nucleophile should be used to study the proposed mechanism of action of DTIC. Our studies utilized various halide ions and found that a chloride ion did a reasonable job as the nucleophile. However, it would be wise to study these reaction pathways with guanine or a structural analogue of guanine in order to better understand the influence of O6-oxygen of guanine on the method of action of DTIC and other triazene containing anti-neoplastic agents.

REFERENCES

1. Canadian Cancer Society/National Cancer Institute of Canada. Canadian Cancer Statistics, Toronto, Canada, www.cancer.ca (2006).
2. N. Saint-Jacques, M. MacIntyre, R. Dewar, G. Johnston. Cancer Statistics in Nova Scotia: A Focus on 1995-1999, Surveillance and Epidemiology Unit, Cancer Care Nova Scotia, www.cancercare.ns.ca, (2002).
3. J. Keith, D. M. Anderson, P. D. Novak, M. A. Elliot. Mosby's Medical, Nursing and Allied Health Dictionary, 6th Edition, Mosby, St. Louis (2002).
4. D. Venes, C. W. Taber. Taber's Cyclopedic Medical Dictionary, 20th Edition, F. A. Davis Company, Philadelphia (2005).
5. K. Vaughan. The Chemistry of Antitumor Agents, Blackie, Glasgow, Chapter 5, 159 (1990).
6. See, for example, (a) J. R. P. Godin, K. Vaughan, K. W. Renton. Canadian Journal of Physiology and Pharmacology, 59, 1234 (1981) (b) S. K. Carter, M. A. Friedman. European Journal of Cancer, 8, 85 (1972), (c) R. L. Comis. Cancer Treatment Reports, 60, 165 (1976), (d) E. S. Newlands, M. F. G. Stevens, S. R. Wedge, R. T. Wheelhouse, C. Brock. Cancer Treatment Review, 23, 35 (1997).
7. Compendium of Pharmaceuticals and Specialties, Canadian Pharmacists Association (2006)
8. S. K. Carter, M. A. Friedman. European Journal of Cancer, 8, 85, (1972).
9. J. R. P. Godin, K. Vaughan, K. W. Renton. Canadian Journal of Physiology and Pharmacology, 59, 1234 (1981).

10. D. A. Clarke, R. K. Barclay, C. C. Stock, R. S. Rondesvedt. Proceedings of the Society for Experimental Biology and Medicine, 90, 484 (1955).

11. E. Carvalho, A. P. Francisco, J. Iley, E. Rose. Bioorganic and Medicinal Chemistry, 8, 1719 (2000) and references therein.

12. T. A. Connors, P. M. Goddard, K. Merai, W. C. J. Ross, D. E. V. Wilman. Biochemical Pharmacology, 25, 241 (1976).

13. M. Julliard, G. Vernin. Industrial and Engineering Chemistry Research Review, 20, 287 (1981).

14. E. Carvalho, J. Iley, M. de J. Perry, E. Rosa. Pharmaceutical Research, 15, 931 (1998).

15. M. Julliard, G. Vernin. Ind. Eng. Chem. Prod. Research Reviews, 20, 287 (1981).

16. K. Vaughan, M. F. G. Stevens. Chemical Society Reviews, 7, 377 (1978).

17. E. Carvalho, J. Iley, M. de Jesus Perry, E. Rosa. Pharmaceutical Research, 15, 931 (1998).

18. C. J. Rutty, D. R. Newell, R. B. Vincent, G. Abel, P. M. Goddard, S. J. Harland, A. H. Calvert. British Journal of Cancer, 48, 140 (1983).

19. C. C. Pye, K. Vaughan, J. F. Glister. Canadian Journal of Chemistry, 80, 447 (2002).

20. K. G. Doucet, C. C. Pye, K. Vaughan, T. G. Enright. Journal of Molecular Structure: THEOCHEM, 801, 21 (2006).

21. K. G. Doucet, C. C. Pye, T. G. Enright. Journal of Molecular Structure: THEOCHEM, 821, 166 (2007).

22. K. G. Doucet, C. C. Pye, T. G. Enright. Canadian Journal of Chemistry, in press.

23. J. M. Gonzales, C. Pak, R. S. Cox, W. D. Allen, H. F. Schaefer III, A. G Császár, G.

Tarczay. Chemistry - A European Journal, 9, 2173 (2003).

24. J. M. Gonzales, R. S. Cox, S. T. Brown, W. D. Allen, H. F. Schaefer III. Journal of Physical Chemistry A, 105, 11327 (2001).
25. J. L Brauman, W. N. Olmstead, C. A. Lieder. Journal of the American Chemical Society, 96, 4030 (1974).
26. C. H. DePuy, S. Gronert, A. Mullin, V. M. Bierbaum Journal of the American Chemical Society, 112, 8650 (1990).
27. H. Wang, W. L. Hase. Journal of the American Chemical Society, 119, 3093 (1997).
28. L. Uggerud. Journal of the Chemical Society, Perkin Transactions 2, 1459 (1999).
29. A. A. Viggiano, A. Midey. Journal of Physical Chemistry A, 104, 6786 (2000).
30. K. Takeuchi, M. Takasuka, E. Shiba, T. Kinoshita, T. Okazaki, J. L. M. Abboud, R. Notario, O. Castano. Journal of the American Chemical Society, 122, 7351 (2000).
31. G. E. Davico, V. M. Bierbaum. Journal of the American Chemical Society, 122, 1740 (2000).
32. M. C. Baschky, S. R. Kass. International Journal of Mass Spectrometry, 196, 411 (2000).
33. A. Pross, S. S. Shaik. New Journal of Chemistry, 13, 427 (1989).
34. K. M. Ervin. International Journal of Mass Spectrometry, 185, 343 (1998).
35. T. Su, H. Wang, W. L. Hase. Journal of Physical Chemistry A, 102, 9819 (1998).
36. H. Tachikawa, M. Igarishi. Chemical Physics Letters, 303, 81 (1999).
37. G. Li, W. L. Hase. Journal of the American Chemical Society, 121, 7124 (1999).
38. S. Raguei, G. Cardini, V. Schetino. Journal of Chemical Physics, 111, 10887 (1999).
39. H. Tachikawa. Journal of Physical Chemistry A, 104, 497 (2000).

40. H. Yamataka. Heteroatom Chemistry, 21, 277 (1999).

41. Y. Okuno. Journal of the American Chemical Society, 122, 2925 (2000).

42. R. C. Dougherty, J. D. Roberts. Organic Mass Spectrometry, 8, 81 (1973).

43. W. N. Olmstead, J. I. Brauman. Journal of the American Chemical Society, 99, 4219 (1977).

44. M. J. Pellerite. Journal of the American Chemical Society, 102, 5993 (1980).

45. M. J. Pellerite, J. I. Brauman. Journal of the American Chemical Society, 105, 2672 (1983).

46. J. A. Dodd, J. I. Brauman, Journal of. Physical Chemistry, 90, 3559 (1986).

47. E. S. Lewis. Journal of. Physical Chemistry, 90, 3756 (1986).

48. S. Hoz, H. Basch, J. L. Wolk, T. Hoz, E. Rozental. Journal of the American Chemical Society, 121, 7724 (1999).

49. D. S. Tonner, T. B. McMahon. Journal of the American Chemical Society, 122, 8783 (2000).

50. Z. Shi, R. J. Boyd. Journal of the American Chemical Society, 112, 6789 (1990).

51. F. M. Bickelhaupt, E. J. Baerands, N. M. M. Nibbering, T. Ziegler. Journal of the American Chemical Society, 115, 9160 (1993).

52. L. Deng, V. Branchadell, T. Ziegler, Journal of the American Chemical Society, 116, 10 645 (1994).

53. M. N. Glukhovtsev, A. Pross, L. Radom, Journal of the American Chemical Society, 117, 2024 (1994).

54. B. D. Wladkowski, W. D. Allen, J. I. Brauman. Journal of Physical Chemistry, 98, 13532 (1994).

55. S. Gronert, G. N. Merrill, S. R. Kass. Journal of Organic Chemistry, 60, 488 (1995).

56. M. N. Glukhovtsev, R. D. Bach, A. Pross, L. Radom. Chemical Physics Letters, 260, 558 (1996).

57. P. Botschwina, M. Horn, S. Seeger, R. Oswald, B. Bunsen-Ges. Physical Chemistry, 101, 387 (1997).

58. F. M. Bickelhaupt. Journal of Computational Chemistry, 20, 114 (1998).

59. M. Igarishi, H. Tachikawa. International Journal of Mass Spectrometry, 181, 151 (1998).

60. M. Aida, H. Yamataka. Journal of Molecular Structure: THEOCHEM, 462, 417 (1999).

61. Y. R. Mo, J. L. Gao. Journal of Computational Chemistry, 21, 1458 (2000).

62. S. Parthiban, G. de Oliveira, J. M. L Martin. Journal of Physical Chemistry A, 105, 895 (2001).

63. A. M. Kuznetsov Journal of Physical Chemistry A, 103, 1239 (1999).

64. S. L. Craig, J. I. Brauman. Journal of the American Chemical Society, 121, 6690 (1999).

65. J. Langer, S. Matejcik, E. Illenberger. Physical Chemistry Chemical Physics, 2, 1001 (2000).

66. W. H. Saunders. Journal of Organic Chemistry, 65, 681 (2000).

67. B. Y. Ma, S. Kumar, C. J. Tsai, Z. J. Hu, R. J. Nussinov. Journal of Theoretical Biology, 203, 383 (2000).

68. H. Jensen, K. Daasbjerg. Journal of the Chemical Society, Perkin Transactions 2, 1251 (2000).

69. M. L. Chabinyc, S. L. Craig, C. K. Regan, J. I Brauman. Science, 279, 1882 (1998).

70. F. Jensen, Introduction to Computational Chemistry, New York, Wiley (1999).

71. A. Szabo, N. S. Ostland, Modern Quantum Chemistry: Introduction to Advanced Electronic Structure Theory, Dover Publications (1996).

72. T. Clark. A Handbook of Computational Chemistry, Wiley, New York (1985).

73. C. J. Cramer. Essentials of Computational Chemistry, John Wiley & Sons (2002).

74. CHEM 6301: *Advanced Electronic Structure Theory* Class Notes, Instructed by Dr. R. Boyd, Department of Chemistry, Dalhousie University, Halifax, Nova Scotia, January to April 2005.

75. CHEM 5301: *Theory of Chemical Bonding* Class Notes, Instructed by Dr. R. Boyd, Department of Chemistry, Dalhousie University, Halifax, Nova Scotia, September to December 2004.

76. CHEM 4241: *Physical Chemistry – Computational Chemistry* Class Notes, Instructed by Dr. S. D. Wetmore, Chemistry Department, Mount Allison University, Sackville, New Brunswick, September to December 2003.

77. P. A. M. Dirac. Mathematical Proceedings of the Cambridge Philosophical Society, 27, Part II, 240 (1930).

78. P. A. M. Dirac. Mathematical Proceedings of the Cambridge Philosophical Society, 26, Part III, 376 (1930).

79. V. Fock. Zeits fur Physik, 61, 126 (1930).

80. C. Møller, M. S. Plesset. Physical Review, 46, 618 (1934).

81. B. Jeziors, R. Moszyns, K. Szalewicz. Chemical Reviews, 94, 1887 (1994).

82. P. Geerlings, F. De Proft, W. Langenaeker. Chemical Reviews, 103, 1793 (2003).

83. W. Kohn, A. D. Becke, R. G. Parr. Journal of Physical Chemistry, 100, 12974 (1996).

84. W. Kohn, P. Hohenberg. Physical Review, 136, B864 (1964).

85. W. Kohn, L. J. Sham. Physical Review, 137, A1697 (1965).

86. W. Kohn, L. J. Sham. Physical Review, 140, A1133 (1965).

87. S. H. Vosko, L. Wilk, M. Nusair. Canadian Journal of Physics, 58, 1200 (1980).

88. J. P. Perdew. Physical Review B, 33, 8822 (1986).

89. M. Grulning, O. V. Gritsenko, S. J. A. van Gisbergen, E. J. Baerends. Journal of Physical Chemistry A, 105, 9211 (2001).

90. R. Colle, O. Salvetti. Theormochimica Acta, 37, 329 (1975).

91. C. Lee, W. Yang, R. G. Parr. Physical Review B, 37, 785 (1988).

92. A. Becke. Physical Review A, 38, 3098 (1988).

93. J. P. Perdew, K. Burke, Y. Wang. Physical Review B, 54, 16533 (1996).

94. J. P. Perdew, K. Burke, M. Ernzerhof. Physical Review Letters, 77, 3865 (1996).

95. Y. Zhang, W. Yang. Physical Review Letters, 80, 890 (1998).

96. M. Filatov, W. Thiel. Molecular Physics, 91, 847 (1997).

97. F. A. Hamprecht, A. J. Cohen, D. J. Tozer, N. C. Handy. Journal of Chemical Physics, 109, 6264 (1998).

98. A. D. Boese, N. L. Doltsinis, N. C. Handy, M. Sprik. Journal of Chemical Physics, 112, 1670 (2000).

99. M. Ludwig, M. Kabickova. Collection of Czechoslovak Chemical Communications, 61, 355 (1996).

100. M. J. Frisch, et al. Gaussian 98, Revision A.9, Gaussian Inc., Pittsburgh, PA (1998).

101. A. P Scott, L. Radom. Journal of Physical Chemistry, 100, 16502 (1996).

102. M. J. Frisch et al. *Gaussian 03*, Revision C.02, Gaussian, Inc., Wallingford CT (2004).

103. M. H Cohen, J. R. Johnson, R. Pazdur. Clinical Cancer Research, 11, 6767 (2005).

104. G. S. Newlands et al. Cancer Treatment Review, 23, 35 (1997).

105. Cancer Care Nova Scotia, Cancer Drug Monographs: Temozolomide, 264 http://www.cancercare.ns.ca/documents/Temozolomide_dm.pdf (2003).

106. Cancer Care Nova Scotia, Neuro-oncology: Temozolomide for CNS Cancer, www.cancercare.ns.ca/documents/Temozolomide_Malignant_Glioma_dg.pdf (2001).

107. O. Fodstad, S. Aamdal, A. Pihl, M. R. Boyd. Cancer Research, 45, 1778 (1985).

108. G. M. Loudon. Organic Chemistry, 3rd Edition, The Benjamin/Cummings Publishing Company Inc., Redwood City, California, 1045 (1995).

109. A. Douhal, F. Lahmani, A. H. Zewail. Journal of Chemical Physics, 207, 477(1996).

110. N. Agmon, Israel Journal of Chemistry, 39, 493 (1999).

111. H. H. Limbach, J. Manz. Berichte der Bunsengesellschaft für physikalische Chemie, 102, 289 (1998).

112. F. T. Marchese, P. H. Mehrotra, D. L. Beveridge. Journal of Physical Chemistry, 88, 5692 (1984).

113. F. T. Marchese, D. L. Beveridge. Chemical Physics Letters, 105, 431 (1984).

114. W. L. Jorgensen, C. J. Swenson. Journal of the American Chemical Society, 107, 1489 (1985).

115. Y. P. Puhovski, B. M. Rode. Journal of Physical Chemistry, 99, 1566 (1995).

116. Y. P. Puhovski, B. M. Rode. Journal of Physical Chemistry, 102, 2920 (1995).

117. M. L. Sanchez, M. A. Aguilar, F. J. Olivares del Valle. Journal of Computational

Chemistry, 18, 313 (1997).

118. S. Chalmet, M. F. Ruiz-Lopez. Journal of Chemical Physics, 113, 1117 (1999).

119. M. W. Wong, K. B. Wiberg, M. J. Frisch. Journal of the American Chemical Society, 114, 1645 (1992).

120. G. P. Jasien, W. J. Stewens. Journal of Chemical Physics, 84, 3271 (1986).

121. F. Sim, A. St. Amant, I. Papai, D. R. Salahub. Journal of the American Chemical Society, 114, 4391 (1992).

122. A. Engdahl, B. Nelander, P. Astrand. Journal of Chemical Physics, 99, 7 (1993).

123. J. C. Contador, M. A. Aguilar, M. L. Sanchez, F. J. Olivares del Valle. Journal of Moleculare Structure: THEOCHEM, 314, 299 (1994).

124. P. R. Rablen, J. W. Lockman, W. L. Jorgensen. Journal of Physical Chemistry A, 102, 3782 (1998).

125. J. Gu, J. Leszczynski. Journal of Physical Chemistry A, 103, 577 (1999).

126. L. Gorb, J. Leszczynski. Journal of the American Chemical Society, 120, 5024 (1998)

127. S. Antonczak, M. F. Ruiz-Lopez, J. L. Rivail. Journal of the American Chemical Society, 116, 3912 (1994).

128. E. S. Kryachko, M. T. Nguyen, T. Zeegers-Huyskens. Journal of Physical Chemistry A, 105, 1934 (2001)

129. G. A. Jeffrey, W. Saenger. Hydrogen Bonding in Biological Structures; Springer: Berlin, Germany (1991)

130. P. Huyskens. Journal of the American Chemical Society, 99, 2578 (1977).

131. L. Goodman, R. S. Sauers. Journal of Computational Chemistry, 28, 269 (2006).

132. T. Clark, J. Chandrasekhar, G. W. Spitznagel, P. v. R. Schleyer. Journal of Computational Chemistry, 4, 294 (1983).

Table S3-1: The calculated N_6-N_7 and N_7-N_8 bond lengths of the (E)-TI configurations

Level of Theory	Bond Length (Å)			
	(E)-TI Im s-trans		(E)-TI Im s-cis	
	N_6-N_7	N_7-N_8	N_6-N_7	N_7-N_8
HF/STO-3G	1.279	1.435	1.279	1.434
HF/3-21G	1.242	1.370	1.244	1.355
HF/6-31G(d)	1.219	1.351	1.219	1.345
HF/6-31+G(d)	1.217	1.350	1.217	1.343
MP2/6-31G(d)	1.282	1.363	1.279	1.360
MP2/6-31+G(d)	1.280	1.362	1.277	1.359
B3LYP/6-31G(d)	1.264	1.360	1.262	1.354
B3LYP/6-31+G(d)	1.260	1.357	1.259	1.351
B3LYP/6-31G(d,p)	1.264	1.357	1.263	1.352

Table S3-2: The calculated ‹($C_1N_2C_3N_4$) and ‹($C_3N_4C_5C_1$) dihedral angles of the (E)-TI configurations.

Level of Theory	Dihedral Angles (degrees)			
	<($C_1N_2C_3N_4$)		<($C_3N_4C_5C_1$)	
	(t)	(c)	(t)	(c)
HF/STO-3G	0.1	0.1	0.1	0.1
HF/3-21G	0.0	0.0	0.0	0.1
HF/6-31G(d)	0.1	0.1	0.1	0.0
HF/6-31+G(d)	0.1	0.1	0.1	0.0
MP2/6-31G(d)	0.1	0.0	0.1	0.1
MP2/6-31+G(d)	0.1	0.0	0.1	0.1
B3LYP/6-31G(d)	0.1	0.0	0.0	0.1
B3LYP/6-31+G(d)	0.1	0.0	0.0	0.1
B3LYP/6-31G(d,p)	0.1	0.0	0.0	0.1

Table S3-3: The ‹($C_5N_6N_7N_8$) and ‹($N_4C_5N_6N_7$) dihedral angles of the (E)-TI configurations.

Level of Theory	Dihedral Angles (degrees)			
	<($C_5N_6N_7N_8$)		<($N_4C_5N_6N_7$)	
	(t)	(c)	(t)	(c)
HF/STO-3G	176.3	176.6	3.1	179.5
HF/3-21G	177.9	179.2	1.1	179.7
HF/6-31G(d)	176.7	176.9	1.9	178.7
HF/6-31+G(d)	177.0	177.1	1.5	178.2
MP2/6-31G(d)	175.1	175.3	2.5	176.8
MP2/6-31+G(d)	175.0	174.9	3.5	173.7
B3LYP/6-31G(d)	175.7	175.9	1.8	178.0
B3LYP/6-31+G(d)	176.1	176.3	1.6	177.9
B3LYP/6-31G(d,p)	175.9	176.1	1.8	178.0

Table S3-4: The ‹($H_9N_8N_7N_6$) and ‹($H_{10}N_8N_7N_6$) dihedral angles of the (E)-TI configurations.

Level of Theory	Dihedral Angles (degrees)			
	<($H_9N_8N_7N_6$)		<($H_{10}N_8N_7N_6$)	
	(t)	(c)	(t)	(c)
HF/STO-3G	143.2	145.2	25.0	26.6
HF/3-21G	163.2	143.2	11.9	5.3
HF/6-31G(d)	150.8	153.0	21.8	22.0
HF/6-31+G(d)	151.9	154.1	22.4	22.4
MP2/6-31G(d)	150.6	152.4	20.3	20.6
MP2/6-31+G(d)	152.4	154.0	20.6	20.6
B3LYP/6-31G(d)	152.1	154.1	19.9	19.7
B3LYP/6-31+G(d)	154.4	156.3	19.8	19.3
B3LYP/6-31G(d,p)	153.2	155.3	19.1	18.7

Table S3-5: The calculated N_6N_7 and N_7N_8 bond lengths of the (Z)-TI configurations.

Level of Theory	Bond Length (Å)			
	N_6-N_7		N_7-N_8	
	(t)	(c)	(t)	(c)
HF/STO-3G	1.269	1.271	1.467	1.443
HF/3-21G	1.227	1.238	1.520	1.401
HF/6-31G(d)	1.217	1.221	1.386	1.352
HF/6-31+G(d)	1.217	1.221	1.382	1.352
MP2/6-31G(d)	1.272	1.279	1.412	1.372
MP2/6-31+G(d)	1.275	1.279	1.405	1.372
B3LYP/6-31G(d)	1.254	1.261	1.417	1.368
B3LYP/6-31+G(d)	1.254	1.260	1.412	1.367
B3LYP/6-31G(d,p)	1.254	1.261	1.415	1.366

Table S3-6: The ‹($C_1N_2C_3N_4$) and ‹($C_3N_4C_5C_1$) dihedral angles of the (Z)-TI configurations.

Level of Theory	Dihedral Angles (degrees)			
	<($C_1N_2C_3N_4$)		<($C_3N_4C_5C_1$)	
	(t)	(c)	(t)	(c)
HF/STO-3G	0.9	0.2	0.2	0.6
HF/3-21G	0.2	0.3	0.1	0.3
HF/6-31G(d)	1.7	0.3	0.5	0.5
HF/6-31+G(d)	1.7	0.3	0.3	0.5
MP2/6-31G(d)	2.0	0.6	0.5	0.5
MP2/6-31+G(d)	2.2	0.5	0.3	0.5
B3LYP/6-31G(d)	2.0	0.5	1.1	0.5
B3LYP/6-31+G(d)	2.0	0.4	0.9	0.4
B3LYP/6-31G(d,p)	1.9	0.5	1.0	0.5

Table S3-7: The calculated ‹($N_8N_7N_6C_5$) and ‹($N_7N_6C_5N_4$) dihedral angles of the (Z)-TI configurations.

Level of Theory	Dihedral Angles (degrees)			
	<($N_8N_7N_6C_5$)		<($N_7N_6C_5N_4$)	
	(t)	(c)	(t)	(c)
HF/STO-3G	0.3	1.3	26.9	161.4
HF/3-21G	1.1	0.8	3.3	163.8
HF/6-31G(d)	1.8	0.5	25.8	163.8
HF/6-31+G(d)	1.8	0.5	29.5	165.1
MP2/6-31G(d)	2.6	1.3	27.2	164.4
MP2/6-31+G(d)	2.6	1.4	32.2	164.5
B3LYP/6-31G(d)	3.0	0.7	20.5	165.7
B3LYP/6-31+G(d)	3.3	0.5	23.1	167.1
B3LYP/6-31G(d,p)	3.0	0.7	20.9	165.6

Table S3-8: The calculated N_6-N_7 and N_7-N_8 bond lengths of the (E)-MTI configurations.

Level of Theory	Bond Length (Å)							
	N_6-N_7				N_7-N_8			
	(t,c)	(t,t)	(c,c)	(c,t)	(t,c)	(t,t)	(c,c)	(c,t)
HF/STO-3G	1.279	1.279	1.280	1.280	1.429	1.433	1.428	1.432
HF/3-21G	1.249	1.244	1.249	1.246	1.350	1.368	1.346	1.356
HF/6-31G(d)	1.223	1.220	1.224	1.221	1.337	1.345	1.329	1.337
HF/6-31+G(d)	1.222	1.219	1.223	1.220	1.335	1.344	1.326	1.336
MP2/6-31G(d)	1.290	1.288	1.287	1.284	1.346	1.352	1.343	1.346
MP2/6-31+G(d)	1.289	1.286	1.286	1.283	1.345	1.352	1.341	1.347
B3LYP/6-31G(d)	1.269	1.268	1.269	1.267	1.346	1.348	1.341	1.342
B3LYP/6-31+G(d)	1.267	1.265	1.267	1.264	1.342	1.346	1.335	1.340
B3LYP/6-31G(d,p)	1.270	1.268	1.269	1.267	1.345	1.347	1.339	1.341

Table S3-9: The calculated ‹($C_1N_2C_3N_4$) and ‹($C_3N_4C_5C_1$) dihedral angles of the (E)-MTI configurations.

Level of Theory	Dihedral Angle (degrees)							
	‹($C_1N_2C_3N_4$)				‹($C_3N_4C_5C_1$)			
	(t,c)	(t,t)	(c,c)	(c,t)	(t,c)	(t,t)	(c,c)	(c,t)
HF/STO-3G	0.1	0.1	0.1	0.1	0.1	0.1	0.1	0.1
HF/3-21G	0.0	0.1	0.1	0.0	0.0	0.0	0.0	0.0
HF/6-31G(d)	0.1	0.1	0.0	0.1	0.1	0.1	0.0	0.0
HF/6-31+G(d)	0.1	0.1	0.0	0.1	0.1	0.1	0.0	0.0
MP2/6-31G(d)	0.1	0.1	0.0	0.0	0.1	0.1	0.1	0.1
MP2/6-31+G(d)	0.0	0.1	0.0	0.0	0.0	0.2	0.3	0.2
B3LYP/6-31G(d)	0.1	0.1	0.0	0.0	0.0	0.0	0.1	0.1
B3LYP/6-31+G(d)	0.1	0.1	0.0	0.0	0.0	0.0	0.1	0.1
B3LYP/6-31G(d,p)	0.1	0.0	0.0	0.0	0.0	0.0	0.1	0.1

Table S3-10: The calculated ‹($N_4C_5N_6N_7$) dihedral angles of the (E)-MTI configurations.

Level of Theory	Dihedral Angle (degrees)			
	(t,c)	(t,t)	(c,c)	(c,t)
HF/STO-3G	2.7	2.5	179.5	179.5
HF/3-21G	0.0	1.0	180.0	179.4
HF/6-31G(d)	1.4	1.4	178.3	178.3
HF/6-31+G(d)	1.0	1.0	177.6	177.9
MP2/6-31G(d)	1.7	1.9	177.1	176.1
MP2/6-31+G(d)	2.5	2.2	172.1	172.7
B3LYP/6-31G(d)	1.1	1.3	178.8	177.9
B3LYP/6-31+G(d)	0.8	1.0	178.7	177.8
B3LYP/6-31G(d,p)	1.1	1.3	178.8	177.9

Table S3-11: The calculated ‹($CN_8N_7N_6$) dihedral angle of the (E)-MTI configurations.

Level of Theory	Dihedral Angle (degrees)			
	(t,c)	(t,t)	(c,c)	(c,t)
HF/STO-3G	25.2	144.3	26.1	146.2
HF/3-21G	0.0	161.5	0.0	166.2
HF/6-31G(d)	17.4	152.4	16.2	154.9
HF/6-31+G(d)	17.5	152.7	15.7	155.0
MP2/6-31G(d)	14.9	152.6	14.0	154.6
MP2/6-31+G(d)	15.0	152.6	13.6	154.4
B3LYP/6-31G(d)	14.0	156.0	12.6	158.3
B3LYP/6-31+G(d)	12.4	157.2	10.1	159.5
B3LYP/6-31G(d,p)	13.1	156.9	11.5	159.4

Table S3-12: The calculated nitrogen-nitrogen bond lengths of the (Z)-MTI

Level of Theory	Bond Length (Å)							
	N_6-N_7				N_7-N_8			
	(c,t)	(t,c)	(c,c)	(t,t)	(c,t)	(t,c)	(c,c)	(t,t)
HF/STO-3G	1.272	1.268	1.268	1.270	1.441	1.491	1.479	1.464
HF/3-21G	1.242	1.228	1.228	1.228	1.394	1.509	1.483	1.506
HF/6-31G(d)	1.224	1.214	1.215	1.218	1.342	1.428	1.409	1.378
HF/6-31+G(d)	1.224	1.214	1.215	1.219	1.341	1.425	1.405	1.373
MP2/6-31G(d)	1.284	1.269	1.273	1.278	1.357	1.465	1.422	1.396
MP2/6-31+G(d)	1.286	1.271	1.276	1.280	1.356	1.455	1.412	1.388
B3LYP/6-31G(d)	1.266	1.248	1.256	1.258	1.354	1.485	1.410	1.398
B3LYP/6-31+G(d)	1.266	1.249	1.259	1.258	1.352	1.472	1.382	1.392
B3LYP/6-31G(d,p)	1.266	1.248	1.259	1.258	1.353	1.486	1.387	1.397

Table S3-13: The ‹($C_1N_2C_3N_4$) and ‹($C_3N_4C_5C_1$) dihedral angles of the (Z)-MTI configurations.

Level of Theory	Dihedral Angle (degrees)							
	‹($C_1N_2C_3N_4$)				‹($C_3N_4C_5C_1$)			
	(c,t)	(t,c)	(c,c)	(t,t)	(c,t)	(t,c)	(c,c)	(t,t)
HF/STO-3G	0.3	0.5	0.1	0.9	0.7	0.1	0.4	0.3
HF/3-21G	0.3	0.3	0.1	0.4	0.4	0.1	0.1	0.1
HF/6-31G(d)	0.3	0.8	0.1	1.7	0.5	0.3	0.1	0.5
HF/6-31+G(d)	0.2	0.9	0.1	1.6	0.4	0.2	0.1	0.3
MP2/6-31G(d)	0.7	1.1	0.3	2.0	0.6	0.1	0.2	0.4
MP2/6-31+G(d)	0.5	1.2	0.2	2.2	0.5	-0.1	0.4	0.4
B3LYP/6-31G(d)	0.6	1.1	0.6	2.1	0.6	0.6	0.2	1.1
B3LYP/6-31+G(d)	0.5	1.1	0.8	2.1	0.4	0.5	0.8	1.0
B3LYP/6-31G(d,p)	0.6	1.0	0.9	2.0	0.5	0.5	0.8	1.1

Table S3-14: The ‹($N_4C_5N_6N_7$) dihedral angle of the (Z)-MTI configurations.

Level of Theory	Dihedral Angle (degrees)			
	(c,t)	(t,c)	(c,c)	(t,t)
HF/STO-3G	159.5	12.7	172.5	31.3
HF/3-21G	163.3	4.2	177.4	5.4
HF/6-31G(d)	162.9	8.6	177.9	27.4
HF/6-31+G(d)	164.2	9.9	178.0	31.7
MP2/6-31G(d)	163.3	13.1	179.6	29.0
MP2/6-31+G(d)	163.2	16.4	179.3	34.7
B3LYP/6-31G(d)	164.3	8.0	175.4	23.0
B3LYP/6-31+G(d)	166.0	9.7	167.1	25.9
B3LYP/6-31G(d,p)	164.2	8.0	167.8	23.2

Table S3-15: The ‹($CN_8N_7N_6$) dihedral angle of the (Z)-MTI configurations.

Level of Theory	Dihedral Angle (degrees)			
	(c,t)	(t,c)	(c,c)	(t,t)
HF/STO-3G	165.4	96.6	90.5	175.4
HF/3-21G	171.3	106.4	94.7	146.7
HF/6-31G(d)	165.1	95.7	88.0	170.5
HF/6-31+G(d)	165.4	93.9	87.5	169.1
MP2/6-31G(d)	164.1	83.4	75.0	166.9
MP2/6-31+G(d)	164.1	79.6	71.4	165.2
B3LYP/6-31G(d)	165.2	91.4	66.9	168.9
B3LYP/6-31+G(d)	165.9	87.9	50.6	168.5
B3LYP/6-31G(d,p)	165.6	96.6	52.5	169.1

Table S3-16: The N_6-N_7 and N_7-N_8 bond lengths of the DTI configurations.

Level of Theory	Bond Length (Å)							
	(E)-DTI				(Z)-DTI			
	(t)	(c)	(t)	(c)	(t)	(c)	(t)	(c)
	N_6-N_7		N_7-N_8		N_6-N_7		N_7-N_8	
HF/STO-3G	1.280	1.280	1.428	1.426	1.268	1.267	1.497	1.484
HF/3-21G	1.247	1.250	1.363	1.350	1.229	1.229	1.505	1.482
HF/6-31G(d)	1.224	1.226	1.337	1.327	1.214	1.214	1.432	1.414
HF/6-31+G(d)	1.223	1.225	1.337	1.326	1.210	1.214	1.430	1.411
MP2/6-31G(d)	1.295	1.291	1.343	1.340	1.269	1.274	1.475	1.429
MP2/6-31+G(d)	1.294	1.291	1.344	1.340	1.271	1.277	1.469	1.419
B3LYP/6-31G(d)	1.272	1.272	1.344	1.338	1.248	1.255	1.495	1.426
B3LYP/6-31+G(d)	1.270	1.270	1.342	1.335	1.248	1.256	1.484	1.418
B3LYP/6-31G(d,p)	1.272	1.272	1.343	1.337	1.247	1.255	1.496	1.425

Table S3-17: The ‹($C_1N_2C_3N_4$) and ‹($C_3N_4C_5C_1$) dihedral angles of the DTI configurations.

Level of Theory	Dihedral Angle (degrees)							
	‹($C_1N_2C_3N_4$) (E)-DTI		‹($C_3N_4C_5C_1$) (E)-DTI		‹($C_1N_2C_3N_4$) (Z)-DTI		‹($C_3N_4C_5C_1$) (Z)-DTI	
	(t)	(c)	(t)	(c)	(t)	(c)	(t)	(c)
HF/STO-3G	0.1	0.1	0.4	0.1	0.1	0.1	0.1	0.3
HF/3-21G	0.0	0.0	0.2	0.1	0.0	0.0	0.1	0.0
HF/6-31G(d)	0.1	0.0	0.6	0.1	0.0	0.1	0.3	0.0
HF/6-31+G(d)	0.1	0.0	0.6	0.0	0.0	0.1	0.2	0.0
MP2/6-31G(d)	0.1	0.1	1.0	0.3	0.0	0.2	0.2	0.1
MP2/6-31+G(d)	0.1	0.1	1.0	0.1	0.1	0.4	0.1	0.0
B3LYP/6-31G(d)	0.0	0.0	0.9	0.4	0.1	0.2	0.5	0.2
B3LYP/6-31+G(d)	0.1	0.0	0.9	0.3	0.0	0.2	0.5	0.2
B3LYP/6-31G(d,p)	0.0	0.0	0.8	0.4	0.1	0.2	0.5	0.2

Table S3-18: The ‹($N_4C_5N_6N_7$) dihedral angle of the DTI configurations.

Level of Theory	Dihedral Angle (degrees)			
	(E)-DTI		(Z)-DTI	
	(t)	(c)	(t)	(c)
HF/STO-3G	2.2	179.3	10.5	173.9
HF/3-21G	0.9	178.7	2.5	178.1
HF/6-31G(d)	1.1	177.2	6.5	179.0
HF/6-31+G(d)	0.5	176.5	7.3	179.2
MP2/6-31G(d)	1.5	175.0	10.5	178.6
MP2/6-31+G(d)	1.6	178.0	11.8	178.3
B3LYP/6-31G(d)	0.8	177.6	6.0	180.0
B3LYP/6-31+G(d)	0.5	177.0	7.0	179.2
B3LYP/6-31G(d,p)	0.9	177.6	6.0	179.8

Table S4-1: The N_6-N_7 and N_7-N_8 triazene moiety bond lengths of the (E)-TIC configurations.

Level of Theory	Bond length (Å)							
	N_6-N_7				N_7-N_8			
	(t,c)	(t,t)	(c,c)	(c,t)	(t,c)	(t,t)	(c,c)	(c,t)
HF/STO-3G	1.280	1.279	1.280	1.277	1.432	1.431	1.429	1.433
HF/3-21G	1.247	1.247	1.250	1.239	1.348	1.347	1.342	1.351
HF/6-31G(d)	1.220	1.220	1.250	1.239	1.342	1.339	1.342	1.351
HF/6-31+G(d)	1.219	1.219	1.224	1.271	1.341	1.339	1.316	1.338
MP2/6-31G(d)	1.283	1.283	1.279	1.277	1.357	1.356	1.343	1.360
MP2/6-31+G(d)	1.281	1.282	1.278	1.277	1.356	1.355	1.339	1.358
B3LYP/6-31G(d)	1.265	1.265	1.266	1.260	1.350	1.349	1.332	1.354
B3LYP/6-31+G(d)	1.262	1.263	1.262	1.258	1.347	1.347	1.334	1.351
B3LYP/6-31G(d,p)	1.265	1.265	1.267	1.260	1.348	1.347	1.328	1.352

Table S4-2: The ‹(OCC_1C_5) and ‹($C_1C_5N_6N_7$) dihedral angles of (E)-TIC configurations.

Level of Theory	Dihedral Angle (degrees)							
	‹(OCC_1C_5)				‹($C_1C_5N_6N_7$)			
	(t,c)	(t,t)	(c,c)	(c,t)	(t,c)	(t,t)	(c,c)	(c,t)
HF/STO-3G	16.1	165.2	23.4	137.4	174.1	176.3	12.7	1.7
HF/3-21G	0.0	180.0	1.8	180.0	180.0	180.0	37.0	0.0
HF/6-31G(d)	2.6	178.4	1.8	180.0	174.6	178.0	37.0	0.0
HF/6-31+G(d)	2.4	179.6	5.7	151.3	174.4	178.0	43.7	38.0
MP2/6-31G(d)	7.1	172.0	11.1	160.2	174.2	176.9	34.8	6.1
MP2/6-31+G(d)	12.7	167.3	14.7	151.1	171.6	174.8	38.7	17.0
B3LYP/6-31G(d)	2.4	176.7	5.5	175.6	176.1	178.4	27.1	2.9
B3LYP/6-31+G(d)	1.7	179.6	6.7	178.5	176.0	178.5	37.9	2.0
B3LYP/6-31G(d,p)	1.2	178.5	4.9	177.4	176.3	178.5	28.5	2.5

Table S4-3: Important hydrogen-nitrogen distances found in the (E)-TIC configurations.

Level of Theory	Hydrogen-Nitrogen Distances (Å)			
	(t,c)	(t,t)	(c,c)	(c,t)
	$N_2\cdots H_{11}$	$N_6\cdots H_{11}$	$N_2\cdots H_{11}$	$N_7\cdots H_{11}$
HF/STO-3G	2.339	2.198	2.296	2.118
HF/3-21G	2.285	2.147	2.272	1.970
HF/6-31G(d)	2.341	2.252	2.272	1.970
HF/6-31+G(d)	2.351	2.260	2.349	2.256
MP2/6-31G(d)	2.298	2.176	2.285	1.994
MP2/6-31+G(d)	2.329	2.191	2.332	2.036
B3LYP/6-31G(d)	2.310	2.178	2.277	1.955
B3LYP/6-31+G(d)	2.328	2.197	2.326	1.967
B3LYP/6-31G(d,p)	2.305	2.173	2.274	1.945

Table S4-4: The N_6-N_7 triazene moiety bond lengths of the (Z)-TIC configurations.

Level of Theory	Bond length (Å)							
	N_6-N_7				N_7-N_8			
	(t,t)	(t,c)	(c,c)	(c,t)	(t,t)	(t,c)	(c,c)	(c,t)
HF/STO-3G	1.269	1.270	1.274	1.272	1.468	1.452	1.426	1.435
HF/3-21G	1.230	1.228	1.252	1.254	1.475	1.485	1.339	1.345
HF/6-31G(d)	1.219	1.253	1.225	1.227	1.365	1.392	1.332	1.325
HF/6-31+G(d)	1.220	1.253	1.224	1.299	1.359	1.392	1.333	1.349
MP2/6-31G(d)	1.276	1.272	1.278	1.283	1.399	1.393	1.349	1.351
MP2/6-31+G(d)	1.277	1.272	1.279	1.276	1.394	1.393	1.351	1.374
B3LYP/6-31G(d)	1.257	1.253	1.266	1.268	1.398	1.392	1.337	1.335
B3LYP/6-31+G(d)	1.257	1.253	1.265	1.255	1.392	1.392	1.337	1.369
B3LYP/6-31G(d,p)	1.257	1.254	1.267	1.268	1.396	1.387	1.334	1.336

Table S4-5: The ‹(OCC_1C_5) dihedral angle of (Z)-TIC configurations

Level of Theory	Dihedral Angle (degrees)							
	‹(OCC_1C_5)				‹($C_1C_5N_6N_7$)			
	(t,t)	(t,c)	(c,c)	(c,t)	(t,t)	(t,c)	(c,c)	(c,t)
HF/STO-3G	151.2	6.2	4.3	132.0	163.8	137.5	48.7	53.4
HF/3-21G	175.6	4.1	4.1	62.7	168.9	165.6	29.6	70.5
HF/6-31G(d)	172.7	6.9	9.6	163.5	151.4	151.3	56.4	82.1
HF/6-31+G(d)	170.4	6.9	9.7	152.4	146.7	151.3	57.9	77.9
MP2/6-31G(d)	177.5	9.6	8.0	130.9	162.6	146.7	47.5	120.5
MP2/6-31+G(d)	157.7	9.6	3.1	152.6	159.5	146.7	46.6	71.0
B3LYP/6-31G(d)	177.6	6.9	6.0	152.4	164.4	151.3	40.0	55.9
B3LYP/6-31+G(d)	174.4	6.9	5.3	159.5	162.3	151.3	42.5	66.7
B3LYP/6-31G(d,p)	176.1	6.2	5.6	147.6	164.1	148.3	37.7	54.1

Table S4-6: Important hydrogen-heteroatom distances of the (Z)-TIC configurations.

Level of Theory	Hydrogen-bond length (Å)				
	(t,t)	(t,c)	(c,c)		(c,t)
	$N_6\cdots H_{11}$	$N_2\cdots H_{11}$	$N_2\cdots H_{11}$	$N_8\text{-}H\cdots O$	$N_9\cdots H_{11}$
HF/STO-3G	2.152	2.354	2.282	1.538	3.894
HF/3-21G	2.126	2.277	2.197	1.668	3.188
HF/6-31G(d)	2.222	2.340	1.864	2.327	3.536
HF/6-31+G(d)	2.235	2.340	2.343	1.874	2.230
MP2/6-31G(d)	2.125	2.341	2.370	1.752	3.168
MP2/6-31+G(d)	2.152	2.341	2.270	1.754	2.053
B3LYP/6-31G(d)	2.125	2.340	2.240	1.696	3.118
B3LYP/6-31+G(d)	2.137	2.340	2.275	1.706	2.058
B3LYP/6-31G(d,p)	2.12	2.340	2.230	1.661	3.119

Table S4-7: N_6-N_7 bond lengths of the triazene moiety of (E)-MTIC configurations.

Level of Theory	N_6-N_7 bond length (Å)							
	(t,c,c)	(t,t,c)	(t,c,t)	(t,t,t)	(c,c,c)	(c,t,c)	(c,c,t)	(c,t,t)
HF/STO-3G	1.253	1.281	1.280	1.280	1.281	1.281	1.277	1.277
HF/3-21G	1.231	1.249	1.251	1.249	1.256	1.256	1.241	1.244
HF/6-31G(d)	1.226	1.223	1.230	1.223	1.227	1.230	1.221	1.224
HF/6-31+G(d)	1.226	1.222	1.226	1.222	1.226	1.230	1.221	1.225
MP2/6-31G(d)	1.291	1.289	1.291	1.288	1.283	1.287	1.283	1.285
MP2/6-31+G(d)	1.291	1.287	1.290	1.288	1.283	1.288	1.283	1.286
B3LYP/6-31G(d)	1.272	1.270	1.272	1.270	1.271	1.273	1.262	1.266
B3LYP/6-31+G(d)	1.271	1.268	1.271	1.269	1.269	1.271	1.263	1.265
B3LYP/6-31G(d,p)	1.273	1.270	1.272	1.270	1.271	1.273	1.265	1.266

Table S4-8: N_7-N_8 bond lengths of the triazene moiety of (E)-MTIC configurations.

Level of Theory	N_7-N_8 bond length (Å)							
	(t,c,c)	(t,t,c)	(t,c,t)	(t,t,t)	(c,c,c)	(c,t,c)	(c,c,t)	(c,t,t)
HF/STO-3G	1.340	1.430	1.424	1.428	1.426	1.422	1.430	1.425
HF/3-21G	1.308	1.349	1.339	1.345	1.329	1.331	1.352	1.344
HF/6-31G(d)	1.325	1.334	1.307	1.330	1.317	1.311	1.330	1.320
HF/6-31+G(d)	1.322	1.334	1.318	1.330	1.315	1.308	1.328	1.315
MP2/6-31G(d)	1.399	1.345	1.339	1.343	1.335	1.332	1.347	1.342
MP2/6-31+G(d)	1.338	1.345	1.337	1.343	1.332	1.328	1.347	1.337
B3LYP/6-31G(d)	1.335	1.338	1.335	1.337	1.323	1.325	1.342	1.340
B3LYP/6-31+G(d)	1.330	1.335	1.329	1.335	1.320	1.320	1.339	1.335
B3LYP/6-31G(d,p)	1.334	1.337	1.334	1.336	1.322	1.324	1.341	1.339

Table S4-9: The ‹(OCC_1C_5) dihedral angle of the (E)-MTIC configurations.

Level of Theory	‹(OCC_1C_5) Dihedral Angle (degrees)							
	(t,c,c)	(t,t,c)	(t,c,t)	(t,t,t)	(c,c,c)	(c,t,c)	(c,c,t)	(c,t,t)
HF/STO-3G	15.8	15.5	164.2	165.7	7.7	7.4	180.0	180.0
HF/3-21G	0.0	0.4	180.0	179.6	1.3	1.8	179.5	180.0
HF/6-31G(d)	0.9	2.3	176.5	177.8	4.9	5.2	155.0	158.5
HF/6-31+G(d)	1.1	2.0	178.8	180.0	4.1	4.5	152.5	155.2
MP2/6-31G(d)	6.2	6.8	171.0	171.4	9.3	9.6	156.8	157.4
MP2/6-31+G(d)	11.1	12.4	167.1	167.0	12.3	12.3	150.0	146.8
B3LYP/6-31G(d)	1.9	2.3	176.0	176.2	5.3	5.5	174.6	174.9
B3LYP/6-31+G(d)	0.4	1.1	179.3	179.4	5.7	6.3	177.8	179.2
B3LYP/6-31G(d,p)	0.3	0.9	177.9	179.2	4.7	5.0	176.8	177.8

Table S4-10: The ‹($C_1C_5N_6N_7$) dihedral angle of the (E)-MTIC configurations.

Level of Theory	‹($C_1C_5N_6N_7$) Dihedral Angle (degrees)							
	(t,c,c)	(t,t,c)	(t,c,t)	(t,t,t)	(c,c,c)	(c,t,c)	(c,c,t)	(c,t,t)
HF/STO-3G	174.9	175.8	176.3	176.8	37.8	38.7	25.2	26.7
HF/3-21G	180.0	178.2	180.0	179.5	32.6	36.9	0.6	0.0
HF/6-31G(d)	176.8	175.5	178.1	178.4	45.9	46.1	37.3	36.0
HF/6-31+G(d)	176.8	175.5	178.3	178.7	49.0	49.3	40.4	41.4
MP2/6-31G(d)	176.3	175.1	177.2	177.1	40.3	42.2	14.0	10.8
MP2/6-31+G(d)	173.3	172.6	175.5	175.5	43.2	46.5	22.1	28.2
B3LYP/6-31G(d)	178.2	177.1	178.8	178.8	32.3	34.8	1.7	2.1
B3LYP/6-31+G(d)	178.5	177.3	179.2	179.1	36.9	39.9	0.4	0.6
B3LYP/6-31G(d,p)	178.3	177.2	178.9	178.8	32.2	35.0	1.6	1.5

Table S4-11: Hydrogen-nitrogen distances of the (E)-MTIC configurations.

Level of Theory	Hydrogen-Nitrogen Distances (Å)							
	(t,c,c)	(t,t,c)	(t,c,t)	(t,t,t)	(c,c,c)	(c,t,c)	(c,c,t)	(c,t,t)
	$H_{11}N_2$	$H_{11}N_2$	$H_{11}N_6$	$H_{11}N_6$	$H_{11}N_2$	$H_{11}N_2$	$H_{11}N_7$	$H_{11}N_7$
HF/STO-3G	2.285	2.338	2.186	2.191	2.303	2.306	2.005	2.009
HF/3-21G	2.341	2.284	2.140	2.144	2.259	2.269	1.970	1.964
HF/6-31G(d)	2.342	2.342	2.228	2.247	2.342	2.342	2.213	2.156
HF/6-31+G(d)	2.350	2.246	2.238	2.253	2.356	2.356	2.248	2.203
MP2/6-31G(d)	2.295	2.296	2.152	2.168	2.285	2.388	2.777	1.992
MP2/6-31+G(d)	2.323	2.325	2.159	2.183	2.326	2.331	2.770	2.042
B3LYP/6-31G(d)	2.308	2.308	2.164	2.172	2.282	2.285	2.760	1.954
B3LYP/6-31+G(d)	2.327	2.327	2.172	2.189	2.317	2.321	2.766	1.965
B3LYP/6-31G(d,p)	2.304	2.304	2.158	2.167	2.278	2.281	2.760	1.944

Table S4-12: The N_6-N_7 bond length of the triazene moiety of (Z)-MTIC configurations.

Level of Theory	N_6-N_7 Bond Length Distances (Å)							
	(t,t,c)	(t,c,c)	(t,t,t)	(t,c,t)	(c,t,c)	(c,t,t)	(c,c,c)	(t,t,c)
HF/STO-3G	1.268	1.268	1.270	1.268	1.274	1.273	-	-
HF/3-21G	1.229	1.226	1.232	1.229	1.261	1.260	-	-
HF/6-31G(d)	1.215	1.213	1.222	1.215	1.229	1.233	1.231	1.231
HF/6-31+G(d)	1.213	1.213	1.232	1.215	1.229	1.232	1.231	1.231
MP2/6-31G(d)	1.268	1.268	1.281	1.274	1.285	1.292	1.284	1.286
MP2/6-31+G(d)	1.278	1.278	1.283	1.276	1.287	1.292	1.286	1.288
B3LYP/6-31G(d)	1.247	1.247	1.262	1.252	1.273	1.275	1.266	1.268
B3LYP/6-31+G(d)	1.249	1.249	1.263	1.253	1.273	1.274	1.267	1.268
B3LYP/6-31G(d,p)	1.247	1.247	1.262	1.252	1.274	1.275	1.266	1.268

Table S4-13: The N_7-N_8 bond length of the triazene moiety of (Z)-MTIC configurations.

Level of Theory	N_6-N_7 Bond Length Distances (Å)							
	(t,t,c)	(t,c,c)	(t,t,t)	(t,c,t)	(c,t,c)	(c,t,t)	(c,c,c)	(t,t,c)
HF/STO-3G	1.449	1.491	1.466	1.490	1.430	1.429	-	-
HF/3-21G	1.478	1.511	1.469	1.500	1.315	1.336	-	-
HF/6-31G(d)	1.401	1.418	1.350	1.419	1.318	1.311	1.302	1.311
HF/6-31+G(d)	1.408	1.408	1.312	1.414	1.318	1.312	1.302	1.311
MP2/6-31G(d)	1.456	1.456	1.382	1.451	1.332	1.325	1.332	1.351
MP2/6-31+G(d)	1.363	1.363	1.372	1.440	1.334	1.325	1.331	1.351
B3LYP/6-31G(d)	1.473	1.473	1.377	1.463	1.322	1.321	1.325	1.333
B3LYP/6-31+G(d)	1.448	1.448	1.370	1.451	1.322	1.319	1.324	1.331
B3LYP/6-31G(d,p)	1.475	1.475	1.376	1.465	1.320	1.321	1.325	1.334

Table S4-14: The ‹(OCC_1C_5) dihedral angle of the (Z)-MTIC configurations.

Level of Theory	‹(OCC_1C_5) Dihedral Angle (degrees)							
	(t,t,c)	(t,c,c)	(t,t,t)	(t,c,t)	(c,t,c)	(c,t,t)	(c,c,c)	(t,t,c)
HF/STO-3G	17.9	15.0	150.8	154.4	16.5	137.1	-	-
HF/3-21G	3.9	1.8	175.8	178.0	2.4	163.6	-	-
HF/6-31G(d)	8.7	11.7	172.4	177.9	10.0	167.5	9.5	152.8
HF/6-31+G(d)	11.9	11.9	161.3	173.1	10.3	161.3	8.1	152.3
MP2/6-31G(d)	12.1	12.1	177.4	179.2	8.5	167.6	0.9	135.3
MP2/6-31+G(d)	11.5	11.5	176.0	158.2	9.7	146.4	1.1	131.9
B3LYP/6-31G(d)	7.7	7.7	177.7	179.3	5.8	166.4	5.7	160.5
B3LYP/6-31+G(d)	10.2	10.2	175.9	175.9	5.1	158.1	4.3	156.4
B3LYP/6-31G(d,p)	6.9	6.9	176.5	177.8	5.3	165.8	7.2	159.2

Table S4-15: The ‹($C_1C_5N_6N_7$) dihedral angle of the (Z)-MTIC configurations.

Level of Theory	‹($C_1C_5N_6N_7$) Dihedral Angle (degrees)							
	(t,t,c)	(t,c,c)	(t,t,t)	(t,c,t)	(c,t,c)	(c,t,t)	(c,c,c)	(t,t,c)
HF/STO-3G	179.4	170.0	161.4	172.9	55.3	57.1	-	-
HF/3-21G	166.1	175.4	169.4	176.0	16.4	69.6	-	-
HF/6-31G(d)	179.1	163.7	146.6	171.9	55.0	77.1	72.9	73.0
HF/6-31+G(d)	156.8	156.8	84.0	170.3	57.2	84.0	71.9	75.2
MP2/6-31G(d)	170.9	170.9	161.0	175.1	44.3	66.3	54.1	53.6
MP2/6-31+G(d)	122.9	122.9	154.2	172.6	50.5	61.0	55.5	54.5
B3LYP/6-31G(d)	173.1	173.1	161.6	176.3	35.2	65.4	59.1	64.3
B3LYP/6-31+G(d)	168.6	168.6	158.5	174.9	38.4	66.4	60.3	66.1
B3LYP/6-31G(d,p)	173.3	173.3	161.4	176.3	32.7	65.2	59.8	63.7

Table S4-16: The hydrogen-heteroatom distances of the (Z)-MTIC configurations.

Level of Theory	Hydrogen-heteroatom Distances (Å)					
	(t,c,c)	(t,t,t)	(t,c,t)	(c,t,c)		(c,t,t)
	$H_{11}\cdots N_2$	$H_{11}\cdots N_6$	$H_{11}\cdots N_2$	$H_{11}\cdots N_2$	N_8-H···O	$H_{11}\cdots N_8$
HF/STO-3G	2.320	2.144	2.151	2.272	1.560	3.851
HF/3-21G	2.262	2.126	2.124	2.173	1.630	3.145
HF/6-31G(d)	2.350	2.193	2.228	2.322	1.887	3.412
HF/6-31+G(d)	2.374	2.196	2.507	2.341	1.908	3.610
MP2/6-31G(d)	2.316	2.122	2.121	2.227	1.747	3.014
MP2/6-31+G(d)	2.401	2.148	2.128	2.269	1.762	3.388
B3LYP/6-31G(d)	2.310	2.130	2.119	2.227	1.694	3.077
B3LYP/6-31G(d)	2.348	2.137	2.130	2.264	1.707	3.277
B3LYP/6-31G(d,p)	2.306	2.127	2.114	2.218	1.659	3.076

Table S4-17: The N_6-N_7 and N_7-N_8 bond lengths of the triazene moiety of the (E)-DTIC configurations.

Level of Theory	Bond Length (Å)							
	N_6-N_7				N_7-N_8			
	(t,c)	(t,t)	(c,c)	(c,t)	(t,c)	(t,t)	(c,c)	(c,t)
HF/STO-3G	1.282	1.281	1.282	1.279	1.423	1.422	1.419	1.426
HF/3-21G	1.254	1.255	1.261	1.245	1.342	1.335	1.322	1.346
HF/6-31G(d)	1.228	1.229	1.234	1.227	1.324	1.319	1.304	1.319
HF/6-31+G(d)	1.227	1.229	1.234	1.227	1.323	1.318	1.301	1.316
MP2/6-31G(d)	1.296	1.295	1.292	1.290	1.336	1.336	1.327	1.339
MP2/6-31+G(d)	1.296	1.296	1.294	1.292	1.336	1.336	1.324	1.337
B3LYP/6-31G(d)	1.275	1.229	1.278	1.269	1.333	1.319	1.318	1.338
B3LYP/6-31+G(d)	1.274	1.275	1.277	1.269	1.330	1.329	1.315	1.335
B3LYP/6-31G(d,p)	1.275	1.276	1.278	1.269	1.333	1.332	1.318	1.338

Table S4-18: The ‹(OCC_1C_5) and ‹($C_1C_5N_6N_7$) dihedral angles of the (E)-DTIC configurations

Level of Theory	Dihedral Angle (degrees)							
	‹(OCC_1C_5)				‹($C_1C_5N_6N_7$)			
	(t,c)	(t,t)	(c,c)	(c,t)	(t,c)	(t,t)	(c,c)	(c,t)
HF/STO-3G	15.5	162.6	9.0	139.9	175.8	176.5	36.7	1.2
HF/3-21G	0.0	179.9	1.3	179.3	179.5	179.4	32.0	1.1
HF/6-31G(d)	0.3	175.7	5.0	155.2	178.1	178.1	44.0	40.3
HF/6-31+G(d)	0.4	178.8	4.0	155.3	178.4	178.6	47.7	43.0
MP2/6-31G(d)	5.1	169.9	9.4	153.7	177.6	176.7	40.4	19.5
MP2/6-31+G(d)	9.6	166.5	11.7	147.6	178.5	175.2	45.5	29.6
B3LYP/6-31G(d)	1.4	175.7	5.2	171.9	179.3	178.1	31.5	3.8
B3LYP/6-31+G(d)	0.2	179.4	5.8	176.0	179.2	178.9	38.0	1.9
B3LYP/6-31G(d,p)	0.7	178.1	4.8	174.3	179.3	178.6	31.7	3.8

Table S4-19: The N_6-N_7 and N_7-N_8 bond lengths of the triazene moiety of the (Z)-DTIC configurations.

Level of Theory	Bond Length (Å)							
	N_6-N_7				N_7-N_8			
	(t,c)	(t,t)	(c,c)	(c,t)	(t,c)	(t,t)	(c,c)	(c,t)
HF/STO-3G	1.268	1.268	1.266	1.267	1.498	1.497	1.489	1.485
HF/3-21G	1.227	1.229	1.224	-	1.508	1.498	1.482	-
HF/6-31G(d)	1.213	1.215	1.210	1.212	1.425	1.424	1.414	1.410
HF/6-31+G(d)	1.213	1.215	1.210	1.213	1.420	1.421	1.412	1.406
MP2/6-31G(d)	1.268	1.274	1.292	1.273	1.468	1.460	1.330	1.433
MP2/6-31+G(d)	1.271	1.277	1.295	-	1.454	1.451	1.327	-
B3LYP/6-31G(d)	1.251	1.252	1.272	1.273	1.611	1.473	1.326	1.330
B3LYP/6-31+G(d)	1.247	1.253	1.273	1.273	1.468	1.462	1.322	1.327
B3LYP/6-31G(d,p)	1.246	1.252	1.272	1.273	1.491	1.474	1.326	1.330

Table S4-20: The ‹(OCC_1C_5) and ‹($C_1C_5N_6N_7$) dihedral angles of the (Z)-DTIC configurations.

Level of Theory	Dihedral Angle (degrees)							
	‹(OCC_1C_5)				‹($C_1C_5N_6N_7$)			
	(t,c)	(t,t)	(c,c)	(c,t)	(t,c)	(t,t)	(c,c)	(c,t)
HF/STO-3G	16.0	155.7	5.2	134.5	172.7	175.2	69.1	51.4
HF/3-21G	1.2	178.7	4.4	-	177.0	177.3	62.9	-
HF/6-31G(d)	11.8	179.4	7.4	92.5	167.7	173.9	64.2	15.3
HF/6-31+G(d)	13.0	174.8	7.4	95.6	164.1	172.8	64.9	19.1
MP2/6-31G(d)	12.2	177.6	2.2	95.4	173.6	176.4	48.2	24.4
MP2/6-31+G(d)	17.2	175.7	0.6	-	169.7	174.3	48.9	-
B3LYP/6-31G(d)	0.0	179.9	6.3	164.8	180.0	177.2	51.7	62.1
B3LYP/6-31+G(d)	10.1	177.0	5.4	160.4	172.7	176.6	53.7	65.0
B3LYP/6-31G(d,p)	6.2	178.3	7.5	164.3	175.3	177.2	52.0	62.1

Table S5-1: The N_1-N_2 and N_2-N_3 triazene moiety bond lengths of the TEMO configurations.

Level of Theory	Bond length (Å)			
	N_1-N_2		N_2-N_3	
	(t)	(c)	(t)	(c)
HF/STO-3G	1.279	1.279	1.479	1.420
HF/3-21G	1.245	1.243	1.408	1.419
HF/6-31G(d)	1.227	1.225	1.355	1.364
HF/6-31+G(d)	1.227	1.225	1.355	1.364
MP2/6-31G(d)	1.295	1.291	1.381	1.389
MP2/6-31+G(d)	1.297	1.293	1.382	1.390
B3LYP/6-31G(d)	1.269	1.265	1.386	1.398
B3LYP/6-31+G(d)	1.269	1.265	1.385	1.397
B3LYP/6-31G(d,p)	1.269	1.265	1.386	1.397

Table S5-2: The ‹(OCC_8C_9) and ‹($C_8C_9N_1N_2$) dihedral angles of the TEMO configurations.

Level of Theory	Dihedral Angle (degrees)			
	‹(OCC_8C_9)		‹($C_8C_9N_1N_2$)	
	(t)	(c)	(t)	(c)
HF/STO-3G	162.6	15.7	179.8	179.9
HF/3-21G	180.0	0.0	180.0	180.0
HF/6-31G(d)	180.0	0.0	180.0	180.0
HF/6-31+G(d)	180.0	0.0	180.0	180.0
MP2/6-31G(d)	174.7	3.4	179.9	179.8
MP2/6-31+G(d)	167.3	10.9	178.2	179.7
B3LYP/6-31G(d)	180.0	0.0	1800	180.0
B3LYP/6-31+G(d)	180.0	0.0	180.0	180.0
B3LYP/6-31G(d,p)	180.0	0.0	180.0	180.0

Table S5-3: The N-H···N hydrogen bond distance of the TEMO configurations.

Level of Theory	Distance (Å)	
	(t)	(c)
	N-H···N_1	N-H···N_7
HF/STO-3G	2.228	2.351
HF/3-21G	2.214	2.308
HF/6-31G(d)	2.302	2.368
HF/6-31+G(d)	2.307	2.374
MP2/6-31G(d)	2.214	2.329
MP2/6-31+G(d)	2.231	2.352
B3LYP/6-31G(d)	2.234	2.339
B3LYP/6-31+G(d)	2.246	2.355
B3LYP/6-31G(d,p)	2.233	2.336

Table S5-4: The triazene moiety bond lengths of the MITO configurations.

Level of Theory	MITO (c,a)		MITO (c,ag)		MITO (c,sg)	
	N_1-N_2	N_2-N_3	N_1-N_2	N_2-N_3	N_1-N_2	N_2-N_3
HF/STO-3G	1.278	1.424	1.278	1.423	1.278	1/425
HF/3-21G	1.241	1.426	1.242	1.420	1.240	1.428
HF/6-31G(d)	1.223	1.369	1.223	1.367	1.223	1.369
HF/6-31+G(d)	1.224	1.369	1.224	1.366	1.223	1.369
MP2/6-31G(d)	1.290	1.393	1.291	1.389	1.289	1.395
MP2/6-31+G(d)	-	-	-	-	-	-
B3LYP/6-31G(d)	1.263	1.403	1.264	1.397	1.262	1.404
B3LYP/6-31+G(d)	1.263	1.402	1.264	1.396	1.262	1.403
B3LYP/6-31G(d,p)	1.263	1.403	1.264	1.397	1.262	1.404

Level of Theory	MITO (t,a)		MITO (t,ag)		MITO (t,sg)	
	N_1-N_2	N_2-N_3	N_1-N_2	N_2-N_3	N_1-N_2	N_2-N_3
HF/STO-3G	1.278	1.420	1.278	1.420	1.278	1.421
HF/3-21G	1.243	1.415	1.243	1.410	1.242	1.416
HF/6-31G(d)	1.225	1.361	1.225	1.359	1.225	1.361
HF/6-31+G(d)	1.225	1.360	1.225	1.358	1.225	1.360
MP2/6-31G(d)	1.295	1.385	1.295	1.380	1.293	1.386
MP2/6-31+G(d)	-	-	-	-	-	-
B3LYP/6-31G(d)	1.267	1.392	1.268	1.387	1.267	1.392
B3LYP/6-31+G(d)	1.268	1.391	1.268	1.385	1.267	1.391
B3LYP/6-31G(d,p)	1.268	1.391	1.268	1.386	1.267	1.391

Table S5-5: The ‹(OCC_8C_9) and ‹($C_8C_9N_1N_2$) dihedral angles of the MITO C=O s-cis configurations.

Level of Theory	dihedral angle (degrees)					
	MITO (c,a)		MITO (c,ag)		MITO (c,sg)	
	‹(OCC_8C_9)	‹($C_8C_9N_1N_2$)	‹(OCC_8C_9)	‹($C_8C_9N_1N_2$)	‹(OCC_8C_9)	‹($C_8C_9N_1N_2$)
HF/STO-3G	15.9	179.4	14.9	179.8	14.9	179.8
HF/3-21G	0.1	179.8	0.4	179.6	0.6	179.7
HF/6-31G(d)	0.1	179.8	0.3	179.7	0.5	179.8
HF/6-31+G(d)	0.2	179.9	0.3	179.7	0.5	179.7
MP2/6-31G(d)	2.7	179.9	0.2	179.7	0.5	179.8
MP2/6-31+G(d)	-	-	-	-	-	-
B3LYP/6-31G(d)	0.2	179.8	0.3	179.7	0.5	179.8
B3LYP/6-31+G(d)	0.3	179.8	0.3	179.7	0.6	179.7
B3LYP/6-31G(d,p)	0.3	179.8	0.3	179.7	0.5	179.8

Table S5-6: The ‹(OCC_8C_9) and ‹($C_8C_9N_1N_2$) dihedral angles of the MITO C=O s-trans configurations.

Level of Theory	dihedral angles (degrees)					
	MITO (t,a)		MITO (t,ag)		MITO (t,sg)	
	‹(OCC_8C_9)	‹($C_8C_9N_1N_2$)	‹(OCC_8C_9)	‹($C_8C_9N_1N_2$)	‹(OCC_8C_9)	‹($C_8C_9N_1N_2$)
HF/STO-3G	162.6	179.5	163.2	179.6	162.9	179.6
HF/3-21G	179.9	179.8	179.7	179.9	179.5	179.9
HF/6-31G(d)	180.0	179.9	179.6	180.0	179.9	179.9
HF/6-31+G(d)	179.9	180.0	179.8	180.0	179.9	179.8
MP2/6-31G(d)	179.9	179.8	174.7	180.0	174.6	179.8
MP2/6-31+G(d)	-	-	-	-	-	-
B3LYP/6-31G(d)	179.9	179.9	180.0	179.9	179.6	179.9
B3LYP/6-31+G(d)	179.8	179.9	180.0	179.9	179.8	179.9
B3LYP/6-31G(d,p)	179.9	179.9	180.0	179.9	179.7	179.9

Table S5-7: The N-H···N hydrogen bond distance of the MITO configurations.

Level of Theory	N-H···N_7 distance (Å)		
	MITO (c,a)	MITO (c,ag)	MITO (c,sg)
HF/STO-3G	2.355	2.351	2.353
HF/3-21G	2.313	2.310	2.310
HF/6-31G(d)	2.372	2.369	2.370
HF/6-31+G(d)	2.377	2.375	2.375
MP2/6-31G(d)	2.333	2.333	2.331
MP2/6-31+G(d)	-	-	-
B3LYP/6-31G(d)	2.344	2.341	2.342
B3LYP/6-31+G(d)	2.358	2.356	2.356
B3LYP/6-31G(d,p)	2.340	2.337	2.338

Level of Theory	N-H···N_1 distance (Å)		
	MITO (t,a)	MITO (t,ag)	MITO (t,sg)
HF/STO-3G	2.239	2.235	2.231
HF/3-21G	2.223	2.221	2.220
HF/6-31G(d)	2.309	2.307	2.306
HF/6-31+G(d)	2.313	2.311	2.301
MP2/6-31G(d)	2.217	2.217	2.217
MP2/6-31+G(d)	-	-	-
B3LYP/6-31G(d)	2.243	2.241	2.240
B3LYP/6-31+G(d)	2.255	2.252	2.250
B3LYP/6-31G(d,p)	2.242	2.239	2.238

Table S6-1: The N_6-N_7 and N_7-N_8 bond lengths of the MTI_T configurations.

Level of Theory	N_6-N_7 Bond Length (Å)			
	(Z)-MTI_T (t,c)	(E)-MTI_T (t,c)	(E)-MTI_T (t,t)	(Z)-MTI_T (c,t)
HF/STO-3G	1.459	1.447	1.449	1.483
HF/3-21G	1.387	1.376	1.368	1.482
HF/6-31G(d)	1.336	1.333	1.327	1.411
HF/6-31+G(d)	1.354	1.366	1.367	1.411
MP2/6-31G(d)	1.367	1.382	1.343	1.446
MP2/6-31+G(d)	1.376	1.382	1.354	1.446
B3LYP/6-31G(d)	1.356	1.344	1.343	1.446
B3LYP/6-31+G(d)	1.356	1.342	1.342	1.444
B3LYP/6-31G(d,p)	1.356	1.344	1.343	1.443

Level of Theory	N_7-N_8 Bond Length (Å)			
	(Z)-MTI_T (t,c)	(E)-MTI_T (t,c)	(E)-MTI_T (t,t)	(Z)-MTI_T (c,t)
HF/STO-3G	1.265	1.270	1.270	1.263
HF/3-21G	1.234	1.234	1.238	1.221
HF/6-31G(d)	1.219	1.215	1.219	1.208
HF/6-31+G(d)	1.216	1.208	1.208	1.208
MP2/6-31G(d)	1.272	1.267	1.282	1.256
MP2/6-31+G(d)	1.272	1.265	1.277	1.256
B3LYP/6-31G(d)	1.256	1.256	1.263	1.237
B3LYP/6-31+G(d)	1.254	1.254	1.260	1.236
B3LYP/6-31G(d,p)	1.256	1.256	1.263	1.237

Table S6-2: The ‹($C_1C_5N_6N_7$) dihedral angle of the MTI_T configurations.

Level of Theory	‹($C_1C_5N_6N_7$) Dihedral Angle (degrees)			
	(Z)-MTI_T (t,c)	(E)-MTI_T (t,c)	(E)-MTI_T (t,t)	(Z)-MTI_T (c,t)
HF/STO-3G	141.6	133.1	124.4	32.5
HF/3-21G	180.0	180.0	179.9	42.7
HF/6-31G(d)	180.0	180.0	179.8	43.5
HF/6-31+G(d)	158.8	88.3	103.9	45.1
MP2/6-31G(d)	162.9	94.7	168.7	44.3
MP2/6-31+G(d)	150.6	81.4	150.9	44.5
B3LYP/6-31G(d)	179.9	180.0	180.0	48.3
B3LYP/6-31+G(d)	180.0	180.0	180.0	50.3
B3LYP/6-31G(d,p)	180.0	180.0	180.0	48.3

Table S6-3: The N_6-N_7 bond lengths of the MTIC_T configurations.

Level of Theory	Bond Length (Å)					
	(Z) (t,c,c)	(Z) (t,t,c)	(E) (t,c,c)	(E) (t,t,c)	(E) (t,c,t)	(E) (t,t,t)
HF/STO-3G	1.456	1.445	1.455	1.444	1.438	1.440
HF/3-21G	1.393	1.380	1.396	1.384	1.380	1.370
HF/6-31G(d)	1.343	1.338	1.357	1.353	1.338	1.340
HF/6-31+G(d)	1.345	1.341	1.359	1.353	1.341	1.341
MP2/6-31G(d)	1.365	1.350	1.379	1.360	1.350	1.345
MP2/6-31+G(d)	1.373	1.355	1.379	1.362	1.355	1.349
B3LYP/6-31G(d)	1.362	1.348	1.368	1.353	1.349	1.347
B3LYP/6-31+G(d)	1.363	1.348	1.368	1.352	1.348	1.346
B3LYP/6-31G(d,p)	1.363	1.349	1.367	1.353	1.349	1.347

Table S6-4: The N_7-N_8 bond length of the MTIC_T configurations.

Level of Theory	N_7-N_8 Bond Length (Å)					
	(Z) (t,c,c)	(Z) (t,t,c)	(E) (t,c,c)	(E) (t,t,c)	(E) (t,c,t)	(E) (t,t,t)
HF/STO-3G	1.265	1.270	1.265	1.270	1.272	1.271
HF/3-21G	1.232	1.232	1.231	1.231	1.232	1.236
HF/6-31G(d)	1.217	1.213	1.214	1.211	1.213	1.216
HF/6-31+G(d)	1.217	1.211	1.214	1.209	1.211	1.214
MP2/6-31G(d)	1.273	1.274	1.270	1.271	1.274	1.281
MP2/6-31+G(d)	1.272	1.271	1.271	1.269	1.271	1.279
B3LYP/6-31G(d)	1.253	1.254	1.252	1.253	1.254	1.261
B3LYP/6-31+G(d)	1.253	1.251	1.252	1.251	1.251	1.258
B3LYP/6-31G(d,p)	1.253	1.254	1.252	1.253	1.254	1.261

Table S6-5: The ‹($C_1C_5N_6N_7$) dihedral angle of the MTIC_T configurations.

Level of Theory	‹($C_1C_5N_6N_7$) Dihedral Angle (degrees)					
	(Z) (t,c,c)	(Z) (t,t,c)	(E) (t,c,c)	(E) (t,t,c)	(E) (t,c,t)	(E) (t,t,t)
HF/STO-3G	134.4	137.1	138.3	141.1	137.2	135.6
HF/3-21G	180.0	180.0	153.3	178.0	180.0	177.2
HF/6-31G(d)	180.0	180.0	152.9	166.7	180.0	166.6
HF/6-31+G(d)	174.2	171.0	166.4	166.3	171.0	164.6
MP2/6-31G(d)	164.2	168.4	149.5	166.2	168.4	169.4
MP2/6-31+G(d)	160.3	163.9	158.7	162.5	163.9	162.5
B3LYP/6-31G(d)	180.0	180.0	171.3	164.0	180.0	174.1
B3LYP/6-31+G(d)	180.0	180.0	171.6	175.5	180.0	175.7
B3LYP/6-31G(d,p)	180.0	180.0	172.5	174.7	180.0	174.6

Table S6-6: The ‹(OCC_1C_5) dihedral angle of the MTIC_T configurations.

Level of Theory	‹(OCC_1C_5) Dihedral Angle (degrees)					
	(Z) (t,c,c)	(Z) (t,t,c)	(E) (t,c,c)	(E) (t,t,c)	(E) (t,c,t)	(E) (t,t,t)
HF/STO-3G	3.6	4.8	156.0	155.6	3.9	153.9
HF/3-21G	0.0	0.0	176.5	153.9	0.0	152.2
HF/6-31G(d)	0.0	0.0	167.0	153.8	0.0	150.9
HF/6-31+G(d)	0.1	0.1	151.7	152.7	0.1	149.3
MP2/6-31G(d)	0.9	0.3	163.3	150.1	0.3	147.8
MP2/6-31+G(d)	0.8	0.2	145.0	145.5	0.2	143.5
B3LYP/6-31G(d)	0.0	0.0	152.8	153.3	0.0	151.5
B3LYP/6-31+G(d)	0.0	0.0	149.9	150.7	0.0	148.6
B3LYP/6-31G(d,p)	0.0	0.0	152.6	153.1	0.0	151.3

Table S6-7: The (E)-MTI (t,t) to (E)-MTI_T (t,c) N_6-N_7 and N_7-N_8 distances.

Level of Theory	Bond Lengths (Å)					
	N_6-N_7			N_7-N_8		
	(E)-MTI (t,t)	TS (t)	(E)-MTI_T (t,c)	(E)-MTI (t,t)	TS (t)	(E)-MTI_T (t,c)
HF/STO-3G	1.279	1.353	1.446	1.433	1.327	1.270
HF/3-21G	1.244	1.323	1.376	1.368	1.286	1.234
HF/6-31G(d)	1.220	1.279	1.333	1.345	1.256	1.215
HF/6-31+G(d)	1.219	1.279	1.366	1.344	1.255	1.208
MP2/6-31G(d)	1.288	1.322	1.382	1.352	1.316	1.267
MP2/6-31+G(d)	1.286	1.324	1.382	1.352	1.318	1.265
B3LYP/6-31G(d)	1.268	1.311	1.344	1.348	1.298	1.256
B3LYP/6-31+G(d)	1.265	1.310	1.342	1.346	1.298	1.254
B3LYP/6-31G(d,p)	1.268	1.311	1.344	1.347	1.290	1.256

Table S6-8: The H-N_6 and H-N_8 distances of the (E)-MTI (t,t) to (E)-MTI_T (t,c) gas-phase tautomerization pathway.

Level of Theory	Bond Lengths (Å)			
	H-N_8		H-N_6	
	(E)-MTI (t,t)	TS (t)	TS (t)	(E)-MTI_T (t,c)
HF/STO-3G	1.037	1.281	1.289	1.035
HF/3-21G	1.003	1.348	1.248	0.999
HF/6-31G(d)	1.002	1.343	1.332	0.998
HF/6-31+G(d)	1.002	1.347	1.335	1.001
MP2/6-31G(d)	1.024	1.389	1.349	1.023
MP2/6-31+G(d)	1.025	1.395	1.356	1.025
B3LYP/6-31G(d)	1.021	1.381	1.345	1.017
B3LYP/6-31+G(d)	1.022	1.385	1.350	1.018
B3LYP/6-31G(d,p)	1.020	1.366	1.331	1.016

Table S6-9: The (E)-MTI (c,t) to (Z)-MTI_T (c,t) GP tautomerization N-N bond lengths.

Level of Theory	Bond Lengths (Å)					
	N_6-N_7			N_7-N_8		
	(E)-MTI (c,t)	TS (c)	(Z)-MTI_T (c,t)	(E)-MTI (c,t)	TS (c)	(Z)-MTI_T (c,t)
HF/STO-3G	1.280	1.358	1.483	1.432	1.325	1.263
HF/3-21G	1.246	1.333	1.482	1.357	1.280	1.221
HF/6-31G(d)	1.221	1.292	1.411	1.337	1.251	1.208
HF/6-31+G(d)	1.220	1.294	1.411	1.336	1.250	1.208
MP2/6-31G(d)	1.284	1.327	1.446	1.348	1.310	1.256
MP2/6-31+G(d)	1.283	1.329	1.446	1.347	1.311	1.256
B3LYP/6-31G(d)	1.267	1.318	1.444	1.342	1.293	1.237
B3LYP/6-31+G(d)	1.264	1.318	1.442	1.340	1.292	1.236
B3LYP/6-31G(d,p)	1.267	1.318	1.443	1.341	1.294	1.237

Table S6-10: The (E)-MTI (c,t) to (Z)-MTI_T (c,t) tautomerization H-N bond lengths.

Level of Theory	Bond Lengths (Å)			
	$H\text{-}N_8$		$H\text{-}N_6$	
	(E)-MTI (c,t)	TS (c)	TS (c)	(Z)-MTI_T (c,t)
HF/STO-3G	1.037	1.276	1.295	1.038
HF/3-21G	1.001	1.345	1.349	1.004
HF/6-31G(d)	1.002	1.331	1.347	0.999
HF/6-31+G(d)	1.002	1.332	1.352	0.999
MP2/6-31G(d)	1.024	1.374	1.366	1.019
MP2/6-31+G(d)	1.025	1.379	1.374	1.019
B3LYP/6-31G(d)	1.021	1.374	1.359	1.016
B3LYP/6-31+G(d)	1.022	1.376	1.366	1.015
B3LYP/6-31G(d,p)	1.020	1.356	1.344	1.015

Table S6-11: $N_6\text{-}N_7$ bond lengths during the water mediated tautomerization of (E)-MTI (t,t) to (E)-MTI_T (t,c).

Level of Theory	$N_6\text{-}N_7$ Bond Length (Å)				
	(E)-MTI (t,t)	RC (t,t)	TS H_2O (t)	PC (t,c)	(E)-MTI_T (t,c)
HF/STO-3G	1.279	1.284	1.345	1.429	1.446
HF/3-21G	1.244	1.258	1.310	1.360	1.376
HF/6-31G(d)	1.220	1.226	1.272	1.331	1.333
HF/6-31+G(d)	1.219	1.224	1.268	1.354	1.366
MP2/6-31G(d)	1.288	1.295	1.314	1.333	1.382
MP2/6-31+G(d)	1.286	1.293	1.312	1.342	1.382
B3LYP/6-31G(d)	1.268	1.276	1.307	1.334	1.344
B3LYP/6-31+G(d)	1.265	1.273	1.304	1.333	1.342
B3LYP/6-31G(d,p)	1.268	1.277	1.308	1.334	1.344

Table S6-12: N_7-N_8 bond lengths during the water mediated tautomerization of (E)-MTI (t,t) to (E)-MTI_T (t,c).

Level of Theory	N_7-N_8 Bond Length (Å)				
	(E)-MTI (t,t)	RC (t,t)	TS H_2O (t)	PC (t,c)	(E)-MTI_T (t,c).
HF/STO-3G	1.433	1.418	1.320	1.274	1.270
HF/3-21G	1.368	1.337	1.281	1.242	1.234
HF/6-31G(d)	1.345	1.329	1.255	1.218	1.215
HF/6-31+G(d)	1.344	1.329	1.252	1.213	1.208
MP2/6-31G(d)	1.352	1.334	1.306	1.284	1.267
MP2/6-31+G(d)	1.352	1.336	1.304	1.280	1.265
B3LYP/6-31G(d)	1.348	1.330	1.294	1.265	1.256
B3LYP/6-31+G(d)	1.346	1.329	1.291	1.262	1.254
B3LYP/6-31G(d,p)	1.347	1.329	1.294	1.265	1.256

Table S6-13: HOH···N_6 distance during the water mediated tautomerization of (E)-MTI (t,t) to (E)-MTI_T (t,c).

Level of Theory	HOH···N_6 Distance (Å)				
	(E)-MTI (t,t)	RC (t,t)	TS H_2O (t)	PC (t,c)	(E)-MTI_T (t,c)
HF/STO-3G	∞	2.427	1.335	1.052	1.035
HF/3-21G	∞	2.002	1.261	1.015	0.999
HF/6-31G(d)	∞	2.255	1.129	1.004	0.998
HF/6-31+G(d)	∞	2.287	1.070	1.004	1.001
MP2/6-31G(d)	∞	2.037	1.274	1.032	1.023
MP2/6-31+G(d)	∞	2.056	1.192	1.030	1.025
B3LYP/6-31G(d)	∞	1.993	1.243	1.033	1.017
B3LYP/6-31+G(d)	∞	2.008	1.176	1.029	1.018
B3LYP/6-31G(d,p)	∞	1.991	1.259	1.032	1.026

Table S6-14: HOH···N_8 distance during the water mediated tautomerization of (E)-MTI (t,t) to (E)-MTI_T (t,c).

Level of Theory	HOH···N_8 Lengths (Å)				
	(E)-MTI (t,t)	RC (t,t)	TS H_2O (t)	PC (t,c)	(E)-MTI_T (t,c)
HF/STO-3G	1.037	1.653	1.312	2.508	∞
HF/3-21G	1.003	1.830	1.262	2.012	∞
HF/6-31G(d)	1.002	1.004	1.137	2.245	∞
HF/6-31+G(d)	1.002	1.004	1.082	2.257	∞
MP2/6-31G(d)	1.024	1.030	1.294	2.018	∞
MP2/6-31+G(d)	1.025	1.029	1.214	2.053	∞
B3LYP/6-31G(d)	1.021	1.030	1.264	1.966	∞
B3LYP/6-31+G(d)	1.022	1.027	1.197	1.994	∞
B3LYP/6-31G(d,p)	1.020	1.029	1.281	1.963	∞

Table S6-15: N_6-N_7 bond length during the water mediated tautomerization of (E)-MTI (c,t) to (Z)-MTI_T (c,t).

Level of Theory	N_6-N_7 Bond Length (Å)				
	(E)-MTI (c,t)	RC (c,t)	TS H_2O (c)	PC (c,t)	(Z)-MTI_T (c,t)
HF/STO-3G	1.280	1.285	1.348	1.428	1.483
HF/3-21G	1.246	1.261	1.315	1.360	1.482
HF/6-31G(d)	1.221	1.229	1.276	1.319	1.411
HF/6-31+G(d)	1.220	1.228	1.274	1.315	1.411
MP2/6-31G(d)	1.284	1.291	1.317	1.356	1.446
MP2/6-31+G(d)	1.283	1.291	1.315	1.359	1.446
B3LYP/6-31G(d)	1.267	1.277	1.309	1.334	1.444
B3LYP/6-31+G(d)	1.264	1.274	1.306	1.333	1.442
B3LYP/6-31G(d,p)	1.267	1.277	1.310	1.334	1.443

Table S6-16: N_7-N_8 bond length during the water mediated tautomerization of (E)-MTI (c,t) to (Z)-MTI_T (c,t).

Level of Theory	N_7-N_8 Bond Length (Å)				
	(E)-MTI (c,t)	RC (c,t)	TS H_2O (c)	PC (c,t)	(Z)-MTI_T (c,t)
HF/STO-3G	1.432	1.416	1.318	1.274	1.263
HF/3-21G	1.357	1.330	1.277	1.243	1.221
HF/6-31G(d)	1.337	1.316	1.251	1.215	1.208
HF/6-31+G(d)	1.336	1.317	1.247	1.213	1.208
MP2/6-31G(d)	1.348	1.328	1.301	1.277	1.256
MP2/6-31+G(d)	1.347	1.329	1.297	1.274	1.256
B3LYP/6-31G(d)	1.342	1.322	1.290	1.265	1.237
B3LYP/6-31+G(d)	1.340	1.322	1.287	1.262	1.236
B3LYP/6-31G(d,p)	1.341	1.321	1.291	1.265	1.237

Table S6-17: HOH···N_6 bond length during the water mediated tautomerization of (E)-MTI (c,t) to (Z)-MTI_T (c,t).

Level of Theory	HOH···N_6 Lengths (Å)				
	(E)-MTI (c,t)	RC (c,t)	TS H_2O (c)	PC (c,t)	(Z)-MTI_T (c,t)
HF/STO-3G	∞	2.493	1.324	1.052	1.038
HF/3-21G	∞	1.973	1.236	1.015	1.004
HF/6-31G(d)	∞	2.201	1.111	1.004	0.999
HF/6-31+G(d)	∞	2.232	1.064	1.003	0.999
MP2/6-31G(d)	∞	2.003	1.248	1.031	1.019
MP2/6-31+G(d)	∞	2.005	1.167	1.030	1.019
B3LYP/6-31G(d)	∞	1.960	1.217	1.033	1.016
B3LYP/6-31+G(d)	∞	1.965	1.150	1.029	1.015
B3LYP/6-31G(d,p)	∞	1.955	1.235	1.032	1.015

Table S6-18: HOH···N_8 distance during the water mediated tautomerization of (E)-MTI (c,t) to (Z)-MTI_T (c,t).

Level of Theory	HOH···N_8 Distance (Å)				
	(E)-MTI (c,t)	RC (c,t)	TS H_2O (c)	PC (c,t)	(Z)-MTI_T (c,t)
HF/STO-3G	1.037	1.048	1.307	2.651	∞
HF/3-21G	1.001	1.012	1.240	2.011	∞
HF/6-31G(d)	1.002	1.003	1.123	2.215	∞
HF/6-31+G(d)	1.002	1.003	1.080	2.256	∞
MP2/6-31G(d)	1.024	1.029	1.264	2.021	∞
MP2/6-31+G(d)	1.025	1.028	1.184	2.046	∞
B3LYP/6-31G(d)	1.021	1.029	1.242	1.966	∞
B3LYP/6-31+G(d)	1.022	1.027	1.180	1.966	∞
B3LYP/6-31G(d,p)	1.020	1.028	1.260	1.962	∞

Table S6-19: H-N_6 and H-N_8 bond lengths during gas-phase tautomerization of (E)-MTIC (t,t,c).

Level of Theory	Bond Lengths (Å)			
	H-N_6		H-N_8	
	TS (t,c)	(E)-MTIC_T (t,c,c)	(E)-MTIC (t,t,c)	TS (t,c)
HF/STO-3G	1.299	1.038	1.037	1.274
HF/3-21G	1.368	1.006	1.002	1.332
HF/6-31G(d)	1.346	1.001	1.002	1.331
HF/6-31+G(d)	1.348	1.003	1.003	1.333
MP2/6-31G(d)	1.359	1.025	1.024	1.373
MP2/6-31+G(d)	1.367	1.028	1.026	1.378
B3LYP/6-31G(d)	1.359	1.025	1.021	1.362
B3LYP/6-31+G(d)	1.363	1.024	1.022	1.367
B3LYP/6-31G(d,p)	1.346	1.002	1.022	1.347

Table S6-20: (E)-MTIC (t,t,c) gas-phase tautomerization N_6-N_7 and N_7-N_8 bond lengths.

Level of Theory	Bond Lengths (Å)					
	N_6-N_7			N_7-N_8		
	(E)-MTIC (t,t,c)	TS (t,c)	(E)-MTIC_T (t,c,c)	(E)-MTIC (t,t,c)	TS (t,c)	(E)-MTIC_T (t,c,c)
HF/STO-3G	1.281	1.359	1.445	1.430	1.320	1.270
HF/3-21G	1.249	1.338	1.380	1.349	1.276	1.232
HF/6-31G(d)	1.223	1.289	1.338	1.334	1.249	1.213
HF/6-31+G(d)	1.222	1.291	1.341	1.334	1.248	1.211
MP2/6-31G(d)	1.289	1.320	1.350	1.345	1.312	1.274
MP2/6-31+G(d)	1.287	1.323	1.355	1.345	1.314	1.271
B3LYP/6-31G(d)	1.270	1.313	1.348	1.338	1.291	1.254
B3LYP/6-31+G(d)	1.268	1.314	1.348	1.335	1.290	1.251
B3LYP/6-31G(d,p)	1.270	1.313	1.349	1.337	1.291	1.254

Table S6-21: (E)-MTIC (t,t,t) to (E)-MTIC_T (t,t,c) gas-phase H-N bond lengths.

Level of Theory	Bond Lengths (Å)			
	H-N_6		H-N_8	
	TS (t,t)	(E)-MTIC_T (t,t,c)	(E)-MTIC (t,t,t)	TS (t,t)
HF/STO-3G	1.302	1.037	1.037	1.271
HF/3-21G	1.355	1.001	1.001	1.345
HF/6-31G(d)	1.341	1.001	1.001	1.335
HF/6-31+G(d)	1.345	1.002	1.002	1.336
MP2/6-31G(d)	1.360	1.024	1.023	1.380
MP2/6-31+G(d)	1.367	1.026	1.025	1.385
B3LYP/6-31G(d)	1.353	1.020	1.021	1378
B3LYP/6-31+G(d)	1.358	1.021	1.021	1.378
B3LYP/6-31G(d,p)	1.337	1.019	1.019	1.361

Table S6-22: (E)-MTIC (t,t,t) to (E)-MTIC_T (t,t,c) gas-phase tautomerization of triazene bond lengths.

Level of Theory	Bond Lengths (Å)					
	N_6-N_7			N_7-N_8		
	(E)-MTIC (t,t,t)	TS (t,t)	(E)-MTIC_T (t,t,c)	(E)-MTIC (t,t,t)	TS (t,t)	(E)-MTIC_T (t,t,c)
HF/STO-3G	1.280	1.362	1.444	1.428	1.320	1.270
HF/3-21G	1.249	1.347	1.384	1.345	1.270	1.231
HF/6-31G(d)	1.223	1.294	1.353	1.330	1.247	1.211
HF/6-31+G(d)	1.222	1.296	1.353	1.330	1.246	1.209
MP2/6-31G(d)	1.288	1.327	1.360	1.343	1.312	1.271
MP2/6-31+G(d)	1.288	1.328	1.362	1.343	1.314	1.269
B3LYP/6-31G(d)	1.270	1.320	1.353	1.337	1.292	1.253
B3LYP/6-31+G(d)	1.269	1.321	1.352	1.335	1.290	1.251
B3LYP/6-31G(d,p)	1.270	1.320	1.353	1.336	1.292	1.253

Table S6-23: Gas-phase tautomerization of (E)-MTIC (c,c,c) H-N_6 and H-N_8 bond lengths.

Level of Theory	Bond Lengths (Å)			
	H-N_6		H-N_8	
	TS (c,c)	(E)-MTIC_T (t,c,c)	(E)-MTIC (c,c,c)	TS (c,c)
HF/STO-3G	1.311	1.038	1.037	1.262
HF/3-21G	1.368	1.006	1.001	1.324
HF/6-31G(d)	1.356	1.001	1.001	1.318
HF/6-31+G(d)	1.361	1.003	1.002	1.319
MP2/6-31G(d)	1.389	1.025	1.023	1.350
MP2/6-31+G(d)	1.398	1.028	1.024	1.354
B3LYP/6-31G(d)	1.368	1.023	1.021	1.363
B3LYP/6-31+G(d)	1.375	1.024	1.022	1.366
B3LYP/6-31G(d,p)	1.353	1.022	1.019	1.347

Table S6-24: Gas-phase tautomerization of MTIC (c,c,c) triazene bond lengths.

Level of Theory	Bond Lengths (Å)					
	N_6-N_7			N_7-N_8		
	(E)-MTIC (c,c,c)	TS (c,c)	(E)-MTIC_T (t,c,c)	(E)-MTIC (c,c,c)	TS (c,c)	(E)-MTIC_T (t,c,c)
HF/STO-3G	1.281	1.371	1.445	1.315	1.426	1.270
HF/3-21G	1.265	1.371	1.380	1.260	1.329	1.232
HF/6-31G(d)	1.227	1.314	1.338	1.236	1.317	1.213
HF/6-31+G(d)	1.226	1.317	1.341	1.234	1.315	1.211
MP2/6-31G(d)	1.283	1.334	1.350	1.296	1.335	1.274
MP2/6-31+G(d)	1.283	1.340	1.355	1.295	1.332	1.271
B3LYP/6-31G(d)	1.271	1.328	1.348	1.279	1.323	1.254
B3LYP/6-31+G(d)	1.269	1.330	1.348	1.276	1.320	1.251
B3LYP/6-31G(d,p)	1.271	1.329	1.349	1.280	1.322	1.254

Table S6-25: The H-N_6 and H-N_8 bond lengths during the gas-phase tautomerization of (E)-MTIC (c,c,t) to (E)-MTIC_T (t,t,c).

Level of Theory	Bond Lengths (Å)			
	H-N_6		H-N_8	
	TS (c,t)	(E)-MTIC_T (t,t,c)	(E)_MTIC (c,c,t)	TS (c,t)
HF/STO-3G	1.307	1.037	1.037	1.265
HF/3-21G	1.355	1.001	1.001	1.342
HF/6-31G(d)	1.348	1.001	1.001	1.330
HF/6-31+G(d)	1.352	1.002	1.002	1.333
MP2/6-31G(d)	1.368	1.024	1.024	1.376
MP2/6-31+G(d)	1.378	1.026	1.026	1.379
B3LYP/6-31G(d)	1.357	1.020	1.021	1.377
B3LYP/6-31+G(d)	1.362	1.021	1.021	1.380
B3LYP/6-31G(d,p)	1.341	1.019	1.019	1.362

Table S6-26: Triazene lengths during the gas-phase tautomerization of (E)-MTIC (c,c,t).

Level of Theory	Bond Lengths (Å)					
	N_6-N_7			N_7-N_8		
	(E)-MTIC (c,c,t)	TS (c,t)	(E)-MTIC_T (t,t,c)	(E)-MTIC (c,c,t)	TS (c,t)	(E)-MTIC_T (t,t,c)
HF/STO-3G	1.277	1.364	1.444	1.430	1.319	1.270
HF/3-21G	1.241	1.334	1.384	1.352	1.274	1.231
HF/6-31G(d)	1.221	1.295	1.353	1.330	1.245	1.211
HF/6-31+G(d)	1.221	1.298	1.353	1.328	1.244	1.209
MP2/6-31G(d)	1.283	1.323	1.360	1.347	1.307	1.271
MP2/6-31+G(d)	1.283	1.327	1.362	1.345	1.307	1.269
B3LYP/6-31G(d)	1.264	1.314	1.353	1.342	1.291	1.253
B3LYP/6-31+G(d)	1.263	1.315	1.352	1.339	1.290	1.251
B3LYP/6-31G(d,p)	1.265	1.314	1.353	1.341	1.292	1.253

Table S6-27: The N_6-N_7 length during the water mediated tautomerization of (E)-MTIC (t,t,c).

Level of Theory	N_6-N_7 bond length (Å)				
	SR	RC (t,t,c)	TS H_2O (t,c)	PC (t,c,c)	SP
HF/STO-3G	1.281	1.283	1.351	1.416	1.445
HF/3-21G	1.249	1.261	1.327	1.389	1.380
HF/6-31G(d)	1.223	1.228	1.251	1.346	1.338
HF/6-31+G(d)	1.222	1.227	1.295	1.346	1.341
MP2/6-31G(d)	1.289	1.292	1.317	1.353	1.350
MP2/6-31+G(d)	1.287	1.291	1.319	1.351	1.355
B3LYP/6-31G(d)	1.270	1.278	1.314	1.356	1.348
B3LYP/6-31+G(d)	1.268	1.275	1.314	1.355	1.348
B3LYP/6-31G(d,p)	1.270	1.278	1.314	1.356	1.349

Table S6-28: The N_7-N_8 length during the water mediated tautomerization of (E)-MTIC (t,t,c).

Level of Theory	N_7-N_8 bond length (Å)				
	SR	RC (t,t,c)	TS H_2O (t,c)	PC (t,c,c)	SP
HF/STO-3G	1.430	1.419	1.316	1.275	1.270
HF/3-21G	1.349	1.328	1.274	1.231	1.232
HF/6-31G(d)	1.334	1.319	1.292	1.212	1.213
HF/6-31+G(d)	1.334	1.319	1.248	1.211	1.211
MP2/6-31G(d)	1.345	1.331	1.308	1.275	1.274
MP2/6-31+G(d)	1.345	1.333	1.306	1.274	1.271
B3LYP/6-31G(d)	1.338	1.323	1.290	1.254	1.254
B3LYP/6-31+G(d)	1.335	1.321	1.288	1.251	1.251
B3LYP/6-31G(d,p)	1.337	1.322	1.291	1.254	1.254

Table S6-29: The HOH···N_6 distance during the water mediated tautomerization of (E)-MTIC (t,t,c).

Level of Theory	HOH···N_6 distance (Å)				
	SR	RC (t,t,c)	TS H_2O (t,c)	PC (t,c,c)	SP
HF/STO-3G	∞	2.343	1.377	1.110	1.038
HF/3-21G	∞	2.61	1.426	1.034	1.006
HF/6-31G(d)	∞	2.389	1.629	1.008	1.001
HF/6-31+G(d)	∞	2.413	1.713	1.008	1.003
MP2/6-31G(d)	∞	2.217	1.397	1.041	1.025
MP2/6-31+G(d)	∞	2.264	1.413	1.039	1.028
B3LYP/6-31G(d)	∞	2.230	1.366	1.044	1.023
B3LYP/6-31+G(d)	∞	2.81	1.363	1.040	1.024
B3LYP/6-31G(d,p)	∞	2.239	1.365	1.045	1.022

Table S6-30: The HOH···N_8 distance during the water mediated tautomerization of (E)-MTIC (t,t,c).

Level of Theory	HOH···N_8 distance (Å)				
	SR	RC (t,t,c)	TS H_2O (t,c)	PC (t,c,c)	SP
HF/STO-3G	1.037	1.059	1.323	3.638	∞
HF/3-21G	1.002	1.024	1.389	3.771	∞
HF/6-31G(d)	1.002	1.007	1.566	3.814	∞
HF/6-31+G(d)	1.003	1.006	1.646	3.877	∞
MP2/6-31G(d)	1.024	1.035	1.390	3.673	∞
MP2/6-31+G(d)	1.026	1.032	1.410	3.791	∞
B3LYP/6-31G(d)	1.021	1.036	1.368	3.701	∞
B3LYP/6-31+G(d)	1.022	1.030	1.369	3.806	∞
B3LYP/6-31G(d,p)	1.020	1.035	1.368	3.714	∞

Table S6-31: The N_6-N_7 length during the water mediated tautomerization of (E)-MTIC (t,t,t).

Level of Theory	N_6-N_7 bond length (Å)				
	SR	RC (t,t,t)	TS H_2O (t,t)	PC (t,t,c)	SP
HF/STO-3G	1.280	1.284	1.351	1.416	1.444
HF/3-21G	1.249	1.264	1.323	1.369	1.384
HF/6-31G(d)	1.223	1.231	1.277	1.332	1.353
HF/6-31+G(d)	1.222	1.230	1.276	1.332	1.353
MP2/6-31G(d)	1.288	1.295	1.318	1.338	1.360
MP2/6-31+G(d)	1.288	2.294	1.317	1.341	1.362
B3LYP/6-31G(d)	1.270	1.280	1.313	1.340	1.353
B3LYP/6-31+G(d)	1.269	1.278	1.310	1.340	1.352
B3LYP/6-31G(d,p)	1.270	1.280	1.314	1.340	1.353

Table S6-32: The N_7-N_8 length during the water mediated tautomerization of (E)-MTIC (t,t,t).

Level of Theory	N_7-N_8 bond length (Å)				
	SR	RC (t,t,t)	TS H_2O (t,t)	PC (t,t,c)	SP
HF/STO-3G	1.428	1.418	1.316	1.275	1.270
HF/3-21G	1.345	1.324	1.273	1.239	1.231
HF/6-31G(d)	1.330	1.312	1.250	1.217	1.211
HF/6-31+G(d)	1.330	1.311	1.246	1.216	1.209
MP2/6-31G(d)	1.343	1.328	1.305	1.282	1.271
MP2/6-31+G(d)	1.343	1.329	1.304	1.280	1.269
B3LYP/6-31G(d)	1.337	1.322	1.290	1.262	1.253
B3LYP/6-31+G(d)	1.335	1.317	1.287	1.259	1.251
B3LYP/6-31G(d,p)	1.336	1.312	1.290	1.262	1.253

Table S6-33: The HOH···N_6 distance during the water mediated tautomerization of (E)-MTIC (t,t,t).

Level of Theory	HOH···N_6 distance (Å)				
	SR	RC (t,t,t)	TS H_2O (t,t)	PC (t,t,c)	SP
HF/STO-3G	∞	2.353	1.367	1.081	1.307
HF/3-21G	∞	2.125	1.282	1.021	1.355
HF/6-31G(d)	∞	2.440	1.104	1.003	1.348
HF/6-31+G(d)	∞	2.493	1.058	1.003	1.352
MP2/6-31G(d)	∞	2.149	1.311	1.031	1.368
MP2/6-31+G(d)	∞	2.224	1.265	1.032	1.378
B3LYP/6-31G(d)	∞	2.122	1.279	1.032	1.357
B3LYP/6-31+G(d)	∞	2.219	1.179	1.030	1.362
B3LYP/6-31G(d,p)	∞	2.110	1.275	1.030	1.341

Table S6-34: The HOH···N_8 distance during the water mediated tautomerization of (E)-MTIC (t,t,t).

Level of Theory	HOH···N_8 distance (Å)				
	SR	RC (t,t,t)	TS H_2O (t,t)	PC (t,t,c)	SP
HF/STO-3G	1.037	1.057	1.323	3.788	∞
HF/3-21G	1.001	1.016	1.282	2.082	∞
HF/6-31G(d)	1.001	1.005	1.127	2.270	∞
HF/6-31+G(d)	1.002	1.005	1.092	2.301	∞
MP2/6-31G(d)	1.023	1.032	1.329	2.035	∞
MP2/6-31+G(d)	1.025	1.031	1.286	2.054	∞
B3LYP/6-31G(d)	1.021	1.037	1.254	1.991	∞
B3LYP/6-31+G(d)	1.021	1.028	1.207	2.051	∞
B3LYP/6-31G(d,p)	1.019	1.031	1.301	1.990	∞

Table S6-35: The N_6-N_7 bond length during the water mediated tautomerization of (E)-MTIC (c,c,c).

Level of Theory	N_6-N_7 bond length (Å)				
	SR	RC (c,c,c)	TS H_2O (c,c)	PC (t,c,c)	SP
HF/STO-3G	1.281	1.288	—	1.416	1.445
HF/3-21G	1.265	1.275	1.338	1.389	1.380
HF/6-31G(d)	1.227	1.237	1.288	1.346	1.338
HF/6-31+G(d)	1.226	1.235	1.284	1.346	1.341
MP2/6-31G(d)	1.283	1.293	1.317	1.353	1.350
MP2/6-31+G(d)	1.283	1.290	1.319	1.351	1.355
B3LYP/6-31G(d)	1.271	1.283	1.320	1.356	1.348
B3LYP/6-31+G(d)	1.269	1.280	1.317	1.355	1.348
B3LYP/6-31G(d,p)	1.271	1.283	1.321	1.356	1.349

Table S6-36: The N_7-N_8 bond length during the water mediated tautomerization of (E)-MTIC (c,c,c).

Level of Theory	N_7-N_8 bond length (Å)				
	SR	RC (c,c,c)	TS H_2O (c,c)	PC (t,c,c)	SP
HF/STO-3G	1.426	1.407	—	1.275	1.270
HF/3-21G	1.329	1.308	1.264	1.231	1.232
HF/6-31G(d)	1.317	1.298	1.242	1.212	1.213
HF/6-31+G(d)	1.315	1.298	1.239	1.211	1.211
MP2/6-31G(d)	1.335	1.317	1.306	1.275	1.274
MP2/6-31+G(d)	1.332	1.323	1.306	1.274	1.271
B3LYP/6-31G(d)	1.323	1.307	1.280	1.254	1.254
B3LYP/6-31+G(d)	1.320	1.306	1.276	1.251	1.251
B3LYP/6-31G(d,p)	1.322	1.308	1.280	1.254	1.254

Table S6-37: The HOH···N_6 distance during the water mediated tautomerization of (E)-MTIC (c,c,c).

Level of Theory	HOH···N_6 distance (Å)				
	SR	RC (c,c,c)	TS H_2O (c,c)	PC (t,c,c)	SP
HF/STO-3G	∞	2.597	—	1.110	1.038
HF/3-21G	∞	1.950	1.254	1.034	1.006
HF/6-31G(d)	∞	2.196	1.120	1.008	1.001
HF/6-31+G(d)	∞	2.221	1.081	1.008	1.003
MP2/6-31G(d)	∞	2.003	1.392	1.041	1.025
MP2/6-31+G(d)	∞	2.942	1.412	1.039	1.028
B3LYP/6-31G(d)	∞	1.953	1.230	1.044	1.023
B3LYP/6-31+G(d)	∞	1.964	1.169	1.040	1.024
B3LYP/6-31G(d,p)	∞	1.972	1.266	1.045	1.022

Table S6-38: The HOH···N_8 distance during the water mediated tautomerization of (E)-MTIC (c,c,c).

Level of Theory	HOH···N_8 distance (Å)				
	SR	RC (c,c,c)	TS H_2O (c,c)	PC (t,c,c)	SP
HF/STO-3G	1.037	1.049	—	3.638	∞
HF/3-21G	1.001	1.014	1.250	3.771	∞
HF/6-31G(d)	1.001	1.004	1.126	3.814	∞
HF/6-31+G(d)	1.002	1.004	1.070	3.877	∞
MP2/6-31G(d)	1.023	1.030	1.390	3.673	∞
MP2/6-31+G(d)	1.024	1.024	1.409	3.791	∞
B3LYP/6-31G(d)	1.021	1.031	1.249	3.701	∞
B3LYP/6-31+G(d)	1.022	1.028	1.190	3.806	∞
B3LYP/6-31G(d,p)	1.019	1.030	1.247	3.714	∞

Table S6-39: The N_6-N_7 bond length during the water mediated tautomerization of (E)-MTIC (c,c,t).

Level of Theory	N_6-N_7 bond length (Å)				
	SR	RC (c,c,t)	TS H_2O (c,t)	PC (t,t,c)	SP
HF/STO-3G	1.277	1.283	—	1.416	1.444
HF/3-21G	1.241	1.257	1.320	1.369	1.384
HF/6-31G(d)	1.221	1.231	1.282	1.332	1.353
HF/6-31+G(d)	1.221	1.230	1.277	1.332	1.353
MP2/6-31G(d)	1.283	1.291	1.319	1.338	1.360
MP2/6-31+G(d)	1.283	1.292	1.319	1.341	1.362
B3LYP/6-31G(d)	1.264	1.274	1.310	1.340	1.353
B3LYP/6-31+G(d)	1.263	1.273	1.248	1.340	1.352
B3LYP/6-31G(d,p)	1.265	1.275	1.311	1.340	1.353

Table S6-40: The N_7-N_8 bond length during the water mediated tautomerization of (E)-MTIC (c,c,t).

Level of Theory	N_7-N_8 bond length (Å)				
	SR	RC (c,c,t)	TS H_2O (c,t)	PC (t,t,c)	SP
HF/STO-3G	1.430	1.415	—	1.275	1.270
HF/3-21G	1.352	1.325	1.273	1.239	1.231
HF/6-31G(d)	1.330	1.306	1.248	1.217	1.211
HF/6-31+G(d)	1.328	1.306	1.245	1.216	1.209
MP2/6-31G(d)	1.347	1.325	1.299	1.282	1.271
MP2/6-31+G(d)	1.345	1.323	1.299	1.280	1.269
B3LYP/6-31G(d)	1.342	1.323	1.288	1.262	1.253
B3LYP/6-31+G(d)	1.339	1.322	1.282	1.259	1.251
B3LYP/6-31G(d,p)	1.341	1.321	1.288	1.262	1.253

Table S6-41: The HOH···N_6 distance during the water mediated tautomerization of (E)-MTIC (c,c,t).

Level of Theory	HOH-N_6 distance (Å)				
	SR	RC (c,c,t)	TS H_2O (c,t)	PC (t,t,c)	SP
HF/STO-3G	∞	2.687	—	1.081	1.307
HF/3-21G	∞	2.042	1.281	1.021	1.355
HF/6-31G(d)	∞	2.249	1.137	1.003	1.348
HF/6-31+G(d)	∞	2.280	1.081	1.003	1.352
MP2/6-31G(d)	∞	2.034	1.292	1.031	1368
MP2/6-31+G(d)	∞	2.039	1.292	1.032	1.378
B3LYP/6-31G(d)	∞	1.993	1.250	1.032	1.357
B3LYP/6-31+G(d)	∞	2.009	1.137	1.030	1.362
B3LYP/6-31G(d,p)	∞	1.995	1.266	1.030	1.341

Table S6-42: The HOH···N_8 distance during the water mediated tautomerization of (E)-MTIC (c,c,t).

Level of Theory	HOH···N_8 distance (Å)				
	SR	RC (c,c,t)	TS H_2O (c,t)	PC (t,t,c)	SP
HF/STO-3G	1.037	1.050	—	3.788	∞
HF/3-21G	1.001	1.810	1.275	2.082	∞
HF/6-31G(d)	1.001	1.004	1.139	2.270	∞
HF/6-31+G(d)	1.002	1.004	1.082	2.301	∞
MP2/6-31G(d)	1.024	1.031	1.298	2.035	∞
MP2/6-31+G(d)	1.026	1.030	1.298	2.054	∞
B3LYP/6-31G(d)	1.021	1.030	1.268	1.991	∞
B3LYP/6-31+G(d)	1.021	1.027	1.139	2.051	∞
B3LYP/6-31G(d,p)	1.019	1.029	1.285	1.990	∞

Table S7-1: Bond length comparison during the (E)-MTI (t,c) + F^- S_N2 pathway

Level of Theory	C-X Distance (Å)					C-N_8 Distance (Å)				
	SR	RC	TS	PC	SP	SR	RC	TS	PC	SP
HF/6-31G(d)	∞	3.549	1.924	1.388	1.365	1.447	1.446	1.853	1.388	∞
HF/6-31+G(d)	∞	3.530	1.902	1.398	1.371	1.448	1.446	1.953	1.398	∞
MP2/6-31G(d)	∞	3.465	1.917	1.425	1.392	1.453	1.454	1.783	1.415	∞
MP2/6-31+G(d)	∞	3.452	1.858	1.437	1.407	1.455	1.453	1.922	1.437	∞
B3LYP/6-31G(d)	∞	3.293	1.988	1.408	1.383	1.455	1.457	1.785	1.408	∞
B3LYP/6-31+G(d)	∞	3.384	1.901	1.426	1.393	1.455	1.454	1.940	1.426	∞
B3LYP/6-31G(d,p)	∞	3.336	1.981	1.408	1.383	1.454	1.454	1.790	1.408	∞

Level of Theory	N_8-N_7 Distance (Å)					N_7-N_6 Distance (Å)				
	SR	RC	TS	PC	SP	SR	RC	TS	PC	SP
HF/6-31G(d)	1.337	1.260	1.274	1.256	1.078	1.223	1.285	1.262	1.297	1.301
HF/6-31+G(d)	1.335	1.262	1.274	1.256	1.079	1.222	1.281	1.261	1.289	1.292
MP2/6-31G(d)	1.346	1.304	1.315	1.312	1.131	1.290	1.330	1.311	1.329	1.333
MP2/6-31+G(d)	1.345	1.306	1.319	1.352	1.131	1.289	1.324	1.308	1.322	1.322
B3LYP/6-31G(d)	1.346	1.289	1.311	1.296	1.106	1.269	1.320	1.297	1.325	1.329
B3LYP/6-31+G(d)	1.342	1.293	1.303	1.296	1.105	1.267	1.308	1.295	1.315	1.317
B3LYP/6-31G(d,p)	1.345	1.290	1.310	1.296	1.106	1.270	1.320	1.298	1.325	1.330

Table S7-2: Bond length comparison during the (E)-MTI (t,t) + F^- S_N2 pathway

Level of Theory	C-X Distance (Å)					$C-N_8$ Distance (Å)				
	SR	RC	TS	PC	SP	SR	RC	TS	PC	SP
HF/6-31G(d)	∞	3.479	1.906	1.384	1.365	1.447	1.442	1.906	1.384	∞
HF/6-31+G(d)	∞	3.452	1.879	1.394	1.371	1.448	1.444	1.879	1.394	∞
MP2/6-31G(d)	∞	3.425	1.906	1.413	1.392	1.453	1.452	1.906	1.413	∞
MP2/6-31+G(d)	∞	3.382	1.843	1.434	1.407	1.455	1.455	1.843	1.434	∞
B3LYP/6-31G(d)	∞	3.310	1.970	1.404	1.383	1.455	1.450	1.970	1.404	∞
B3LYP/6-31+G(d)	∞	3.320	1.877	1.426	1.393	1.455	1.451	1.877	1.426	∞
B3LYP/6-31G(d,p)	∞	3.309	1.962	1.404	1.383	1.454	1.450	1.962	1.404	∞

Level of Theory	N_8-N_7 Distance (Å)					N_7-N_6 Distance (Å)				
	SR	RC	TS	PC	SP	SR	RC	TS	PC	SP
HF/6-31G(d)	1.337	1.259	1.263	1.249	1.245	1.223	1.282	1.268	1.302	1.310
HF/6-31+G(d)	1.335	1.258	1.264	1.252	1.245	1.222	1.278	1.268	1.297	1.303
MP2/6-31G(d)	1.346	1.308	1.299	1.299	1.296	1.290	1.321	1.313	1.334	1.340
MP2/6-31+G(d)	1.345	1.307	1.304	1.303	1.299	1.289	1.316	1.312	1.328	1.334
B3LYP/6-31G(d)	1.346	1.297	1.292	1.382	1.279	1.269	1.312	1.302	1.330	1.337
B3LYP/6-31+G(d)	1.342	1.294	1.288	1.285	1.282	1.267	1.304	1.302	1.322	1.328
B3LYP/6-31G(d,p)	1.345	1.295	1.291	1.283	1.279	1.270	1.313	1.303	1.329	1.337

Table S7-3: Bond length comparison during the (E)-MTI (c,c) + F^- S_N2 pathway

Level of Theory	C-X Distance (Å)					C-N_8 Distance (Å)				
	SR	RC	TS	PC	SP	SR	RC	TS	PC	SP
HF/6-31G(d)	∞	3.474	1.920	1.388	1.365	1.447	1.448	1.858	3.136	∞
HF/6-31+G(d)	∞	3.493	1.899	1.398	1.371	1.448	1.448	1.958	3.190	∞
MP2/6-31G(d)	∞	3.343	1.906	1.416	1.392	1.453	1.455	1.794	3.012	∞
MP2/6-31+G(d)	∞	3.415	1.851	1.438	1.407	1.455	1.455	1.932	3.043	∞
B3LYP/6-31G(d)	∞	3.215	1.980	1.409	1.383	1.455	1.459	1.793	3.063	∞
B3LYP/6-31+G(d)	∞	3.346	1.894	1.430	1.393	1.455	1.456	1.951	3.099	∞
B3LYP/6-31G(d,p)	∞	3.233	1.972	1.409	1.383	1.454	1.460	1.798	3.046	∞

Level of Theory	N_8-N_7 Distance (Å)					N_7-N_6 Distance (Å)				
	SR	RC	TS	PC	SP	SR	RC	TS	PC	SP
HF/6-31G(d)	1.337	1.256	1.269	1.252	1.251	1.223	1.290	1.266	1.302	1.306
HF/6-31+G(d)	1.335	1.257	1.268	1.253	1.251	1.222	1.286	1.266	1.295	1.398
MP2/6-31G(d)	1.346	1.302	1.313	1.309	1.309	1.290	1.329	1.309	1.331	1.335
MP2/6-31+G(d)	1.345	1.304	1.316	1.311	1.309	1.289	1.323	1.306	1.322	1.323
B3LYP/6-31G(d)	1.346	1.288	1.306	1.393	1.293	1.269	1.321	1.298	1.327	1.332
B3LYP/6-31+G(d)	1.342	1.290	1.297	1.292	1.291	1.267	1.310	1.297	1.317	1.318
B3LYP/6-31G(d,p)	1.345	1.288	1.305	1.293	1.293	1.270	1.322	1.298	1.327	1.332

Table S7-4: Bond length comparison during the (E)-MTI (c,t) + F^- S_N2 pathway

Level of Theory	C-X Distance (Å)					C-N_8 Distance (Å)				
	SR	RC	TS	PC	SP	SR	RC	TS	PC	SP
HF/6-31G(d)	∞	3.535	1.912	1.385	1.365	1.447	1.443	1.841	3.051	∞
HF/6-31+G(d)	∞	3.486	1.886	1.395	1.371	1.448	1.445	1.939	3.104	∞
MP2/6-31G(d)	∞	3.509	1.909	1.413	1.392	1.453	1.453	1.773	2.938	∞
MP2/6-31+G(d)	∞	3.415	1.847	1.434	1.407	1.455	1.456	1.914	2.973	∞
B3LYP/6-31G(d)	∞	3.390	1.974	1.405	1.383	1.455	1.451	1.771	2.972	∞
B3LYP/6-31+G(d)	∞	3.342	1.882	1.426	1.393	1.455	1.452	1.924	3.002	∞
B3LYP/6-31G(d,p)	∞	3.392	1.965	1.405	1.383	1.454	1.451	1.776	2.959	∞

Level of Theory	N_8-N_7 Distance (Å)					N_7-N_6 Distance (Å)				
	SR	RC	TS	PC	SP	SR	RC	TS	PC	SP
HF/6-31G(d)	1.337	1.254	1.259	1.254	1.242	1.223	1.287	1.273	1.308	1.315
HF/6-31+G(d)	1.335	1.252	1.258	1.247	1.243	1.222	1.284	1.273	1.303	1.309
MP2/6-31G(d)	1.346	1.307	1.295	1.296	1.292	1.290	1.320	1.313	1.335	1.342
MP2/6-31+G(d)	1.345	1.305	1.300	1.299	1.295	1.289	1.314	1.311	1.329	1.336
B3LYP/6-31G(d)	1.346	1.293	1.288	1.279	1.276	1.269	1.314	1.304	1.332	1.339
B3LYP/6-31+G(d)	1.342	1.291	1.283	1.282	1.278	1.267	1.304	1.303	1.324	1.330
B3LYP/6-31G(d,p)	1.345	1.293	1.287	1.280	1.276	1.270	1.314	1.304	1.331	1.340

Table S7-5: Bond length comparison during the (Z)-MTI (c,t) + F^- S_N2 pathway

Level of Theory	C-X Distance (Å)					$C-N_8$ Distance (Å)				
	SR	RC	TS	PC	SP	SR	RC	TS	PC	SP
HF/6-31G(d)	∞	3.121	1,908	1.386	1.365	1.447	1.449	1.848	3.044	∞
HF/6-31+G(d)	∞	3,221	1.881	1.396	1.371	1.448	1.451	1.946	3.102	∞
MP2/6-31G(d)	∞	3.071	1.840	1.415	1.392	1.453	1.461	1.926	2.932	∞
MP2/6-31+G(d)	∞	3.204	1.840	1.436	1.407	1.455	1.464	1.926	2.968	∞
B3LYP/6-31G(d)	∞	3.045	1.971	1.406	1.383	1.455	1.458	1.782	2.977	∞
B3LYP/6-31+G(d)	∞	3.134	1.875	1.428	1.393	1.455	1.462	1.939	3.011	∞
B3LYP/6-31G(d,p)	∞	3.043	1.963	1.406	1.383	1.454	1.458	1.787	2.965	∞

Level of Theory	N_8-N_7 Distance (Å)					N_7-N_6 Distance (Å)				
	SR	RC	TS	PC	SP	SR	RC	TS	PC	SP
HF/6-31G(d)	1.337	1.267	1.265	1.252	1.249	1.223	1.277	1.272	1.305	1.313
HF/6-31+G(d)	1.335	1.267	1.246	1.255	1.251	1.222	1.277	1.275	1.302	1.308
MP2/6-31G(d)	1.346	1.320	1.308	1.304	1.301	1.290	1.313	1.317	1.336	1.344
MP2/6-31+G(d)	1.345	1.322	1.308	1.308	1.305	1.289	1.313	1.312	1.335	1.341
B3LYP/6-31G(d)	1.346	1.307	1.296	1.287	1.284	1.269	1.302	1.303	1.331	1.339
B3LYP/6-31+G(d)	1.342	1.308	1.292	1.290	1.287	1.267	1.299	1.306	1.326	1.333
B3LYP/6-31G(d,p)	1.345	1.307	1.295	1.287	1.284	1.270	1.302	1.303	1.331	1.339

Table S7-6: Bond length comparison during the (Z)-MTI (t,c) + F^- S_N2 pathway

Level of Theory	C-X Distance (Å)					$C-N_8$ Distance (Å)				
	SR	RC	TS	PC	SP	SR	RC	TS	PC	SP
HF/6-31G(d)	∞	3.407	1.961	1.387	1.365	1.447	1.440	1.862	4.696	∞
HF/6-31+G(d)	∞	3.404	1.932	1.396	1.371	1.448	1.444	1.959	4.762	∞
MP2/6-31G(d)	∞	3.523	1.996	1.415	1.392	1.453	1.449	1.777	4.573	∞
MP2/6-31+G(d)	∞	3.573	1.914	1.436	1.407	1.455	1.453	1.909	4.648	∞
B3LYP/6-31G(d)	∞	3.511	2.063	1.406	1.383	1.455	1.447	1.782	4.567	∞
B3LYP/6-31+G(d)	∞	3.398	1.971	1.427	1.393	1.455	1.451	1.922	4.690	∞
B3LYP/6-31G(d,p)	∞	3.526	2.056	1.406	1.383	1.454	1.446	1.785	4.556	∞

Level of Theory	N_8-N_7 Distance (Å)					N_7-N_6 Distance (Å)				
	SR	RC	TS	PC	SP	SR	RC	TS	PC	SP
HF/6-31G(d)	1.337	1.344	1.347	1.273	1.382	1.223	1.226	1.236	1.284	1.223
HF/6-31+G(d)	1.335	1.340	1.335	1.276	1.377	1.222	1.227	1.239	1.280	1.223
MP2/6-31G(d)	1.346	1.379	1.376	1.330	1.398	1.290	1.285	1.296	1.321	1.286
MP2/6-31+G(d)	1.345	1.355	1.366	1.334	1.394	1.289	1.288	1.299	1.317	1.286
B3LYP/6-31G(d)	1.346	1.377	1.377	1.315	1.406	1.269	1.265	1.279	1.313	1.266
B3LYP/6-31+G(d)	1.342	1.349	1.363	1.316	1.400	1.267	1.270	1.279	1.309	1.264
B3LYP/6-31G(d,p)	1.345	1.377	1.377	1.316	1.402	1.270	1.265	1.279	1.312	1.264

Table S7-7: Bond length comparison during the (Z)-MTI (c,c) + F^- S_N2 pathway

Level of Theory	C-X Distance (Å)					C-N_8 Distance (Å)				
	SR	RC	TS	PC	SP	SR	RC	TS	PC	SP
HF/6-31G(d)	∞	3.417	1.982	1.384	1.365	1.447	1.449	1.855	1.384	∞
HF/6-31+G(d)	∞	3.468	1.955	1.392	1.371	1.448	1.449	1.952	1.392	∞
MP2/6-31G(d)	∞	3.257	1.986	1.412	1.392	1.453	1.454	1.775	1.412	∞
MP2/6-31+G(d)	∞	3.344	1.911	1.431	1.407	1.455	1.455	1.906	1.431	∞
B3LYP/6-31G(d)	∞	3.152	2.046	1.403	1.383	1.455	1.459	1.787	1.403	∞
B3LYP/6-31+G(d)	∞	3.268	1.971	1.422	1.393	1.455	1.457	1.920	1.422	∞
B3LYP/6-31G(d,p)	∞	3.155	2.037	1.403	1.383	1.454	1.460	1.791	1.403	∞

Level of Theory	N_8-N_7 Distance (Å)					N_7-N_6 Distance (Å)				
	SR	RC	TS	PC	SP	SR	RC	TS	PC	SP
HF/6-31G(d)	1.337	1.260	1.324	1.263	1.260	1.223	1.293	1.242	1.293	1.396
HF/6-31+G(d)	1.335	1.261	1.312	1.261	1.261	1.222	1.291	1.247	1.292	1.292
MP2/6-31G(d)	1.346	1.314	1.342	1.321	1.391	1.290	1.327	1.300	1.326	1.327
MP2/6-31+G(d)	1.345	1.315	1.341	1.321	1.322	1.289	1.324	1.302	1.325	1.323
B3LYP/6-31G(d)	1.346	1.295	1.338	1.304	1.301	1.269	1.328	1.286	1.320	1.323
B3LYP/6-31+G(d)	1.342	1.299	1.334	1.303	1.301	1.267	1.306	1.285	1.316	1.317
B3LYP/6-31G(d,p)	1.345	1.294	1.338	1.304	1.301	1.270	1.319	1.287	1.320	1.323

Table S7-8: Bond length comparison during the (Z)-MTI (t,t) + F^- S_N2 pathway

Level of Theory	C-X Distance (Å)					C-N_8 Distance (Å)				
	SR	RC	TS	PC	SP	SR	RC	TS	PC	SP
HF/6-31G(d)	∞	3.684	1.907	1.386	1.365	1.447	1.440	1.848	3.038	∞
HF/6-31+G(d)	∞	3.765	1.879	1.396	1.371	1.448	1.442	1.947	3.101	∞
MP2/6-31G(d)	∞	3.524	1.906	1.414	1.392	1.453	1.449	1.785	2.932	∞
MP2/6-31+G(d)	∞	3.572	1.844	1.436	1.407	1.455	1.452	1.918	2.973	∞
B3LYP/6-31G(d)	∞	3.510	1.971	1.405	1.383	1.455	1.447	1.1782	2.980	∞
B3LYP/6-31+G(d)	∞	3.397	1.877	1.427	1.393	1.455	1.451	1.935	3.015	∞
B3LYP/6-31G(d,p)	∞	3.527	1.966	1.405	1.383	1.454	1.446	1.786	2.968	∞

Level of Theory	N_8-N_7 Distance (Å)					N_7-N_6 Distance (Å)				
	SR	RC	TS	PC	SP	SR	RC	TS	PC	SP
HF/6-31G(d)	1.337	1.367	1.265	1.259	1.260	1.223	1.223	1.273	1.300	1.396
HF/6-31+G(d)	1.335	1.363	1.267	1.260	1.261	1.222	1.223	1.275	1.299	1.292
MP2/6-31G(d)	1.346	1.376	1.305	1.311	1.391	1.290	1.285	1.314	1.332	1.327
MP2/6-31+G(d)	1.345	1.375	1.307	1.309	1.322	1.289	1.288	1.312	1.338	1.323
B3LYP/6-31G(d)	1.346	1.376	1.310	1.296	1.301	1.269	1.265	1.296	1.325	1.323
B3LYP/6-31+G(d)	1.342	1.349	1.298	1.295	1.301	1.267	1.270	1.303	1.324	1.317
B3LYP/6-31G(d,p)	1.345	1.377	1.309	1.296	1.301	1.270	1.265	1.296	1.324	1.323

Table S7-9: Bond length comparison during the (E)-MTI (t,c) + Cl^- S_N2 pathway

Level of Theory	C-X Distance (Å)					C-N_8 Distance (Å)				
	SR	RC	TS	PC	SP	SR	RC	TS	PC	SP
HF/6-31G(d)	∞	3.883	2.270	1.824	1.785	1.447	1.436	2.175	3.103	∞
HF/6-31+G(d)	∞	3.944	2.289	1.824	1.786	1.448	1.438	2.181	3.183	∞
MP2/6-31G(d)	∞	3.777	2.208	1.810	1.780	1.453	1.441	2.066	3.000	∞
MP2/6-31+G(d)	∞	3.840	2.221	1.809	1.802	1.455	1.443	2.073	3.083	∞
B3LYP/6-31G(d)	∞	3.742	2.241	1.849	1.803	1.455	1.445	2.156	2.979	∞
B3LYP/6-31+G(d)	∞	3.823	2.259	1.847	1.805	1.455	1.447	2.161	3.071	∞
B3LYP/6-31G(d,p)	∞	3.721	2.245	1.850	1.803	1.454	1.445	2.157	2.963	∞

Level of Theory	N_8-N_7 Distance (Å)					N_7-N_6 Distance (Å)				
	SR	RC	TS	PC	SP	SR	RC	TS	PC	SP
HF/6-31G(d)	1.337	1.284	1.270	1.256	1.255	1.223	1.245	1.271	1.296	1.301
HF/6-31+G(d)	1.335	1.284	1.272	1.259	1.256	1.222	1.243	1.266	1.289	1.292
MP2/6-31G(d)	1.346	1.307	1.320	1.309	1.312	1.290	1.306	1.314	1.331	1.333
MP2/6-31+G(d)	1.345	1.307	1.321	1.315	1.313	1.289	1.305	1.209	1.322	1.322
B3LYP/6-31G(d)	1.346	1.302	1.303	1.295	1.296	1.269	1.291	1.304	1.323	1.329
B3LYP/6-31+G(d)	1.342	1.302	1.302	1.296	1.295	1.267	1.287	1.298	1.315	1.317
B3LYP/6-31G(d,p)	1.345	1.302	1.302	1.295	1.295	1.270	1.292	1.304	1.323	1.330

Table S7-10: Bond length comparison during the (E)-MTI (t,t) + Cl^- S_N2 pathway

Level of Theory	C-X Distance (Å)					C-N_8 Distance (Å)				
	SR	RC	TS	PC	SP	SR	RC	TS	PC	SP
HF/6-31G(d)	∞	3.552	2.242	1.818	1.365	1.447	1.438	2.159	2.983	∞
HF/6-31+G(d)	∞	3.590	2.257	1.818	1.371	1.448	1.441	2.166	3.067	∞
MP2/6-31G(d)	∞	3.478	2.195	1.805	1.392	1.453	1.443	2.068	2.899	∞
MP2/6-31+G(d)	∞	3.520	2.206	1.806	1.407	1.455	1.447	2.072	2.968	∞
B3LYP/6-31G(d)	∞	3.467	2.222	1.841	1.383	1.455	1.444	2.145	2.883	∞
B3LYP/6-31+G(d)	∞	3.511	2.234	1.841	1.393	1.455	1.447	2.140	2.961	∞
B3LYP/6-31G(d,p)	∞	3.456	2.223	1.842	1.383	1.454	1.444	2.135	2.857	∞

Level of Theory	N_8-N_7 Distance (Å)					N_7-N_6 Distance (Å)				
	SR	RC	TS	PC	SP	SR	RC	TS	PC	SP
HF/6-31G(d)	1.337	1.293	1.262	1.250	1.245	1.223	1.238	1.276	1.301	1.310
HF/6-31+G(d)	1.335	1.300	1.264	1.253	1.245	1.222	1.234	1.272	1.296	1.303
MP2/6-31G(d)	1.346	1.309	1.305	1.300	1.296	1.290	1.302	1.317	1.333	1.340
MP2/6-31+G(d)	1.345	1.313	1.308	1.304	1.299	1.289	1.299	1.313	1.328	1.334
B3LYP/6-31G(d)	1.346	1.306	1.291	1.283	1.279	1.269	1.286	1.310	1.328	1.337
B3LYP/6-31+G(d)	1.342	1.306	1.288	1.286	1.282	1.267	1.282	1.306	1.321	1.328
B3LYP/6-31G(d,p)	1.345	1.306	1.286	1.284	1.279	1.270	1.286	1.311	1.328	1.337

Table S7-11: Bond length comparison during the (E)-MTI (c,c) + Cl^- S_N2 pathway

Level of Theory	C-X Distance (Å)					C-N_8 Distance (Å)				
	SR	RC	TS	PC	SP	SR	RC	TS	PC	SP
HF/6-31G(d)	∞	3.710	2.266	1.825	1.365	1.447	1.437	2.182	3.091	∞
HF/6-31+G(d)	∞	3.758	2.285	1.824	1.371	1.448	1.439	2.187	3.167	∞
MP2/6-31G(d)	∞	3.624	2.201	1.810	1.392	1.453	1.441	2.077	3.000	∞
MP2/6-31+G(d)	∞	3.708	2.213	1.810	1.407	1.455	1.444	2.085	3.074	∞
B3LYP/6-31G(d)	∞	3.624	2.235	1.852	1.383	1.455	1.446	2.172	2.975	∞
B3LYP/6-31+G(d)	∞	3.691	2.253	1.848	1.393	1.455	1.448	2.176	3.083	∞
B3LYP/6-31G(d,p)	∞	3.611	2.239	1.853	1.383	1.454	1.446	2.174	2.953	∞

Level of Theory	N_8-N_7 Distance (Å)					N_7-N_6 Distance (Å)				
	SR	RC	TS	PC	SP	SR	RC	TS	PC	SP
HF/6-31G(d)	1.337	1.280	1.285	1.253	1.251	1.223	1.248	1.277	1.302	1.306
HF/6-31+G(d)	1.335	1.279	1.266	1.254	1.251	1.222	1.246	1.272	1.295	1.398
MP2/6-31G(d)	1.346	1.307	1.318	1.309	1.309	1.290	1.304	1.313	1.331	1.335
MP2/6-31+G(d)	1.345	1.306	1.317	1.311	1.309	1.289	1.303	1.308	1.322	1.323
B3LYP/6-31G(d)	1.346	1.301	1.292	1.293	1.293	1.269	1.292	1.306	1.325	1.332
B3LYP/6-31+G(d)	1.342	1.300	1.297	1.293	1.291	1.267	1.288	1.299	1.316	1.318
B3LYP/6-31G(d,p)	1.345	1.301	1.297	1.293	1.293	1.270	1.292	1.306	1.325	1.332

Table S7-12: Bond length comparison during the (E)-MTI (c,t) + Cl^- S_N2 pathway

Level of Theory	C-X Distance (Å)					C-N_8 Distance (Å)				
	SR	RC	TS	PC	SP	SR	RC	TS	PC	SP
HF/6-31G(d)	∞	3.624	2.249	1.818	1.365	1.447	1.438	2.156	3.009	∞
HF/6-31+G(d)	∞	3.672	2.265	1.818	1.371	1.448	1.440	2.161	3.095	∞
MP2/6-31G(d)	∞	3.553	2.198	1.805	1.392	1.453	1.443	2.063	2.920	∞
MP2/6-31+G(d)	∞	3.639	2.211	1.806	1.407	1.455	1.446	2.067	3.004	∞
B3LYP/6-31G(d)	∞	3.533	2.224	1.840	1.383	1.455	1.444	2.141	2.901	∞
B3LYP/6-31+G(d)	∞	3.594	2.237	1.840	1.393	1.455	1.447	2.142	2.983	∞
B3LYP/6-31G(d,p)	∞	3.520	2.226	1.840	1.383	1.454	1.444	2.143	2.890	∞

Level of Theory	N_8-N_7 Distance (Å)					N_7-N_6 Distance (Å)				
	SR	RC	TS	PC	SP	SR	RC	TS	PC	SP
HF/6-31G(d)	1.337	1.285	1.276	1.246	1.242	1.223	1.242	1.281	1.306	1.315
HF/6-31+G(d)	1.335	1.285	1.259	1.248	1.243	1.222	1.240	1.278	1.302	1.309
MP2/6-31G(d)	1.346	1.309	1.301	1.296	1.292	1.290	1.298	1.317	1.334	1.342
MP2/6-31+G(d)	1.345	1.309	1.304	1.299	1.295	1.289	1.296	1.312	1.329	1.336
B3LYP/6-31G(d)	1.346	1.305	1.287	1.280	1.276	1.269	1.286	1.312	1.329	1.339
B3LYP/6-31+G(d)	1.342	1.304	1.286	1.282	1.278	1.267	1.281	1.306	1.323	1.330
B3LYP/6-31G(d,p)	1.345	1.305	1.287	1.281	1.276	1.270	1.286	1.312	1.329	1.340

Table S7-13: Bond length comparison during the (Z)-MTI (c,t) + Cl^- S_N2 pathway

Level of Theory	C-X Distance (Å)					$C-N_8$ Distance (Å)				
	SR	RC	TS	PC	SP	SR	RC	TS	PC	SP
HF/6-31G(d)	∞	3.520	2.239	1.820	1.365	1.447	1.455	2.169	3.002	∞
HF/6-31+G(d)	∞	3.553	2.256	1.820	1.371	1.448	1.447	2.171	3.086	∞
MP2/6-31G(d)	∞	3.432	2.187	1.807	1.392	1.453	1.450	2.080	2.920	∞
MP2/6-31+G(d)	∞	3.446	2.201	1.808	1.407	1.455	1.457	2.080	2.995	∞
B3LYP/6-31G(d)	∞	3.440	2.208	1.842	1.383	1.455	1.450	2.166	2.923	∞
B3LYP/6-31+G(d)	∞	3.479	2.223	1.841	1.393	1.455	1.452	2.163	3.013	∞
B3LYP/6-31G(d,p)	∞	3.427	2.210	1.842	1.383	1.454	1.450	2.168	2.911	∞

Level of Theory	N_8-N_7 Distance (Å)					N_7-N_6 Distance (Å)				
	SR	RC	TS	PC	SP	SR	RC	TS	PC	SP
HF/6-31G(d)	1.337	1.321	1.263	1.253	1.249	1.223	1.321	1.263	1.304	1.313
HF/6-31+G(d)	1.335	1.321	1.265	1.255	1.251	1.222	1.321	1.265	1.3-1	1.308
MP2/6-31G(d)	1.346	1.325	1.308	1.305	1.301	1.290	1.325	1.308	1.335	1.344
MP2/6-31+G(d)	1.345	1.335	1.311	1.309	1.305	1.289	1.335	1.311	1.334	1.341
B3LYP/6-31G(d)	1.346	1.322	1.292	1.288	1.284	1.269	1.322	1.292	1.329	1.339
B3LYP/6-31+G(d)	1.342	1.318	1.292	1.290	1.287	1.267	1.319	1.292	1.325	1.333
B3LYP/6-31G(d,p)	1.345	1.319	1.292	1.288	1.284	1.270	1.319	1.292	1.329	1.339

Table S7-14: Bond length comparison during the (Z)-MTI (t,c) + Cl^- S_N2 pathway

Level of Theory	C-X Distance (Å)					C-N_8 Distance (Å)				
	SR	RC	TS	PC	SP	SR	RC	TS	PC	SP
HF/6-31G(d)	∞	3.793	2.290	1.821	1.365	1.447	1.445	2.175	4.596	∞
HF/6-31+G(d)	∞	3.796	2.308	1.821	1.371	1.448	1.448	2.175	4.676	∞
MP2/6-31G(d)	∞	3.700	2.249	1.807	1.392	1.453	1.452	2.070	4.478	∞
MP2/6-31+G(d)	∞	3.677	2.263	1.808	1.407	1.455	1.457	2.063	4.579	∞
B3LYP/6-31G(d)	∞	3.740	2.304	1.839	1.383	1.455	1.450	2.141	3.083	∞
B3LYP/6-31+G(d)	∞	3.764	2.316	1.839	1.393	1.455	1.453	2.143	4.590	∞
B3LYP/6-31G(d,p)	∞	3.725	2.309	1.841	1.383	1.454	1.449	2.142	4.456	∞

Level of Theory	N_8-N_7 Distance (Å)					N_7-N_6 Distance (Å)				
	SR	RC	TS	PC	SP	SR	RC	TS	PC	SP
HF/6-31G(d)	1.337	1.340	1.321	1.273	1.382	1.223	1.225	1.248	1.284	1.223
HF/6-31+G(d)	1.335	1.338	1.320	1.276	1.377	1.222	1.225	1.247	1.280	1.223
MP2/6-31G(d)	1.346	1.351	1.362	1.329	1.398	1.290	1.287	1.303	1.321	1.286
MP2/6-31+G(d)	1.345	1.356	1.361	1.334	1.394	1.289	1.288	1.303	1.317	1.286
B3LYP/6-31G(d)	1.346	1.349	1.354	1.304	1.406	1.269	1.268	1.286	1.320	1.266
B3LYP/6-31+G(d)	1.342	1.349	1.351	1.316	1.400	1.267	1.268	1.285	1.308	1.264
B3LYP/6-31G(d,p)	1.345	1.347	1.355	1.315	1.402	1.270	1.269	1.286	1.312	1.264

Table S7-15: Bond length comparison during the (Z)-MTI (c,c) + Cl^- S_N2 pathway

Level of Theory	C-X Distance (Å)					C-N_8 Distance (Å)				
	SR	RC	TS	PC	SP	SR	RC	TS	PC	SP
HF/6-31G(d)	∞	3.617	2.312	1.814	1.365	1.447	1.453	2.168	3.317	∞
HF/6-31+G(d)	∞	2.661	2.331	1.813	1.371	1.448	1.454	2.167	3.764	∞
MP2/6-31G(d)	∞	3.537	2.251	1.803	1.392	1.453	1.454	2.071	3.085	∞
MP2/6-31+G(d)	∞	3.583	2.262	1.803	1.407	1.455	1.455	2.063	3.855	∞
B3LYP/6-31G(d)	∞	3.537	2.301	1.839	1.383	1.455	1.456	2.145	3.083	∞
B3LYP/6-31+G(d)	∞	3.590	2.316	1.831	1.393	1.455	1.458	2.143	3.506	∞
B3LYP/6-31G(d,p)	∞	3.542	2.305	1.840	1.383	1.454	1.456	2.147	3.067	∞

Level of Theory	N_8-N_7 Distance (Å)					N_7-N_6 Distance (Å)				
	SR	RC	TS	PC	SP	SR	RC	TS	PC	SP
HF/6-31G(d)	1.337	1.305	1.299	1.262	1.260	1.223	1.239	1.257	1.294	1.396
HF/6-31+G(d)	1.335	1.306	1.298	1.261	1.261	1.222	1.239	1.257	1.292	1.292
MP2/6-31G(d)	1.346	1.328	1.342	1.320	1.391	1.290	1.297	1.304	1.327	1.327
MP2/6-31+G(d)	1.345	1.327	1.340	1.321	1.322	1.289	1.299	1.306	1.325	1.323
B3LYP/6-31G(d)	1.346	1.319	1.328	1.304	1.301	1.269	1.281	1.293	1.320	1.323
B3LYP/6-31+G(d)	1.342	1.319	1.326	1.302	1.301	1.267	1.281	1.291	1.316	1.317
B3LYP/6-31G(d,p)	1.345	1.317	1.329	1.305	1.301	1.270	1.282	1..293	1.320	1.323

Table S7-16: Bond length comparison during the (Z)-MTI (t,t) + Cl^- S_N2 pathway

Level of Theory	C-X Distance (Å)					$C-N_8$ Distance (Å)				
	SR	RC	TS	PC	SP	SR	RC	TS	PC	SP
HF/6-31G(d)	∞	3.786	2.239	1.812	1.365	1.447	1.445	2.168	2.985	∞
HF/6-31+G(d)	∞	3.797	2.256	1.812	1.371	1.448	1.448	2.170	3.082	∞
MP2/6-31G(d)	∞	3.689	-	1.806	1.392	1.453	1.452	-	2.922	∞
MP2/6-31+G(d)	∞	-	-	-	1.407	1.455	-	-	-	∞
B3LYP/6-31G(d)	∞	3.740	2.208	1.840	1.383	1.455	1.450	2.166	2.926	∞
B3LYP/6-31+G(d)	∞	3.745	2.223	1.840	1.393	1.455	1.453	2.164	3.013	∞
B3LYP/6-31G(d,p)	∞	3.706	2.210	1.841	1.383	1.454	1.450	2.168	2.916	∞

Level of Theory	N_8-N_7 Distance (Å)					N_7-N_6 Distance (Å)				
	SR	RC	TS	PC	SP	SR	RC	TS	PC	SP
HF/6-31G(d)	1.337	1.339	1.263	1.259	1.260	1.223	1.225	1.281	1.299	1.396
HF/6-31+G(d)	1.335	1.338	1.265	1.261	1.261	1.222	1.225	1.279	1.299	1.292
MP2/6-31G(d)	1.346	1.351	-	1.311	1.391	1.290	1.287	-	1.331	1.327
MP2/6-31+G(d)	1.345	-	-	-	1.322	1.289	-	-	-	1.323
B3LYP/6-31G(d)	1.346	1.349	1.292	1.296	1.301	1.269	1.268	1.312	1.323	1.323
B3LYP/6-31+G(d)	1.342	1.349	1.293	1.295	1.301	1.267	1.268	1.310	1.323	1.317
B3LYP/6-31G(d,p)	1.345	1.348	1.292	1.297	1.301	1.270	1.269	1.312	1.322	1.323

Table S7-17: Bond length comparison during the (E)-MTI (t,c) + Br^- S_N2 pathway

Level of Theory	C-X Distance (Å)					C-N_8 Distance (Å)				
	SR	RC	TS	PC	SP	SR	RC	TS	PC	SP
HF/6-31G(d)	∞	3.872	2.400	1.993	1.948	1.447	1.437	2.183	3.071	∞
HF/6-31+G(d)	∞	3.953	2.409	1.984	1.946	1.448	1.453	2.193	3.413	∞
MP2/6-31G(d)	∞	3.734	2.327	1.988	1.951	1.453	1.441	2.104	2.943	∞
MP2/6-31+G(d)	∞	3.824	2.343	1.979	1.950	1.455	1.444	2.103	3.328	∞
B3LYP/6-31G(d)	∞	3.737	2.369	2.016	1.966	1.455	1.445	2.162	2.942	∞
B3LYP/6-31+G(d)	∞	3.842	2.382	2.002	1.965	1.455	1.447	2.163	3.306	∞
B3LYP/6-31G(d,p)	∞	3.725	2.372	2.015	1.963	1.454	1.445	2.162	3.202	∞

Level of Theory	N_8-N_7 Distance (Å)					N_7-N_6 Distance (Å)				
	SR	RC	TS	PC	SP	SR	RC	TS	PC	SP
HF/6-31G(d)	1.337	1.284	1.270	1.257	1.078	1.223	1.245	1.272	1.296	1.301
HF/6-31+G(d)	1.335	1.285	1.272	1.257	1.079	1.222	1.242	1.266	1.291	1.292
MP2/6-31G(d)	1.346	1.307	1.321	1.312	1.131	1.290	1.306	1.315	1.329	1.333
MP2/6-31+G(d)	1.345	1.307	1.323	1.314	1.131	1.289	1.304	1.309	1.323	1.322
B3LYP/6-31G(d)	1.346	1.302	1.304	1.295	1.106	1.269	1.291	1.304	1.323	1.329
B3LYP/6-31+G(d)	1.342	1.303	1.303	1.295	1.105	1.267	1.286	1.297	1.216	1.317
B3LYP/6-31G(d,p)	1.345	1.302	1.304	1.294	1.106	1.270	1.291	1.304	1.324	1.330

Table S7-18: Bond length comparison during the (E)-MTI (t,t) + Br^- S_N2 pathway

Level of Theory	C-X Distance (Å)					C-N_8 Distance (Å)				
	SR	RC	TS	PC	SP	SR	RC	TS	PC	SP
HF/6-31G(d)	∞	3.658	2.372	1.985	1.948	1.447	1.438	2.186	2.967	∞
HF/6-31+G(d)	∞	3.691	2.377	1.973	1.946	1.448	1.440	2.177	3.045	∞
MP2/6-31G(d)	∞	3.558	2.320	1.982	1.951	1.453	1.444	2.098	2.862	∞
MP2/6-31+G(d)	∞	3.572	2.327	1.971	1.950	1.455	1.447	2.107	2.938	∞
B3LYP/6-31G(d)	∞	3.553	2.352	2.007	1.966	1.455	1.444	2.141	2.852	∞
B3LYP/6-31+G(d)	∞	3.585	2.355	1.995	1.965	1.455	1.447	2.143	2.926	∞
B3LYP/6-31G(d,p)	∞	3.540	2.354	2.005	1.963	1.454	1.444	2.157	2.842	∞

Level of Theory	N_8-N_7 Distance (Å)					N_7-N_6 Distance (Å)				
	SR	RC	TS	PC	SP	SR	RC	TS	PC	SP
HF/6-31G(d)	1.337	1.291	1.262	1.250	1.245	1.223	1.239	1.276	1.301	1.310
HF/6-31+G(d)	1.335	1.291	1.264	1.253	1.245	1.222	1.237	1.272	1.295	1.303
MP2/6-31G(d)	1.346	1.310	1.300	1.300	1.296	1.290	1.301	1.318	1.332	1.340
MP2/6-31+G(d)	1.345	1.310	1.311	1.304	1.299	1.289	1.299	1.313	1.328	1.334
B3LYP/6-31G(d)	1.346	1.307	1.286	1.284	1.279	1.269	1.286	1.311	1.327	1.337
B3LYP/6-31+G(d)	1.342	1.307	1.288	1.286	1.282	1.267	1.281	1.305	1.321	1.328
B3LYP/6-31G(d,p)	1.345	1.307	1.293	1.284	1.279	1.270	1.286	1.309	1.327	1.337

Table S7-19: Bond length comparison during the (E)-MTI (c,c) + Br^- S_N2 pathway

Level of Theory	C-X Distance (Å)					C-N_8 Distance (Å)				
	SR	RC	TS	PC	SP	SR	RC	TS	PC	SP
HF/6-31G(d)	∞	3.760	2.395	1.994	1.948	1.447	1.438	2.190	3.061	∞
HF/6-31+G(d)	∞	3.820	2.406	1.983	1.946	1.448	1.440	2.199	3.095	∞
MP2/6-31G(d)	∞	3.654	2.321	1.989	1.951	1.453	1.442	2.117	2.955	∞
MP2/6-31+G(d)	∞	3.708	2.328	1.979	1.950	1.455	1.444	2.121	2.973	∞
B3LYP/6-31G(d)	∞	3.645	2.364	2.021	1.966	1.455	1.446	2.178	2.929	∞
B3LYP/6-31+G(d)	∞	3.708	2.376	2.007	1.965	1.455	1.448	2.177	2.974	∞
B3LYP/6-31G(d,p)	∞	3.633	2.367	2.020	1.963	1.454	1.446	2.178	2.912	∞

Level of Theory	N_8-N_7 Distance (Å)					N_7-N_6 Distance (Å)				
	SR	RC	TS	PC	SP	SR	RC	TS	PC	SP
HF/6-31G(d)	1.337	1.281	1.265	1.253	1.251	1.223	1.247	1.277	1.301	1.306
HF/6-31+G(d)	1.335	1.281	1.266	1.254	1.251	1.222	1.245	1.272	1.294	1.398
MP2/6-31G(d)	1.346	1.308	1.318	1.209	1.309	1.290	1.303	1.314	1.330	1.335
MP2/6-31+G(d)	1.345	1.307	1.318	1.311	1.309	1.289	1.301	1.308	1.322	1.323
B3LYP/6-31G(d)	1.346	1.302	1.299	1.293	1.293	1.269	1.290	1.306	1.324	1.332
B3LYP/6-31+G(d)	1.342	1.301	1.298	1.293	1.291	1.267	1.286	1.299	1.316	1.318
B3LYP/6-31G(d,p)	1.345	1.301	1.299	1.293	1.293	1.270	1.291	1.305	1.324	1.332

Table S7-20: Bond length comparison during the (E)-MTI (c,t) + Br^- S_N2 pathway

Level of Theory	C-X Distance (Å)					C-N_8 Distance (Å)				
	SR	RC	TS	PC	SP	SR	RC	TS	PC	SP
HF/6-31G(d)	∞	3.707	2.379	1.986	1.948	1.447	1.438	2.165	2.997	∞
HF/6-31+G(d)	∞	3.763	2.384	1.970	1.946	1.448	1.440	2.172	3.277	∞
MP2/6-31G(d)	∞	3.607	2.327	1.982	1.951	1.453	1.444	2.104	2.880	∞
MP2/6-31+G(d)	∞	3.654	2.343	1.971	1.950	1.455	1.447	2.103	3.219	∞
B3LYP/6-31G(d)	∞	3.587	2.369	2.005	1.966	1.455	1.445	2.161	2.876	∞
B3LYP/6-31+G(d)	∞	3.629	2.382	1.991	1.965	1.455	1.447	2.163	2.975	∞
B3LYP/6-31G(d,p)	∞	3.573	2.372	2.003	1.963	1.454	1.445	2.162	2.868	∞

Level of Theory	N_8-N_7 Distance (Å)					N_7-N_6 Distance (Å)				
	SR	RC	TS	PC	SP	SR	RC	TS	PC	SP
HF/6-31G(d)	1.337	1.286	1.257	1.264	1.242	1.223	1.241	1.281	1.306	1.315
HF/6-31+G(d)	1.335	1.286	1.259	1.246	1.243	1.222	1.239	1.277	1.303	1.309
MP2/6-31G(d)	1.346	1.309	1.321	1.297	1.292	1.290	1.298	1.315	1.333	1.342
MP2/6-31+G(d)	1.345	1.309	1.323	1.298	1.295	1.289	1.295	1.309	1.329	1.336
B3LYP/6-31G(d)	1.346	1.305	1.304	1.281	1.276	1.269	1.285	1.304	1.329	1.339
B3LYP/6-31+G(d)	1.342	1.304	1.303	1.283	1.278	1.267	1.280	1.297	1.322	1.330
B3LYP/6-31G(d,p)	1.345	1.305	1.304	1.281	1.276	1.270	1.286	1.304	1.328	1.340

Table S7-21: Bond length comparison during the (Z)-MTI (c,t) + Br^- S_N2 pathway

Level of Theory	C-X Distance (Å)					$C-N_8$ Distance (Å)				
	SR	RC	TS	PC	SP	SR	RC	TS	PC	SP
HF/6-31G(d)	∞	3.629	2.368	1.988	1.948	1.447	1.444	2.179	2.978	∞
HF/6-31+G(d)	∞	3.684	2.376	1.976	1.946	1.448	1.444	2.181	3.264	∞
MP2/6-31G(d)	∞	3.523	2.308	1.957	1.951	1.453	1.452	2.125	2.924	∞
MP2/6-31+G(d)	∞	3.566	2.308	1.957	1.950	1.455	1.453	2.125	2.922	∞
B3LYP/6-31G(d)	∞	3.540	2.337	2.007	1.966	1.455	1.450	2.177	2.890	∞
B3LYP/6-31+G(d)	∞	3.576	2.344	1.996	1.965	1.455	1.452	2.169	2.915	∞
B3LYP/6-31G(d,p)	∞	3.527	2.339	2.005	1.963	1.454	1.450	2.177	2.882	∞

Level of Theory	N_8-N_7 Distance (Å)					N_7-N_6 Distance (Å)				
	SR	RC	TS	PC	SP	SR	RC	TS	PC	SP
HF/6-31G(d)	1.337	1.307	1.263	1.253	1.249	1.223	1.234	1.281	1.303	1.313
HF/6-31+G(d)	1.335	1.295	1.265	1.254	1.251	1.222	1.237	1.279	1.302	1.308
MP2/6-31G(d)	1.346	1.328	1.309	1.310	1.301	1.290	1.292	1.320	1.334	1.344
MP2/6-31+G(d)	1.345	1.322	1.309	1.310	1.305	1.289	1.293	1.320	1.333	1.341
B3LYP/6-31G(d)	1.346	1.319	1.293	1.288	1.284	1.269	1.276	1.312	1.328	1.339
B3LYP/6-31+G(d)	1.342	1.318	1.293	1.291	1.287	1.267	1.276	1.309	1.323	1.333
B3LYP/6-31G(d,p)	1.345	1.319	1.293	1.288	1.284	1.270	1.277	1.312	1.328	1.339

Table S7-22: Bond length comparison during the (Z)-MTI (t,c) + Br^- S_N2 pathway

Level of Theory	C-X Distance (Å)					C-N_8 Distance (Å)				
	SR	RC	TS	PC	SP	SR	RC	TS	PC	SP
HF/6-31G(d)	∞	3.719	2.419	1.989	1.948	1.447	1.447	2.180	4.562	∞
HF/6-31+G(d)	∞	3.856	2.426	1.979	1.946	1.448	1.444	2.181	4.632	∞
MP2/6-31G(d)	∞	3.613	2.366	1.985	1.951	1.453	1.454	2.821	4.442	∞
MP2/6-31+G(d)	∞	3.741	2.376	1.977	1.950	1.455	1.459	2.091	4.540	∞
B3LYP/6-31G(d)	∞	3.785	2.433	1.2005	1.966	1.455	1.450	2.147	4.439	∞
B3LYP/6-31+G(d)	∞	3.862	2.438	1.997	1.965	1.455	1.448	2.139	4.576	∞
B3LYP/6-31G(d,p)	∞	3.774	2.438	2.003	1.963	1.454	1.449	2.146	4.434	∞

Level of Theory	N_8-N_7 Distance (Å)					N_7-N_6 Distance (Å)				
	SR	RC	TS	PC	SP	SR	RC	TS	PC	SP
HF/6-31G(d)	1.337	1.335	1.321	1.272	1.382	1.223	1.226	1.249	1.284	1.223
HF/6-31+G(d)	1.335	1.337	1,319	1.275	1.377	1.222	1.226	1.248	1.280	1.223
MP2/6-31G(d)	1.346	1.348	1,361	1.328	1.398	1.290	1.287	1.304	1.321	1.286
MP2/6-31+G(d)	1.345	1.355	1,359	1.333	1.394	1.289	1.287	1.303	1.317	1.286
B3LYP/6-31G(d)	1.346	1.347	1.353	1.313	1.406	1.269	1.269	1.287	1.313	1.266
B3LYP/6-31+G(d)	1.342	1.335	1.350	1.315	1.400	1.267	1.270	1.285	1.309	1.264
B3LYP/6-31G(d,p)	1.345	1.345	1.355	1.314	1.402	1.270	1.269	1.286	1.312	1.264

Table S7-23: Bond length comparison during the (Z)-MTI (c,c) + Br^- S_N2 pathway

Level of Theory	C-X Distance (Å)					C-N_8 Distance (Å)				
	SR	RC	TS	PC	SP	SR	RC	TS	PC	SP
HF/6-31G(d)	∞	3.705	2.440	1.980	1.948	1.447	1.454	2.172	3.290	∞
HF/6-31+G(d)	∞	3.779	2.446	1.965	1.946	1.448	1.454	2.172	3.730	∞
MP2/6-31G(d)	∞	3.602	2.369	1.980	1.951	1.453	1.456	2.107	3.035	∞
MP2/6-31+G(d)	∞	2.658	2.377	1.964	1.950	1.455	1.456	2.088	3.595	∞
B3LYP/6-31G(d)	∞	3.594	2.438	2.102	1.966	1.455	1.458	2.150	2.974	∞
B3LYP/6-31+G(d)	∞	3.668	2.434	1.977	1.965	1.455	1.458	2.139	3.558	∞
B3LYP/6-31G(d,p)	∞	3.580	2.431	1.977	1.963	1.454	1.457	2.151	3.280	∞

Level of Theory	N_8-N_7 Distance (Å)					N_7-N_6 Distance (Å)				
	SR	RC	TS	PC	SP	SR	RC	TS	PC	SP
HF/6-31G(d)	1.337	1.309	1.299	1.262	1.260	1.223	1.237	1.258	1.294	1.396
HF/6-31+G(d)	1.335	1.307	1.297	1.261	1.261	1.222	1.238	1.257	1.292	1.292
MP2/6-31G(d)	1.346	1.331	1.341	1.321	1.391	1.290	1.295	1.305	1.326	1.327
MP2/6-31+G(d)	1.345	1.330	1.340	1.322	1.322	1.289	1.298	1.305	1.323	1.323
B3LYP/6-31G(d)	1.346	1.321	1.328	1.307	1.301	1.269	1.280	1.293	1.317	1.323
B3LYP/6-31+G(d)	1.342	1.320	1.326	1.302	1.301	1.267	1.280	1.291	1.317	1.317
B3LYP/6-31G(d,p)	1.345	1.319	1.328	1.306	1.301	1.270	1.281	1.293	1.317	1.323

Table S7-24: Bond length comparison during the (Z)-MTI (t,t) + Br^- S_N2 pathway

Level of Theory	C-X Distance (Å)					C-N_8 Distance (Å)				
	SR	RC	TS	PC	SP	SR	RC	TS	PC	SP
HF/6-31G(d)	∞	3.720	2.368	1.989	1.948	1.447	1.447	2.179	2.970	∞
HF/6-31+G(d)	∞	3.856	2.376	1.977	1.946	1.448	1.449	2.181	3.059	∞
MP2/6-31G(d)	∞	3.612	-	1.983	1.951	1.453	1.454	-	2.881	∞
MP2/6-31+G(d)	∞	-	-	-	1.950	1.455	-	-	-	∞
B3LYP/6-31G(d)	∞	3.780	2.338	2.005	1.966	1.455	1.450	2.176	2.900	∞
B3LYP/6-31+G(d)	∞	3.861	2.344	1.994	1.965	1.455	1.448	2.169	2.935	∞
B3LYP/6-31G(d,p)	∞	3.774	2.339	2.003	1.963	1.454	1.449	2.178	2.892	∞

Level of Theory	N_8-N_7 Distance (Å)					N_7-N_6 Distance (Å)				
	SR	RC	TS	PC	SP	SR	RC	TS	PC	SP
HF/6-31G(d)	1.337	1.335	1.263	1.279	1.260	1.223	1.226	1.281	1.298	1.396
HF/6-31+G(d)	1.335	1.337	1.265	1.261	1.261	1.222	1.226	1.279	1.298	1.292
MP2/6-31G(d)	1.346	1.348	-	1.312	1.391	1.290	1.287	-	1.331	1.327
MP2/6-31+G(d)	1.345	-	-	-	1.322	1.289	-	-	-	1.323
B3LYP/6-31G(d)	1.346	1.347	1.293	1.297	1.301	1.269	1.269	1.312	1.322	1.323
B3LYP/6-31+G(d)	1.342	1.335	1.293	1.296	1.301	1.267	1.270	1.309	1.322	1.317
B3LYP/6-31G(d,p)	1.345	1.345	1.293	1.297	1.301	1.270	1.269	1.312	1.321	1.323

Table S7-25: Bond length comparison during the (Z)-MTI_T (t,c) + F^- S_N2 pathway

Level of Theory	C-X Distance (Å)					C-N_8 Distance (Å)				
	SR	RC	TS	PC	SP	SR	RC	TS	PC	SP
HF/6-31G(d)	∞	3.217	1,883	1.388	1.365	1.455	1.452	1.892	4.862	∞
HF/6-31+G(d)	∞	3.244	2.186	1.398	1.371	1.456	1.451	1.727	5.991	∞
MP2/6-31G(d)	∞	3.233	2.143	1.416	1.392	1.465	1.463	1.612	4.100	∞
MP2/6-31+G(d)	∞	3.216	2.096	1.438	1.407	1.466	1.463	1.715	4.035	∞
B3LYP/6-31G(d)	∞	3.186	2.152	1.407	1.383	1.467	1.468	1.707	5.793	∞
B3LYP/6-31+G(d)	∞	3.197	2.163	1.430	1.398	1.467	1.466	1.728	5.473	∞
B3LYP/6-31G(d,p)	∞	3.152	2.135	1.407	1.383	1.467	1.468	1.679	5.558	∞

Level of Theory	N_8-N_7 Distance (Å)					N_7-N_6 Distance (Å)				
	SR	RC	TS	PC	SP	SR	RC	TS	PC	SP
HF/6-31G(d)	1.219	1.241	1.189	1.078	1.078	1.336	1.315	1.501	4.663	∞
HF/6-31+G(d)	1.216	1.241	1.110	1.078	1.079	1.354	1.315	2.150	4.111	∞
MP2/6-31G(d)	1.273	1.298	1.172	1.136	1.131	1.367	1.343	1.981	3.799	∞
MP2/6-31+G(d)	1.272	1.297	1.169	1.135	1.131	1.376	1.345	2.072	3.770	∞
B3LYP/6-31G(d)	1.256	1.277	1.188	1.113	1.106	1.356	1.341	1.728	3.942	∞
B3LYP/6-31+G(d)	1.256	1.275	1.158	1.109	1.105	1.356	1.342	2.016	3.046	∞
B3LYP/6-31G(d,p)	1.256	1.277	1.182	1.113	1.106	1.356	1.342	1.797	3.953	∞

Table S7-26: Bond length comparison during the (E)-MTI_T (t,c) + F^- S_N2 pathway

Level of Theory	C-X Distance (Å)					C-N_8 Distance (Å)				
	SR	RC	TS	PC	SP	SR	RC	TS	PC	SP
HF/6-31G(d)	∞	5.138	1.859	1.388	1.365	1.450	1.445	1.902	4.862	∞
HF/6-31+G(d)	∞	5.055	1.829	1.398	1.371	1.452	1.445	1.996	5.991	∞
MP2/6-31G(d)	∞	5.442	2.047	1.416	1.392	1.464	1.458	1.726	4.100	∞
MP2/6-31+G(d)	∞	5.130	-	1.438	1.407	1.464	1.460	-	4.035	∞
B3LYP/6-31G(d)	∞	5.414	2.010	1.407	1.383	1.459	1.455	1.782	5.793	∞
B3LYP/6-31+G(d)	∞	5.072	2.152	1.430	1.398	1.459	1.456	1.738	5.473	∞
B3LYP/6-31G(d,p)	∞	5.401	2.079	1.407	1.383	1.459	1.455	1.800	5.558	∞

Level of Theory	N_8-N_7 Distance (Å)					N_7-N_6 Distance (Å)				
	SR	RC	TS	PC	SP	SR	RC	TS	PC	SP
HF/6-31G(d)	1.215	1.240	1.193	1.078	1.078	1.333	1.308	1.460	4.663	∞
HF/6-31+G(d)	1.208	1.236	1.190	1.078	1.079	1.366	1.308	1.471	4.111	∞
MP2/6-31G(d)	1.267	1.302	1.194	1.136	1.131	1.382	1.329	1.750	3.799	∞
MP2/6-31+G(d)	1.265	1.297	-	1.135	1.131	1.382	1.329	-	3.770	∞
B3LYP/6-31G(d)	1.256	1.283	1.201	1.113	1.106	1.344	1.327	1.586	3.942	∞
B3LYP/6-31+G(d)	1.254	1.275	1.160	1.109	1.105	1.342	1.327	1.981	3.046	∞
B3LYP/6-31G(d,p)	1.256	1.283	1.152	1.113	1.106	1.344	1.372	2.261	3.953	∞

Table S7-27: Bond length comparison during the (E)-MTI_T (t,t) + F^- S_N2 pathway

Level of Theory	C-X Distance (Å)					$C-N_8$ Distance (Å)				
	SR	RC	TS	PC	SP	SR	RC	TS	PC	SP
HF/6-31G(d)	∞	5.640	1,883	1.388	1.365	1.451	1.444	1.892	4.862	∞
HF/6-31+G(d)	∞	5.467	2.186	1.398	1.371	1.452	1.446	1.727	5.991	∞
MP2/6-31G(d)	∞	5.834	2.143	1.416	1.392	1.463	1.456	1.612	4.100	∞
MP2/6-31+G(d)	∞	5.550	2.096	1.438	1.407	1.465	1.460	1.715	4.035	∞
B3LYP/6-31G(d)	∞	5.803	2.152	1.407	1.383	1.460	1.453	1.707	5.793	∞
B3LYP/6-31+G(d)	∞	5.498	2.163	1.430	1.398	1.461	1.457	1.728	5.473	∞
B3LYP/6-31G(d,p)	∞	5.794	2.135	1.407	1.383	1.460	1.453	1.679	5.558	∞

Level of Theory	N_8-N_7 Distance (Å)					N_7-N_6 Distance (Å)				
	SR	RC	TS	PC	SP	SR	RC	TS	PC	SP
HF/6-31G(d)	1.219	1.257	1.189	1.078	1.078	1.327	1.291	1.501	4.663	∞
HF/6-31+G(d)	1.208	1.254	1.110	1.078	1.079	1.367	1.293	2.150	4.111	∞
MP2/6-31G(d)	1.282	1.320	1.172	1.136	1.131	1.343	1.320	1.981	3.799	∞
MP2/6-31+G(d)	1.277	1.316	1.169	1.135	1.131	1.354	1.321	2.072	3.770	∞
B3LYP/6-31G(d)	1.263	1.302	1.188	1.113	1.106	1.343	1.314	1.728	3.942	∞
B3LYP/6-31+G(d)	1.260	1.293	1.158	1.109	1.105	1.342	1.316	2.016	3.046	∞
B3LYP/6-31G(d,p)	1.263	1.303	1.182	1.113	1.106	1.343	1.314	1.797	3.953	∞

Table S7-28: Bond length comparison during the (Z)-MTI_T (c,t) + F^- S_N2 pathway

Level of Theory	C-X Distance (Å)					C-N_8 Distance (Å)				
	SR	RC	TS	PC	SP	SR	RC	TS	PC	SP
HF/6-31G(d)	∞	4.948	1.859	1.388	1.365	1.456	1.458	1.902	4.862	∞
HF/6-31+G(d)	∞	3.295	1.829	1.398	1.371	1.456	1.453	1.996	5.991	∞
MP2/6-31G(d)	∞	4.970	2.047	1.416	1.392	1.468	1.460	1.726	4.100	∞
MP2/6-31+G(d)	∞	4.100	-	1.438	1.407	1.470	1.472	-	4.035	∞
B3LYP/6-31G(d)	∞	5.420	2.010	1.407	1.383	1.469	1.462	1.782	5.793	∞
B3LYP/6-31+G(d)	∞	4.334	2.152	1.430	1.398	1.469	1.473	1.738	5.473	∞
B3LYP/6-31G(d,p)	∞	3.273	2.079	1.407	1.383	1.469	1.469	1.800	5.558	∞

Level of Theory	N_8-N_7 Distance (Å)					N_7-N_6 Distance (Å)				
	SR	RC	TS	PC	SP	SR	RC	TS	PC	SP
HF/6-31G(d)	1.208	1.224	1.193	1.078	1.078	1.411	1.375	1.460	4.663	∞
HF/6-31+G(d)	1.208	1.238	1.190	1.078	1.079	1.411	1.318	1.471	4.111	∞
MP2/6-31G(d)	1.256	1.303	1.194	1.136	1.131	1.446	1.349	1.750	3.799	∞
MP2/6-31+G(d)	1.256	1.270	-	1.135	1.131	1.446	1.400	-	3.770	∞
B3LYP/6-31G(d)	1.237	1.265	1.201	1.113	1.106	1.444	1.367	1.586	3.942	∞
B3LYP/6-31+G(d)	1.236	1.251	1.160	1.109	1.105	1.442	1.390	1.981	3.046	∞
B3LYP/6-31G(d,p)	1.237	1.276	1.152	1.113	1.106	1.443	1.339	2.261	3.953	∞

Table S7-29: Bond length comparison during the (Z)-MTI_T (t,c) + Cl^- S_N2 pathway

Level of Theory	C-X Distance (Å)					C-N_8 Distance (Å)				
	SR	RC	TS	PC	SP	SR	RC	TS	PC	SP
HF/6-31G(d)	∞	5.740	2.656	1.829	1.785	1.450	1.446	1.780	4.791	∞
HF/6-31+G(d)	∞	5.760	2.656	1.825	1.786	1.452	1.447	1.780	5.803	∞
MP2/6-31G(d)	∞	3.504	2.373	1.815	1.779	1.464	1.464	1.888	3.992	∞
MP2/6-31+G(d)	∞	3.544	2.389	1.812	1.780	1.464	1.464	1.880	3.819	∞
B3LYP/6-31G(d)	∞	5.641	2.538	1.867	1.803	1.459	1.457	1.917	4.641	∞
B3LYP/6-31+G(d)	∞	5.647	2.552	1.853	1.805	1.459	1.457	1.907	5.261	∞
B3LYP/6-31G(d,p)	∞	5.619	2.546	1.869	1.803	1.459	1.457	1.916	4.645	∞

Level of Theory	N_8-N_7 Distance (Å)					N_7-N_6 Distance (Å)				
	SR	RC	TS	PC	SP	SR	RC	TS	PC	SP
HF/6-31G(d)	1.215	1.221	1.104	1.078	1.078	1.333	1.320	2.212	4.375	∞
HF/6-31+G(d)	1.208	1.219	1.104	1.078	1.079	1.366	1.320	2.212	4.109	∞
MP2/6-31G(d)	1.267	1.282	1.172	1.135	1.131	1.382	1.348	2.182	3.857	∞
MP2/6-31+G(d)	1.265	1.282	1.172	1.135	1.131	1.382	1.356	2.196	3.853	∞
B3LYP/6-31G(d)	1.256	1.266	1.143	1.113	1.106	1.344	1.333	2.307	3.925	∞
B3LYP/6-31+G(d)	1.254	1.262	1.142	1.111	1.105	1.342	1.332	2.329	3.920	∞
B3LYP/6-31G(d,p)	1.256	1.266	1.143	1.113	1.106	1.344	1.333	2.319	3.938	∞

Table S7-30: Bond length comparison during the (E)-MTI_T (t,c) + Cl^- S_N2 pathway

Level of Theory	C-X Distance (Å)					C-N_8 Distance (Å)				
	SR	RC	TS	PC	SP	SR	RC	TS	PC	SP
HF/6-31G(d)	∞	6.141	2.656	1.829	1.785	1.451	1.449	1.780	4.791	∞
HF/6-31+G(d)	∞	6.147	2.656	1.825	1.786	1.452	1.450	1.780	5.803	∞
MP2/6-31G(d)	∞	6.110	2.373	1.815	1.779	1.463	1.460	1.889	3.992	∞
MP2/6-31+G(d)	∞	6.080	2.389	1.812	1.780	1.465	1.462	1.880	3.819	∞
B3LYP/6-31G(d)	∞	6.097	2.538	1.867	1.803	1.460	1.457	1.917	4.641	∞
B3LYP/6-31+G(d)	∞	6.098	2.552	1.853	1.805	1.461	1.460	1.907	5.261	∞
B3LYP/6-31G(d,p)	∞	6.076	2.546	1.869	1.803	1.460	1.457	1.916	4.645	∞

Level of Theory	N_8-N_7 Distance (Å)					N_7-N_6 Distance (Å)				
	SR	RC	TS	PC	SP	SR	RC	TS	PC	SP
HF/6-31G(d)	1.219	1.232	1.104	1.078	1.078	1.327	1.306	2.212	4.375	∞
HF/6-31+G(d)	1.208	1.230	1.104	1.078	1.079	1.367	1.306	2.212	4.109	∞
MP2/6-31G(d)	1.282	1.299	1.172	1.135	1.131	1.343	1.322	2.182	3.857	∞
MP2/6-31+G(d)	1.277	1.298	1.172	1.135	1.131	1.354	1.321	2.196	3.853	∞
B3LYP/6-31G(d)	1.263	1.280	1.143	1.113	1.106	1.343	1.321	2.307	3.925	∞
B3LYP/6-31+G(d)	1.260	1.276	1.142	1.111	1.105	1.342	1.321	2.329	3.920	∞
B3LYP/6-31G(d,p)	1.263	1.280	1.143	1.113	1.106	1.343	1.321	2.319	3.938	∞

Table S7-31: Bond length comparison during the (E)-MTI_T (t,t) + Cl^- S_N2 pathway

Level of Theory	C-X Distance (Å)					C-N_8 Distance (Å)				
	SR	RC	TS	PC	SP	SR	RC	TS	PC	SP
HF/6-31G(d)	∞	5.900	2.656	1.829	1.785	1.456	1.461	1.780	4.791	∞
HF/6-31+G(d)	∞	5.989	2.656	1.825	1.786	1.456	1.460	1.780	5.803	∞
MP2/6-31G(d)	∞	5.758	2.373	1.815	1.779	1.468	1.464	1.888	3.992	∞
MP2/6-31+G(d)	∞	5.770	2.389	1.812	1.780	1.470	1.465	1.880	3.819	∞
B3LYP/6-31G(d)	∞	5.799	2.538	1.867	1.803	1.469	1.465	1.917	4.641	∞
B3LYP/6-31+G(d)	∞	5.850	2.552	1.853	1.805	1.469	1.465	1.907	5.261	∞
B3LYP/6-31G(d,p)	∞	5.775	2.546	1.869	1.803	1.469	1.465	1.916	4.645	∞

Level of Theory	N_8-N_7 Distance (Å)					N_7-N_6 Distance (Å)				
	SR	RC	TS	PC	SP	SR	RC	TS	PC	SP
HF/6-31G(d)	1.208	1.212	1.104	1.078	1.078	1.411	1.406	2.212	4.375	∞
HF/6-31+G(d)	1.208	1.212	1.104	1.078	1.079	1.411	1.404	2.212	4.109	∞
MP2/6-31G(d)	1.256	1.277	1.172	1.135	1.131	1.446	1.388	2.182	3.857	∞
MP2/6-31+G(d)	1.256	1.259	1.172	1.135	1.131	1.446	1.381	2.196	3.853	∞
B3LYP/6-31G(d)	1.237	1.258	1.143	1.113	1.106	1.444	1.382	2.307	3.925	∞
B3LYP/6-31+G(d)	1.236	1.267	1.142	1.111	1.105	1.442	1.382	2.329	3.920	∞
B3LYP/6-31G(d,p)	1.237	1.258	1.143	1.113	1.106	1.443	1.381	2.319	3.938	∞

Table S7-32: Bond length comparison during the (Z)-MTI_T (t,t) + Cl^- S_N2 pathway

Level of Theory	C-X Distance (Å)					C-N_8 Distance (Å)				
	SR	RC	TS	PC	SP	SR	RC	TS	PC	SP
HF/6-31G(d)	∞	5.900	2.656	1.829	1.785	1.455	1.461	1.780	4.791	∞
HF/6-31+G(d)	∞	5.989	2.656	1.825	1.786	1.456	1.460	1.780	5.803	∞
MP2/6-31G(d)	∞	5/758	2.373	1.815	1.779	1.465	1.464	1.889	3.992	∞
MP2/6-31+G(d)	∞	5.770	2.389	1.812	1.780	1.466	1.465	1.880	3.819	∞
B3LYP/6-31G(d)	∞	5.799	2.538	1.867	1.803	1.467	1.465	1.917	4.641	∞
B3LYP/6-31+G(d)	∞	5.850	2.552	1.853	1.805	1.467	1.465	1.907	5.261	∞
B3LYP/6-31G(d,p)	∞	5.775	2.546	1.869	1.803	1.467	1.465	1.916	4.645	∞

Level of Theory	N_8-N_7 Distance (Å)					N_7-N_6 Distance (Å)				
	SR	RC	TS	PC	SP	SR	RC	TS	PC	SP
HF/6-31G(d)	1.219	1.212	1.104	1.078	1.078	1.336	1.406	2.212	4.375	∞
HF/6-31+G(d)	1.216	1.212	1.104	1.078	1.079	1.354	1.404	2.212	4.109	∞
MP2/6-31G(d)	1.273	1.277	1.172	1.135	1.131	1.367	1.388	2.182	3.857	∞
MP2/6-31+G(d)	1.272	1.259	1.172	1.135	1.131	1.376	1.381	2.196	3.853	∞
B3LYP/6-31G(d)	1.256	1.258	1.143	1.113	1.106	1.356	1.382	2.307	3.925	∞
B3LYP/6-31+G(d)	1.256	1.257	1.142	1.111	1.105	1.356	1.382	2.329	3.920	∞
B3LYP/6-31G(d,p)	1.256	1.258	1.143	1.113	1.106	1.356	1.381	2.319	3.938	∞

Table S7-33: Bond length comparison during the (Z)-MTI_T (t,c) + Br^- S_N2 pathway

Level of Theory	C-X Distance (Å)					C-N_8 Distance (Å)				
	SR	RC	TS	PC	SP	SR	RC	TS	PC	SP
HF/6-31G(d)	∞	3.721	2.783	2.003	1.948	1.455	1.456	1.783	4.728	∞
HF/6-31+G(d)	∞	3.766	2.847	1.967	1.946	1.456	1.456	1.753	4.298	∞
MP2/6-31G(d)	∞	3.645	2.783	2.004	1.951	1.465	1.464	1.783	3.967	∞
MP2/6-31+G(d)	∞	3.614	2.520	1.978	1.950	1.466	1.467	1.895	3.719	∞
B3LYP/6-31G(d)	∞	3.644	2.675	2.062	1.966	1.467	1.467	1.902	4.627	∞
B3LYP/6-31+G(d)	∞	3.706	2.691	2.030	1.965	1.467	1.466	1.912	4.508	∞
B3LYP/6-31G(d,p)	∞	3.615	2.681	2.060	1.963	1.467	1.467	1.897	4.630	∞

Level of Theory	N_8-N_7 Distance (Å)					N_7-N_6 Distance (Å)				
	SR	RC	TS	PC	SP	SR	RC	TS	PC	SP
HF/6-31G(d)	1.219	1.223	1.104	1.078	1.078	1.336	1.331	2.210	4.390	∞
HF/6-31+G(d)	1.216	1.223	1.098	1.078	1.079	1.354	1.331	2.295	6.095	∞
MP2/6-31G(d)	1.273	1.283	1.104	1.135	1.131	1.367	1.347	2.210	3.869	∞
MP2/6-31+G(d)	1.272	1.262	1.172	1.135	1.131	1.376	1.352	2.01	4.046	∞
B3LYP/6-31G(d)	1.256	1.262	1.144	1.112	1.106	1.356	1.352	2.313	3.958	∞
B3LYP/6-31+G(d)	1.256	1.261	1.142	1.110	1.105	1.356	1.352	2.338	3.995	∞
B3LYP/6-31G(d,p)	1.256	1.262	1.144	1.112	1.106	1.356	1.352	2.320	3.963	∞

Table S7-34: Bond length comparison during the (E)-MTI_T (t,c) + Br^- S_N2 pathway

Level of Theory	C-X Distance (Å)					C-N_8 Distance (Å)				
	SR	RC	TS	PC	SP	SR	RC	TS	PC	SP
HF/6-31G(d)	∞	5.970	2.783	2.003	1.948	1.450	1.446	1.783	4.728	∞
HF/6-31+G(d)	∞	5.932	2.847	1.967	1.946	1.452	1.447	1.753	4.298	∞
MP2/6-31G(d)	∞	5.925	2.793	2.004	1.951	1.464	1.460	1.783	3.967	∞
MP2/6-31+G(d)	∞	5.896	2.520	1.978	1.950	1.464	1.461	1.895	3.719	∞
B3LYP/6-31G(d)	∞	5.868	2.675	2.062	1.966	1.459	1.457	1.902	4.627	∞
B3LYP/6-31+G(d)	∞	5.866	2.691	2.030	1.965	1.459	1.457	1.912	4.508	∞
B3LYP/6-31G(d,p)	∞	5.961	2.681	2.060	1.963	1.459	1.446	1.897	4.630	∞

Level of Theory	N_8-N_7 Distance (Å)					N_7-N_6 Distance (Å)				
	SR	RC	TS	PC	SP	SR	RC	TS	PC	SP
HF/6-31G(d)	1.215	1.221	1.105	1.078	1.078	1.333	1.319	2.210	4.390	∞
HF/6-31+G(d)	1.208	1.291	1.098	1.078	1.079	1.366	1.320	2.295	6.095	∞
MP2/6-31G(d)	1.267	1.286	1.205	1.135	1.131	1.382	1.329	2.210	3.869	∞
MP2/6-31+G(d)	1.265	1.284	1.172	1.135	1.131	1.382	1.329	2.201	4.046	∞
B3LYP/6-31G(d)	1.256	1.266	1.144	1.112	1.106	1.344	1.332	2.313	3.958	∞
B3LYP/6-31+G(d)	1.254	1.261	1.142	1.110	1.105	1.342	1.332	2.338	3.995	∞
B3LYP/6-31G(d,p)	1.256	1.221	1.144	1.112	1.106	1.344	1.320	2.380	3.963	∞

Table S7-35: Bond length comparison during the (E)-MTI_T (t,t) + Br^- S_N2 pathway

Level of Theory	C-X Distance (Å)					C-N_8 Distance (Å)				
	SR	RC	TS	PC	SP	SR	RC	TS	PC	SP
HF/6-31G(d)	∞	6.393	2.783	2.003	1.948	1.451	1.449	1.783	4.728	∞
HF/6-31+G(d)	∞	6.322	2.847	1.967	1.946	1.452	1.454	1.753	4.298	∞
MP2/6-31G(d)	∞	6.369	2.783	2.004	1.951	1.463	1.460	1.783	3.967	∞
MP2/6-31+G(d)	∞	6.332	2.520	1.978	1.950	1.465	1.462	1.895	3.719	∞
B3LYP/6-31G(d)	∞	6.343	2.675	2.062	1.966	1.460	1.457	1.902	4.627	∞
B3LYP/6-31+G(d)	∞	6.303	2.691	2.030	1.965	1.461	1.459	1.912	4.508	∞
B3LYP/6-31G(d,p)	∞	6.272	2.681	2.060	1.963	1.460	1.457	1.897	4.630	∞

Level of Theory	N_8-N_7 Distance (Å)					N_7-N_6 Distance (Å)				
	SR	RC	TS	PC	SP	SR	RC	TS	PC	SP
HF/6-31G(d)	1.219	1.232	1.104	1.078	1.078	1.327	1.232	2.210	4.390	∞
HF/6-31+G(d)	1.208	1.229	1.098	1.078	1.079	1.367	1.229	2.295	6.095	∞
MP2/6-31G(d)	1.282	1.298	1.104	1.135	1.131	1.343	1.298	2.210	3.869	∞
MP2/6-31+G(d)	1.277	1.296	1.172	1.135	1.131	1.354	1.296	2.01	4.046	∞
B3LYP/6-31G(d)	1.263	1.279	1.144	1.112	1.106	1.343	1.279	2.313	3.958	∞
B3LYP/6-31+G(d)	1.260	1.275	1.142	1.110	1.105	1.342	1.275	2.338	3.995	∞
B3LYP/6-31G(d,p)	1.263	1.280	1.144	1.112	1.106	1.343	1.280	2.320	3.963	∞

Table S7-36: Bond length comparison during the (Z)-MTI_T (t,t) + Br^- S_N2 pathway

Level of Theory	C-X Distance (Å)					C-N_8 Distance (Å)				
	SR	RC	TS	PC	SP	SR	RC	TS	PC	SP
HF/6-31G(d)	∞	6.000	2.783	2.003	1.948	1.456	1.461	1.783	4.728	∞
HF/6-31+G(d)	∞	6.035	2.847	1.967	1.946	1.456	1.460	1.753	4.298	∞
MP2/6-31G(d)	∞	5.874	2.793	2.004	1.951	1.468	1.464	1.783	3.967	∞
MP2/6-31+G(d)	∞	5.834	2.520	1.978	1.950	1.470	1.465	1.895	3.719	∞
B3LYP/6-31G(d)	∞	5.920	2.675	2.062	1.966	1.469	1.465	1.902	4.627	∞
B3LYP/6-31+G(d)	∞	5.927	2.691	2.030	1.965	1.469	1.465	1.912	4.508	∞
B3LYP/6-31G(d,p)	∞	5.899	2.681	2.060	1.963	1.469	1.465	1.897	4.630	∞

Level of Theory	N_8-N_7 Distance (Å)					N_7-N_6 Distance (Å)				
	SR	RC	TS	PC	SP	SR	RC	TS	PC	SP
HF/6-31G(d)	1.208	1.212	1.105	1.078	1.078	1.411	1.406	2.210	4.390	∞
HF/6-31+G(d)	1.208	1.212	1.098	1.078	1.079	1.411	1.404	2.295	6.095	∞
MP2/6-31G(d)	1.256	1.277	1.205	1.135	1.131	1.446	1.288	2.210	3.869	∞
MP2/6-31+G(d)	1.256	1.279	1.172	1.135	1.131	1.446	1.383	2.201	4.046	∞
B3LYP/6-31G(d)	1.237	1.258	1.144	1.112	1.106	1.444	1.383	2.313	3.958	∞
B3LYP/6-31+G(d)	1.236	1.256	1.142	1.110	1.105	1.442	1.383	2.338	3.995	∞
B3LYP/6-31G(d,p)	1.237	1.258	1.144	1.112	1.106	1.443	1.382	2.380	3.963	∞

Table S8-1: Bond length comparison during the (E)-MTIC (t,c,c) + F^- S_N2 pathway

Level of Theory	C-X Distance (Å)					C-N_8 Distance (Å)				
	SR	RC	TS	PC	SP	SR	RC	TS	PC	SP
HF/6-31G(d)	∞	3.598	1.954	1.390	1.365	1.449	1.451	1.822	3.575	∞
HF/6-31+G(d)	∞	3.583	1.931	1.401	1.371	1.450	1.451	1.923	3.675	∞
B3LYP/6-31G(d)	∞	3.336	2.016	1.409	1.383	1.455	1.461	1.760	3.517	∞
B3LYP/6-31+G(d)	∞	3.443	1.935	1.430	1.393	1.456	1.460	1.899	3.629	∞
B3LYP/6-31G(d,p)	∞	3.384	2.088	1.409	1.383	1.454	1.462	1.764	3.551	∞

Level of Theory	N_8-N_7 Distance (Å)					N_7-N_6 Distance (Å)				
	SR	RC	TS	PC	SP	SR	RC	TS	PC	SP
HF/6-31G(d)	1.325	1.246	1.263	1.241	1.241	1.226	1.303	1.272	1.320	1.321
HF/6-31+G(d)	1.322	1.248	1.262	1.242	1.243	1.226	1.300	1.272	1.313	1.313
B3LYP/6-31G(d)	1.335	1.280	1.304	1.283	1.285	1.272	1.332	1.305	1.340	1.342
B3LYP/6-31+G(d)	1.330	1.283	1.293	1.283	1.284	1.271	1.322	1.303	1.332	1.331
B3LYP/6-31G(d,p)	1.334	1.281	1.303	1.284	1.285	1.273	1.332	1.305	1.340	1.342

Table S8-2: Bond length comparison during the (E)-MTIC (t,t,c) + F^- S_N2 pathway

Level of Theory	C-X Distance (Å)					C-N_8 Distance (Å)				
	SR	RC	TS	PC	SP	SR	RC	TS	PC	SP
HF/6-31G(d)	∞	3.392	1.922	1.382	1.365	1.445	1.445	1.824	3.073	∞
HF/6-31+G(d)	∞	3.413	1.893	1.392	1.371	1.447	1.446	1.924	3.123	∞
B3LYP/6-31G(d)	∞	3.151	1.988	1.402	1.383	1.450	1.452	1.748	2.982	∞
B3LYP/6-31+G(d)	∞	3.293	1.894	1.423	1.393	1.451	1.454	1.902	3.020	∞
B3LYP/6-31G(d,p)	∞	3.159	1.979	1.402	1.383	1.449	1.453	1.751	2.969	∞

Level of Theory	N_8-N_7 Distance (Å)					N_7-N_6 Distance (Å)				
	SR	RC	TS	PC	SP	SR	RC	TS	PC	SP
HF/6-31G(d)	1.334	1.244	1.252	1.273	1.235	1.223	1.303	1.280	1.322	1.329
HF/6-31+G(d)	1.334	1.243	1.252	1.240	1.236	1.222	1.300	1.281	1.318	1.325
B3LYP/6-31G(d)	1.338	1.283	1.282	1.274	1.270	1.270	1.325	1.310	1.343	1.351
B3LYP/6-31+G(d)	1.335	1.283	1.279	1.276	1.273	1.268	1.318	1.312	1.337	1.343
B3LYP/6-31G(d,p)	1.337	1.284	1.280	1.274	1.270	1.270	1.325	1.311	1.343	1.351

Table S8-3: Bond length comparison during the (E)-MTIC (t,c,t) + F^- S_N2 pathway

Level of Theory	C-X Distance (Å)					C-N_8 Distance (Å)				
	SR	RC	TS	PC	SP	SR	RC	TS	PC	SP
HF/6-31G(d)	∞	3.574	1.942	1.382	1.365	1.446	1.449	1.821	3.155	∞
HF/6-31+G(d)	∞	3.577	1.917	1.392	1.371	1.446	1.449	1.921	3.212	∞
B3LYP/6-31G(d)	∞	3.251	2.005	1.402	1.383	1.453	1.459	1.754	3.044	∞
B3LYP/6-31+G(d)	∞	3.438	1.919	1.422	1.393	1.453	1.458	1.903	3.097	∞
B3LYP/6-31G(d,p)	∞	3.286	1.996	1.402	1.383	1.452	1.460	1.759	3.024	∞

Level of Theory	N_8-N_7 Distance (Å)					N_7-N_6 Distance (Å)				
	SR	RC	TS	PC	SP	SR	RC	TS	PC	SP
HF/6-31G(d)	1.307	1.247	1.264	1.245	1.243	1.230	1.299	1.269	1.301	1.314
HF/6-31+G(d)	1.318	1.249	1.263	1.246	1.244	1.226	1.296	1.270	1.303	1.307
B3LYP/6-31G(d)	1.335	1.281	1.303	1.287	1.286	1.272	1.327	1.301	1.331	1.335
B3LYP/6-31+G(d)	1.329	1.284	1.293	1.287	1.285	1.271	1.319	1.301	1.323	1.326
B3LYP/6-31G(d,p)	1.334	1.281	1.301	1.287	1.286	1.272	1.327	1.301	1.330	1.335

Table S8-4: Bond length comparison during the (E)-MTIC (t,t,t) + F^- S_N2 pathway

Level of Theory	C-X Distance (Å)					C-N_8 Distance (Å)				
	SR	RC	TS	PC	SP	SR	RC	TS	PC	SP
HF/6-31G(d)	∞	3.590	1.933	1.381	1.365	1.447	1.444	1.810	3.087	∞
HF/6-31+G(d)	∞	3.525	1.903	1.390	1.371	1.448	1.445	1.909	3.135	∞
B3LYP/6-31G(d)	∞	3.382	1.998	1.401	1.383	1.451	1.452	1.737	2.994	∞
B3LYP/6-31+G(d)	∞	3.395	1.906	1.422	1.393	1.453	1.453	1.886	3.033	∞
B3LYP/6-31G(d,p)	∞	3.760	1.989	1.402	1.383	1.450	1.449	1.741	2.98	∞

Level of Theory	N_8-N_7 Distance (Å)					N_7-N_6 Distance (Å)				
	SR	RC	TS	PC	SP	SR	RC	TS	PC	SP
HF/6-31G(d)	1.330	1.245	1.252	1.238	1.235	1.223	1.297	1.276	1.316	1.323
HF/6-31+G(d)	1.330	1.244	1.252	1.240	1.237	1.222	1.294	1.278	1.313	1.319
B3LYP/6-31G(d)	1.337	1.285	1.284	1.274	1.271	1.270	1.318	1.306	1.336	1.343
B3LYP/6-31+G(d)	1.335	1.285	1.276	1.276	1.273	1.269	1.312	1.308	1.332	1.338
B3LYP/6-31G(d,p)	1.336	1.291	1.283	1.274	1.271	1.270	1.315	1.306	1.336	1.343

Table S8-5: Bond length comparison during the (E)-MTIC (c,c,c) + F^- S_N2 pathway

Level of Theory	C-X Distance (Å)					C-N_8 Distance (Å)				
	SR	RC	TS	PC	SP	SR	RC	TS	PC	SP
HF/6-31G(d)	∞	3.589	1.930	1.388	1.365	1.448	1.447	1.826	3.411	∞
HF/6-31+G(d)	∞	3.525	1.900	1.398	1.371	1.449	1.448	1.927	3.537	∞
B3LYP/6-31G(d)	∞	3.445	1.990	1.407	1.383	1.450	1.455	1.755	3.343	∞
B3LYP/6-31+G(d)	∞	3.378	1.899	1.428	1.393	1.453	1.456	1.905	3.397	∞
B3LYP/6-31G(d,p)	∞	3.445	1.981	1.408	1.383	1.449	1.455	1.760	3.333	∞

Level of Theory	N_8-N_7 Distance (Å)					N_7-N_6 Distance (Å)				
	SR	RC	TS	PC	SP	SR	RC	TS	PC	SP
HF/6-31G(d)	1.317	1.239	1.248	1.232	1.232	1.227	1.308	1.286	1.329	1.332
HF/6-31+G(d)	1.315	1.238	1.247	1.234	1.233	1.226	1.304	1.287	1.325	1.328
B3LYP/6-31G(d)	1.323	1.281	1.280	1.268	1.267	1.271	1.325	1.312	1.347	1.352
B3LYP/6-31+G(d)	1.320	1.279	1.274	1.269	1.268	1.269	1.317	1.314	1.341	1.344
B3LYP/6-31G(d,p)	1.322	1.281	1.279	1.268	1.267	1.271	1.325	1.313	1.347	1.352

Table S8-6: Bond length comparison during the (E)-MTIC (c,t,c) + F^- S_N2 pathway

Level of Theory	C-X Distance (Å)					C-N_8 Distance (Å)				
	SR	RC	TS	PC	SP	SR	RC	TS	PC	SP
HF/6-31G(d)	∞	3.419	1.933	1.387	1.365	1.447	1.454	1.845	3.157	∞
HF/6-31+G(d)	∞	3.475	1.909	1.396	1.371	1.447	1.451	1.947	3.211	∞
B3LYP/6-31G(d)	∞	3.165	1.993	1.407	1.383	1.454	1.463	1.777	3.075	∞
B3LYP/6-31+G(d)	∞	3.344	1.906	1.428	1.393	1.455	1.461	1.937	3.122	∞
B3LYP/6-31G(d,p)	∞	3.179	1.984	1.407	1.383	1.453	1.464	1.782	3.057	∞

Level of Theory	N_8-N_7 Distance (Å)					N_7-N_6 Distance (Å)				
	SR	RC	TS	PC	SP	SR	RC	TS	PC	SP
HF/6-31G(d)	1.311	1.245	1.256	1.239	1.238	1.230	1.306	1.279	1.320	1.325
HF/6-31+G(d)	1.308	1.246	1.254	1.240	1.238	1.230	1.302	1.280	1.314	1.317
B3LYP/6-31G(d)	1.325	1.278	1.293	1.282	1.281	1.273	1.332	1.305	1.338	1.344
B3LYP/6-31+G(d)	1.320	1.280	1.285	1.280	1.278	1.271	1.323	1.306	1.330	1.333
B3LYP/6-31G(d,p)	1.324	1.278	1.292	1.282	1.281	1.273	1.332	1.306	1.338	1.344

Table S8-7: Bond length comparison during the (E)-MTIC (c,c,t) + F^- S_N2 pathway

Level of Theory	C-X Distance (Å)					C-N_8 Distance (Å)				
	SR	RC	TS	PC	SP	SR	RC	TS	PC	SP
HF/6-31G(d)	∞	3.583	1.932	1.381	1.365	1.447	1.444	1.812	3.124	∞
HF/6-31+G(d)	∞	3.528	1.903	1.390	1.371	1.448	1.445	1.910	3.168	∞
B3LYP/6-31G(d)	∞	3.211	1.996	1.400	1.383	1.452	1.455	1.744	3.025	∞
B3LYP/6-31+G(d)	∞	3.385	1.907	1.421	1.393	1.454	1.453	1.888	3.062	∞
B3LYP/6-31G(d,p)	∞	3.218	1.987	1.400	1.383	1.451	1.456	1.748	3.009	∞

Level of Theory	N_8-N_7 Distance (Å)					N_7-N_6 Distance (Å)				
	SR	RC	TS	PC	SP	SR	RC	TS	PC	SP
HF/6-31G(d)	1.330	1.247	1,256	1.240	1.237	1.221	1.291	1.270	1.307	1.313
HF/6-31+G(d)	1.328	1.246	1.255	1.242	1.239	1.221	1.288	1.272	1.303	1.309
B3LYP/6-31G(d)	1.342	1.288	1.291	1.277	1.274	1.262	1.310	1.298	1.326	1.332
B3LYP/6-31+G(d)	1.339	1.288	1.284	1.279	1.276	1.263	1.305	1.299	1.321	1.326
B3LYP/6-31G(d,p)	1.341	1.288	1.290	1.277	1.274	1.265	1.310	1.298	1.325	1.331

Table S8-8: Bond length comparison during the (E)-MTIC (c,t,t) + F^- S_N2 pathway

Level of Theory	C-X Distance (Å)					C-N_8 Distance (Å)				
	SR	RC	TS	PC	SP	SR	RC	TS	PC	SP
HF/6-31G(d)	∞	3.527	1.944	1.385	1.365	1.446	1.448	1.827	3.163	∞
HF/6-31+G(d)	∞	3.547	1.919	1.401	1.371	1.446	1.449	1.927	3.675	∞
B3LYP/6-31G(d)	∞	3.205	2.003	1.404	1.383	1.453	1.458	1.760	3.081	∞
B3LYP/6-31+G(d)	∞	3.425	1.920	1.425	1.393	1.454	1.457	1.909	3.125	∞
B3LYP/6-31G(d,p)	∞	3.226	1.995	1.404	1.383	1.452	1.459	1.764	3.063	∞

Level of Theory	N_8-N_7 Distance (Å)					N_7-N_6 Distance (Å)				
	SR	RC	TS	PC	SP	SR	RC	TS	PC	SP
HF/6-31G(d)	1.320	1.250	1.266	1.247	1.245	1.224	1.290	1.263	1.301	1.305
HF/6-31+G(d)	1.315	1.252	1.265	1.242	1.246	1.225	1.287	1.265	1.313	1.299
B3LYP/6-31G(d)	1.340	1.285	1.306	1.290	1.289	1.266	1.316	1.292	1.320	1.325
B3LYP/6-31+G(d)	1.335	1.288	1.297	1.290	1.288	1.265	1.308	1.293	1.314	1.316
B3LYP/6-31G(d,p)	1.339	1.285	1.306	1.290	1.289	1.266	1.316	1.293	1.320	1.324

Table S8-9: Bond length comparison during the (Z)-MTIC (t,t,c) + F^- S_N2 pathway

Level of Theory	C-X Distance (Å)					C-N_8 Distance (Å)				
	SR	RC	TS	PC	SP	SR	RC	TS	PC	SP
HF/6-31G(d)	∞	3.372	1.983	1.389	1.365	1.469	1.444	1.837	4.792	∞
HF/6-31+G(d)	∞	3.870	1.951	1.400	1.371	1.470	1.445	1.934	4.849	∞
B3LYP/6-31G(d)	∞	3.486	2.080	1.408	1.383	1.481	1.449	1.757	4.787	∞
B3LYP/6-31+G(d)	∞	3.396	1.991	1.430	1.393	1.483	1.453	1.890	4.854	∞
B3LYP/6-31G(d,p)	∞	3.518	2.074	1.408	1.383	1.481	1.447	1.760	4.838	∞

Level of Theory	N_8-N_7 Distance (Å)					N_7-N_6 Distance (Å)				
	SR	RC	TS	PC	SP	SR	RC	TS	PC	SP
HF/6-31G(d)	1.418	1.360	1.338	1.262	1.400	1.213	1.220	1.239	1.300	1.245
HF/6-31+G(d)	1.408	1.358	1.326	1.264	1.367	1.213	1.219	1.244	1.296	1.222
B3LYP/6-31G(d)	1.473	1.370	1.369	1.308	1.390	1.247	1.263	1.282	1.323	1.265
B3LYP/6-31+G(d)	1.448	1.345	1.354	1.308	1.386	1.249	1.271	1.282	1.319	1.263
B3LYP/6-31G(d,p)	1.475	1.369	1.370	1.309	1.386	1.247	1.264	1.281	1.323	1.266

Table S8-10: Bond length comparison during the (Z)-MTIC (t,c,c) + F^- S_N2 pathway

Level of Theory	C-X Distance (Å)					$C-N_8$ Distance (Å)				
	SR	RC	TS	PC	SP	SR	RC	TS	PC	SP
HF/6-31G(d)	∞	3.372	1.983	1.389	1.365	1.469	1.444	1.837	4.792	∞
HF/6-31+G(d)	∞	3.870	1.951	1.400	1.371	1.470	1.445	1.934	4.849	∞
B3LYP/6-31G(d)	∞	3.468	2.080	1.408	1.383	1.481	1.449	1.757	4.787	∞
B3LYP/6-31+G(d)	∞	3.396	1.991	1.430	1.393	1.483	1.453	1.890	4.854	∞
B3LYP/6-31G(d,p)	∞	3.518	2.074	1.408	1.383	1.481	1.447	1.760	4.838	∞

Level of Theory	N_8-N_7 Distance (Å)					N_7-N_6 Distance (Å)				
	SR	RC	TS	PC	SP	SR	RC	TS	PC	SP
HF/6-31G(d)	1.418	1.360	1.338	1.262	1.400	1.213	1.220	1.239	1.300	1.245
HF/6-31+G(d)	1.408	1.358	1.326	1.264	1.367	1.213	1.219	1.244	1.296	1.222
B3LYP/6-31G(d)	1.473	1.370	1.369	1.308	1.390	1.247	1.263	1.282	1.328	1.265
B3LYP/6-31+G(d)	1.448	1.245	1.354	1.308	1.386	1.249	1.271	1.282	1.319	1.263
B3LYP/6-31G(d,p)	1.475	1.369	1.370	1.309	1.386	1.247	1.264	1.281	1.323	1.266

Table S8-11: Bond length comparison during the (Z)-MTIC (t,t,t) + F^- S_N2 pathway

Level of Theory	C-X Distance (Å)					C-N_8 Distance (Å)				
	SR	RC	TS	PC	SP	SR	RC	TS	PC	SP
HF/6-31G(d)	∞	3.372	2.000	1.281	1.365	1.453	1.441	1.819	4.412	∞
HF/6-31+G(d)	∞	3.364	1.969	1.289	1.371	1.449	1.444	1.915	4.347	∞
B3LYP/6-31G(d)	∞	3.489	2.095	1.400	1.383	1.463	1.447	1.741	4.386	∞
B3LYP/6-31+G(d)	∞	3.367	2.009	1.419	1.393	1.464	1.450	1.868	4.353	∞
B3LYP/6-31G(d,p)	∞	3.510	2.087	1.400	1.383	1.462	1.446	1.744	4.090	∞

Level of Theory	N_8-N_7 Distance (Å)					N_7-N_6 Distance (Å)				
	SR	RC	TS	PC	SP	SR	RC	TS	PC	SP
HF/6-31G(d)	1.350	1.319	1.335	1.259	1.361	1.222	1.232	1.239	1.299	1.225
HF/6-31+G(d)	1.312	1.315	1.323	1.261	1.357	1.232	1.234	1.244	1.295	1.225
B3LYP/6-31G(d)	1.377	1.355	1.364	1.304	1.281	1.262	1.269	1.283	1.321	1.268
B3LYP/6-31+G(d)	1.370	1.328	1.350	1.304	1.276	1.263	1.277	1.283	1.317	1.268
B3LYP/6-31G(d,p)	1.376	1.354	1.364	1.306	1.377	1.262	1.269	1.283	1.318	1.270

Table S8-12: Bond length comparison during the (Z)-MTIC (t,c,t) + F^- S_N2 pathway

Level of Theory	C-X Distance (Å)					C-N_8 Distance (Å)				
	SR	RC	TS	PC	SP	SR	RC	TS	PC	SP
HF/6-31G(d)	∞	3.158	1.932	1.381	1.365	1.469	1.451	1.817	4.409	∞
HF/6-31+G(d)	∞	3.276	1.900	1.389	1.371	1.471	1.452	1.918	4.343	∞
B3LYP/6-31G(d)	∞	3.490	2.003	1.400	1.383	1.483	1.447	1.745	4.385	∞
B3LYP/6-31+G(d)	∞	3.369	1.905	1.418	1.393	1.485	1.450	1.893	4.360	∞
B3LYP/6-31G(d,p)	∞	3.188	1.994	1.400	1.383	1.483	1.466	1.749	4.375	∞

Level of Theory	N_8-N_7 Distance (Å)					N_7-N_6 Distance (Å)				
	SR	RC	TS	PC	SP	SR	RC	TS	PC	SP
HF/6-31G(d)	1.419	1.268	1.261	1.259	1.361	1.215	1.280	1.276	1.299	1.225
HF/6-31+G(d)	1.414	1.270	1.261	1.261	1.357	1.215	1.278	1.280	1.295	1.225
B3LYP/6-31G(d)	1.463	1.354	1.301	1.304	1.381	1.252	1.269	1.301	1.321	1.268
B3LYP/6-31+G(d)	1.451	1.327	1.292	1.304	1.376	1.253	1.278	1.307	1.317	1.268
B3LYP/6-31G(d,p)	1.465	1.290	1.300	1.305	1.377	1.252	1.327	1.301	1.321	1.270

Table S8-13: Bond length comparison during the (Z)-MTIC (c,t,c) + F^- S_N2 pathway

Level of Theory	C-X Distance (Å)					C-N_8 Distance (Å)				
	SR	RC	TS	PC	SP	SR	RC	TS	PC	SP
HF/6-31G(d)	∞	3.257	1.920	1.387	1.365	1.450	1.446	1.836	3.184	∞
HF/6-31+G(d)	∞	3.435	1.889	1.397	1.371	1.451	1.447	1.937	3.291	∞
B3LYP/6-31G(d)	∞	3.485	1.977	1.407	1.383	1.454	1.449	1.772	3.085	∞
B3LYP/6-31+G(d)	∞	3.396	1.880	1.428	1.393	1.457	1.453	1.920	3.149	∞
B3LYP/6-31G(d,p)	∞	3.242	1.969	1.407	1.383	1.453	1.453	1.770	3.072	∞

Level of Theory	N_8-N_7 Distance (Å)					N_7-N_6 Distance (Å)				
	SR	RC	TS	PC	SP	SR	RC	TS	PC	SP
HF/6-31G(d)	1.318	1.248	1.248	1.233	1.230	1.229	1.296	1.285	1.333	1.340
HF/6-31+G(d)	1.318	1.347	1.248	1.235	1.233	1.229	1.224	1.289	1.330	1.335
B3LYP/6-31G(d)	1.322	1.370	1.275	1.270	1.267	1.273	1.263	1.317	1.350	1.357
B3LYP/6-31+G(d)	1.322	1.345	1.273	1.270	1.268	1.273	1.271	1.319	1.348	1.354
B3LYP/6-31G(d,p)	1.320	1.287	1.274	1.270	1.267	1.274	1.317	1.317	1.350	1.357

Table S8-14: Bond length comparison during the (Z)-MTIC (c,t,t) + F^- S_N2 pathway

Level of Theory	C-X Distance (Å)					C-N_8 Distance (Å)				
	SR	RC	TS	PC	SP	SR	RC	TS	PC	SP
HF/6-31G(d)	∞	3.157	1.932	1.383	1.365	1.447	1.451	1.817	3.089	∞
HF/6-31+G(d)	∞	3.276	1.900	1.392	1.371	1.449	1.452	1.918	3.139	∞
B3LYP/6-31G(d)	∞	3.489	2.003	1.402	1.383	1.450	1.477	1.745	3.024	∞
B3LYP/6-31+G(d)	∞	3.370	1.905	1.422	1.393	1.452	1.450	1.893	3.064	∞
B3LYP/6-31G(d,p)	∞	3.509	1.994	1.402	1.383	1.449	1.446	1.749	3.012	∞

Level of Theory	N_8-N_7 Distance (Å)					N_7-N_6 Distance (Å)				
	SR	RC	TS	PC	SP	SR	RC	TS	PC	SP
HF/6-31G(d)	1.311	1.266	1.261	1.249	1.245	1.233	1.279	1.276	1.312	1.321
HF/6-31+G(d)	1.312	1.270	1.261	1.251	1.248	1.232	1.278	1.280	1.310	1.317
B3LYP/6-31G(d)	1.321	1.355	1.301	1.286	1.284	1.275	1.269	1.301	1.332	1.340
B3LYP/6-31+G(d)	1.319	1.327	1.292	1.287	1.284	1.274	1.278	1.307	1.331	1.337
B3LYP/6-31G(d,p)	1.321	1.354	1.300	1.287	1.284	1.275	1.269	1.301	1.332	1.339

Table S8-15: Bond length comparison during the (Z)-MTIC (c,c,c) + F^- S_N2 pathway

Level of Theory	C-X Distance (Å)					C-N_8 Distance (Å)				
	SR	RC	TS	PC	SP	SR	RC	TS	PC	SP
HF/6-31G(d)	∞	3.601	1.867	1.384	1.365	1.450	1.451	1.962	3.134	∞
HF/6-31+G(d)	∞	3.584	1.951	1.400	1.371	1.450	1.451	1.934	4.845	∞
B3LYP/6-31G(d)	∞	3.336	1.850	1.405	1.383	1.457	1.461	1.988	3.047	∞
B3LYP/6-31+G(d)	∞	3.442	1.991	1.425	1.393	1.459	1.460	1.820	3.076	∞
B3LYP/6-31G(d,p)	∞	3.384	1.848	1.405	1.383	1.456	1.462	1.996	3.031	∞

Level of Theory	N_8-N_7 Distance (Å)					N_7-N_6 Distance (Å)				
	SR	RC	TS	PC	SP	SR	RC	TS	PC	SP
HF/6-31G(d)	1.302	1.256	1.307	1.245	1.400	1.231	1.303	1.249	1.310	1.300
HF/6-31+G(d)	1.302	1.248	1.326	1.264	1.367	1.231	1.300	1.244	1.296	1.296
B3LYP/6-31G(d)	1.325	1.280	1.330	1.284	1.390	1.266	1.332	1.283	1.331	1.328
B3LYP/6-31+G(d)	1.324	1.283	1.354	1.284	1.386	1.267	1.322	1.282	1.325	1.319
B3LYP/6-31G(d,p)	1.325	1.281	1.330	1.284	1.386	1.266	1.332	1.283	1.331	1.323

Table S8-16: Bond length comparison during the (Z)-MTIC (c,c,t) + F^- S_N2 pathway

Level of Theory	C-X Distance (Å)					C-N_8 Distance (Å)				
	SR	RC	TS	PC	SP	SR	RC	TS	PC	SP
HF/6-31G(d)	∞	3.515	1.874	1.281	1.365	1.457	1.451	1.931	4.412	∞
HF/6-31+G(d)	∞	3.584	1.846	1.289	1.371	1.458	1.451	1.951	4.347	∞
B3LYP/6-31G(d)	∞	3.336	2.095	1.400	1.383	1.463	1.461	1.741	4.386	∞
B3LYP/6-31+G(d)	∞	3.442	2.009	1.419	1.393	1.465	1.460	1.868	4.353	∞
B3LYP/6-31G(d,p)	∞	3.384	1.843	1.400	1.383	1.463	1.462	1.958	4.090	∞

Level of Theory	N_8-N_7 Distance (Å)					N_7-N_6 Distance (Å)				
	SR	RC	TS	PC	SP	SR	RC	TS	PC	SP
HF/6-31G(d)	1.311	1.238	1.286	1.259	1.361	1.231	1.336	1.257	1.299	1.225
HF/6-31+G(d)	1.311	1.248	1.320	1.261	1.357	1.231	1.300	1.292	1.295	1.225
B3LYP/6-31G(d)	1.333	1.280	1.364	1.304	1.281	1.268	1.332	1.283	1.321	1.268
B3LYP/6-31+G(d)	1.331	1.283	1.350	1.304	1.276	1.268	1.322	1.283	1.317	1.268
B3LYP/6-31G(d,p)	1.334	1.281	1.320	1.306	1.377	1.268	1.332	1.293	1.318	1.270

Table S8-17: Bond length comparison during the (E)-MTIC (t,c,c) + Cl^- S_N2 pathway

Level of Theory	C-X Distance (Å)					C-N_8 Distance (Å)				
	SR	RC	TS	PC	SP	SR	RC	TS	PC	SP
HF/6-31G(d)	∞	3.963	2.313	1.829	1.404	1.449	1.440	2.130	3.532	∞
HF/6-31+G(d)	∞	4.024	2.328	1.829	1.365	1.450	1.441	2.140	3.629	∞
B3LYP/6-31G(d)	∞	3.792	2.287	1.846	1.383	1.455	1.448	2.095	3.491	∞
B3LYP/6-31+G(d)	∞	3.874	2.302	1.845	1.393	1.456	1.450	2.105	3.590	∞
B3LYP/6-31G(d,p)	∞	3.774	2.289	1.847	1.383	1.454	1.448	2.098	3.478	∞

Level of Theory	N_8-N_7 Distance (Å)					N_7-N_6 Distance (Å)				
	SR	RC	TS	PC	SP	SR	RC	TS	PC	SP
HF/6-31G(d)	1.334	1.273	1.258	1.241	1.241	1.226	1.253	1.282	1.320	1.321
HF/6-31+G(d)	1.334	1.273	1.260	1.242	1.243	1.226	1.253	1.268	1.313	1.313
B3LYP/6-31G(d)	1.338	1.294	1.294	1.284	1.285	1.272	1.298	1.311	1.339	1.342
B3LYP/6-31+G(d)	1.335	1.294	1.293	1.283	1.284	1.271	1.295	1.306	1.331	1.331
B3LYP/6-31G(d,p)	1.337	1.293	1.294	1.284	1.285	1.273	1.299	1.311	1.339	1.342

Table S8-18: Bond length comparison during the (E)-MTIC (t,t,c) + Cl^- S_N2 pathway

Level of Theory	C-X Distance (Å)					C-N_8 Distance (Å)				
	SR	RC	TS	PC	SP	SR	RC	TS	PC	SP
HF/6-31G(d)	∞	3.366	2.270	1.813	1.404	1.445	1.443	2.127	3.028	∞
HF/6-31+G(d)	∞	3.504	2.280	1.814	1.365	1.447	1.444	2.136	3.108	∞
B3LYP/6-31G(d)	∞	3.393	2.252	1.836	1.383	1.450	1.447	2.094	2.923	∞
B3LYP/6-31+G(d)	∞	3.425	2.259	1.836	1.393	1.451	1.450	2.107	3.009	∞
B3LYP/6-31G(d,p)	∞	3.383	2.252	1.836	1.383	1.449	1.447	2.097	2.910	∞

Level of Theory	N_8-N_7 Distance (Å)					N_7-N_6 Distance (Å)				
	SR	RC	TS	PC	SP	SR	RC	TS	PC	SP
HF/6-31G(d)	1.334	1.275	1.250	1.238	1.235	1.223	1.250	1.289	1.321	1.329
HF/6-31+G(d)	1.334	1.279	1.252	1.240	1.236	1.222	1.254	1.286	1.317	1.325
B3LYP/6-31G(d)	1.338	1.298	1.278	1.275	1.270	1.270	1.292	1.319	1.341	1.351
B3LYP/6-31+G(d)	1.335	1.298	1.279	1.277	1.273	1.268	1.288	1.315	1.336	1.343
B3LYP/6-31G(d,p)	1.337	1.298	1.278	1.275	1.270	1.270	1.292	1.319	1.340	1.351

Table S8-19: Bond length comparison during the (E)-MTIC (t,c,t) + Cl^- S_N2 pathway

Level of Theory	C-X Distance (Å)					C-N_8 Distance (Å)				
	SR	RC	TS	PC	SP	SR	RC	TS	PC	SP
HF/6-31G(d)	∞	3.819	2.294	1.813	1.404	1.446	1.413	2.126	3.123	∞
HF/6-31+G(d)	∞	3.880	2.308	1.813	1.365	1.446	1.440	2.133	3.237	∞
B3LYP/6-31G(d)	∞	3.697	2.279	1.837	1.383	1.453	1.446	2.095	2.2971	∞
B3LYP/6-31+G(d)	∞	3.778	2.287	1.835	1.393	1.453	1.448	2.109	3.085	∞
B3LYP/6-31G(d,p)	∞	3.680	2.280	1.838	1.383	1.452	1.446	2.098	2.957	∞

Level of Theory	N_8-N_7 Distance (Å)					N_7-N_6 Distance (Å)				
	SR	RC	TS	PC	SP	SR	RC	TS	PC	SP
HF/6-31G(d)	1.307	1.272	1.259	1.245	1.243	1.230	1.252	1.280	1.310	1.314
HF/6-31+G(d)	1.318	1.272	1.260	1.246	1.244	1.226	1.251	1.276	1.304	1.307
B3LYP/6-31G(d)	1.335	1.294	1.294	1.287	1.286	1.272	1.296	1.307	1.330	1.335
B3LYP/6-31+G(d)	1.329	1.294	1.291	1.287	1.285	1.271	1.293	1.306	1.323	1.326
B3LYP/6-31G(d,p)	1.334	1.294	1.294	1.287	1.286	1.272	1.296	1.307	1.330	1.335

Table S8-20: Bond length comparison during the (E)-MTIC (t,t,t) + Cl^- S_N2 pathway

Level of Theory	C-X Distance (Å)					C-N_8 Distance (Å)				
	SR	RC	TS	PC	SP	SR	RC	TS	PC	SP
HF/6-31G(d)	∞	3.605	2.285	1.811	1.404	1.447	1.439	2.108	3.049	∞
HF/6-31+G(d)	∞	3.663	2.294	1.812	1.365	1.448	1.441	2.117	3.130	∞
B3LYP/6-31G(d)	∞	3.536	2.269	1.833	1.383	1.451	1.445	2.071	2.940	∞
B3LYP/6-31+G(d)	∞	3.617	2.275	1.833	1.393	1.453	1.447	2.084	3.027	∞
B3LYP/6-31G(d,p)	∞	3.523	2.269	1.833	1.383	1.450	1.445	2.075	2.928	∞

Level of Theory	N_8-N_7 Distance (Å)					N_7-N_6 Distance (Å)				
	SR	RC	TS	PC	SP	SR	RC	TS	PC	SP
HF/6-31G(d)	1.330	1.278	1.251	1.239	1.235	1.223	1.239	1.285	1.315	1.323
HF/6-31+G(d)	1.330	1.278	1.253	1.241	1.237	1.222	1.244	1.283	1.312	1.319
B3LYP/6-31G(d)	1.337	1.300	1.279	1.275	1.271	1.270	1.289	1.314	1.334	1.343
B3LYP/6-31+G(d)	1.335	1.299	1.280	1.277	1.273	1.269	1.287	1.311	1.331	1.338
B3LYP/6-31G(d,p)	1.336	1.299	1.279	1.275	1.271	1.270	1.290	1.313	1.334	1.343

Table S8-21: Bond length comparison during the (E)-MTIC (c,c,c) + Cl^- S_N2 pathway

Level of Theory	C-X Distance (Å)					$C-N_8$ Distance (Å)				
	SR	RC	TS	PC	SP	SR	RC	TS	PC	SP
HF/6-31G(d)	∞	3.647	2.278	1.821	1.404	1.448	1.441	2.133	3.340	∞
HF/6-31+G(d)	∞	3.682	2.286	1.822	1.365	1.449	1.443	2.144	3.392	∞
B3LYP/6-31G(d)	∞	3.566	2.252	1.829	1.383	1.450	1.447	2.103	3.250	∞
B3LYP/6-31+G(d)	∞	3.662	2.258	1.839	1.393	1.453	1.448	2.114	3.333	∞
B3LYP/6-31G(d,p)	∞	3.553	2.252	1.840	1.383	1.449	1.447	2.107	3.241	∞

Level of Theory	N_8-N_7 Distance (Å)					N_7-N_6 Distance (Å)				
	SR	RC	TS	PC	SP	SR	RC	TS	PC	SP
HF/6-31G(d)	1.317	1.272	1.245	1.233	1.232	1.227	1.251	1.296	1.328	1.332
HF/6-31+G(d)	1.315	1.270	1.246	1.235	1.233	1.226	1.251	1.293	1.324	1.328
B3LYP/6-31G(d)	1.323	1.294	1.275	1.268	1.267	1.271	1.292	1.321	1.345	1.352
B3LYP/6-31+G(d)	1.320	1.294	1.274	1.269	1.268	1.269	1.289	1.317	1.340	1.344
B3LYP/6-31G(d,p)	1.322	1.294	1.275	1.268	1.267	1.271	1.292	1.321	1.345	1.352

Table S8-22: Bond length comparison during the (E)-MTIC (c,t,c) + Cl^- S_N2 pathway

Level of Theory	C-X Distance (Å)					C-N_8 Distance (Å)				
	SR	RC	TS	PC	SP	SR	RC	TS	PC	SP
HF/6-31G(d)	∞	3.633	2.286	1.821	1.404	1.447	1.441	2.160	3.124	∞
HF/6-31+G(d)	∞	3.689	2.291	1.821	1.365	1.447	1.442	2.174	3.199	∞
B3LYP/6-31G(d)	∞	3.539	2.262	1.847	1.383	1.454	1.449	2.142	3.005	∞
B3LYP/6-31+G(d)	∞	3.608	2.272	1.844	1.393	1.455	1.451	2.154	3.111	∞
B3LYP/6-31G(d,p)	∞	3.529	2.264	1.848	1.383	1.453	1.449	2.145	2.988	∞

Level of Theory	N_8-N_7 Distance (Å)					N_7-N_6 Distance (Å)				
	SR	RC	TS	PC	SP	SR	RC	TS	PC	SP
HF/6-31G(d)	1.311	1.270	1.251	1.240	1.238	1.230	1.256	1.291	1.319	1.325
HF/6-31+G(d)	1.308	1.271	1.252	1.240	1.238	1.230	1.254	1.287	1.314	1.317
B3LYP/6-31G(d)	1.325	1.293	1.285	1.281	1.281	1.273	1.297	1.314	1.337	1.344
B3LYP/6-31+G(d)	1.320	1.292	1.283	1.280	1.278	1.271	1.294	1.310	1.330	1.333
B3LYP/6-31G(d,p)	1.324	1.292	1.284	1.282	1.281	1.273	1.298	1.314	1.337	1.344

Table S8-23: Bond length comparison during the (E)-MTIC (c,c,t) + Cl^- S_N2 pathway

Level of Theory	C-X Distance (Å)					C-N_8 Distance (Å)				
	SR	RC	TS	PC	SP	SR	RC	TS	PC	SP
HF/6-31G(d)	∞	3.608	2.287	1.810	1.404	1.447	1.439	2.109	3.102	∞
HF/6-31+G(d)	∞	3.657	2.298	1.811	1.365	1.448	1.441	2.118	3.174	∞
B3LYP/6-31G(d)	∞	3.532	2.271	1.833	1.383	1.452	1.444	2.079	2.980	∞
B3LYP/6-31+G(d)	∞	3.595	2.277	1.833	1.393	1.454	1.447	2.089	3.061	∞
B3LYP/6-31G(d,p)	∞	3.515	2.273	1.834	1.383	1.451	1.444	2.082	2.964	∞

Level of Theory	N_8-N_7 Distance (Å)					N_7-N_6 Distance (Å)				
	SR	RC	TS	PC	SP	SR	RC	TS	PC	SP
HF/6-31G(d)	1.330	1.281	1.254	1.241	1.237	1.221	1.241	1.278	1.306	1.313
HF/6-31+G(d)	1.328	1.281	1.255	1.243	1.239	1.221	1.240	1.276	1.303	1.309
B3LYP/6-31G(d)	1.342	1.302	1.287	1.278	1.274	1.262	1.282	1.304	1.324	1.332
B3LYP/6-31+G(d)	1.339	1.302	1.287	1.280	1.276	1.263	1.280	1.302	1.320	1.326
B3LYP/6-31G(d,p)	1.341	1.302	1.288	1.279	1.274	1.265	1.283	1.304	1.324	1.331

Table S8-24: Bond length comparison during the (E)-MTIC (c,t,t) + Cl^- S_N2 pathway

Level of Theory	C-X Distance (Å)					C-N_8 Distance (Å)				
	SR	RC	TS	PC	SP	SR	RC	TS	PC	SP
HF/6-31G(d)	∞	3.800	2.294	1.817	1.404	1.446	1.438	2.137	3.138	∞
HF/6-31+G(d)	∞	3.974	2.308	1.817	1.365	1.446	1.440	2.144	3.205	∞
B3LYP/6-31G(d)	∞	3.679	2.281	1.841	1.383	1.453	1.445	2.100	3.022	∞
B3LYP/6-31+G(d)	∞	3.763	2.285	1.839	1.393	1.454	1.448	2.119	3.119	∞
B3LYP/6-31G(d,p)	∞	3.662	2.285	1.841	1.383	1.452	1.445	2.102	3.006	∞

Level of Theory	N_8-N_7 Distance (Å)					N_7-N_6 Distance (Å)				
	SR	RC	TS	PC	SP	SR	RC	TS	PC	SP
HF/6-31G(d)	1.320	1.276	1.261	1.247	1.245	1.224	1.247	1.274	1.301	1.305
HF/6-31+G(d)	1.315	1.276	1.262	1.248	1.246	1.225	1.246	1.270	1.296	1.299
B3LYP/6-31G(d)	1.340	1.298	1.297	1.289	1.289	1.266	1.287	1.299	1.319	1.325
B3LYP/6-31+G(d)	1.335	1.298	1.294	1.290	1.288	1.265	1.285	1.296	1.314	1.316
B3LYP/6-31G(d,p)	1.339	1.298	1.297	1.290	1.289	1.266	1.288	1.299	1.319	1.324

Table S8-25: Bond length comparison during the (Z)-MTIC (t,t,c) + Cl^- S_N2 pathway

Level of Theory	C-X Distance (Å)					C-N_8 Distance (Å)				
	SR	RC	TS	PC	SP	SR	RC	TS	PC	SP
HF/6-31G(d)	∞	3.735	2.322	1.826	1.404	1.469	1.449	2.134	4.762	∞
HF/6-31+G(d)	∞	3.812	2.336	1.827	1.365	1.470	1.450	2.132	4.817	∞
B3LYP/6-31G(d)	∞	3.640	2.339	1.845	1.383	1.481	1.453	2.090	4.787	∞
B3LYP/6-31+G(d)	∞	3.687	2.347	1.844	1.393	1.483	1.456	2.097	4.848	∞
B3LYP/6-31G(d,p)	∞	3.636	2.344	1.845	1.383	1.481	1.452	2.092	4.788	∞

Level of Theory	N_8-N_7 Distance (Å)					N_7-N_6 Distance (Å)				
	SR	RC	TS	PC	SP	SR	RC	TS	PC	SP
HF/6-31G(d)	1.418	1.335	1.315	1.262	1.400	1.213	1.225	1.253	1.300	1.305
HF/6-31+G(d)	1.408	1.334	1.312	1.264	1.367	1.213	1.225	1.253	1.296	1.299
B3LYP/6-31G(d)	1.473	1.342	1.350	1.307	1.390	1.247	1.269	1.288	1.324	1.325
B3LYP/6-31+G(d)	1.448	1.343	1.345	1.307	1.386	1.249	1.267	1.288	1.319	1.316
B3LYP/6-31G(d,p)	1.475	1.341	1.352	1.308	1.386	1.247	1.269	1.288	1.323	1.324

Table S8-26: Bond length comparison during the (Z)-MTIC (t,c,c) + Cl^- S_N2 pathway

Level of Theory	C-X Distance (Å)					C-N_8 Distance (Å)				
	SR	RC	TS	PC	SP	SR	RC	TS	PC	SP
HF/6-31G(d)	∞	3.735	2.322	1.826	1.404	1.469	1.449	2.134	4.762	∞
HF/6-31+G(d)	∞	3.812	2.336	1.827	1.365	1.470	1.450	2.139	4.817	∞
B3LYP/6-31G(d)	∞	3.640	2.339	1.845	1.383	1.481	1.453	2.090	4.787	∞
B3LYP/6-31+G(d)	∞	3.687	2.347	1.844	1.393	1.483	1.456	2.097	4.848	∞
B3LYP/6-31G(d,p)	∞	3.636	2.3444	1.845	1.383	1.481	1.452	2.092	4.788	∞

Level of Theory	N_8-N_7 Distance (Å)					N_7-N_6 Distance (Å)				
	SR	RC	TS	PC	SP	SR	RC	TS	PC	SP
HF/6-31G(d)	1.418	1.335	1.315	1.262	1.400	1.213	1.225	1.253	1.300	1.245
HF/6-31+G(d)	1.408	1.334	1.312	1.264	1.367	1.213	1.225	1.253	1.296	1.222
B3LYP/6-31G(d)	1.473	1.342	1.350	1.307	1.390	1.247	1.269	1.288	1.324	1.265
B3LYP/6-31+G(d)	1.448	1.343	1.345	1.307	1.386	1.249	1.267	1.288	1.319	1.263
B3LYP/6-31G(d,p)	1.475	1.341	1.352	1.308	1.386	1.247	1.269	1.288	1.323	1.266

Table S8-27: Bond length comparison during the (Z)-MTIC (t,t,t) + Cl^- S_N2 pathway

Level of Theory	C-X Distance (Å)					C-N_8 Distance (Å)				
	SR	RC	TS	PC	SP	SR	RC	TS	PC	SP
HF/6-31G(d)	∞	3.662	2.346	1.809	1.404	1.453	1.447	2.106	4.405	∞
HF/6-31+G(d)	∞	3.692	2.359	1.810	1.365	1.449	1.449	2.111	4.323	∞
B3LYP/6-31G(d)	∞	3.695	2.359	1.828	1.383	1.463	1.450	2.062	4.338	∞
B3LYP/6-31+G(d)	∞	3.717	2.367	1.825	1.393	1.464	1.453	2.069	4.541	∞
B3LYP/6-31G(d,p)	∞	3.682	2.363	1.825	1.383	1.462	1.449	2.064	4.438	∞

Level of Theory	N_8-N_7 Distance (Å)					N_7-N_6 Distance (Å)				
	SR	RC	TS	PC	SP	SR	RC	TS	PC	SP
HF/6-31G(d)	1.350	1.316	1.311	1.259	1.361	1.222	1.232	1.252	1.299	1.225
HF/6-31+G(d)	1.312	1.317	1.309	1.261	1.357	1.232	1.232	1.253	1.295	1.225
B3LYP/6-31G(d)	1.377	1.330	1.345	1.303	1.281	1.262	1.274	1.288	1.321	1.268
B3LYP/6-31+G(d)	1.370	1.329	1.341	1.304	1.276	1.263	1.274	1.288	1.316	1.268
B3LYP/6-31G(d,p)	1.376	1.327	1.346	1.304	1.377	1.262	1.275	1.288	1.317	1.270

Table S8-28: Bond length comparison during the (Z)-MTIC (t,c,t) + Cl^- S_N2 pathway

Level of Theory	C-X Distance (Å)					C-N_8 Distance (Å)				
	SR	RC	TS	PC	SP	SR	RC	TS	PC	SP
HF/6-31G(d)	∞	3.611	2.276	1.809	1.404	1.469	1.450	2.121	4.405	∞
HF/6-31+G(d)	∞	3.678	2.286	1.810	1.365	1.471	1.451	2.131	4.323	∞
B3LYP/6-31G(d)	∞	3.694	2.261	1.828	1.383	1.483	1.450	2.090	4.338	∞
B3LYP/6-31+G(d)	∞	3.717	2.268	1.825	1.393	1.485	1.453	2.009	4.541	∞
B3LYP/6-31G(d,p)	∞	3.682	2.262	1.825	1.383	1.483	1.449	2.093	4.438	∞

Level of Theory	N_8-N_7 Distance (Å)					N_7-N_6 Distance (Å)				
	SR	RC	TS	PC	SP	SR	RC	TS	PC	SP
HF/6-31G(d)	1.419	1.281	1.261	1.259	1.361	1.215	1.271	1.284	1.299	1.225
HF/6-31+G(d)	1.414	1.272	1.261	1.261	1.357	1.215	1.278	1.284	1.295	1.225
B3LYP/6-31G(d)	1.463	1.329	1.294	1.303	1.381	1.252	1.274	1.309	1.321	1.268
B3LYP/6-31+G(d)	1.451	1.329	1.292	1.304	1.376	1.253	1.274	1.310	1.316	1.268
B3LYP/6-31G(d,p)	1.465	1.327	1.294	1.304	1.377	1.252	1.275	1.309	1.317	1.270

Table S8-29: Bond length comparison during the (Z)-MTIC (c,t,c) + Cl^- S_N2 pathway

Level of Theory	C-X Distance (Å)					C-N_8 Distance (Å)				
	SR	RC	TS	PC	SP	SR	RC	TS	PC	SP
HF/6-31G(d)	∞	3.734	2.257	1.826	1.404	1.450	1.449	2.152	4.762	∞
HF/6-31+G(d)	∞	3.812	2.266	1.827	1.365	1.451	1.450	2.160	4.817	∞
B3LYP/6-31G(d)	∞	3.640	2.235	1.845	1.383	1.454	1.453	2.127	4.787	∞
B3LYP/6-31+G(d)	∞	6.687	2.241	1.844	1.393	1.457	1.456	2.136	4.848	∞
B3LYP/6-31G(d,p)	∞	3.636	2.234	1.845	1.383	1.453	1.452	2.351	4.788	∞

Level of Theory	N_8-N_7 Distance (Å)					N_7-N_6 Distance (Å)				
	SR	RC	TS	PC	SP	SR	RC	TS	PC	SP
HF/6-31G(d)	1.318	1.335	1.247	1.262	1.230	1.229	1.225	1.296	1.300	1.340
HF/6-31+G(d)	1.318	1.334	1.248	1.264	1.233	1.229	1.225	1.295	1.296	1.335
B3LYP/6-31G(d)	1.322	1.342	1.275	1.307	1.267	1.273	1.269	1.324	1.324	1.357
B3LYP/6-31+G(d)	1.322	1.343	1.273	1.307	1.268	1.273	1.267	1.324	1.319	1.354
B3LYP/6-31G(d,p)	1.320	1.341	1.274	1.308	1.267	1.274	1.269	1.324	1.323	1.357

Table S8-30: Bond length comparison during the (Z)-MTIC (c,t,t) + Cl^- S_N2 pathway

Level of Theory	C-X Distance (Å)					$C-N_8$ Distance (Å)				
	SR	RC	TS	PC	SP	SR	RC	TS	PC	SP
HF/6-31G(d)	∞	3.612	2.276	1.809	1.404	1.447	1.450	2.121	4.405	∞
HF/6-31+G(d)	∞	3.680	2.286	1.810	1.365	1.449	1.451	2.131	4.323	∞
B3LYP/6-31G(d)	∞	3.686	2.261	1.828	1.383	1.450	1.450	2.090	4.338	∞
B3LYP/6-31+G(d)	∞	3.717	2.268	1.825	1.393	1.452	1.453	2.099	4.541	∞
B3LYP/6-31G(d,p)	∞	3.682	2.262	1.825	1.383	1.449	1.449	2.093	4.438	∞

Level of Theory	N_8-N_7 Distance (Å)					N_7-N_6 Distance (Å)				
	SR	RC	TS	PC	SP	SR	RC	TS	PC	SP
HF/6-31G(d)	1.311	1.280	1.261	1.259	1.245	1.233	1.271	1.284	1.299	1.321
HF/6-31+G(d)	1.312	1.272	1.262	1.261	1.248	1.232	1.278	1.284	1.295	1.317
B3LYP/6-31G(d)	1.321	1.328	1.294	1.303	1.284	1.275	1.274	1.309	1.321	1.340
B3LYP/6-31+G(d)	1.319	1.329	1.292	1.304	1.284	1.274	1.274	1.310	1.316	1.337
B3LYP/6-31G(d,p)	1.321	1.327	1.294	1.304	1.284	1.275	1.275	1.309	1.317	1.339

Table S8-31: Bond length comparison during the (Z)-MTIC (c,c,c) + Cl^- S_N2 pathway

Level of Theory	C-X Distance (Å)					C-N_8 Distance (Å)				
	SR	RC	TS	PC	SP	SR	RC	TS	PC	SP
HF/6-31G(d)	∞	3.963	2.322	1.826	1.404	1.450	1.440	1.253	1.300	∞
HF/6-31+G(d)	∞	4.024	2.336	1.827	1.365	1.450	1.441	1.253	1.296	∞
B3LYP/6-31G(d)	∞	3.799	2.339	1.845	1.383	1.457	1.448	1.288	1.324	∞
B3LYP/6-31+G(d)	∞	3.874	2.347	1.844	1.393	1.459	1.450	1.288	1.319	∞
B3LYP/6-31G(d,p)	∞	3.778	2.3444	1.845	1.383	1.456	1.448	1.288	1.323	∞

Level of Theory	N_8-N_7 Distance (Å)					N_7-N_6 Distance (Å)				
	SR	RC	TS	PC	SP	SR	RC	TS	PC	SP
HF/6-31G(d)	1.302	1.273	1.315	1.262	1.400	1.231	1.253	1.253	1.300	1.245
HF/6-31+G(d)	1.302	1.273	1.312	1.264	1.367	1.231	1.253	1.253	1.296	1.222
B3LYP/6-31G(d)	1.325	1.294	1.350	1.307	1.390	1.266	1.298	1.288	1.324	1.265
B3LYP/6-31+G(d)	1.324	1.294	1.345	1.307	1.386	1.267	1.295	1.288	1.319	1.263
B3LYP/6-31G(d,p)	1.325	1.293	1.352	1.308	1.386	1.266	1.298	1.288	1.323	1.266

Table S8-32: Bond length comparison during the (Z)-MTIC (c,c,t) + Cl^- S_N2 pathway

Level of Theory	C-X Distance (Å)					C-N_8 Distance (Å)				
	SR	RC	TS	PC	SP	SR	RC	TS	PC	SP
HF/6-31G(d)	∞	3.612	2.346	1.809	1.404	1.457	1.450	2.106	4.405	∞
HF/6-31+G(d)	∞	3.680	2.359	1.810	1.365	1.458	1.451	2.111	4.323	∞
B3LYP/6-31G(d)	∞	3.686	2.359	1.828	1.383	1.463	1.450	2.062	4.338	∞
B3LYP/6-31+G(d)	∞	3.717	2.367	1.825	1.393	1.465	1.453	2.069	4.541	∞
B3LYP/6-31G(d,p)	∞	3.682	2.363	1.825	1.383	1.463	1.449	2.064	4.438	∞

Level of Theory	N_8-N_7 Distance (Å)					N_7-N_6 Distance (Å)				
	SR	RC	TS	PC	SP	SR	RC	TS	PC	SP
HF/6-31G(d)	1.311	1.280	1.311	1.259	1.361	1.231	1.271	1.252	1.299	1.225
HF/6-31+G(d)	1.311	1.272	1.309	1.261	1.357	1.231	1.278	1.253	1.295	1.225
B3LYP/6-31G(d)	1.333	1.328	1.345	1.303	1.281	1.268	1.274	1.288	1.321	1.268
B3LYP/6-31+G(d)	1.331	1.329	1.341	1.304	1.276	1.268	1.274	1.288	1.316	1.268
B3LYP/6-31G(d,p)	1.334	1.327	1.346	1.304	1.377	1.268	1.275	1.288	1.317	1.270

Table S8-33: Bond length comparison during the (E)-MTIC (t,c,c) + Br^- S_N2 pathway

Level of Theory	C-X Distance (Å)					C-N_8 Distance (Å)				
	SR	RC	TS	PC	SP	SR	RC	TS	PC	SP
HF/6-31G(d)	∞	3.955	2.444	1.998	1.948	1.449	1.440	2.136	3.511	∞
HF/6-31+G(d)	∞	4.038	2.450	1.987	1.946	1.450	1.442	2.151	3.518	∞
B3LYP/6-31G(d)	∞	3.775	2.417	2.011	1.966	1.455	1.448	2.099	3.463	∞
B3LYP/6-31+G(d)	∞	3.887	2.426	1.999	1.965	1.456	1.450	2.108	3.485	∞
B3LYP/6-31G(d,p)	∞	3.759	2.418	2.009	1.963	1.454	1.448	2.101	3.455	∞

Level of Theory	N_8-N_7 Distance (Å)					N_7-N_6 Distance (Å)				
	SR	RC	TS	PC	SP	SR	RC	TS	PC	SP
HF/6-31G(d)	1.325	1.273	1.258	1.241	1.241	1.226	1.252	1.282	1.320	1.321
HF/6-31+G(d)	1.322	1.274	1.259	1.242	1.243	1.226	1.250	1.278	1.314	1.313
B3LYP/6-31G(d)	1.335	1.294	1.295	1.284	1.285	1.272	1.297	1.311	1.339	1.342
B3LYP/6-31+G(d)	1.330	1.294	1.291	1.283	1.284	1.271	1.293	1.306	1.332	1.331
B3LYP/6-31G(d,p)	1.334	1.294	1.294	1.284	1.285	1.273	1.298	1.311	1.338	1.342

Table S8-34: Bond length comparison during the (E)-MTIC (t,t,c) + Br^- S_N2 pathway

Level of Theory	C-X Distance (Å)					C-N_8 Distance (Å)				
	SR	RC	TS	PC	SP	SR	RC	TS	PC	SP
HF/6-31G(d)	∞	3.457	2.401	1.979	1.948	1.445	1.443	2.134	3.019	∞
HF/6-31+G(d)	∞	3.491	2.400	1.962	1.946	1.447	1.445	2.146	3.213	∞
B3LYP/6-31G(d)	∞	3.480	2.384	1.999	1.966	1.450	1.448	2.100	2.908	∞
B3LYP/6-31+G(d)	∞	3.487	2.412	1.987	1.965	1.451	1.451	2.109	2.981	∞
B3LYP/6-31G(d,p)	∞	3.470	1.410	1.997	1.963	1.449	1.448	2.101	2.902	∞

Level of Theory	N_8-N_7 Distance (Å)					N_7-N_6 Distance (Å)				
	SR	RC	TS	PC	SP	SR	RC	TS	PC	SP
HF/6-31G(d)	1.334	1.276	1.250	1.238	1.235	1.223	1.249	1.289	1.320	1.329
HF/6-31+G(d)	1.334	1.276	1.252	1.240	1.236	1.222	1.247	1.286	1.317	1.325
B3LYP/6-31G(d)	1.338	1.299	1.279	1.275	1.270	1.270	1.291	1.319	1.340	1.351
B3LYP/6-31+G(d)	1.335	1.298	1.291	1.277	1.273	1.268	1.287	1.303	1.335	1.343
B3LYP/6-31G(d,p)	1.337	1.298	1.295	1.275	1.270	1.270	1.292	1.307	1.340	1.351

Table S8-35: Bond length comparison during the (E)-MTIC (t,c,t) + Br^- S_N2 pathway

Level of Theory	C-X Distance (Å)					C-N_8 Distance (Å)				
	SR	RC	TS	PC	SP	SR	RC	TS	PC	SP
HF/6-31G(d)	∞	3.812	2.425	1.980	1.948	1.446	1.439	2.132	3.105	∞
HF/6-31+G(d)	∞	2.891	2.430	1.962	1.946	1.446	1.440	2.142	4.099	∞
B3LYP/6-31G(d)	∞	3.694	2.439	2.003	1.966	1.453	1.447	2.099	2.935	∞
B3LYP/6-31+G(d)	∞	3.789	2.412	1.986	1.965	1.453	1.448	2.109	3.111	∞
B3LYP/6-31G(d,p)	∞	3.680	2.410	2.001	1.963	1.452	1.447	2.101	2.924	∞

Level of Theory	N_8-N_7 Distance (Å)					N_7-N_6 Distance (Å)				
	SR	RC	TS	PC	SP	SR	RC	TS	PC	SP
HF/6-31G(d)	1.307	1.273	1.259	1.245	1.243	1.230	1.252	1.280	1.309	1.314
HF/6-31+G(d)	1.318	1.273	1.260	1.242	1.244	1.226	1.250	1.276	1.309	1.307
B3LYP/6-31G(d)	1.335	1.295	1.295	1.287	1.286	1.272	1.294	1.307	1.329	1.335
B3LYP/6-31+G(d)	1.329	1.294	1.291	1.287	1.285	1.271	1.291	1.303	1.323	1.326
B3LYP/6-31G(d,p)	1.334	1.294	1.295	1.287	1.286	1.272	1.295	1.307	1.329	1.335

Table S8-36: Bond length comparison during the (E)-MTIC (t,t,t) + Br^- S_N2 pathway

Level of Theory	C-X Distance (Å)					C-N_8 Distance (Å)				
	SR	RC	TS	PC	SP	SR	RC	TS	PC	SP
HF/6-31G(d)	∞	3.672	2.416	1.978	1.948	1.447	1.440	2.114	3.042	∞
HF/6-31+G(d)	∞	3.720	2.414	1.961	1.946	1.448	1.442	2.126	3.225	∞
B3LYP/6-31G(d)	∞	3.578	2.401	1.986	1.966	1.451	1.446	2.078	3.159	∞
B3LYP/6-31+G(d)	∞	3.634	2.396	1.986	1.965	1.453	1.448	2.084	3.159	∞
B3LYP/6-31G(d,p)	∞	3.577	2.401	1.984	1.963	1.450	1.445	2.080	3.158	∞

Level of Theory	N_8-N_7 Distance (Å)					N_7-N_6 Distance (Å)				
	SR	RC	TS	PC	SP	SR	RC	TS	PC	SP
HF/6-31G(d)	1.330	1.279	1.251	1.239	1.235	1.223	1.245	1.285	1.315	1.323
HF/6-31+G(d)	1.330	1.279	1.252	1.240	1.237	1.222	1.243	1.283	1.312	1.319
B3LYP/6-31G(d)	1.337	1.300	1.280	1.275	1.271	1.270	1.289	1.313	1.334	1.343
B3LYP/6-31+G(d)	1.335	1.300	1.280	1.275	1.273	1.269	1.286	1.311	1.334	1.338
B3LYP/6-31G(d,p)	1.336	1.299	1.280	1.275	1.271	1.270	1.290	1.313	1.334	1.343

Table S8-37: Bond length comparison during the (E)-MTIC (c,c,c) + Br^- S_N2 pathway

Level of Theory	C-X Distance (Å)					C-N_8 Distance (Å)				
	SR	RC	TS	PC	SP	SR	RC	TS	PC	SP
HF/6-31G(d)	∞	3.720	2.409	1,987	1.948	1.448	1.442	2.140	3.316	∞
HF/6-31+G(d)	∞	3.790	2.407	1.877	1.946	1.449	1.443	2.155	3.351	∞
B3LYP/6-31G(d)	∞	3.618	2.383	2.001	1.966	1.450	1.447	2.110	3.226	∞
B3LYP/6-31+G(d)	∞	3.692	2.380	1.992	1.965	1.453	1.450	2.116	3.303	∞
B3LYP/6-31G(d,p)	∞	3.604	2.383	1.999	1.963	1.449	1.447	2.113	3.217	∞

Level of Theory	N_8-N_7 Distance (Å)					N_7-N_6 Distance (Å)				
	SR	RC	TS	PC	SP	SR	RC	TS	PC	SP
HF/6-31G(d)	1.317	1.251	1.245	1.233	1.232	1.227	1.442	1.296	1.327	1.332
HF/6-31+G(d)	1.315	1.272	1.246	1.234	1.233	1.226	1.249	1.293	1.323	1.328
B3LYP/6-31G(d)	1.323	1.295	1.275	1.268	1.267	1.271	1.291	1.321	1.345	1.352
B3LYP/6-31+G(d)	1.320	1.294	1.273	1.269	1.268	1.269	1.287	1.317	1.339	1.344
B3LYP/6-31G(d,p)	1.322	1.294	1.275	1.268	1.267	1.271	1.292	1.321	1.345	1.352

Table S8-38: Bond length comparison during the (E)-MTIC (c,t,c) + Br^- S_N2 pathway

Level of Theory	C-X Distance (Å)					C-N_8 Distance (Å)				
	SR	RC	TS	PC	SP	SR	RC	TS	PC	SP
HF/6-31G(d)	∞	3.706	2.416	1.988	1.948	1.447	1.441	2.167	3.114	∞
HF/6-31+G(d)	∞	3.759	2.391	1.969	1.946	1.447	1.443	2.146	3.679	∞
B3LYP/6-31G(d)	∞	3.592	2.392	1.999	1.966	1.454	1.450	2.146	2.944	∞
B3LYP/6-31+G(d)	∞	3.656	2.394	1.984	1.965	1.455	1.451	2.155	3.008	∞
B3LYP/6-31G(d,p)	∞	3.580	2.394	1.997	1.963	1.453	1.449	2.148	2.937	∞

Level of Theory	N_8-N_7 Distance (Å)					N_7-N_6 Distance (Å)				
	SR	RC	TS	PC	SP	SR	RC	TS	PC	SP
HF/6-31G(d)	1.311	1.271	1.251	1.240	1.238	1.230	1.255	1.291	1.319	1.325
HF/6-31+G(d)	1.308	1.271	1.284	1.238	1.238	1.230	1.253	1.314	1.318	1.317
B3LYP/6-31G(d)	1.325	1.293	1.285	1.278	1.281	1.273	1.296	1.314	1.324	1.344
B3LYP/6-31+G(d)	1.320	1.292	1.283	1.280	1.278	1.271	1.292	1.309	1.320	1.333
B3LYP/6-31G(d,p)	1.324	1.293	1.285	1.279	1.281	1.273	1.297	1.314	1.323	1.344

Table S8-39: Bond length comparison during the (E)-MTIC (c,c,t) + Br^- S_N2 pathway

Level of Theory	C-X Distance (Å)					C-N_8 Distance (Å)				
	SR	RC	TS	PC	SP	SR	RC	TS	PC	SP
HF/6-31G(d)	∞	3.681	2.419	1.977	1.948	1.447	1.444	2.115	3.082	∞
HF/6-31+G(d)	∞	3.727	2.404	1.965	1.946	1.448	1.441	2.086	3.121	∞
B3LYP/6-31G(d)	∞	3.585	2.404	1.998	1.966	1.452	1.445	2.086	2.943	∞
B3LYP/6-31+G(d)	∞	3.638	2.406	1.986	1.965	1.454	1.447	2.092	3.017	∞
B3LYP/6-31G(d,p)	∞	3.574	2.405	1.997	1.963	1.451	1.445	2.088	2.933	∞

Level of Theory	N_8-N_7 Distance (Å)					N_7-N_6 Distance (Å)				
	SR	RC	TS	PC	SP	SR	RC	TS	PC	SP
HF/6-31G(d)	1.330	1.281	1.254	1.241	1.237	1.221	1.240	1.278	1.306	1.313
HF/6-31+G(d)	1.328	1.281	1.289	1.243	1.239	1.221	1.239	1.304	1.303	1.309
B3LYP/6-31G(d)	1.342	1.302	1.289	1.278	1.274	1.262	1.282	1.304	1.324	1.332
B3LYP/6-31+G(d)	1.339	1.302	1.291	1.280	1.276	1.263	1.280	1.300	1.320	1.326
B3LYP/6-31G(d,p)	1.341	1.302	1.289	1.278	1.274	1.265	1.283	1.304	1.324	1.331

Table S8-40: Bond length comparison during the (E)-MTIC (c,t,t) + Br^- S_N2 pathway

Level of Theory	C-X Distance (Å)					C-N_8 Distance (Å)				
	SR	RC	TS	PC	SP	SR	RC	TS	PC	SP
HF/6-31G(d)	∞	3.791	2.425	1.984	1.948	1.446	1.439	2.143	3.112	∞
HF/6-31+G(d)	∞	3.849	2.428	1.976	1.946	1.446	1.440	1.254	3.121	∞
B3LYP/6-31G(d)	∞	3.682	2.410	2.005	1.966	1.453	1.442	2.104	3.018	∞
B3LYP/6-31+G(d)	∞	3.753	2.408	1.995	1.965	1.454	1.448	2.120	3.016	∞
B3LYP/6-31G(d,p)	∞	3.672	2.412	2.003	1.963	1.452	1.445	2.106	3.002	∞

Level of Theory	N_8-N_7 Distance (Å)					N_7-N_6 Distance (Å)				
	SR	RC	TS	PC	SP	SR	RC	TS	PC	SP
HF/6-31G(d)	1.320	1.276	1.261	1.247	1.245	1.224	1.256	1.274	1.301	1.305
HF/6-31+G(d)	1.315	1.277	1.262	1.248	1.246	1.225	1.244	1.271	1.395	1.299
B3LYP/6-31G(d)	1.340	1.299	1.298	1.289	1.289	1.266	1.287	1.299	1.319	1.325
B3LYP/6-31+G(d)	1.335	1.299	1.294	1.290	1.288	1.265	1.284	1.296	1.313	1.316
B3LYP/6-31G(d,p)	1.339	1.298	1.298	1.290	1.289	1.266	1.287	1.299	1.319	1.324

Table S8-41: Bond length comparison during the (Z)-MTIC (c,c,t) + Br^- S_N2 pathway

Level of Theory	C-X Distance (Å)					C-N_8 Distance (Å)				
	SR	RC	TS	PC	SP	SR	RC	TS	PC	SP
HF/6-31G(d)	∞	3.728	2.452	1.996	1.948	1.469	1.450	2.139	4.745	∞
HF/6-31+G(d)	∞	3.923	2.454	1.985	1.946	1.470	1.450	2.144	4.675	∞
B3LYP/6-31G(d)	∞	3.637	2.468	2.01	1.966	1.481	1.454	2.096	4.768	∞
B3LYP/6-31+G(d)	∞	3.783	2.468	1.997	1.965	1.483	1.458	2.093	4.696	∞
B3LYP/6-31G(d,p)	∞	3.636	2.472	2.008	1.963	1.481	1.453	2.096	4.767	∞

Level of Theory	N_8-N_7 Distance (Å)					N_7-N_6 Distance (Å)				
	SR	RC	TS	PC	SP	SR	RC	TS	PC	SP
HF/6-31G(d)	1.418	1.333	1.314	1.261	1.400	1.213	1.226	1.253	1.301	1.245
HF/6-31+G(d)	1.408	1.333	1.312	1.263	1.367	1.213	1.225	1.253	1.296	1.222
B3LYP/6-31G(d)	1.473	1.339	1.349	1.306	1.390	1.247	1.269	1.289	1.324	1.265
B3LYP/6-31+G(d)	1.448	1.347	1.345	1.307	1.386	1.249	1.266	1.288	1.319	1.263
B3LYP/6-31G(d,p)	1.475	1.339	1.351	1.308	1.386	1.247	1.269	1.289	1.323	1.266

Table S8-42: Bond length comparison during the (Z)-MTIC (t,c,c) + Br^- S_N2 pathway

Level of Theory	C-X Distance (Å)					C-N_8 Distance (Å)				
	SR	RC	TS	PC	SP	SR	RC	TS	PC	SP
HF/6-31G(d)	∞	3.730	2.453	1.996	1.948	1.469	1.450	2.138	4.745	∞
HF/6-31+G(d)	∞	3.924	2.467	1.985	1.946	1.470	1.405	2.096	4.673	∞
B3LYP/6-31G(d)	∞	3.638	2.470	2.010	1.966	1.481	1.454	2.095	4.768	∞
B3LYP/6-31+G(d)	∞	3.783	2.470	1.997	1.965	1.483	1.458	2.093	4.696	∞
B3LYP/6-31G(d,p)	∞	3.636	2.473	2.008	1.963	1.481	1.453	2.095	4.767	∞

Level of Theory	N_8-N_7 Distance (Å)					N_7-N_6 Distance (Å)				
	SR	RC	TS	PC	SP	SR	RC	TS	PC	SP
HF/6-31G(d)	1.418	1.333	1.315	1.261	1.400	1.213	1.226	1.253	1.301	1.245
HF/6-31+G(d)	1.408	1.333	1.349	1.263	1.367	1.213	1.225	1.289	1.296	1.222
B3LYP/6-31G(d)	1.473	1.339	1.350	1.306	1.390	1.247	1.269	1.289	1.324	1.265
B3LYP/6-31+G(d)	1.448	1.346	1.346	1.307	1.386	1.249	1.266	1.288	1.319	1.263
B3LYP/6-31G(d,p)	1.475	1.339	1.351	1.308	1.386	1.247	1.269	1.289	1.323	1.266

Table S8-43: Bond length comparison during the (Z)-MTIC (t,t,t) + Br^- S_N2 pathway

Level of Theory	C-X Distance (Å)					C-N_8 Distance (Å)				
	SR	RC	TS	PC	SP	SR	RC	TS	PC	SP
HF/6-31G(d)	∞	3.656	2.476	1.975	1.948	1.453	1.448	2.109	4.402	∞
HF/6-31+G(d)	∞	3.802	2.479	1.959	1.946	1.449	1.449	2.116	4.288	∞
B3LYP/6-31G(d)	∞	3.730	2.488	1.990	1.966	1.463	1.448	2.006	4.324	∞
B3LYP/6-31+G(d)	∞	3.816	2.488	1.973	1.965	1.464	1.450	2.0065	4.295	∞
B3LYP/6-31G(d,p)	∞	3.716	2.491	1.990	1.963	1.462	1.448	2.006	4.308	∞

Level of Theory	N_8-N_7 Distance (Å)					N_7-N_6 Distance (Å)				
	SR	RC	TS	PC	SP	SR	RC	TS	PC	SP
HF/6-31G(d)	1.350	1.315	1.311	1.258	1.361	1.222	1.233	1.253	1.300	1.225
HF/6-31+G(d)	1.312	1.318	1.308	1.261	1.357	1.232	1.232	1.253	1.395	1.225
B3LYP/6-31G(d)	1.377	1.332	1.345	1.303	1.281	1.262	1.276	1.289	1.321	1.268
B3LYP/6-31+G(d)	1.370	1.322	1.341	1.304	1.276	1.263	1.276	1.288	1.318	1.268
B3LYP/6-31G(d,p)	1.376	1.322	1.346	1.303	1.377	1.262	1.276	1.289	1.321	1.270

Table S8-44: Bond length comparison during the (Z)-MTIC (t,c,t) + Br^- S_N2 pathway

Level of Theory	C-X Distance (Å)					C-N_8 Distance (Å)				
	SR	RC	TS	PC	SP	SR	RC	TS	PC	SP
HF/6-31G(d)	∞	3.656	2.407	1.975	1.948	1.469	1.448	2.128	4.402	∞
HF/6-31+G(d)	∞	3.803	2.406	1.959	1.946	1.471	1.449	2.141	4.288	∞
B3LYP/6-31G(d)	∞	3.732	2.393	1.990	1.966	1.483	1.449	2.096	4.324	∞
B3LYP/6-31+G(d)	∞	3.816	2.390	1.973	1.965	1.485	1.450	2.101	4.295	∞
B3LYP/6-31G(d,p)	∞	3.727	2.394	1.990	1.963	1.483	1.448	2.098	4.308	∞

Level of Theory	N_8-N_7 Distance (Å)					N_7-N_6 Distance (Å)				
	SR	RC	TS	PC	SP	SR	RC	TS	PC	SP
HF/6-31G(d)	1.419	1.315	1.261	1.258	1.361	1.215	1.233	1.284	1.300	1.225
HF/6-31+G(d)	1.414	1.317	1.262	1.261	1.357	1.215	1.232	1.284	1.395	1.225
B3LYP/6-31G(d)	1.463	1.322	1.295	1.303	1.381	1.252	1.276	1.309	1.321	1.268
B3LYP/6-31+G(d)	1.451	1.322	1.294	1.304	1.376	1.253	1.276	1.309	1.318	1.268
B3LYP/6-31G(d,p)	1.465	1.322	1.295	1.303	1.377	1.252	1.276	1.309	1.321	1.270

Table S8-45: Bond length comparison during the (Z)-MTIC (c,t,c) + Br^- S_N2 pathway

Level of Theory	C-X Distance (Å)					C-N_8 Distance (Å)				
	SR	RC	TS	PC	SP	SR	RC	TS	PC	SP
HF/6-31G(d)	∞	3.728	2.387	1.996	1.948	1.450	1.450	2.160	4.745	∞
HF/6-31+G(d)	∞	3.923	2.387	1.985	1.946	1.451	1.450	2.167	4.673	∞
B3LYP/6-31G(d)	∞	2.637	2.371	2.010	1.966	1.454	1.454	2.128	4.768	∞
B3LYP/6-31+G(d)	∞	3.783	2.366	1.997	1.965	1.457	1.458	2.131	4.696	∞
B3LYP/6-31G(d,p)	∞	3.636	2.371	2.008	1.963	1.453	1.453	2.131	4.767	∞

Level of Theory	N_8-N_7 Distance (Å)					N_7-N_6 Distance (Å)				
	SR	RC	TS	PC	SP	SR	RC	TS	PC	SP
HF/6-31G(d)	1.318	1.333	1.247	1.261	1.230	1.229	1.226	1.296	1.301	1.340
HF/6-31+G(d)	1.318	1.333	1.249	1.263	1.233	1.229	1.225	1.295	1.296	1.335
B3LYP/6-31G(d)	1.322	1.339	1.276	1.306	1.267	1.273	1.269	1.323	1.324	1.357
B3LYP/6-31+G(d)	1.322	1.347	1.275	1.307	1.268	1.273	1.266	1.322	1.319	1.354
B3LYP/6-31G(d,p)	1.320	1.339	1.276	1.308	1.267	1.274	1.269	1.323	1.323	1.357

Table S8-46: Bond length comparison during the (Z)-MTIC (c,t,t) + Br^- S_N2 pathway

Level of Theory	C-X Distance (Å)					C-N_8 Distance (Å)				
	SR	RC	TS	PC	SP	SR	RC	TS	PC	SP
HF/6-31G(d)	∞	3.656	2.407	1.975	1.948	1.447	1.448	2.128	4.402	∞
HF/6-31+G(d)	∞	3.802	2.406	1.959	1.946	1.449	1.449	2.141	4.288	∞
B3LYP/6-31G(d)	∞	3.733	2.393	1.990	1.966	1.450	1.449	2.097	4.324	∞
B3LYP/6-31+G(d)	∞	3.816	2.389	1.973	1.965	1.452	1.450	2.101	4.295	∞
B3LYP/6-31G(d,p)	∞	3.726	2.394	1.990	1.963	1.449	1.448	2.098	4.308	∞

Level of Theory	N_8-N_7 Distance (Å)					N_7-N_6 Distance (Å)				
	SR	RC	TS	PC	SP	SR	RC	TS	PC	SP
HF/6-31G(d)	1.311	1.315	1.261	1.258	1.245	1.233	1.233	1.284	1.300	1.321
HF/6-31+G(d)	1.312	1.318	1.262	1.261	1.248	1.232	1.232	1.284	1.395	1.317
B3LYP/6-31G(d)	1.321	1.323	1.295	1.303	1.284	1.275	1.276	1.309	1.321	1.340
B3LYP/6-31+G(d)	1.319	1.322	1.294	1.304	1.284	1.274	1.276	1.309	1.318	1.337
B3LYP/6-31G(d,p)	1.321	1.322	1.295	1.303	1.284	1.275	1.276	1.309	1.321	1.339

Table S8-47: Bond length comparison during the (Z)-MTIC (c,c,c) + Br^- S_N2 pathway

Level of Theory	C-X Distance (Å)					C-N_8 Distance (Å)				
	SR	RC	TS	PC	SP	SR	RC	TS	PC	SP
HF/6-31G(d)	∞	3.955	2.453	1.996	1.948	1.450	1.440	2.138	4.745	∞
HF/6-31+G(d)	∞	4.038	2.467	1.985	1.946	1.450	1.442	2.096	4.673	∞
B3LYP/6-31G(d)	∞	3.773	2.470	2.010	1.966	1.457	1.448	2.095	4.768	∞
B3LYP/6-31+G(d)	∞	3.887	2.470	1.997	1.965	1.459	1.450	2.093	4.696	∞
B3LYP/6-31G(d,p)	∞	3.758	2.473	2.008	1.963	1.456	1.448	2.095	4.767	∞

Level of Theory	N_8-N_7 Distance (Å)					N_7-N_6 Distance (Å)				
	SR	RC	TS	PC	SP	SR	RC	TS	PC	SP
HF/6-31G(d)	1.302	1.273	1.315	1.261	1.400	1.231	1.252	1.253	1.301	1.245
HF/6-31+G(d)	1.302	1.274	1.349	1.263	1.367	1.231	1.250	1.289	1.296	1.222
B3LYP/6-31G(d)	1.325	1.294	1.350	1.306	1.390	1.266	1.297	1.289	1.324	1.265
B3LYP/6-31+G(d)	1.324	1.294	1.346	1.307	1.386	1.267	1.293	1.288	1.319	1.263
B3LYP/6-31G(d,p)	1.325	1.294	1.351	1.308	1.386	1.266	1.298	1.289	1.323	1.266

Table S8-48: Bond length comparison during the (Z)-MTIC (c,c,t) + Br^- S_N2 pathway

Level of Theory	C-X Distance (Å)					C-N_8 Distance (Å)				
	SR	RC	TS	PC	SP	SR	RC	TS	PC	SP
HF/6-31G(d)	∞	3.656	2.476	1.975	1.948	1.457	1.448	2.109	4.402	∞
HF/6-31+G(d)	∞	3.802	2.479	1.959	1.946	1.458	1.449	2.116	4.288	∞
B3LYP/6-31G(d)	∞	3.733	2.488	1.990	1.966	1.463	1.449	2.006	4.324	∞
B3LYP/6-31+G(d)	∞	3.816	2.488	1.973	1.965	1.465	1.450	2.0065	4.295	∞
B3LYP/6-31G(d,p)	∞	3.726	2.491	1.990	1.963	1.463	1.448	2.006	4.308	∞

Level of Theory	N_8-N_7 Distance (Å)					N_7-N_6 Distance (Å)				
	SR	RC	TS	PC	SP	SR	RC	TS	PC	SP
HF/6-31G(d)	1.311	1.315	1.311	1.258	1.361	1.231	1.233	1.253	1.300	1.225
HF/6-31+G(d)	1.311	1.318	1.308	1.261	1.357	1.231	1.232	1.253	1.395	1.225
B3LYP/6-31G(d)	1.333	1.323	1.345	1.303	1.281	1.268	1.276	1.289	1.321	1.268
B3LYP/6-31+G(d)	1.331	1.322	1.341	1.304	1.276	1.268	1.276	1.288	1.318	1.268
B3LYP/6-31G(d,p)	1.334	1.322	1.346	1.303	1.377	1.268	1.276	1.289	1.321	1.270

Table S8-49: Bond length comparison during the (Z)-MTIC_T (t,c,c) + F^- S_N2 pathway

Level of Theory	C-X Distance (Å)					C-N_8 Distance (Å)				
	SR	RC	TS	PC	SP	SR	RC	TS	PC	SP
HF/6-31G(d)	∞	3.490	1,910	1.385	1.365	1.457	1.457	1.857	4.568	∞
HF/6-31+G(d)	∞	3.662	2.335	1.395	1.371	1.456	1.457	1.612	5.973	∞
B3LYP/6-31G(d)	∞	2.281	2.097	1.404	1.383	1.468	1.474	1.751	4.326	∞
B3LYP/6-31+G(d)	∞	3.807	2.119	1.425	1.393	1.468	1.472	1.778	4.873	∞
B3LYP/6-31G(d,p)	∞	3.362	2.092	1.404	1.383	1.468	1.474	1.762	4.336	∞

Level of Theory	N_8-N_7 Distance (Å)					N_7-N_6 Distance (Å)				
	SR	RC	TS	PC	SP	SR	RC	TS	PC	SP
HF/6-31G(d)	1.217	1.231	1.185	1.078	1.078	1.343	1.339	1.513	3.499	∞
HF/6-31+G(d)	1.217	1.232	1.097	1.078	1.079	1.345	1.336	2.280	4.185	∞
B3LYP/6-31G(d)	1.253	1.269	1.149	1.108	1.106	1.362	1.363	2.223	3.412	∞
B3LYP/6-31+G(d)	1.253	1.270	1.143	1.106	1.105	1.363	1.357	2.297	3.701	∞
B3LYP/6-31G(d,p)	1.253	1.269	1.148	1.109	1.106	1.363	1.363	2.246	3.407	∞

Table S8-50: Bond length comparison during the (E)-MTIC_T (t,c,c) + F^- S_N2 pathway

Level of Theory	C-X Distance (Å)					C-N_8 Distance (Å)				
	SR	RC	TS	PC	SP	SR	RC	TS	PC	SP
HF/6-31G(d)	∞	4.647	1.865	1.385	1.365	1.449	1.446	1.894	4.568	∞
HF/6-31+G(d)	∞	4.701	1.833	1.395	1.371	1.450	1.446	1.990	5.973	∞
B3LYP/6-31G(d)	∞	4.616	2.196	1.404	1.383	1.459	1.456	1.671	4.326	∞
B3LYP/6-31+G(d)	∞	4.658	2.2.16	1.425	1.393	1.453	1.456	1.676	4.873	∞
B3LYP/6-31G(d,p)	∞	4.619	2.177	1.404	1.383	1.459	1.456	1.689	4.336	∞

Level of Theory	N_8-N_7 Distance (Å)					N_7-N_6 Distance (Å)				
	SR	RC	TS	PC	SP	SR	RC	TS	PC	SP
HF/6-31G(d)	1.213	1.229	1.193	1.078	1.078	1.338	1.330	1.453	3.499	∞
HF/6-31+G(d)	1.211	1.227	1.190	1.078	1.079	1.341	1.330	1.463	4.185	∞
B3LYP/6-31G(d)	1.254	1.272	1.137	1.108	1.106	1.348	1.345	2.360	3.412	∞
B3LYP/6-31+G(d)	1.251	1.267	1.156	1.106	1.105	1.348	1.344	1.968	3.701	∞
B3LYP/6-31G(d,p)	1.254	1.272	1.135	1.109	1.106	1.349	1.345	2.383	3.407	∞

Table S8-51: Bond length comparison during the (Z)-MTIC_T (t,t,c) + F^- S_N2 pathway

Level of Theory	C-X Distance (Å)					C-N_8 Distance (Å)				
	SR	RC	TS	PC	SP	SR	RC	TS	PC	SP
HF/6-31G(d)	∞	3.279	1.905	1.383	1.365	1.457	.1456	1.858	4.50	∞
HF/6-31+G(d)	∞	3.431	2.394	1.393	1.371	1.456	1.456	1.534	6.375	∞
B3LYP/6-31G(d)	∞	3.039	2.168	1.403	1.383	1.468	1.471	1.641	4.292	∞
B3LYP/6-31+G(d)	∞	3.045	2.228	1.424	1.393	1.467	1.468	1.614	6.783	∞
B3LYP/6-31G(d,p)	∞	3.035	2.158	1.403	1.383	1.468	1.471	1.650	4.248	∞

Level of Theory	N_8-N_7 Distance (Å)					N_7-N_6 Distance (Å)				
	SR	RC	TS	PC	SP	SR	RC	TS	PC	SP
HF/6-31G(d)	1.214	1.230	1.184	1.078	1.078	1.357	1.339	1.525	3.573	∞
HF/6-31+G(d)	1.214	1.231	1.118	1.078	1.079	1.359	1.338	1.988	4.195	∞
B3LYP/6-31G(d)	1.252	1.266	1.147	1.107	1.106	1.368	1.361	2.205	3.557	∞
B3LYP/6-31+G(d)	1.252	1.260	1.151	1.107	1.105	1.368	1.365	2.091	4.094	∞
B3LYP/6-31G(d,p)	1.252	1.267	1.145	1.107	1.106	1.367	1.361	2.226	3.557	∞

Table S8-52: Bond length comparison during the (E)-MTIC_T (t,t,c) + F^- S_N2 pathway

Level of Theory	C-X Distance (Å)					C-N_8 Distance (Å)				
	SR	RC	TS	PC	SP	SR	RC	TS	PC	SP
HF/6-31G(d)	∞	4.615	1.876	1.383	1.365	1.450	1.445	1.879	4.50	∞
HF/6-31+G(d)	∞	4.716	1.843	1.393	1.371	1.451	1.446	1.976	6.375	∞
B3LYP/6-31G(d)	∞	4.787	2.188	1.403	1.383	1.459	1.456	1.673	4.292	∞
B3LYP/6-31+G(d)	∞	4.842	2.198	1.424	1.393	1.459	1.457	1.683	6.783	∞
B3LYP/6-31G(d,p)	∞	4.773	2.170	1.403	1.383	1.459	1.456	1.692	4.248	∞

Level of Theory	N_8-N_7 Distance (Å)					N_7-N_6 Distance (Å)				
	SR	RC	TS	PC	SP	SR	RC	TS	PC	SP
HF/6-31G(d)	1.231	1.231	1.192	1.078	1.078	1.384	1.325	1.464	3.573	∞
HF/6-31+G(d)	1.211	1.227	1.190	1.078	1.079	1.353	1.328	1.471	4.195	∞
B3LYP/6-31G(d)	1.253	1.273	1.137	1.107	1.106	1.353	1.339	2.365	3.557	∞
B3LYP/6-31+G(d)	1.251	1.264	1.161	1.107	1.105	1.352	1.340	1.936	4.094	∞
B3LYP/6-31G(d,p)	1.253	1.273	1.135	1.107	1.106	1.353	1.340	2.397	3.557	∞

Table S8-53: Bond length comparison during the (E)-MTIC_T (t,c,t) + F^- S_N2 pathway

Level of Theory	C-X Distance (Å)					C-N_8 Distance (Å)				
	SR	RC	TS	PC	SP	SR	RC	TS	PC	SP
HF/6-31G(d)	∞	5.102	1.874	1.385	1.365	1.449	1.446	1.882	4.568	∞
HF/6-31+G(d)	∞	5.111	1.840	1.395	1.371	1.450	1.448	1.981	5.973	∞
B3LYP/6-31G(d)	∞	5.134	2.004	1.404	1.383	1.459	1.454	1.772	4.326	∞
B3LYP/6-31+G(d)	∞	5.169	2.211	1.425	1.393	1.458	1.458	1.675	4.873	∞
B3LYP/6-31G(d,p)	∞	5.144	1.990	1.404	1.383	1.459	1.454	1.781	4.336	∞

Level of Theory	N_8-N_7 Distance (Å)					N_7-N_6 Distance (Å)				
	SR	RC	TS	PC	SP	SR	RC	TS	PC	SP
HF/6-31G(d)	1.213	1.249	1.192	1.078	1.078	1.380	1.308	1.467	3.499	∞
HF/6-31+G(d)	1.211	1.246	1.192	1.078	1.079	1.338	1.310	1.467	4.185	∞
B3LYP/6-31G(d)	1.254	1.295	1.212	1.108	1.106	1.349	1.327	1.540	3.412	∞
B3LYP/6-31+G(d)	1.251	1.289	1.159	1.106	1.105	1.348	1.328	1.990	3.701	∞
B3LYP/6-31G(d,p)	1.254	1.297	1.214	1.109	1.106	1.349	1.326	1.533	3.407	∞

Table S8-54: Bond length comparison during the (E)-MTIC_T (t,t,t) + F^- S_N2 pathway

Level of Theory	C-X Distance (Å)					C-N_8 Distance (Å)				
	SR	RC	TS	PC	SP	SR	RC	TS	PC	SP
HF/6-31G(d)	∞	5.106	1.886	1.383	1.365	1.452	1.447	1.869	4.50	∞
HF/6-31+G(d)	∞	5.183	1.853	1.393	1.371	1.453	1.448	1.967	6.375	∞
B3LYP/6-31G(d)	∞	5.269	2.184	1.403	1.383	1.460	1.445	1.675	4.292	∞
B3LYP/6-31+G(d)	∞	5.358	2.218	1.424	1.393	1.462	1.459	1.666	6.783	∞
B3LYP/6-31G(d,p)	∞	5.264	2.167	1.403	1.383	1.461	1.455	1.693	4.248	∞

Level of Theory	N_8-N_7 Distance (Å)					N_7-N_6 Distance (Å)				
	SR	RC	TS	PC	SP	SR	RC	TS	PC	SP
HF/6-31G(d)	1.216	1.245	1.194	1.078	1.078	1.340	1.310	1.464	3.573	∞
HF/6-31+G(d)	1.214	1.241	1.189	1.078	1.079	1.341	1.313	1.482	4.195	∞
B3LYP/6-31G(d)	1.261	1.290	1.137	1.107	1.106	1.347	1.326	2.376	3.557	∞
B3LYP/6-31+G(d)	1.258	1.277	1.161	1.107	1.105	1.346	1.327	1.964	4.094	∞
B3LYP/6-31G(d,p)	1.261	1.291	1.135	1.107	1.106	1.347	1.326	2.400	3.557	∞

Table S8-55: Bond length comparison during the (Z)-MTIC_T (t,c,c) + Cl^- S_N2 pathway

Level of Theory	C-X Distance (Å)					C-N_8 Distance (Å)				
	SR	RC	TS	PC	SP	SR	RC	TS	PC	SP
HF/6-31G(d)	∞	4.275	2.771	1.819	1.365	1.457	1.456	1.657	4.652	∞
HF/6-31+G(d)	∞	4.226	2.973	1.818	1.371	1.456	1.456	1.533	6.055	∞
B3LYP/6-31G(d)	∞	4.393	2.558	1.848	1.383	1.468	1.472	1.847	4.505	∞
B3LYP/6-31+G(d)	∞	4.394	2.576	1.843	1.393	1.468	1.472	1.834	5.639	∞
B3LYP/6-31G(d,p)	∞	4.293	2.562	1.848	1.383	1.468	1.474	1.847	4.991	∞

Level of Theory	N_8-N_7 Distance (Å)					N_7-N_6 Distance (Å)				
	SR	RC	TS	PC	SP	SR	RC	TS	PC	SP
HF/6-31G(d)	1.217	1.232	1.093	1.078	1.078	1.343	1.337	2.324	3.585	∞
HF/6-31+G(d)	1.217	1.233	1.086	1.078	1.079	1.345	1.334	2.391	4.234	∞
B3LYP/6-31G(d)	1.253	1.268	1.141	1.117	1.106	1.362	1.364	2.299	3.548	∞
B3LYP/6-31+G(d)	1.253	1.270	1.139	1.106	1.105	1.363	1.358	2.338	3.381	∞
B3LYP/6-31G(d,p)	1.253	1.262	1.141	1.108	1.106	1.363	1.375	2.309	2.964	∞

Table S8-56: Bond length comparison during the (E)-MTIC_T (t,c,c) + Cl^- S_N2 pathway

Level of Theory	C-X Distance (Å)					C-N_8 Distance (Å)				
	SR	RC	TS	PC	SP	SR	RC	TS	PC	SP
HF/6-31G(d)	∞	4.909	2.771	1.819	1.365	1.457	1.446	1.657	4.652	∞
HF/6-31+G(d)	∞	4.957	2.973	1.818	1.371	1.456	1.446	1.533	6.055	∞
B3LYP/6-31G(d)	∞	4.979	2.558	1.848	1.383	1.468	1.457	1.847	4.505	∞
B3LYP/6-31+G(d)	∞	5.076	2.576	1.843	1.393	1.468	1.457	1.834	5.639	∞
B3LYP/6-31G(d,p)	∞	4.967	2.562	1.848	1.383	1.468	1.457	1.847	4.991	∞

Level of Theory	N_8-N_7 Distance (Å)					N_7-N_6 Distance (Å)				
	SR	RC	TS	PC	SP	SR	RC	TS	PC	SP
HF/6-31G(d)	1.217	1.229	1.093	1.078	1.078	1.343	1.332	2.324	3.585	∞
HF/6-31+G(d)	1.217	1.227	1.086	1.078	1.079	1.345	1.330	2.391	4.234	∞
B3LYP/6-31G(d)	1.253	1.256	1.141	1.117	1.106	1.362	1.359	2.299	3.548	∞
B3LYP/6-31+G(d)	1.253	1.253	1.139	1.106	1.105	1.363	1.357	2.338	3.381	∞
B3LYP/6-31G(d,p)	1.253	1.257	1.141	1.108	1.106	1.363	1.358	2.309	2.964	∞

Table S8-57: Bond length comparison during the (Z)-MTIC_T (t,t,c) + Cl^- S_N2 pathway

Level of Theory	C-X Distance (Å)					C-N_8 Distance (Å)				
	SR	RC	TS	PC	SP	SR	RC	TS	PC	SP
HF/6-31G(d)	∞	3.883	2.773	1.816	1.365	1.457	1.456	1.647	4.568	∞
HF/6-31+G(d)	∞	3.950	2.944	1.187	1.371	1.456	1.456	1.540	6.403	∞
B3LYP/6-31G(d)	∞	3.518	2.571	2.412	1.383	1.468	1.468	1.841	4.421	∞
B3LYP/6-31+G(d)	∞	3.553	2.585	1.840	1.393	1.467	1.467	1.832	4.890	∞
B3LYP/6-31G(d,p)	∞	3.504	2.575	1.844	1.383	1.468	1.468	1.841	3.456	∞

Level of Theory	N_8-N_7 Distance (Å)					N_7-N_6 Distance (Å)				
	SR	RC	TS	PC	SP	SR	RC	TS	PC	SP
HF/6-31G(d)	1.214	1.230	1.095	1.078	1.078	1.357	1.341	2.295	3.586	∞
HF/6-31+G(d)	1.214	1.232	1.090	1.078	1.079	1.359	1.336	2.325	4.205	∞
B3LYP/6-31G(d)	1.252	1.253	1.143	1.107	1.106	1.368	1.377	2.297	3.558	∞
B3LYP/6-31+G(d)	1.252	1.255	1.142	1.105	1.105	1.368	1.376	2.324	3.880	∞
B3LYP/6-31G(d,p)	1.252	1.253	1.143	1.107	1.106	1.367	1.376	2.308	3.559	∞

Table S8-58: Bond length comparison during the (E)-MTIC_T (t,t,c) + Cl^- S_N2 pathway

Level of Theory	C-X Distance (Å)					C-N_8 Distance (Å)				
	SR	RC	TS	PC	SP	SR	RC	TS	PC	SP
HF/6-31G(d)	∞	5.425	2.773	1.816	1.365	1.457	1.447	1.647	4.568	∞
HF/6-31+G(d)	∞	5.484	2.944	1.187	1.371	1.456	1.448	1.540	6.403	∞
B3LYP/6-31G(d)	∞	5.323	2.571	2.412	1.383	1.468	1.458	1.841	4.421	∞
B3LYP/6-31+G(d)	∞	5.402	2.585	1.840	1.393	1.467	1.458	1.832	4.890	∞
B3LYP/6-31G(d,p)	∞	5.308	2.575	1.844	1.383	1.468	1.458	1.841	3.456	∞

Level of Theory	N_8-N_7 Distance (Å)					N_7-N_6 Distance (Å)				
	SR	RC	TS	PC	SP	SR	RC	TS	PC	SP
HF/6-31G(d)	1.214	1.214	1.095	1.078	1.078	1.357	1.344	2.295	3.586	∞
HF/6-31+G(d)	1.214	1.213	1.090	1.078	1.079	1.359	1.345	2.325	4.205	∞
B3LYP/6-31G(d)	1.252	1.258	1.143	1.107	1.106	1.368	1.349	2.297	3.558	∞
B3LYP/6-31+G(d)	1.252	1.255	1.142	1.105	1.105	1.368	1.348	2.324	3.880	∞
B3LYP/6-31G(d,p)	1.252	1.259	1.143	1.107	1.106	1.367	1.349	2.308	3.559	∞

Table S8-59: Bond length comparison during the (E)-MTIC_T (t,c,t) + Cl^- S_N2 pathway

Level of Theory	C-X Distance (Å)					C-N_8 Distance (Å)				
	SR	RC	TS	PC	SP	SR	RC	TS	PC	SP
HF/6-31G(d)	∞	5.311	2.771	1.819	1.365	1.457	1.447	1.657	4.652	∞
HF/6-31+G(d)	∞	5.365	2.973	1.818	1.371	1.456	1.448	1.533	6.055	∞
B3LYP/6-31G(d)	∞	5.514	2.558	1.848	1.383	1.468	1.459	1.847	4.505	∞
B3LYP/6-31+G(d)	∞	5.623	2.576	1.843	1.393	1.468	1.461	1.834	5.639	∞
B3LYP/6-31G(d,p)	∞	5.492	2.562	1.848	1.383	1.468	1.459	1.847	4.991	∞

Level of Theory	N_8-N_7 Distance (Å)					N_7-N_6 Distance (Å)				
	SR	RC	TS	PC	SP	SR	RC	TS	PC	SP
HF/6-31G(d)	1.217	1.247	1.093	1.078	1.078	1.343	1.447	2.324	3.585	∞
HF/6-31+G(d)	1.217	1.246	1.086	1.078	1.079	1.345	1.448	2.391	4.234	∞
B3LYP/6-31G(d)	1.253	1.273	1.141	1.117	1.106	1.362	1.459	2.299	3.548	∞
B3LYP/6-31+G(d)	1.253	1.268	1.139	1.106	1.105	1.363	1.461	2.338	3.381	∞
B3LYP/6-31G(d,p)	1.253	1.274	1.141	1.108	1.106	1.363	1.459	2.309	2.964	∞

Table S8-60: Bond length comparison during the (E)-MTIC_T (t,t,t) + Cl^- S_N2 pathway

Level of Theory	C-X Distance (Å)					C-N_8 Distance (Å)				
	SR	RC	TS	PC	SP	SR	RC	TS	PC	SP
HF/6-31G(d)	∞	6.040	2.773	1.816	1.365	1.457	1.450	1.647	4.568	∞
HF/6-31+G(d)	∞	6.289	2.944	1.187	1.371	1.456	1.450	1.540	6.403	∞
B3LYP/6-31G(d)	∞	5.782	2.571	2.412	1.383	1.468	1.459	1.841	4.421	∞
B3LYP/6-31+G(d)	∞	5.844	2.585	1.840	1.393	1.467	1.461	1.832	4.890	∞
B3LYP/6-31G(d,p)	∞	5.758	2.575	1.844	1.383	1.468	1.459	1.841	3.456	∞

Level of Theory	N_8-N_7 Distance (Å)					N_7-N_6 Distance (Å)				
	SR	RC	TS	PC	SP	SR	RC	TS	PC	SP
HF/6-31G(d)	1.214	1.224	1.095	1.078	1.078	1.357	1.323	2.295	3.586	∞
HF/6-31+G(d)	1.214	1.215	1.090	1.078	1.079	1.359	1.343	2.325	4.205	∞
B3LYP/6-31G(d)	1.252	1.271	1.143	1.107	1.106	1.368	1.334	2.297	3.558	∞
B3LYP/6-31+G(d)	1.252	1.267	1.142	1.105	1.105	1.368	1.334	2.324	3.880	∞
B3LYP/6-31G(d,p)	1.252	1.272	1.143	1.107	1.106	1.367	1.333	2.308	3.559	∞

Table S8-61: Bond length comparison during the (Z)-MTIC_T (t,c,c) + Br^- S_N2 pathway

Level of Theory	C-X Distance (Å)					C-N_8 Distance (Å)				
	SR	RC	TS	PC	SP	SR	RC	TS	PC	SP
HF/6-31G(d)	∞	4.150	2.895	1.988	1.948	1.457	1.457	1.662	4.643	∞
HF/6-31+G(d)	∞	4.237	3.115	1.965	1.946	1.456	1.457	1.534	6.745	∞
B3LYP/6-31G(d)	∞	4.031	2.696	2.023	1.966	1.468	1.475	1.835	4.382	∞
B3LYP/6-31+G(d)	∞	4.045	2.714	1.983	1.965	1.468	1.474	1.840	5.864	∞
B3LYP/6-31G(d,p)	∞	4.032	2.698	2.022	1.963	1.468	1.475	1.831	4.422	∞

Level of Theory	N_8-N_7 Distance (Å)					N_7-N_6 Distance (Å)				
	SR	RC	TS	PC	SP	SR	RC	TS	PC	SP
HF/6-31G(d)	1.217	1.231	1.094	1.078	1.078	1.343	1.338	2.314	3.581	∞
HF/6-31+G(d)	1.217	1.233	1.084	1.078	1.079	1.345	1.335	2.443	3.580	∞
B3LYP/6-31G(d)	1.253	1.260	1.141	1.107	1.106	1.362	1.380	2.302	3.563	∞
B3LYP/6-31+G(d)	1.253	1.260	1.139	1.105	1.105	1.363	1.376	2.347	3.580	∞
B3LYP/6-31G(d,p)	1.253	1.260	1.141	1.107	1.106	1.363	1.379	2.311	3.559	∞

Table S8-62: Bond length comparison during the (E)-MTIC_T (t,c,c) + Br^- S_N2 pathway

Level of Theory	C-X Distance (Å)					C-N_8 Distance (Å)				
	SR	RC	TS	PC	SP	SR	RC	TS	PC	SP
HF/6-31G(d)	∞	6.077	2.895	1.988	1.948	1.449	1.449	1.662	4.643	∞
HF/6-31+G(d)	∞	6.213	3.115	1.965	1.946	1.450	1.449	1.534	6.745	∞
B3LYP/6-31G(d)	∞	6.065	2.696	2.023	1.966	1.459	1.460	1.835	4.382	∞
B3LYP/6-31+G(d)	∞	6.171	2.714	1.983	1.965	1.453	1.460	1.840	5.864	∞
B3LYP/6-31G(d,p)	∞	6.088	2.698	2.022	1.963	1.459	1.460	1.831	4.422	∞

Level of Theory	N_8-N_7 Distance (Å)					N_7-N_6 Distance (Å)				
	SR	RC	TS	PC	SP	SR	RC	TS	PC	SP
HF/6-31G(d)	1.213	1.213	1.094	1.078	1.078	1.338	1.346	2.314	3.581	∞
HF/6-31+G(d)	1.211	1.211	1.084	1.078	1.079	1.341	1.350	2.443	3.580	∞
B3LYP/6-31G(d)	1.254	1.257	1.141	1.107	1.106	1.348	1.347	2.302	3.563	∞
B3LYP/6-31+G(d)	1.251	1.253	1.139	1.105	1.105	1.348	1.347	2.347	3.580	∞
B3LYP/6-31G(d,p)	1.254	1.258	1.141	1.107	1.106	1.349	1.346	2.311	3.559	∞

Table S8-63: Bond length comparison during the (Z)-MTIC_T (t,t,c) + Br^- S_N2 pathway

Level of Theory	C-X Distance (Å)					C-N_8 Distance (Å)				
	SR	RC	TS	PC	SP	SR	RC	TS	PC	SP
HF/6-31G(d)	∞	3.759	2.895	1.985	1.948	1.457	1.458	1.662	4.554	∞
HF/6-31+G(d)	∞	3.815	3.115	1.974	1.946	1.456	1.458	1.534	5.955	∞
B3LYP/6-31G(d)	∞	3.641	2.696	2.016	1.966	1.468	1.468	1.835	4.318	∞
B3LYP/6-31+G(d)	∞	3.702	2.714	1.995	1.965	1.467	1.469	1.840	4.673	∞
B3LYP/6-31G(d,p)	∞	3.624	2.698	2.015	1.963	1.468	1.468	1.831	4.356	∞

Level of Theory	N_8-N_7 Distance (Å)					N_7-N_6 Distance (Å)				
	SR	RC	TS	PC	SP	SR	RC	TS	PC	SP
HF/6-31G(d)	1.214	1.215	1.094	1.078	1.078	1.357	1.365	2.314	3.597	∞
HF/6-31+G(d)	1.214	1.215	1.084	1.078	1.079	1.359	1.368	2.443	4.082	∞
B3LYP/6-31G(d)	1.252	1.252	1.141	1.107	1.106	1.368	1.379	2.302	3.572	∞
B3LYP/6-31+G(d)	1.252	1.252	1.139	1.105	1.105	1.368	1.379	2.347	3.843	∞
B3LYP/6-31G(d,p)	1.252	1.253	1.141	1.107	1.106	1.367	1.379	2.311	3.576	∞

Table S8-64: Bond length comparison during the (E)-MTIC_T (t,t,c) + Br^- S_N2 pathway

Level of Theory	C-X Distance (Å)					C-N_8 Distance (Å)				
	SR	RC	TS	PC	SP	SR	RC	TS	PC	SP
HF/6-31G(d)	∞	5.580	2.895	1.985	1.948	1.450	1.447	1.662	4.554	∞
HF/6-31+G(d)	∞	5.434	3.115	1.974	1.946	1.451	1.447	1.534	5.955	∞
B3LYP/6-31G(d)	∞	5.435	2.696	2.016	1.966	1.459	1.458	1.835	4.318	∞
B3LYP/6-31+G(d)	∞	5.591	2.714	1.995	1.965	1.459	1.458	1.840	4.673	∞
B3LYP/6-31G(d,p)	∞	5.382	2.698	2.015	1.963	1.459	1.458	1.831	4.356	∞

Level of Theory	N_8-N_7 Distance (Å)					N_7-N_6 Distance (Å)				
	SR	RC	TS	PC	SP	SR	RC	TS	PC	SP
HF/6-31G(d)	1.231	1.215	1.094	1.078	1.078	1.384	1.345	2.314	3.597	∞
HF/6-31+G(d)	1.211	1.212	1.084	1.078	1.079	1.353	1.350	2.443	4.082	∞
B3LYP/6-31G(d)	1.253	1.258	1.141	1.107	1.106	1.353	1.350	2.302	3.572	∞
B3LYP/6-31+G(d)	1.251	1.255	1.139	1.105	1.105	1.352	1.349	2.347	3.843	∞
B3LYP/6-31G(d,p)	1.253	1.258	1.141	1.107	1.106	1.353	1.350	2.311	3.576	∞

Table S8-65: Bond length comparison during the (E)-MTIC_T (t,c,t) + Br^- S_N2 pathway

Level of Theory	C-X Distance (Å)					C-N_8 Distance (Å)				
	SR	RC	TS	PC	SP	SR	RC	TS	PC	SP
HF/6-31G(d)	∞	5.604	2.895	1.988	1.948	1.449	1.450	1.662	4.643	∞
HF/6-31+G(d)	∞	6.383	3.115	1.965	1.946	1.450	1.448	1.534	6.745	∞
B3LYP/6-31G(d)	∞	5.622	2.696	2.023	1.966	1.459	1.459	1.835	4.382	∞
B3LYP/6-31+G(d)	∞	6.041	2.714	1.983	1.965	1.458	1.491	1.840	5.864	∞
B3LYP/6-31G(d,p)	∞	5.590	2.698	2.022	1.963	1.459	1.459	1.831	4.422	∞

Level of Theory	N_8-N_7 Distance (Å)					N_7-N_6 Distance (Å)				
	SR	RC	TS	PC	SP	SR	RC	TS	PC	SP
HF/6-31G(d)	1.213	1.223	1.094	1.078	1.078	1.380	1.326	2.314	3.581	∞
HF/6-31+G(d)	1.211	1.208	1.084	1.078	1.079	1.338	1.360	2.443	3.580	∞
B3LYP/6-31G(d)	1.254	1.271	1.141	1.107	1.106	1.349	1.334	2.302	3.563	∞
B3LYP/6-31+G(d)	1.251	1.266	1.139	1.105	1.105	1.348	1.335	2.347	3.580	∞
B3LYP/6-31G(d,p)	1.254	1.273	1.141	1.107	1.106	1.349	1.333	2.311	3.559	∞

Table S8-66: Bond length comparison during the (E)-MTIC_T (t,t,t) + Br^- S_N2 pathway

Level of Theory	C-X Distance (Å)					C-N_8 Distance (Å)				
	SR	RC	TS	PC	SP	SR	RC	TS	PC	SP
HF/6-31G(d)	∞	6.263	2.895	1.985	1.948	1.452	1.450	1.662	4.554	∞
HF/6-31+G(d)	∞	6.474	3.115	1.974	1.946	1.453	1.450	1.534	5.955	∞
B3LYP/6-31G(d)	∞	5.905	2.696	2.016	1.966	1.460	1.459	1.835	4.318	∞
B3LYP/6-31+G(d)	∞	6.044	2.714	1.995	1.965	1.462	1.461	1.840	4.673	∞
B3LYP/6-31G(d,p)	∞	5.839	2.698	2.015	1.963	1.461	1.459	1.831	4.356	∞

Level of Theory	N_8-N_7 Distance (Å)					N_7-N_6 Distance (Å)				
	SR	RC	TS	PC	SP	SR	RC	TS	PC	SP
HF/6-31G(d)	1.216	1.223	1.094	1.078	1.078	1.340	1.324	2.314	3.597	∞
HF/6-31+G(d)	1.214	1.214	1.084	1.078	1.079	1.341	1.342	2.443	4.082	∞
B3LYP/6-31G(d)	1.261	1.270	1.141	1.107	1.106	1.347	1.335	2.302	3.572	∞
B3LYP/6-31+G(d)	1.258	1.266	1.139	1.105	1.105	1.346	1.335	2.347	3.843	∞
B3LYP/6-31G(d,p)	1.261	1.271	1.141	1.107	1.106	1.347	1.334	2.311	3.576	∞

APPENDIX I: ABSOLUTE ENERGIES

CONFIGURATIONS & TAUTOMERS

Level of Theory	(E)-TI (t)	(E)-TI (c)	(Z)-TI (t)	(Z)-TI (c)	(E)-MTI (t,c)	(E)-MTI (t,t)
HF/STO-3G	-388.79210	-388.78867	-388.77284	-388.77849	-422.31824	-422.31940
HF/3-21G	-388.81017	-388.80668	-388.78268	-388.79434	-425.28652	-425.28486
HF/6-31G(d)	-388.81560	-388.81245	-388.79400	-388.79993	-427.70918	-427.70902
HF/6-31+G(d)	-388.81564	-388.81250	-388.79404	-388.79990	-427.72312	-427.72280
MP2/6-31G(d)	-390.28309	-390.27987	-390.26679	-390.27388	-429.03413	-429.03250
MP2/6-31+G(d)	-390.28303	-390.27981	-390.26659	-390.27371	-429.06534	-429.06351
B3LYP/6-31G(d)	-391.16100	-391.15822	-391.14237	-391.14895	-430.33032	-430.32990
B3LYP/6-31+G(d)	-391.16117	-391.15839	-391.14242	-391.14901	-430.35151	-430.35069
B3LYP/6-31G(d,p)	-391.16110	-391.15833	-391.14246	-391.14905	-430.34429	-430.34373

Level of Theory	(E)-MTI (c,c)	(E)-MTI (c,t)	(Z)-MTI (c,t)	(Z)-MTI (t,c)	(Z)-MTI (c,c)	(Z)-MTI (t,t)
HF/STO-3G	-422.31774	-422.31893	-422.30614	-422.30276	-422.30172	-422.30373
HF/3-21G	-425.28534	-425.28362	-425.27168	-425.26925	-425.26621	-425.26918
HF/6-31G(d)	-427.70679	-427.70660	-427.69446	-427.68526	-427.68380	-427.68894
HF/6-31+G(d)	-427.72049	-427.72004	-427.70667	-427.69726	-427.69594	-427.70110
MP2/6-31G(d)	-429.03132	-429.02978	-429.02395	-429.01430	-429.01299	-429.01709
MP2/6-31+G(d)	-429.06247	-429.06064	-429.05324	-429.04349	-429.04258	-429.04646
B3LYP/6-31G(d)	-430.32789	-430.32758	-430.31924	-430.30823	-430.30671	-430.31254
B3LYP/6-31+G(d)	-430.34897	-430.34825	-430.33809	-430.32669	-430.32610	-430.33108
B3LYP/6-31G(d,p)	-430.34184	-430.34141	-430.33315	-430.32196	-430.32059	-430.32629

Level of Theory	(E)-DTI (t)	(E)-DTI (c)	(Z)-DTI (t)	(Z)-DTI (c)	(E)-TIC (t,c)	(E)-TIC (t,t)
HF/STO-3G	-626.46566	-626.46261	-626.44744	-626.44620	-549.30478	-549.30166
HF/3-21G	-630.95916	-630.95202	-630.93724	-630.93385	-553.32756	-553.32062
HF/6-31G(d)	-634.53163	-634.52487	-634.50172	-634.49917	-556.46918	-556.46244
HF/6-31+G(d)	-634.55017	-634.54342	-634.51864	-634.51625	-556.48817	-556.48137
MP2/6-31G(d)	-636.45222	-636.44758	-636.42796	-636.42709	-558.12274	-558.11811
MP2/6-31+G(d)	-636.49801	-636.49322	-636.47253	-636.47130	-558.16631	-558.16123
B3LYP/6-31G(d)	-638.35148	-638.34673	-638.31803	-638.32214	-559.72508	-559.72085
B3LYP/6-31+G(d)	-638.38144	-638.37642	-638.35001	-638.34975	-559.75536	-559.75072
B3LYP/6-31G(d,p)	-638.37144	-638.36664	-638.34254	-638.34208	-559.74334	-559.73910

Level of Theory	(E)-TIC (c,c)	(E)-TIC (c,t)	(Z)-TIC (t,t)	(Z)-TIC (t,c)	(Z)-TIC (c,c)	(Z)-TIC (c,t)
HF/STO-3G	-549.30160	-549.29702	-549.28679	-549.28897	-549.30023	-549.28241
HF/3-21G	-553.32531	-553.31350	-553.30320	-553.30695	-553.32645	-553.29865
HF/6-31G(d)	-556.46686	-556.45454	-556.44354	-556.43943	-556.46006	-556.44288
HF/6-31+G(d)	-556.48378	-556.47324	-556.46118	-556.45733	-556.47721	-556.45638
MP2/6-31G(d)	-558.11724	-558.11219	-558.10493	-558.10691	-558.11984	-558.10341
MP2/6-31+G(d)	-558.16184	-558.15541	-558.14630	-558.14902	-558.16108	-558.14270
B3LYP/6-31G(d)	-559.72009	-559.71546	-559.70551	-559.70662	-559.72323	-559.70159
B3LYP/6-31+G(d)	-559.75180	-559.74501	-559.73332	-559.73484	-559.75040	-559.72785
B3LYP/6-31G(d,p)	-559.73843	-559.73371	-559.72350	-559.72465	-559.74177	-559.72007

Level of Theory	(E)-MTIC (t,c,c)	(E)-MTIC (t,t,c)	(E)-MTIC (t,c,t)	(E)-MTIC (t,t,t)	(E)-MTIC (c,c,c)	(E)-MTIC (c,t,c)
HF/STO-3G	-587.88497	-587.88600	-587.88190	-587.88295	-587.88296	-587.88199
HF/3-21G	-592.14445	-592.14192	-592.13726	-592.13521	-592.14030	-592.14161
HF/6-31G(d)	-595.50108	-595.50027	-595.49433	-595.49375	-595.49828	-595.49867
HF/6-31+G(d)	-595.52007	-595.51885	-595.51329	-595.51232	-595.51721	-595.51786
MP2/6-31G(d)	-597.28740	-597.28501	-597.28271	-597.28062	-597.28154	-597.28336
MP2/6-31+G(d)	-597.33220	-597.32923	-597.32721	-597.32451	-597.32693	-597.32928
B3LYP/6-31G(d)	-599.03876	-599.03774	-599.03413	-599.03361	-599.03441	-599.03475
B3LYP/6-31+G(d)	-599.06940	-599.06765	-599.06439	-599.06319	-599.06464	-599.06548
B3LYP/6-31G(d,p)	-599.05796	-599.05680	-599.05330	-599.05265	-599.05342	-599.05384

Level of Theory	(E)-MTIC (c,c,t)	(E)-MTIC (c,t,t)	(Z)-MTIC (t,t,c)	(Z)-MTIC (t,c,c)	(Z)-MTIC (t,t,t)	(Z)-MTIC (t,c,t)
HF/STO-3G	-587.87600	-587.87492	-587.86712	-587.86745	-587.86679	-587.86604
HF/3-21G	-592.12807	-592.13013	-592.12106	-592.12093	-592.11753	-592.11739
HF/6-31G(d)	-595.48582	-595.48604	-595.47218	-595.47145	-595.47410	-595.46859
HF/6-31+G(d)	-595.50416	-595.50468	-595.48865	-595.48865	-595.49206	-595.48573
MP2/6-31G(d)	-597.27482	-597.27640	-597.26395	-597.26395	-597.26626	-597.26280
MP2/6-31+G(d)	-597.31893	-597.32069	-597.30906	-597.30906	-597.30891	-597.30525
B3LYP/6-31G(d)	-599.02799	-599.02862	-599.01159	-599.01159	-599.01659	-599.01100
B3LYP/6-31+G(d)	-599.05726	-599.05809	-599.03923	-599.03923	-599.04438	-599.03861
B3LYP/6-31G(d,p)	-599.04702	-599.04778	-599.03053	-599.03053	-599.03554	-599.02993

Level of Theory	(Z)-MTIC (c,t,c)	(Z)-MTIC (c,t,t)	(Z)-MTIC (c,c,c)	(Z)-MTIC (c,c,t)	(E)-DTIC (t,c)	(E)-DTIC (t,t)
HF/STO-3G	-587.88085	-587.86331	-	-	-626.46566	-626.46261
HF/3-21G	-592.14084	-592.11374	-	-	-630.95916	-630.95202
HF/6-31G(d)	-595.49044	-595.47459	-595.47211	-595.46165	-634.53163	-634.52487
HF/6-31+G(d)	-595.50754	-595.49206	-595.49018	-595.47965	-634.55017	-634.54342
MP2/6-31G(d)	-597.28215	-597.26695	-597.26688	-597.25799	-636.45222	-636.44758
MP2/6-31+G(d)	-597.32479	-597.31080	-597.31235	-597.30322	-636.49801	-636.49322
B3LYP/6-31G(d)	-599.03530	-599.01570	-599.01590	-599.00517	-638.35148	-638.34673
B3LYP/6-31+G(d)	-599.06237	-599.04384	-599.04527	-599.03432	-638.38144	-638.37642
B3LYP/6-31G(d,p)	-599.05473	-599.03471	-599.03511	-599.02419	-638.37144	-638.36664

Level of Theory	(E)-DTIC (c,c)	(E)-DTIC (c,t)	(Z)-DTIC (t,c)	(Z)-DTIC (t,t)	(Z)-DTIC (c,c)	(Z)-DTIC (c,t)
HF/STO-3G	-626.46267	-626.45788	-626.44744	-626.44620	-626.44455	-626.43979
HF/3-21G	-630.95715	-630.94469	-630.93724	-630.93385	-630.93198	-
HF/6-31G(d)	-634.52948	-634.51662	-634.50172	-634.49917	-634.49890	-634.49133
HF/6-31+G(d)	-634.54829	-634.53473	-634.51864	-634.51625	-634.51648	-634.50912
MP2/6-31G(d)	-636.44842	-636.44145	-636.42796	-636.42709	-636.43316	-636.41867
MP2/6-31+G(d)	-636.49554	-636.48695	-636.47253	-636.47130	-636.47980	-
B3LYP/6-31G(d)	-638.34446	-638.34090	-638.31803	-638.32214	-638.32891	-638.31677
B3LYP/6-31+G(d)	-638.37800	-638.36986	-638.35001	-638.34975	-638.35760	-638.34533
B3LYP/6-31G(d,p)	-638.36772	-638.36078	-638.34254	-638.34208	-638.34889	-638.33654

Level of Theory	(Z)-MTI_T (t,c)	(E)-MTI_T (t,c)	(E)-MTI_T (t,t)
HF/STO-3G	-422.30613	-422.31740	-422.31591
HF/3-21G	-425.27081	-425.2834498	-425.28355
HF/6-31G(d)	-427.68912	-427.7032117	-427.70207
HF/6-31+G(d)	-427.70166	-427.7188477	-427.71685
MP2/6-31G(d)	-429.01555	-429.0250201	-429.028201
MP2/6-31+G(d)	-429.04460	-429.0570805	-429.05872
B3LYP/6-31G(d)	-430.31230	-430.3227522	-430.32492
B3LYP/6-31+G(d)	-430.33124	-430.343486	-430.34508
B3LYP/6-31G(d,p)	-430.32669	-430.3369344	-430.33921

Level of Theory	(Z)-MTI_T (c,t)	(Z)-MTIC_T (t,c,c)	(E)-MTIC_T (t,c,c)	(Z)-MTIC_T (t,t,c)	(E)-MTIC_T (t,t,c)	(E)-MTIC_T (t,c,t)
HF/STO-3G	-422.30088	-587.88197	-587.89083	-587.87485	-587.88470	-587.89023
HF/3-21G	-425.262995	-592.15157	-592.15943	-592.12005	-592.13190	-592.16195
HF/6-31G(d)	-427.68150	-595.49996	-595.51104	-595.47764	-595.49150	-595.51131
HF/6-31+G(d)	-427.69393	-595.51716	-595.52964	-595.49445	-595.50978	-595.52959
MP2/6-31G(d)	-429.00924	-597.28527	-597.29129	-597.26611	-597.27436	-597.29697
MP2/6-31+G(d)	-429.03975	-597.32770	-597.33537	-597.30839	-597.31846	-597.34007
B3LYP/6-31G(d)	-430.30146	-599.03818	-599.04548	-599.01654	-599.02624	-599.04975
B3LYP/6-31+G(d)	-430.32109	-599.06632	-599.07539	-599.04402	-599.05562	-599.07876
B3LYP/6-31G(d,p)	-430.31536	-599.05786	-599.06497	-599.03572	-599.04527	-599.06935

Level of Theory	(E)-MTIC_T (t,t,t)	TEMO (t)	TEMO (c)	MITO (t,a)	MITO (t,ag)	MITO (t,sg)
HF/STO-3G	-587.88361	-697.98479	-697.98612	-1190.56348	-1190.56450	-1190.56372
HF/3-21G	-592.13232	-703.09404	-703.09905	-1198.63136	-1198.63137	-1198.63193
HF/6-31G(d)	-595.48962	-707.08381	-707.08784	-1205.02010	-1205.01916	-1205.01982
HF/6-31+G(d)	-595.50754	-707.10127	-707.10511	-1205.03821	-1205.03718	-1205.03787
MP2/6-31G(d)	-597.27806	-709.16700	-709.16905	-1207.36292	-1207.36300	-1207.36326
MP2/6-31+G(d)	-597.32144	-709.21180	-709.21380	-	-	-
B3LYP/6-31G(d)	-599.02884	-711.17627	-711.17855	-1210.08433	-1210.08372	-1210.08422
B3LYP/6-31+G(d)	-599.05741	-711.20534	-711.20752	-1210.11481	-1210.11417	-1210.11459
B3LYP/6-31G(d,p)	-599.04798	-711.18867	-711.19098	-1210.09799	-1210.09748	-1210.09795

Level of Theory	MITO (c,a)	MITO (c,ag)	MITO (c,sg)
HF/STO-3G	-1190.56505	-1190.56613	-1190.56484
HF/3-21G	-1198.63689	-1198.63716	-1198.63677
HF/6-31G(d)	-1205.02454	-1205.02380	-1205.02359
HF/6-31+G(d)	-1205.04247	-1205.04160	-1205.04144
MP2/6-31G(d)	-1207.36528	-1207.36543	-1207.36514
MP2/6-31+G(d)	-	-	-
B3LYP/6-31G(d)	-1210.08690	-1210.08639	-1210.08634
B3LYP/6-31+G(d)	-1210.11728	-1210.11670	-1210.11658
B3LYP/6-31G(d,p)	-1210.10059	-1210.10018	-1210.10011

TAUTOMERIZATION REACTION PATHWAYS

Level of Theory	(E)-MTI (t,t) TS	(E)-MTI (c,t) TS	(E)-MTI (t,t) TS H_2O	(E)-MTI (c,t) TS H_2O	(E)-MTIC (t,t,c) TS	(E)-MTIC (t,t,t) TS
HF/STO-3G	-422.22788	-422.22814	-497.27396	-497.27205	-587.79831	-587.79252
HF/3-21G	-425.20102	-425.20059	-500.86384	-500.86168	-592.06596	-592.04854
HF/6-31G(d)	-427.61445	-427.61493	-503.66972	-503.66958	-595.41308	-595.39976
HF/6-31+G(d)	-427.62633	-427.62706	-503.69098	-503.69151	-595.43047	-595.41701
MP2/6-31G(d)	-428.96859	-428.96795	-505.21255	-505.20927	-597.22464	-597.21491
MP2/6-31+G(d)	-428.99787	-428.99746	-505.25193	-505.25031	-597.26770	-597.25810
B3LYP/6-31G(d)	-430.26290	-430.26208	-506.72663	-506.72363	-598.97559	-598.96403
B3LYP/6-31+G(d)	-430.28122	-430.28053	-506.75403	-506.72363	-599.00374	-598.99196
B3LYP/6-31G(d,p)	-430.27945	-430.27849	-506.75431	-506.75102	-598.99740	-598.98561

Level of Theory	(E)-MTIC (c,c,c) TS	(E)-MTIC (c,c,t) TS	E)-MTIC (t,t,c) TS H_2O	(E)-MTIC (t,t,t) TS H_2O	(E)-MTIC (c,c,c) TS H_2O	(E)-MTIC (c,c,t) TS H_2O
HF/STO-3G	-587.79676	-587.78848	-662.84818	-662.84122	-	-
HF/3-21G	-592.06362	-592.04558	-667.73532	-667.71257	-667.72353	-667.70572
HF/6-31G(d)	-595.41135	-595.39687	-671.47372	-671.45458	-671.46498	-671.44979
HF/6-31+G(d)	-595.42884	-595.41395	-671.49704	-671.47946	-671.49187	-671.47608
MP2/6-31G(d)	-597.22219	-597.21327	-673.47458	-673.46068	-673.47458	-673.45601
MP2/6-31+G(d)	-597.26616	-597.25632	-673.52707	-673.51290	-673.52707	-673.51000
B3LYP/6-31G(d)	-598.97150	-598.96203	-675.44281	-675.42843	-675.43330	-675.42347
B3LYP/6-31+G(d)	-598.99941	-598.98919	-675.47813	-675.46389	-675.47079	-675.45971
B3LYP/6-31G(d,p)	-598.99306	-598.98362	-675.47621	-675.46138	-675.46583	-675.45625

Level of Theory	(E)-MTIC (t,t,c) H_2O	(E)-MTIC (t,t,t) H_2O	(E)-MTIC (c,c,c) H_2O	(E)-MTIC (c,c,t) H_2O	(E)-MTIC (t,c,c) H_2O	(E)-MTIC (t,t,c) H_2O
HF/STO-3G	-662.87117	-662.8644	-662.86172	-662.85634	-662.88283	-662.86882
HF/3-21G	-667.76614	-667.74357	-667.75208	-667.73692	-667.77728	-667.74396
HF/6-31G(d)	-671.53106	-671.51567	-671.52070	-671.50703	-671.53503	-671.51232
HF/6-31+G(d)	-671.55584	-671.53954	-671.54482	-671.53086	-671.55868	-671.53541
MP2/6-31G(d)	-673.50845	-673.49575	-673.49730	-673.48868	-673.50778	-673.48986
MP2/6-31+G(d)	-673.56416	-673.55096	-673.55767	-673.54376	-673.56233	-673.54377
B3LYP/6-31G(d)	-675.47335	-675.45972	-675.46266	-675.45391	-675.47483	-675.45429
B3LYP/6-31+G(d)	-675.51290	-675.49779	-675.50127	-675.49151	-675.51275	-675.4914
B3LYP/6-31G(d,p)	-675.50294	-675.48934	-675.49106	-675.48372	-675.50497	-675.48413

Level of Theory	(E)-MTI (t,t) H_2O	(E)-MTI (c,t) H_2O	(E)-MTI (t,c) H_2O	(Z)-MTI (c,t) H_2O
HF/STO-3G	-497.29851	-497.296326	-497.29773	-497.29757
HF/3-21G	-500.89587	-500.893206	-500.894849	-500.894849
HF/6-31G(d)	-503.73068	-503.726845	-503.725959	-503.725649
HF/6-31+G(d)	-503.749584	-503.745443	-503.745185	-503.745108
MP2/6-31G(d)	-505.247804	-505.243522	-505.241684	-505.239849
MP2/6-31+G(d)	-505.288922	-505.284795	-505.282305	-505.282071
B3LYP/6-31G(d)	-506.757786	-506.754275	-506.752151	-506.752151
B3LYP/6-31+G(d)	-506.786855	-506.78316	-506.780804	-506.780804
B3LYP/6-31G(d,p)	-506.782362	-506.778918	-506.776997	-506.776997

S_N2 REACTION PATHWAYS – FLUORIDE

Level of Theory	RC (E)-MTI (t,c) F^-	RC (E)-MTI (t,t) F^-	RC (E)-MTI (c,c) F^-	RC (E)-MTI (c,t) F^-	RC (Z)-MTI (c,t) F^-	RC (Z)-MTI (t,c) F^-
HF/6-31G(d)	-527.16313	-527.15654	-527.15909	-527.15593	-527.14516	-527.15939
HF/6-31+G(d)	-527.20091	-527.19448	-527.19685	-527.19430	-527.18014	-527.20016
MP2/6-31G(d)	-528.68793	-528.67896	-528.68146	-528.67546	-528.67271	-528.69342
MP2/6-31+G(d)	-528.76042	-528.75111	-528.75410	-528.74851	-528.74118	-528.74118
B3LYP/6-31G(d)	-530.21789	-530.21131	-530.21263	-530.20852	-530.20351	-530.22354
B3LYP/6-31+G(d)	-530.28235	-530.27482	-530.27691	-530.27305	-530.26049	-530.28307
B3LYP/6-31G(d,p)	-530.23544	-530.22882	-530.23008	-530.22596	-530.22114	-530.24067

Level of Theory	RC (Z)-MTI (c,c) F^-	RC (Z)-MTI (t,t) F^-	(E)-MTI (t,c) F^- TS	(E)-MTI (t,t) F^- TS	(E)-MTI (c,c) F^- TS	(E)-MTI (c,t) F^- TS
HF/6-31G(d)	-527.12434	-527.16583	-527.06456	-527.07088	-527.06478	-527.06714
HF/6-31+G(d)	-527.16111	-527.19957	-527.11789	-527.12233	-527.11806	-527.11889
MP2/6-31G(d)	-528.65699	-528.69342	-528.58412	-528.59006	-528.58207	-528.58397
MP2/6-31+G(d)	-528.76055	-528.76055	-528.67465	-528.67885	-528.67266	-528.67330
B3LYP/6-31G(d)	-530.18628	-530.22354	-530.12592	-530.13201	-530.12448	-530.12697
B3LYP/6-31+G(d)	-530.28307	-530.28307	-530.20532	-530.20993	-530.20409	-530.20549
B3LYP/6-31G(d,p)	-530.20380	-530.24067	-530.14094	-530.14695	-530.13940	-530.14185

Level of Theory	(Z)-MTI (c,t) F^- TS	(Z)-MTI (t,c) F^- TS	(Z)-MTI (c,c) F^- TS	(Z)-MTI (t,t) F^- TS	PC (E)-MTI (t,c) F^-	PC (E)-MTI (t,t) F^-
HF/6-31G(d)	-527.05317	-527.05153	-527.04508	-527.05046	-527.13495	-527.13898
HF/6-31+G(d)	-527.10358	-527.10364	-527.09842	-527.10130	-527.17148	-527.17386
MP2/6-31G(d)	-528.66376	-528.57762	-528.57012	-528.57608	-528.64434	-528.64908
MP2/6-31+G(d)	-528.66376	-528.66909	-528.66246	-528.66135	-528.71227	-528.71527
B3LYP/6-31G(d)	-530.11636	-530.11675	-530.10960	-530.11278	-530.18398	-530.18860
B3LYP/6-31+G(d)	-530.19297	-530.19522	-530.18895	-530.18918	-530.24022	-530.24308
B3LYP/6-31G(d,p)	-530.13132	-530.13185	-530.12463	-530.12770	-530.19868	-530.20304

Level of Theory	PC (E)-MTI (c,c) F^-	PC (E)-MTI (c,t) F^-	PC (Z)-MTI (c,t) F^-	PC (Z)-MTI (t,c) F^-	PC (Z)-MTI (c,c) F^-	PC (Z)-MTI (t,t) F^-
HF/6-31G(d)	-527.13386	-527.13626	-527.12012	-527.13470	-527.12721	-527.11674
HF/6-31+G(d)	-527.17068	-527.17144	-527.15460	-527.17017	-527.16338	-527.15160
MP2/6-31G(d)	-528.64054	-528.64374	-528.63321	-528.65054	-528.63990	-528.63072
MP2/6-31+G(d)	-528.70908	-528.71064	-528.69907	-528.71713	-528.71713	-528.69738
B3LYP/6-31G(d)	-530.18079	-530.18400	-530.17089	-530.18748	-530.18628	-530.16822
B3LYP/6-31+G(d)	-530.23759	-530.23914	-530.22486	-530.24177	-530.24945	-530.22158
B3LYP/6-31G(d,p)	-530.19540	-530.19837	-530.18540	-530.20246	-530.20380	-530.18271

Level of Theory	RC (Z)-MTI_T (t,c) F^-	RC (E)-MTI_T (t,c) F^-	RC (E)-MTI_T (t,t) F^-	RC (Z)-MTI_T (c,t) F^-	(Z)-MTI_T (t,c) F^- TS	(E)-MTI_T (t,c) F^- TS
HF/6-31G(d)	-527.15980	-527.15772	-527.15846	-527.13114	-527.04548	-527.05484
HF/6-31+G(d)	-527.19432	-527.19549	-527.19543	-527.19449	-527.10455	-527.10592
MP2/6-31G(d)	-528.68570	-528.67945	-528.68701	-528.66479	-528.57801	-528.57085
MP2/6-31+G(d)	-528.75302	-528.75046	-528.75677	-528.75044	-528.67603	-
B3LYP/6-31G(d)	-530.21510	-530.21179	-530.21700	-530.20465	-530.11557	-530.11261
B3LYP/6-31+G(d)	-530.27295	-530.27356	-530.27769	-530.26448	-530.19868	-530.19686
B3LYP/6-31G(d,p)	-530.23292	-530.22936	-530.23485	-530.23699	-530.13101	-530.16839

Level of Theory	(E)-MTI_T (t,t) F^- TS	(Z)-MTI_T (c,t) F^- TS	PC (Z)-MTI_T (t,c) F^-	PC (E)-MTI_T (t,c) F^-	PC (E)-MTI_T (t,t) F^-	PC (Z)-MTI_T (c,t) F^-
HF/6-31G(d)	-527.05414	-527.06513	-527.21412	-527.21440	-527.21440	-527.21440
HF/6-31+G(d)	-527.10455	-527.11162	-527.25170	-527.25171	-527.25171	-527.25170
MP2/6-31G(d)	-528.57801	-528.57085	-528.71235	-528.71235	-528.71235	-528.71235
MP2/6-31+G(d)	-528.67603	-	-528.78213	-528.78213	-528.78213	-528.78213
B3LYP/6-31G(d)	-530.11557	-530.15234	-530.23161	-530.23092	-530.23092	-530.23092
B3LYP/6-31+G(d)	-530.19868	-530.21523	-530.28654	-530.28654	-530.28654	-530.28654
B3LYP/6-31G(d,p)	-530.13101	-530.16839	-530.24691	-530.24629	-530.24629	-530.24629

Level of Theory	RC (E)-MTIC (t,c,c) F^-	RC (E)-MTIC (t,t,c) F^-	RC (E)-MTIC (t,c,t) F^-	RC (E)-MTIC (t,t,t) F^-	RC (E)-MTIC (c,c,c) F^-	RC (E)-MTIC (c,t,c) F^-
HF/6-31G(d)	-694.96517	-694.95676	-694.97175	-694.96754	-694.95392	-694.95218
HF/6-31+G(d)	-695.00700	-694.99834	-695.01340	-695.00953	-694.99622	-694.99380
B3LYP/6-31G(d)	-698.93486	-698.92665	-698.94157	-698.93678	-698.92092	-698.92135
B3LYP/6-31+G(d)	-699.00737	-698.99734	-699.01328	-699.00849	-698.99347	-698.99299
B3LYP/6-31G(d,p)	-698.95748	-698.94913	-698.96425	-698.95992	-698.94333	-698.94377

Level of Theory	RC (E)-MTIC (c,c,t) F^-	RC (E)-MTIC (c,t,t) F^-	RC (Z)-MTIC (t,t,c) F^-	RC (Z)-MTIC (t,c,c) F^-	RC (Z)-MTIC (t,t,t) F^-	RC (Z)-MTIC (t,c,t) F^-
HF/6-31G(d)	-694.95655	-694.96036	-694.96657	-694.94733	-694.95910	-694.95674
HF/6-31+G(d)	-694.99822	-695.00171	-695.00582	-694.98572	-695.00353	-694.99524
B3LYP/6-31G(d)	-698.92896	-698.93374	-698.93751	-698.93751	-698.94314	-698.94307
B3LYP/6-31+G(d)	-699.00006	-699.00462	-699.00336	-699.00336	-699.01068	-699.01065
B3LYP/6-31G(d,p)	-698.95147	-698.95651	-698.95958	-698.95958	-698.96550	-698.93226

Level of Theory	RC (Z)-MTIC (c,t,c) F^-	RC (Z)-MTIC (c,t,t) F^-	RC (Z)-MTIC (c,c,c) F^-	RC (Z)-MTIC (c,c,t) F^-	(E)-MTIC (t,c,c) F^- TS	(E)-MTIC (t,t,c) F^- TS
HF/6-31G(d)	-694.93833	-694.95705	-694.96517	-694.93323	-694.85863	-694.86994
HF/6-31+G(d)	-695.00032	-694.99524	-695.00700	-695.00700	-694.91695	-694.92603
B3LYP/6-31G(d)	-698.93751	-698.94314	-698.93486	-698.93486	-698.83602	-698.84628
B3LYP/6-31+G(d)	-699.00336	-699.01068	-699.00737	-699.00737	-698.92468	-698.93366
B3LYP/6-31G(d,p)	-698.93287	-698.96550	-698.95748	-698.95748	-698.85615	-698.86633

Level of Theory	(E)-MTIC (t,c,t) F^- TS	(E)-MTIC (t,t,t) F^- TS	(E)-MTIC (c,c,c) F^- TS	(E)-MTIC (c,t,c) F^- TS	(E)-MTIC (c,c,t) F^- TS	(E)-MTIC (c,t,t) F^- TS
HF/6-31G(d)	-694.86888	-694.87413	-694.85899	-694.85890	-694.86221	-694.86002
HF/6-31+G(d)	-694.92706	-694.93043	-694.91582	-694.91737	-694.91862	-694.91771
B3LYP/6-31G(d)	-698.84603	-698.85092	-698.83403	-698.83443	-698.84235	-698.84033
B3LYP/6-31+G(d)	-698.93485	-698.93829	-698.92196	-698.92303	-698.92948	-698.92816
B3LYP/6-31G(d,p)	-698.86625	-698.87108	-698.85394	-698.85437	-698.86252	-698.86055

Level of Theory	(Z)-MTIC (t,t,c) F^- TS	(Z)-MTIC (t,c,c) F^- TS	(Z)-MTIC (t,t,t) F^- TS	(Z)-MTIC (t,c,t) F^- TS	(Z)-MTIC (c,t,c) F^- TS	(Z)-MTIC (c,t,t) F^- TS
HF/6-31G(d)	-694.84430	-694.84385	-694.84968	-694.85113	-694.84627	-694.85113
HF/6-31+G(d)	-694.90129	-694.90129	-694.90738	-694.90682	-694.90170	-694.90682
B3LYP/6-31G(d)	-698.82662	-698.82621	-698.83362	-698.83092	-698.82584	-698.83092
B3LYP/6-31+G(d)	-698.91382	-698.91344	-698.92096	-698.91685	-698.91154	-698.91685
B3LYP/6-31G(d,p)	-698.84682	-698.84647	-698.85391	-698.85108	-698.84589	-698.85108

Level of Theory	(Z)-MTIC (c,c,c) F^- TS	(Z)-MTIC (c,c,t) F^- TS	PC (E)-MTIC (t,c,c) F^-	PC (E)-MTIC (t,t,c) F^-	PC (E)-MTI (t,c,t) F^-	PC (E)-MTIC (t,t,t) F^-
HF/6-31G(d)	-694.84578	-694.84918	-694.94080	-694.94410	-694.94695	-694.95140
HF/6-31+G(d)	-694.90129	-694.90738	-694.98071	-694.98233	-694.98720	-694.98944
B3LYP/6-31G(d)	-698.83559	-698.84100	-698.90431	-698.90831	-698.91030	-698.91572
B3LYP/6-31+G(d)	-698.91344	-698.92096	-698.96826	-698.97074	-698.97479	-698.97773
B3LYP/6-31G(d,p)	-698.85556	-698.86112	-698.92403	-698.92766	-698.92995	-698.93517

Level of Theory	PC (E)-MTIC (c,c,c) F^-	PC (E)-MTIC (c,t,c) F^-	PC (E)-MTIC (c,c,t) F^-	PC (E)-MTIC (c,t,t) F^-	PC (Z)-MTIC (t,t,c) F^-	PC (Z)-MTIC (t,c,c) F^-
HF/6-31G(d)	-694.93509	-694.93291	-694.94008	-694.93728	-694.93847	-694.93848
HF/6-31+G(d)	-694.97359	-694.97296	-694.97842	-694.98071	-694.97753	-694.97753
B3LYP/6-31G(d)	-698.89852	-698.89449	-698.90727	-698.90446	-698.90662	-698.90667
B3LYP/6-31+G(d)	-698.96090	-698.95891	-698.96966	-698.96775	-698.96893	-698.96893
B3LYP/6-31G(d,p)	-698.91787	-698.91394	-698.92684	-698.92424	-698.92045	-698.92045

Level of Theory	PC (Z)-MTIC (t,t,t) F^-	PC (Z)-MTIC (t,c,t) F^-	PC (Z)-MTIC (c,t,c) F^-	PC (Z)-MTIC (c,t,t) F^-	PC (Z)-MTIC (c,c,c) F^-	PC (Z)-MTIC (c,c,t) F^-
HF/6-31G(d)	-694.94467	-694.94467	-694.91787	-694.92633	-694.91702	-694.94467
HF/6-31+G(d)	-694.98340	-694.98340	-694.95543	-694.96384	-694.97753	-694.98340
B3LYP/6-31G(d)	-698.91271	-698.91271	-698.88541	-698.89464	-698.88171	-698.91271
B3LYP/6-31+G(d)	-698.97472	-698.97472	-698.94699	-698.95560	-698.94601	-698.97472
B3LYP/6-31G(d,p)	-698.93240	-698.93266	-698.90484	-698.91419	-698.90120	-698.93240

Level of Theory	RC (Z)-MTIC_T (t,c,c) F^-	RC (E)-MTIC_T (t,c,c) F^-	RC (Z)-MTIC_T (t,t,c) F^-	RC (E)-MTIC_T (t,t,c) F^-	RC (E)-MTIC_T (t,c,t) F^-	RC (E)-MTIC_T (t,t,t) F^-
HF/6-31G(d)	-694.96084	-694.95716	-694.96343	-694.96566	-694.95604	-694.96240
HF/6-31+G(d)	-695.00068	-694.99832	-695.00172	-695.00504	-694.99586	-695.00134
B3LYP/6-31G(d)	-698.92861	-698.92362	-698.93861	-698.93770	-698.92730	-698.94015
B3LYP/6-31+G(d)	-698.99451	-698.99222	-699.00165	-699.00177	-698.99479	-699.00603
B3LYP/6-31G(d,p)	-698.95139	-698.94620	-698.96144	-698.96044	-698.95031	-698.96324

Level of Theory	(Z)-MTIC_T (t,c,c) F^- TS	(E)-MTIC_T (t,c,c) F^- TS	(Z)-MTIC_T (t,t,c) F^- TS	(E)-MTIC_T (t,t,c) F^- TS	(E)-MTIC_T (t,c,t) F^- TS	(E)-MTIC_T (t,t,t) F^- TS
HF/6-31G(d)	-694.85094	-694.86317	-694.84416	-694.85316	-694.86469	-694.85157
HF/6-31+G(d)	-694.93570	-694.91884	-694.91884	-694.90873	-694.91944	-694.90617
B3LYP/6-31G(d)	-698.88248	-698.83906	-698.83492	-698.82851	-698.84122	-698.83133
B3LYP/6-31+G(d)	-698.95372	-698.92942	-698.92366	-698.91767	-698.93244	-698.91984
B3LYP/6-31G(d,p)	-698.90359	-698.86007	-698.85579	-698.84953	-698.86175	-698.85236

Level of Theory	PC (Z)-MTIC_T (t,c,c) F^-	PC (E)-MTIC_T (t,c,c) F^-	PC (Z)-MTIC_T (t,t,c) F^-	PC (E)-MTIC_T (t,t,c) F^-	PC (E)-MTIC_T (t,c,t) F^-	PC (E)-MTIC_T (t,t,t) F^-
HF/6-31G(d)	-695.04161	-695.04161	-695.03178	-695.03178	-695.04161	-695.03178
HF/6-31+G(d)	-695.08161	-695.08161	-695.07108	-695.07108	-695.08161	-695.07108
B3LYP/6-31G(d)	-698.97070	-698.97070	-698.96093	-698.96093	-698.97070	-698.96093
B3LYP/6-31+G(d)	-699.03505	-699.03505	-699.02521	-699.02521	-699.03505	-699.02521
B3LYP/6-31G(d,p)	-698.99070	-698.99070	-698.98084	-698.98084	-698.99070	-698.98084

S_N2 REACTION PATHWAYS CON'T – CHLORIDE

Level of Theory	RC (E)-MTI (t,c) Cl^-	RC (E)-MTI (t,t) Cl^-	RC (E)-MTI (c,c) Cl^-	RC (E)-MTI (c,t) Cl^-	RC (Z)-MTI (c,t) Cl^-	RC (Z)-MTI (t,c) Cl^-	RC (Z)-MTI (c,c) Cl^-
HF/6-31G(d)	-887.26973	-887.26059	-887.26503	-887.26028	-887.24570	-887.26072	-887.23493
HF/6-31+G(d)	-887.29358	-887.28438	-887.28873	-887.28384	-887.26778	-887.28173	-887.25727
MP2/6-31G(d)	-888.73144	-888.72005	-888.72509	-888.71817	-888.71108	-888.72893	-888.70302
MP2/6-31+G(d)	-888.77959	-888.76790	-888.77313	-888.76588	-888.75828	-888.77603	-888.75065
B3LYP/6-31G(d)	-890.62764	-890.61823	-890.62228	-890.61700	-890.60611	-890.62335	-890.59830
B3LYP/6-31+G(d)	-890.66432	-890.65464	-890.65896	-890.65357	-890.64089	-890.65661	-890.63330
B3LYP/6-31G(d,p)	-890.64236	-890.63291	-890.63696	-890.63160	-890.62075	-890.63812	-890.61287

Level of Theory	RC (Z)-MTI (t,t) Cl^-	(E)-MTI (t,c) Cl^- TS	(E)-MTI (t,t) Cl^- TS	(E)-MTI (c,c) Cl^- TS	(E)-MTI (c,t) Cl^- TS	(Z)-MTI (c,t) Cl^- TS	(Z)-MTI (t,c) Cl^- TS
HF/6-31G(d)	-887.26072	-887.17469	-887.17820	-887.17454	-887.17512	-887.16080	-887.16424
HF/6-31+G(d)	-887.28173	-887.20035	-887.20272	-887.20028	-887.19976	-887.18433	-887.18787
MP2/6-31G(d)	-888.72892	-888.64204	-888.64573	-888.63937	-888.63988	-888.63187	-888.64021
MP2/6-31+G(d)	-888.77602	-888.69234	-888.69510	-888.69021	-888.68976	-888.68012	-888.68935
B3LYP/6-31G(d)	-890.62335	-890.54978	-890.55334	-890.54807	-890.54868	-890.53775	-890.54431
B3LYP/6-31+G(d)	-890.65659	-890.58786	-890.59027	-890.58642	-890.58616	-890.57355	-890.58030
B3LYP/6-31G(d,p)	-890.63807	-890.56426	-890.56742	-890.56251	-890.56286	-890.55209	-890.55885

Level of Theory	(Z)-MTI (c,c) Cl^- TS	(Z)-MTI (t,t) Cl^- TS	PC (E)-MTI (t,c) Cl^-	PC (E)-MTI (t,t) Cl^-	PC (E)-MTI (c,c) Cl^-	PC (E)-MTI (c,t) Cl^-	PC (Z)-MTI (c,t) Cl^-
HF/6-31G(d)	-887.16013	-887.16080	-887.19568	-887.19863	-887.19469	-887.19621	-887.18040
HF/6-31+G(d)	-887.18432	-887.18433	-887.22301	-887.22456	-887.22220	-887.22241	-887.20582
MP2/6-31G(d)	-888.63279	-	-888.66520	-888.66900	-888.66159	-888.66394	-888.65376
MP2/6-31+G(d)	-888.68305	-	-888.71705	-888.71936	-888.71395	-888.71510	-888.70377
B3LYP/6-31G(d)	-890.53740	-890.53775	-890.56236	-890.56563	-890.55950	-890.56128	-890.54866
B3LYP/6-31+G(d)	-890.57459	-890.57355	-890.60226	-890.60424	-890.59976	-890.60049	-890.58650
B3LYP/6-31G(d,p)	-890.55177	-890.55209	-890.57674	-890.57972	-890.57379	-890.57532	-890.56283

Level of Theory	PC (Z)-MTI (t,c) Cl^-	PC (Z)-MTI (c,c) Cl^-	PC (Z)-MTI (t,t) Cl^-	RC (Z)-MTI_T (t,c) Cl^-	RC (E)-MTI_T (t,c) Cl^-	RC (E)-MTI_T (t,t) Cl^-	RC (Z)-MTI_T (c,t) Cl^-
HF/6-31G(d)	-887.19500	-887.18762	-887.17697	-887.25403	-887.25362	-887.25852	-887.24901
HF/6-31+G(d)	-887.22136	-887.21488	-887.20279	-887.27523	-887.27660	-887.28133	-887.27037
MP2/6-31G(d)	-888.67114	-888.66079	-888.65115	-888.71829	-888.71829	-888.72299	-888.71379
MP2/6-31+G(d)	-888.72179	-888.71512	-888.70205	-888.76396	-888.76396	-888.77032	-888.75867
B3LYP/6-31G(d)	-890.56526	-890.55261	-890.54577	-890.61312	-890.61043	-890.61919	-890.60695
B3LYP/6-31+G(d)	-890.60338	-890.59303	-890.58314	-890.64694	-890.64618	-890.65427	-890.64013
B3LYP/6-31G(d,p)	-890.57988	-890.56688	-890.55993	-890.62821	-890.62542	-890.63426	-890.62179

Level of Theory	(Z)-MTI_T (t,c) Cl^- TS	(E)-MTI_T (t,c) Cl^- TS	(E)-MTI_T (t,t) Cl^- TS	(Z)-MTI_T (c,t) Cl^- TS	PC (Z)-MTI_T (t,c) Cl^-	PC (E)-MTI_T (t,c) Cl^-	PC (E)-MTI_T (t,t) Cl^-
HF/6-31G(d)	-887.17849	-887.17849	-887.17849	-887.17849	-887.27423	-887.27423	-887.27423
HF/6-31+G(d)	-887.20310	-887.20310	-887.20310	-887.20310	-887.30262	-887.30262	-887.30262
MP2/6-31G(d)	-888.66348	-888.66348	-888.66348	-888.66348	-888.73263	-888.73263	-888.73263
MP2/6-31+G(d)	-888.71277	-888.71277	-888.71277	-888.71277	-888.78690	-888.78690	-888.78690
B3LYP/6-31G(d)	-890.56436	-890.56436	-890.56436	-890.56436	-890.60981	-890.60981	-890.60981
B3LYP/6-31+G(d)	-890.59917	-890.59917	-890.59917	-890.59917	-890.64982	-890.64982	-890.64982
B3LYP/6-31G(d,p)	-890.57936	-890.57936	-890.57936	-890.57936	-890.62485	-890.62485	-890.62485

Level of Theory	PC (Z)-MTI_T (c,t) Cl^-
HF/6-31G(d)	-887.27423
HF/6-31+G(d)	-887.30262
MP2/6-31G(d)	-888.73263
MP2/6-31+G(d)	-888.78690
B3LYP/6-31G(d)	-890.60981
B3LYP/6-31+G(d)	-890.64982
B3LYP/6-31G(d,p)	-890.62485

Level of Theory	RC (E)-MTIC (t,c,c) Cl^-	RC (E)-MTIC (t,t,c) Cl^-	RC (E)-MTIC (t,c,t) Cl^-	RC (E)-MTIC (t,t,t) Cl^-	RC (E)-MTIC (c,c,c) Cl^-	RC (E)-MTIC (c,t,c) Cl^-	RC (E)-MTIC (c,c,t) Cl^-
HF/6-31G(d)	-1055.06501	-1055.04997	-1055.06712	-1055.05934	-1055.05187	-1055.05376	-1055.05035
HF/6-31+G(d)	-1055.09371	-1055.07910	-1055.09573	-1055.08779	-1055.08056	-1055.08263	-1055.07844
B3LYP/6-31G(d)	-1059.33962	-1059.32573	-1059.34327	-1059.33559	-1059.32475	-1059.32662	-1059.32948
B3LYP/6-31+G(d)	-1059.38556	-1059.37076	-1059.38885	-1059.38104	-1059.37048	-1059.37249	-1059.37426
B3LYP/6-31G(d,p)	-1059.35947	-1059.34556	-1059.36326	-1059.35558	-1059.34441	-1059.34637	-1059.34945

Level of Theory	RC (E)-MTIC (c,t,t) Cl^-	RC (Z)-MTIC (t,t,c) Cl^-	RC (Z)-MTIC (t,c,c) Cl^-	RC (Z)-MTIC (t,t,t) Cl^-	RC (Z)-MTIC (t,c,t) Cl^-	RC (Z)-MTIC (c,t,c) Cl^-	RC (Z)-MTIC (c,t,t) Cl^-
HF/6-31G(d)	-1055.05611	-1055.05587	-1055.05561	-1055.05636	-1055.00687	-1055.05587	-1055.00694
HF/6-31+G(d)	-1055.08444	-1055.08213	-1055.08213	-1055.08227	-1055.03386	-1055.08213	-1055.03389
B3LYP/6-31G(d)	-1059.33533	-1059.33317	-1059.33287	-1059.33880	-1059.33880	-1059.33317	-1059.33873
B3LYP/6-31+G(d)	-1059.38029	-1059.37530	-1059.37494	-1059.38109	-1059.38109	-1059.37530	-1059.38109
B3LYP/6-31G(d,p)	-1059.35538	-1059.35310	-1059.35283	-1059.35898	-1059.35898	-1059.35310	-1059.35898

Level of Theory	RC (Z)-MTIC (c,c,c) Cl^-	RC (Z)-MTIC (c,c,t) Cl^-	(E)-MTIC (t,c,c) Cl^- TS	(E)-MTIC (t,t,c) Cl^- TS	(E)-MTIC (t,c,t) Cl^- TS	(E)-MTIC (t,t,t) Cl^- TS	(E)-MTIC (c,c,c) Cl^- TS
HF/6-31G(d)	-1055.06501	-1055.00694	-1054.97140	-1054.97854	-1054.97952	-1054.98340	-1054.96880
HF/6-31+G(d)	-1055.09371	-1055.03389	-1055.00114	-1055.00700	-1055.00968	-1055.01176	-1054.99772
B3LYP/6-31G(d)	-1059.33962	-1059.33873	-1059.26159	-1059.26882	-1059.27014	-1059.27402	-1059.25713
B3LYP/6-31+G(d)	-1059.38556	-1059.38109	-1059.30836	-1059.31449	-1059.31713	-1059.31938	-1059.30336
B3LYP/6-31G(d,p)	-1059.35947	-1059.35898	-1059.28104	-1059.28808	-1059.28964	-1059.29337	-1059.27629

Level of Theory	(E)-MTIC (c,t,c) Cl^- TS	(E)-MTIC (c,c,t) Cl^- TS	(E)-MTIC (c,t,t) Cl^- TS	(Z)-MTIC (t,t,c) Cl^- TS	(Z)-MTIC (t,c,c) Cl^- TS	(Z)-MTIC (t,t,t) Cl^- TS	(Z)-MTIC (t,c,t) Cl^- TS
HF/6-31G(d)	-1054.97042	-1054.97147	-1054.97108	-1054.95853	-1054.95813	-1054.96509	-1054.96039
HF/6-31+G(d)	-1055.00025	-1055.00001	-1055.00082	-1054.98631	-1054.98631	-1054.99308	-1054.98824
B3LYP/6-31G(d)	-1059.25905	-1059.26531	-1059.26488	-1059.25484	-1059.25450	-1059.26222	-1059.25410
B3LYP/6-31+G(d)	-1059.30565	-1059.31064	-1059.31083	-1059.29937	-1059.29904	-1059.30694	-1059.29810
B3LYP/6-31G(d,p)	-1059.27842	-1059.28470	-1059.28448	-1059.27445	-1059.27415	-1059.28186	-1059.27353

Level of Theory	(Z)-MTIC (c,t,c) Cl^- TS	(Z)-MTIC (c,t,t) Cl^- TS	(Z)-MTIC (c,c,c) Cl^- TS	(Z)-MTIC (c,c,t) Cl^- TS	PC (E)-MTIC (t,c,c) Cl^-	PC (E)-MTIC (t,t,c) Cl^-	PC (E)-MTIC (t,c,t) Cl^-
HF/6-31G(d)	-1054.95520	-1054.96039	-1054.95813	-1054.96509	-1055.00241	-1055.00345	-1055.00650
HF/6-31+G(d)	-1054.98305	-1054.98824	-1054.98631	-1054.99308	-1055.03313	-1055.03285	-1055.03782
B3LYP/6-31G(d)	-1059.24824	-1059.25410	-1059.25450	-1059.26222	-1059.28329	-1059.28489	-1059.28707
B3LYP/6-31+G(d)	-1059.29270	-1059.29810	-1059.29904	-1059.30694	-1059.33075	-1059.33170	-1059.33583
B3LYP/6-31G(d,p)	-1059.26761	-1059.27353	-1059.27415	-1059.28186	-1059.30260	-1059.30391	-1059.30641

Level of Theory	PC (E)-MTIC (t,t,t) Cl^-	PC (E)-MTIC (c,c,c) Cl^-	PC (E)-MTIC (c,t,c) Cl^-	PC (E)-MTIC (c,c,t) Cl^-	PC (E)-MTIC (c,t,t) Cl^-	PC (Z)-MTIC (t,t,c) Cl^-	PC (Z)-MTIC (t,c,c) Cl^-
HF/6-31G(d)	-1055.01061	-1054.99651	-1054.99346	-1054.99919	-1054.99740	-1054.99973	-1054.99973
HF/6-31+G(d)	-1055.03987	-1055.02581	-1055.02432	-1055.02879	-1055.02787	-1055.02962	-1055.02962
B3LYP/6-31G(d)	-1059.29208	-1059.27718	-1059.27276	-1059.28343	-1059.28209	-1059.28504	-1059.28504
B3LYP/6-31+G(d)	-1059.33857	-1059.32332	-1059.32090	-1059.33040	-1059.32935	-1059.33111	-1059.33111
B3LYP/6-31G(d,p)	-1059.31119	-1059.29622	-1059.29189	-1059.30268	-1059.30153	-1059.30478	-1059.30478

Level of Theory	PC (Z)-MTIC (t,t,t) Cl^-	PC (Z)-MTIC (t,c,t) Cl^-	PC (Z)-MTIC (c,t,c) Cl^-	PC (Z)-MTIC (c,t,t) Cl^-	PC (Z)-MTIC (c,c,c) Cl^-	PC (Z)-MTIC (c,c,t) Cl^-
HF/6-31G(d)	-1055.00450	-1055.00450	-1054.99973	-1055.00450	-1054.97723	-1055.00450
HF/6-31+G(d)	-1055.03434	-1055.03434	-1055.02962	-1055.03434	-1055.02962	-1055.03434
B3LYP/6-31G(d)	-1059.28964	-1059.28964	-1059.28504	-1059.28964	-1059.25917	-1059.28964
B3LYP/6-31+G(d)	-1059.33631	-1059.33631	-1059.33111	-1059.33631	-1059.30759	-1059.33631
B3LYP/6-31G(d,p)	-1059.30940	-1059.30940	-1059.30478	-1059.30940	-1059.27836	-1059.30940

Level of Theory	RC (Z)-MTIC_T (t,c,c) Cl^-	RC (E)-MTIC_T (t,c,c) Cl^-	RC (Z)-MTIC_T (t,t,c) Cl^-	RC (E)-MTIC_T (t,t,c) Cl^-	RC (E)-MTIC_T (t,c,t) Cl^-	RC (E)-MTIC_T (t,t,t) Cl^-
HF/6-31G(d)	-1055.01047	-1055.00927	-1055.01246	-1055.05370	-1055.00818	-1055.05466
HF/6-31+G(d)	-1055.03870	-1055.03740	-1055.03979	-1055.08123	-1055.03491	-1055.08255
B3LYP/6-31G(d)	-1059.29847	-1059.31147	-1059.32898	-1059.32740	-1059.31695	-1059.33283
B3LYP/6-31+G(d)	-1059.34255	-1059.35765	-1059.37153	-1059.37170	-1059.36162	-1059.37612
B3LYP/6-31G(d,p)	-1059.32159	-1059.33154	-1059.34908	-1059.34749	-1059.33735	-1059.35312

Level of Theory	(Z)-MTIC_T (t,c,c) Cl^- TS	(E)-MTIC_T (t,c,c) Cl^- TS	(Z)-MTIC_T (t,t,c) Cl^- TS	(E)-MTIC_T (t,t,c) Cl^- TS	(E)-MTIC_T (t,c,t) Cl^- TS	(E)-MTIC_T (t,t,t) Cl^- TS
HF/6-31G(d)	-1054.99703	-1054.99703	-1054.98322	-1054.98322	-1054.99703	-1054.98322
HF/6-31+G(d)	-1055.02828	-1055.02828	-1055.01328	-1055.01328	-1055.02828	-1055.01328
B3LYP/6-31G(d)	-1059.29228	-1059.29228	-1059.28175	-1059.28175	-1059.29228	-1059.28175
B3LYP/6-31+G(d)	-1059.33605	-1059.33605	-1059.32482	-1059.32482	-1059.33605	-1059.32482
B3LYP/6-31G(d,p)	-1059.31219	-1059.31219	-1059.30158	-1059.30158	-1059.31219	-1059.30158

Level of Theory	PC (Z)-MTIC_T (t,c,c) Cl^-	PC (E)-MTIC_T (t,c,c) Cl^-	PC (Z)-MTIC_T (t,t,c) Cl^-	PC (E)-MTIC_T (t,t,c) Cl^-	PC (E)-MTIC_T (t,c,t) Cl^-	PC (E)-MTIC_T (t,t,t) Cl^-
HF/6-31G(d)	-1055.10125	-1055.10125	-1055.09115	-1055.09115	-1055.10125	-1055.09115
HF/6-31+G(d)	-1055.13232	-1055.13232	-1055.12161	-1055.12161	-1055.13232	-1055.12161
B3LYP/6-31G(d)	-1059.34717	-1059.34717	-1059.33766	-1059.33766	-1059.34717	-1059.33766
B3LYP/6-31+G(d)	-1059.39626	-1059.39626	-1059.38556	-1059.38556	-1059.39626	-1059.38556
B3LYP/6-31G(d,p)	-1059.36744	-1059.36744	-1059.35729	-1059.35729	-1059.36744	-1059.35729

S_N2 REACTION PATHWAYS CON'T – BROMIDE

Level of Theory	RC (E)-MTI (t,c) Br^-	RC (E)-MTI (t,t) Br^-	RC (E)-MTI (c,c) Br^-	RC (E)-MTI (c,t) Br^-	RC (Z)-MTI (c,t) Br^-	RC (Z)-MTI (t,c) Br^-	RC (Z)-MTI (c,c) Br^-
HF/6-31G(d)	-2997.68243	-2997.67423	-2997.67816	-2997.67382	-2997.66046	-2997.67417	-2997.64841
HF/6-31+G(d)	-2997.72600	-2997.71783	-2997.72146	-2997.71724	-2997.70148	-2997.71508	-2997.68975
MP2/6-31G(d)	-2999.13227	-2999.12233	-2999.12652	-2999.12031	-2999.11424	-2999.12934	-2999.10494
MP2/6-31+G(d)	-2999.19686	-2999.18680	-2999.19104	-2999.18484	-2999.17673	-2999.19291	-2999.16880
B3LYP/6-31G(d)	-3002.13769	-3002.12945	-3002.13280	-3002.12814	-3002.11891	-3002.13436	-3002.10920
B3LYP/6-31+G(d)	-3002.19313	-3002.18493	-3002.18817	-3002.18373	-3002.17190	-3002.18587	-3002.16242
B3LYP/6-31G(d,p)	-3002.15248	-3002.14398	-3002.14744	-3002.14260	-3002.13342	-3002.14911	-3002.12371

Level of Theory	RC (Z)-MTI (t,t) Br^-	(E)-MTI (t,c) Br^- TS	(E)-MTI (t,t) Br^- TS	(E)-MTI (c,c) Br^- TS	(E)-MTI (c,t) Br^- TS	(Z)-MTI (c,t) Br^- TS	(Z)-MTI (t,c) Br^- TS
HF/6-31G(d)	-2997.67417	-2997.58738	-2997.59062	-2997.58725	-2997.58756	-2997.57329	-2997.57723
HF/6-31+G(d)	-2997.71508	-2997.63065	-2997.63266	-2997.63069	-2997.62973	-2997.61450	-2997.61971
MP2/6-31G(d)	-2999.12934	-2999.04224	-2999.04503	-2999.03954	-2999.04224	-2999.03380	-2999.04106
MP2/6-31+G(d)	-2999.19291	-2999.10861	-2999.11090	-2999.10655	-2999.10861	-2999.10167	-2999.10762
B3LYP/6-31G(d)	-3002.13436	-3002.06154	-3002.06449	-3002.05986	-3002.06154	-3002.04959	-3002.05640
B3LYP/6-31+G(d)	-3002.18587	-3002.11667	-3002.11877	-3002.11532	-3002.11667	-3002.10532	-3002.11070
B3LYP/6-31G(d,p)	-3002.14911	-3002.07632	-3002.07936	-3002.07460	-3002.07633	-3002.06427	-3002.07126

Level of Theory	(Z)-MTI (c,c) Br^- TS	(Z)-MTI (t,t) Br^- TS	PC (E)-MTI (t,c) Br^-	PC (E)-MTI (t,t) Br^-	PC (E)-MTI (c,c) Br^-	PC (E)-MTI (c,t) Br^-	PC (Z)-MTI (c,t) Br^-
HF/6-31G(d)	-2997.57323	-2997.57329	-2997.60408	-2997.60666	-2997.60317	-2997.60425	-2997.58856
HF/6-31+G(d)	-2997.61648	-2997.61450	-2997.65202	-2997.65037	-2997.64844	-2997.64973	-2997.63181
MP2/6-31G(d)	-2999.03380	-	-2999.05710	-2999.06046	-2999.05364	-2999.05539	-2999.04537
MP2/6-31+G(d)	-2999.10167	-	-2999.12927	-2999.12774	-2999.12305	-2999.12581	-2999.11236
B3LYP/6-31G(d)	-3002.04959	-3002.04921	-3002.07116	-3002.07405	-3002.06843	-3002.06966	-3002.05714
B3LYP/6-31+G(d)	-3002.10532	-3002.10227	-3002.13133	-3002.13009	-3002.12620	-3002.12643	-3002.11236
B3LYP/6-31G(d,p)	-3002.06427	-3002.06387	-3002.08660	-3002.08864	-3002.08320	-3002.08418	-3002.07179

Level of Theory	PC (Z)-MTI (t,c) Br^-	PC (Z)-MTI (c,c) Br^-	PC (Z)-MTI (t,t) Br^-	RC (Z)-MTI_T (t,c) Br^-	RC (E)-MTI_T (t,c) Br^-	RC (E)-MTI_T (t,t) Br^-	RC (Z)-MTI_T (c,t) Br^-
HF/6-31G(d)	-2997.60316	-2997.59577	-2997.58513	-2997.66824	-2997.66735	-2997.67175	-2997.66272
HF/6-31+G(d)	-2997.64959	-2997.64364	-2997.62868	-2997.70812	-2997.71006	-2997.71417	-2997.70260
MP2/6-31G(d)	-2999.06279	-2999.05251	-2999.04269	-2999.12105	-2999.11485	-2999.12445	-2999.11581
MP2/6-31+G(d)	-2999.13294	-2999.12711	-	-2999.18195	-2999.17880	-2999.18785	-2999.17752
B3LYP/6-31G(d)	-3002.07377	-3002.06121	-3002.05420	-3002.12498	-3002.12139	-3002.12973	-3002.11823
B3LYP/6-31+G(d)	-3002.13170	-3002.12196	-3002.10896	-3002.17640	-3002.17597	-3002.18346	-3002.16908
B3LYP/6-31G(d,p)	-3002.08887	-3002.07659	-3002.06883	-3002.14017	-3002.13639	-3002.14492	-3002.13291

Level of Theory	(Z)-MTI_T (t,c) Br^- TS	(E)-MTI_T (t,c) Br^- TS	(E)-MTI_T (t,t) Br^- TS	(Z)-MTI_T (c,t) Br^- TS	PC (Z)-MTI_T (t,c) Br^-	PC (E)-MTI_T (t,c) Br^-	PC (E)-MTI_T (t,t) Br^-
HF/6-31G(d)	-2997.59354	-2997.59354	-2997.59354	-2997.59354	-2997.68264	-2997.68264	-2997.68264
HF/6-31+G(d)	-2997.63608	-2997.63608	-2997.63608	-2997.63608	-2997.73015	-2997.73015	-2997.73015
MP2/6-31G(d)	-2999.06665	-2999.06665	-2999.06665	-2999.06665	-2999.12478	-2999.12478	-2999.12478
MP2/6-31+G(d)	-2999.13187	-2999.13187	-2999.13187	-2999.13187	-2999.19739	-2999.19739	-2999.19739
B3LYP/6-31G(d)	-3002.07913	-3002.07913	-3002.07913	-3002.07913	-3002.11921	-3002.11921	-3002.11921
B3LYP/6-31+G(d)	-3002.13057	-3002.13057	-3002.13057	-3002.13057	-3002.17754	-3002.17754	-3002.17754
B3LYP/6-31G(d,p)	-3002.09422	-3002.09422	-3002.09422	-3002.09422	-3002.13472	-3002.13472	-3002.13472

Level of Theory	PC (Z)-MTI_T (c,t) Br^-	RC (E)-MTIC (t,c,c) Br^-	RC (E)-MTIC (t,t,c) Br^-	RC (E)-MTIC (t,c,t) Br^-	RC (E)-MTI (t,t,t) Br^-	RC (E)-MTIC (c,c,c) Br^-	RC (E)-MTIC (c,t,c) Br^-
HF/6-31G(d)	-2997.68264	-	-	-	-	-	-
HF/6-31+G(d)	-2997.73015	-	-	-	-	-	-
MP2/6-31G(d)	-2999.12478	-3165.47728	-3165.46331	-3165.47953	-3165.47248	-3165.46523	-3165.46701
MP2/6-31+G(d)	-2999.19739	-3165.52590	-3165.51229	-3165.52797	-3165.52081	-3165.51376	-3165.51543
B3LYP/6-31G(d)	-3002.11921	-3170.84928	-3170.83696	-3170.85305	-3170.84611	-3170.83554	-3170.83730
B3LYP/6-31+G(d)	-3002.17754	-3170.91416	-3170.90117	-3170.91746	-3170.91048	-3170.90033	-3170.90183
B3LYP/6-31G(d,p)	-3002.13472	-3170.86930	-3170.85662	-3170.87322	-3170.86613	-3170.85511	-3170.85700

Level of Theory	RC (E)-MTIC (c,c,t) Br^-	RC (E)-MTIC (c,t,t) Br^-	RC (Z)-MTIC (t,t,c) Br^-	RC (Z)-MTIC (t,c,c) Br^-	RC (Z)-MTIC (t,t,t) Br^-	RC (Z)-MTIC (t,c,t) Br^-	RC (Z)-MTIC (c,t,c) Br^-
MP2/6-31G(d)	-3165.46357	-3165.46862	-3165.46971	-3165.46945	-3165.46989	-3165.46989	-3165.46971
MP2/6-31+G(d)	-3165.51175	-3165.51671	-3165.51592	-3165.51592	-3165.51589	-3165.51589	-3165.51592
B3LYP/6-31G(d)	-3170.84008	-3170.84517	-3170.84463	-3170.84433	-3170.84953	-3170.84954	-3170.84463
B3LYP/6-31+G(d)	-3170.90413	-3170.90910	-3170.90547	-3170.90547	-3170.91086	-3170.91086	-3170.90547
B3LYP/6-31G(d,p)	-3170.86004	-3170.86537	-3170.86466	-3170.86466	-3170.86975	-3170.86975	-3170.86466

Level of Theory	RC (Z)-MTIC (c,t,t) Br^-	RC (Z)-MTIC (c,c,c) Br^-	RC (Z)-MTIC (c,c,t) Br^-	(E)-MTIC (t,c,c) Br^- TS	(E)-MTIC (t,t,c) Br^- TS	(E)-MTIC (t,c,t) Br^- TS
HF/6-31G(d)	-3165.46989	-3165.47728	-3165.46989	-3165.38409	-3165.39096	-3165.39204
HF/6-31+G(d)	-3165.51589	-3165.52590	-3165.51589	-3165.43194	-3165.43707	-3165.44055
B3LYP/6-31G(d)	-3170.84954	-3170.84928	-3170.84954	-3170.77331	-3170.78013	-3170.78181
B3LYP/6-31+G(d)	-3170.91086	-3170.91416	-3170.91086	-3170.83740	-3170.84640	-3170.84640
B3LYP/6-31G(d,p)	-3170.86975	-3170.86930	-3170.86975	-3170.79306	-3170.80162	-3170.80162

Level of Theory	(E)-MTIC (t,t,t) Br^- TS	(E)-MTIC (c,c,c) Br^- TS	(E)-MTIC (c,t,c) Br^- TS	(E)-MTIC (c,c,t) Br^- TS	(E)-MTIC (c,t,t) Br^- TS	(Z)-MTIC (t,t,c) Br^- TS
HF/6-31G(d)	-3165.39581	-3165.38131	-3165.38314	-3165.38388	-3165.38365	-3165.37151
HF/6-31+G(d)	-3165.44181	-3165.42787	-3165.43076	-3165.43006	-3165.43135	-3165.41819
B3LYP/6-31G(d)	-3170.78529	-3170.76856	-3170.77077	-3170.77680	-3170.77657	-3170.76700
B3LYP/6-31+G(d)	-3170.84783	-3170.83187	-3170.83468	-3170.83906	-3170.83976	-3170.82984
B3LYP/6-31G(d,p)	-3170.80495	-3170.78802	-3170.79044	-3170.79651	-3170.79648	-3170.78693

Level of Theory	(Z)-MTIC (t,c,c) Br^- TS	(Z)-MTIC (t,t,t) Br^- TS	(Z)-MTIC (t,c,t) Br^- TS	(Z)-MTIC (c,t,c) Br^- TS	(Z)-MTIC (c,t,t) Br^- TS	(Z)-MTIC (c,c,c) Br^- TS
HF/6-31G(d)	-3165.37111	-3165.37808	-3165.37285	-3165.36772	-3165.37285	-3165.37111
HF/6-31+G(d)	-3165.41819	-3165.42496	-3165.41834	-3165.41390	-3165.41834	-3165.41819
B3LYP/6-31G(d)	-3170.76665	-3170.77434	-3170.76551	-3170.75972	-3170.76551	-3170.76665
B3LYP/6-31+G(d)	-3170.82951	-3170.83724	-3170.82681	-3170.82206	-3170.82681	-3170.82951
B3LYP/6-31G(d,p)	-3170.78662	-3170.79429	-3170.78525	-3170.77940	-3170.78525	-3170.78662

Level of Theory	(Z)-MTIC (c,c,t) Br^- TS	PC (E)-MTIC (t,c,c) Br^-	PC (E)-MTIC (t,t,c) Br^-	PC (E)-MTIC (t,c,t) Br^-	PC (E)-MTIC (t,t,t) Br^-	PC (E)-MTIC (c,c,c) Br^-
HF/6-31G(d)	-3165.37808	-3165.41103	-3165.41136	-3165.41449	-3165.41844	-3165.40497
HF/6-31+G(d)	-3165.42496	-3165.46209	-3165.45921	-3165.46699	-3165.46616	-3165.45303
B3LYP/6-31G(d)	-3170.77434	-3170.79201	-3170.79316	-3170.79548	-3170.80059	-3170.78585
B3LYP/6-31+G(d)	-3170.83724	-3170.85971	-3170.85763	-3170.86293	-3170.86511	-3170.85054
B3LYP/6-31G(d,p)	-3170.79429	-3170.81188	-3170.81266	-3170.81532	-3170.82027	-3170.80540

Level of Theory	PC (E)-MTIC (c,t,c) Br^-	PC (E)-MTIC (c,c,t) Br^-	PC (E)-MTIC (c,t,t) Br^-	PC (Z)-MTIC (t,t,c) Br^-	PC (Z)-MTIC (t,c,c) Br^-	PC (Z)-MTIC (t,t,t) Br^-
HF/6-31G(d)	-3165.40183	-3165.40699	-3165.40562	-3165.40819	-3165.40819	-3165.41248
HF/6-31+G(d)	-3165.45432	-3165.45455	-3165.45385	-3165.45848	-3165.45848	-3165.46401
B3LYP/6-31G(d)	-3170.79160	-3170.79160	-3170.79071	-3170.79364	-3170.79364	-3170.79797
B3LYP/6-31+G(d)	-3170.85624	-3170.85610	-3170.85552	-3170.86003	-3170.86003	-3170.86561
B3LYP/6-31G(d,p)	-3170.81137	-3170.81133	-3170.81064	-3170.81388	-3170.81388	-3170.81805

Level of Theory	PC (Z)-MTIC (t,c,t) Br^-	PC (Z)-MTIC (c,t,c) Br^-	PC (Z)-MTIC (c,t,t) Br^-	PC (Z)-MTIC (c,c,c) Br^-	PC (Z)-MTIC (c,c,t) Br^-	RC (Z)-MTIC_T (t,c,c) Br^-
HF/6-31G(d)	-3165.41248	-3165.40819	-3165.41248	-3165.38550	-3165.41248	-3165.41549
HF/6-31+G(d)	-3165.46401	-3165.45848	-3165.46401	-3165.45848	-3165.46401	-3165.45836
B3LYP/6-31G(d)	-3170.79797	-3170.79364	-3170.79797	-3170.79364	-3170.79797	-3170.80978
B3LYP/6-31+G(d)	-3170.86561	-3170.86003	-3170.86561	-3170.86003	-3170.86561	-3170.87129
B3LYP/6-31G(d,p)	-3170.81805	-3170.81388	-3170.81805	-3170.81388	-3170.81805	-3170.83271

Level of Theory	RC (E)-MTIC_T (t,c,c) Br^-	RC (Z)-MTIC_T (t,t,c) Br^-	RC (E)-MTIC_T (t,t,c) Br^-	RC (E)-MTIC_T (t,c,t) Br^-	RC (E)-MTIC_T (t,t,t) Br^-
HF/6-31G(d)	-3165.48281	-3165.46771	-3165.46743	-3165.45558	-3165.46806
HF/6-31+G(d)	-3165.52909	-3165.51263	-3165.51467	-3165.52562	-3165.51623
B3LYP/6-31G(d)	-3170.85084	-3170.84142	-3170.83833	-3170.82674	-3170.84322
B3LYP/6-31+G(d)	-3170.91265	-3170.90194	-3170.90111	-3170.90457	-3170.90457
B3LYP/6-31G(d,p)	-3170.87073	-3170.86129	-3170.85830	-3170.84718	-3170.86346

Level of Theory	(Z)-MTIC_T (t,c,c) Br^- TS	(E)-MTIC_T (t,c,c) Br^- TS
HF/6-31G(d)	-3165.41196	-3165.41196
HF/6-31+G(d)	-3165.46121	-3165.46121
B3LYP/6-31G(d)	-3170.80684	-3170.80684
B3LYP/6-31+G(d)	-3170.86754	-3170.86754
B3LYP/6-31G(d,p)	-3170.82683	-3170.82683

Level of Theory	(Z)-MTIC_T (t,t,c) Br^- TS	(E)-MTIC_T (t,t,c) Br^- TS	(E)-MTIC_T (t,c,t) Br^- TS	(E)-MTIC_T (t,t,t) Br^- TS	PC (Z)-MTIC_T (t,c,c) Br^-
HF/6-31G(d)	-3165.39811	-3165.39811	-3165.41196	-3165.39811	-3165.50936
HF/6-31+G(d)	-3165.44602	-3165.44602	-3165.46121	-3165.44602	-3165.56251
B3LYP/6-31G(d)	-3170.79649	-3170.79649	-3170.80684	-3170.79649	-3170.85585
B3LYP/6-31+G(d)	-3170.85627	-3170.85627	-3170.86754	-3170.85627	-3170.92672
B3LYP/6-31G(d,p)	-3170.81639	-3170.81639	-3170.82683	-3170.81639	-3170.87601

Level of Theory	PC (E)-MTIC_T (t,c,c) Br^-	PC (Z)-MTIC_T (t,t,c) Br^-	PC (E)-MTIC_T (t,t,c) Br^-	PC (E)-MTIC_T (t,c,t) Br^-	PC (E)-MTIC_T (t,t,t) Br^-
HF/6-31G(d)	-3165.50936	-3165.49917	-3165.49917	-3165.50936	-3165.49917
HF/6-31+G(d)	-3165.56251	-3165.54929	-3165.54929	-3165.56251	-3165.54929
B3LYP/6-31G(d)	-3170.85585	-3170.84621	-3170.84621	-3170.85585	-3170.84621
B3LYP/6-31+G(d)	-3170.92672	-3170.91373	-3170.91373	-3170.92672	-3170.91373
B3LYP/6-31G(d,p)	-3170.87601	-3170.86632	-3170.86632	-3170.87601	-3170.86632

S_N2 REACTION PATHWAYS SEPARATED REACTANTS AND SEPARATED PRODUCTS

Level of Theory	F^-	Cl^-	Br^-	N_2	CH_3F	CH_3Cl	CH_3Br
HF/6-31G(d)	-99.35048	-459.52600	-2569.93750	-108.94395	-139.03462	-499.09315	-2609.50068
HF/6-31+G(d)	-99.41859	-459.53966	-2569.97127	-108.94702	-139.04423	-499.09416	-2609.51457
MP2/6-31G(d)	-99.52661	-459.65210	-2570.05281	-109.25528	-139.33586	-499.35456	-2609.74482
MP2/6-31+G(d)	-99.62385	-459.67115	-2570.05281	-109.26193	-139.35350	-499.35747	-2609.76014
B3LYP/6-31G(d)	-99.75409	-460.25223	-2571.76134	-109.52413	-139.73392	-500.10853	-2611.61665
B3LYP/6-31+G(d)	-99.85970	-460.27473	-2571.80318	-109.52978	-139.75108	-500.11152	-2611.63240
B3LYP/6-31G(d,p)	-99.75409	-460.25223	-2571.76134	-109.52413	-139.73829	-500.11255	-2611.62112

Level of Theory	Post (E)-MTI $(t,c)^-$	Post (E)-MTI $(t,t)^-$	Post (E)-MTI $(c,c)^-$	Post (E)-MTI $(c,t)^-$	Post (Z)-MTI $(c,t)^-$	Post (Z)-MTI $(t,c)^-$	Post (Z)-MTI $(c,c)^-$
HF/6-31G(d)	-388.08492	-388.09203	-388.08362	-388.08890	-388.07193	-388.10110	-388.08002
HF/6-31+G(d)	-388.11393	-388.11833	-388.11327	-388.11547	-388.09777	-388.12560	-388.10848
MP2/6-31G(d)	-389.28973	-389.29762	-389.28539	-389.29185	-389.28040	-389.31292	-389.28704
MP2/6-31+G(d)	-389.34258	-389.34716	-389.33942	-389.34210	-389.32940	-389.36016	-389.33917
B3LYP/6-31G(d)	-390.43380	-390.44146	-390.42997	-390.43649	-390.42253	-390.45154	-390.42831
B3LYP/6-31+G(d)	-390.47602	-390.48055	-390.47336	-390.47622	-390.46098	-390.48810	-390.46967
B3LYP/6-31G(d,p)	-390.44391	-390.45138	-390.43998	-390.44634	-390.43248	-390.46125	-390.43837

Level of Theory	Post (Z)-MTI $(t,t)^-$	5-imidazoyl amide$^-$	5-(4-carbox amido) imidazoyl amide$^-$ (c)	5-(4-carbox amido) imidazoyl amide$^-$ (t)	Post (E)-MTIC $(t,c,c)^-$	Post (E)-MTIC $(t,t,c)^-$	Post (E)-MTIC $(t,c,t)^-$
HF/STO-3G	-	-275.55819	-441.16206	-441.16206	-548.61441	-548.62358	-548.62389
HF/3-21G	-	-277.63566	-444.53362	-444.53362	-552.73474	-552.74827	-552.74698
HF/6-31G(d)	-388.06856	-279.21788	-447.04804	-447.04804	-555.88985	-555.89774	-555.90078
HF/6-31+G(d)	-388.09475	-279.24565	-447.07749	-447.07749	-555.92149	-555.92805	-555.93294
MP2/6-31G(d)	-389.27829	-280.09383	-448.38217	-448.38217	-557.55237	-557.56155	-557.56394
MP2/6-31+G(d)	-389.32788	-280.14130	-448.43984	-448.43984	-557.61642	-557.62288	-557.62807
B3LYP/6-31G(d)	-390.42034	-280.95049	-449.69554	-449.69554	-559.15380	-559.16274	-559.16452
B3LYP/6-31+G(d)	-390.45809	-280.99013	-449.74158	-449.74158	-559.20300	-559.20944	-559.21399
B3LYP/6-31G(d,p)	-390.43027	-280.96127	-449.71095	-449.71095	-559.16882	-559.17758	-559.17968

Level of Theory	Post (E)-MTIC $(t,t,t)^-$	Post (E)-MTIC $(c,c,c)^-$	Post (E)-MTIC $(c,t,c)^-$	Post (E)-MTIC $(c,c,t)^-$	Post (E)-MTIC $(c,t,t)^-$	Post (Z)-MTIC $(t,t,c)^-$	Post (Z)-MTIC $(t,c,c)^-$
HF/STO-3G	-548.63088	-548.61455	-548.61026	-548.62261	-548.61544	-548.64557	-548.64591
HF/3-21G	-552.75664	-552.73536	-552.72953	-552.74568	-552.73569	-552.75461	-552.75461
HF/6-31G(d)	-555.90635	-555.88606	-555.88391	-555.89529	-555.88923	-555.90337	-555.90337
HF/6-31+G(d)	-555.93574	-555.91569	-555.91642	-555.92500	-555.92137	-555.93132	-555.93132
MP2/6-31G(d)	-557.57039	-557.54809	-557.54380	-557.56168	-557.55495	-557.57565	-557.57565
MP2/6-31+G(d)	-557.63104	-557.61118	-557.61019	-557.62319	-557.61935	-557.63506	-557.63506
B3LYP/6-31G(d)	-559.17084	-559.14928	-559.14509	-559.16291	-559.15629	-559.16946	-559.16946
B3LYP/6-31+G(d)	-559.21702	-559.19627	-559.19564	-559.20928	-559.20554	-559.21380	-559.21380
B3LYP/6-31G(d,p)	-559.18580	-559.16402	-559.15994	-559.17802	-559.17152	-559.18433	-559.18433